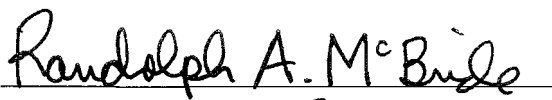





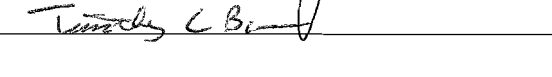
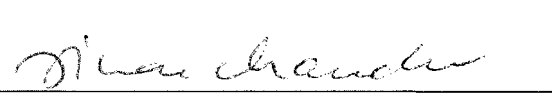


MORPHODYNAMIC CHANGES OF THE PARRAMORE-CEDAR BARRIER-  
ISLAND SYSTEM AND WACHAPREAGUE INLET, VIRGINIA FROM 1852 TO  
2011: A MODEL OF BARRIER ISLAND AND TIDAL INLET EVOLUTION ALONG  
THE SOUTHERN DELMARVA PENINSULA, USA

by

Trent Michael Richardson  
A Dissertation  
Submitted to the  
Graduate Faculty  
of  
George Mason University  
in Partial Fulfillment of  
the Requirements for the Degree  
of  
Doctor of Philosophy  
Environmental Science and Public Policy

Committee:

	Dr. Randolph A. McBride, Dissertation Director
	Dr. Sheryl L. Beach, Committee Member
	Dr. Richard J. Diecchio, Committee Member
	Dr. Michael S. Fenster, Committee Member, Randolph Macon College
	Dr. Albert Torzilli, Graduate Program Director
	Dr. Robert Jonas, Department Chairperson
	Dr. Timothy L. Born, Associate Dean for Student and Academic Affairs, College of Science
	Dr. Vikas Chandhoke, Dean, College of Science

Date: May 2, 2012 Spring Semester 2012  
George Mason University  
Fairfax, VA

Morphodynamic Changes of the Parramore-Cedar Barrier-Island System and  
Wachapreague Inlet, Virginia from 1852 to 2011: a Model of Barrier Island and Tidal  
Inlet Evolution along the Southern Delmarva Peninsula, USA

A dissertation submitted in partial fulfillment of the requirements for the degree of  
Doctor of Philosophy at George Mason University

by

Trent Michael Richardson  
Master of Science  
George Mason University, 1999  
Dual Bachelor of Arts  
Mary Washington College, 1997

Director: Randolph A. McBride, Associate Professor  
Department of Environmental Science and Policy and Department of Atmospheric,  
Oceanic, and Earth Sciences

Spring Semester 2012  
George Mason University  
Fairfax, VA





This work is licensed under a [creative commons attribution-noncommercial 3.0 unported license](https://creativecommons.org/licenses/by-nc/3.0/).

## **DEDICATION**

This research is dedicated to my family, Elizabeth, Lillian, and Beauregard. Liz has endured long days and nights and repeatedly accommodated my schedule. I am both fortunate and grateful for this sacrifice. Not to be forgotten, my parents provided the financial support and encouragement to complete these studies, while my grandparents laid the foundation for this success many years ago through their own hard work.

Lillie and Beau may read this dedication one day far into the future. If so then I hope you have learned the joy of education, the reward of a challenge, the value of discipline, and your responsibility to humanity, our country, and the Earth.

## ACKNOWLEDGMENTS

Acknowledging all the people who have generously provided their expertise and time over the past many years is a difficult task.

Firstly, I'm deeply appreciative of the guidance and friendship of Dr. Randolph McBride who was the driving force and primary reason for the completion of this research. A special thanks is also given to Dr. Michael Fenster who served as an outside committee member from Randolph Macon College. In addition, I'm also very appreciative of Dr. Sheryl Beach and Dr. Richard Diecchio for their contributions to this study. And finally, I want to acknowledge my previous advisors for setting me on this doctoral path, specifically Dr. Barry Haack (George Mason University) and Dr. Donald Rallis (University of Mary Washington).

Of course no doctoral research is possible without data and I have many to thank for their assistance in both the collection and analysis of the shoreline and tidal inlet data contained in this study. I thank Nitesh Patel and Julia Nord for serving as companions and assistants during shoreline surveys. I also thank Kevin Moyer for his guidance on tidal inlet surveys and tidal corrections.

In the execution and further refinement of this work, I humbly thank Domenick Alario for his extensive mapping and graphics support during my most pressing hours. I'm also appreciative of Margo Harris for her watchful eye and proofreading skills during the final push for the final dissertation.

I also received support on statistical techniques, and in particular, the refinement of the English to metric unit conversions of cross-sectional area to tidal prism and tidal prism to ebb-tidal delta volumes. Specifically, David Walnut, Professor in the Department of Mathematical Sciences, Chris Seminack for his contributions to the development of a modified tidal prism equation, and Jeffrey Topp.

In addition, I've received support from a host of colleagues both past and present, but in particular, I'm grateful to John Loyd and Renee Orr for both their patience and encouragement during this long process.

And finally, I wish to thank the Eastern Shore Laboratory of the Virginia Institute of Marine Science for their logistical assistance during the course of many years of research. But in particular, Sean Fate for his well-guided transportation to the islands and assistance with data collection and the overarching support of Dr. Mark Luckenbach.

## TABLE OF CONTENTS

	Page
List of Tables .....	ix
List of Figures .....	xi
List of Equations .....	xx
Abstract .....	xxi
Chapter One: Introduction .....	1
Statement of the Problem .....	1
Research Questions .....	13
Multiple Working Hypotheses .....	14
Overall Goal and Scientific Objectives .....	16
Scope of the Study .....	17
Chapter Two: Regional Setting .....	19
Geology of the Southern Delmarva Peninsula .....	19
Coastal Geomorphology .....	21
Coastal Processes .....	25
Area of Investigation .....	26
Parramore Island .....	26
Cedar Island .....	27
Wachapreague Inlet .....	30
Chapter Three: Data Sets and Methods .....	32
Shoreline Data Sets .....	32
Data Sources, Proxies, and GPS .....	35
Shoreline Accuracy Assessment .....	39
Shoreline Analysis Methodology .....	41
Shoreline Change Statistics .....	41
Shoreline Cells .....	44
Bathymetric Data Sets .....	48

<i>In Situ</i> Inlet Survey Methodology (2007–2011).....	48
Bathymetric Data Set Errors.....	53
Tidal Prism Calculations .....	55
Jarrett Equation Modifications .....	58
Ebb-Tidal Delta Calculations .....	61
Chapter Four: Related Studies and Concepts.....	64
Barrier-Island Formation.....	64
The Barrier-Island System .....	68
Tidal Inlets and Tidal Deltas .....	73
Coastal Morphodynamics and Drivers of Shoreline Change .....	79
Sediment Supply.....	79
Storminess .....	87
Relative Sea-Level Rise versus Storm Activity as Principal Drivers.....	88
Coastal Change Studies.....	91
Chapter Five: Results.....	96
Parramore Island .....	96
Cell 0: Northern, Bay-Side Shoreline.....	101
Cell 1: Wachapreague Inlet-Throat Shoreline .....	101
Cell 2: Northern, Inlet-Influenced Shoreline .....	103
Cell 3: North-Central, Open-Ocean Shoreline .....	105
Cell 4: Southern, Washover-Dominated, Open-Ocean Shoreline .....	107
Cell 5: Southern Spit Shoreline .....	108
Cells 3–4: Non-Inlet Influenced, Open-Ocean Shoreline.....	109
Cedar Island.....	114
Cell 0: Metompkin Inlet and Coast Guard Breach-Influenced Shoreline .....	116
Cell 1: Coast-Guard Breach-Throat Shoreline .....	118
Cell 2: Northern, Breach-Influenced Shoreline .....	119
Cell 3: North-Central, Marsh-Backed, Open-Ocean Shoreline .....	120
Cell 4: South-Central, Bay-Backed, Open-Ocean Shoreline.....	121
Cell 5: Southern Spit Shoreline .....	122
Cells 3–4: Non-Inlet-Influenced, Open-Ocean Shoreline .....	124
Wachapreague Inlet.....	129

Shoreline Changes of Wachapreague Inlet: 1852 to 2010 .....	129
Wachapreague Inlet Bathymetric Surveys (2007–2011).....	130
Historical Tidal Inlet Bathymetric Surveys (1852–1972) .....	134
Historical Metrics of Wachapreague Inlet.....	134
Parramore Island Summary .....	144
Cedar Island Summary .....	147
Wachapreague Inlet Summary .....	153
Chapter Six: Discussion.....	157
Drivers of Change to the Barrier-Island System .....	158
Relative Sea-Level Rise and the Three-Stage Model of Runaway Transgression ..	159
Southern Extension of Large Arc of Erosion .....	161
Updrift Island Breaching .....	165
Increased Storminess .....	178
A Six-Stage Model of Coastal Change and Barrier-Island Evolution .....	189
Stage 1 ( $\geq 2,000$ Years B.P.): Original Shoreline .....	189
Stage 2 (2000 to 500 Years B.P.): Updrift Sediment Trapping and Recurved Spit and Arc of Erosion Development.....	191
Stage 3 (500 to 200 years B.P.): Continued Spit Development and Southern Extension of the Large Arc of Erosion.....	194
Stage 4 (200 to 150 years B.P.): Morphodynamic Changes to Cedar Island, Virginia .....	195
Stage 5 (50 to 40 years B.P.): Morphodynamic Changes to Parramore Island, Virginia.....	200
Stage 6 (10 to 100 years into the future): Evolution of the Parramore–Cedar Barrier Island and Wachapreague Tidal Inlet System .....	205
Chapter Seven: Conclusions .....	209
Summary of the Study.....	209
Conclusions of the Findings.....	210
Future Research.....	218
Appendix A: Parramore Island Shoreline Results .....	219
Appendix B: Cedar Island Shoreline Results.....	244
References.....	269

## LIST OF TABLES

Table	Page
Table 1: Parramore Island shoreline data sets (NOS T-sheets and GPS shoreline position surveys).....	34
Table 2: Cedar Island shoreline data sets (NOS T-sheets and GPS shoreline position surveys).....	35
Table 3: Maximum root-mean-square (rms) shoreline change error (Parramore Island, Virginia).....	40
Table 4: Maximum root-mean-square (rms) shoreline change error (Cedar Island, Virginia).....	40
Table 5: Wachapreague Inlet bathymetric data sets (H-sheets and bathymetric surveys)	49
Table 6: Jarrett (1976) regression equations of tidal prism and cross-sectional area .....	57
Table 7: Processes of coastal change (Kraft and Chrzastowski, 1985). .....	84
Table 8: Comparison of long-term incremental time periods by end point rate (m/yr) and shoreline cell of Parramore Island, Virginia .....	99
Table 9: Long-term (1852–1998) and short-term (1998–2010) end point and linear regression rates (m/yr) by shoreline cell of Parramore Island .....	100
Table 10: Comparison of long-term incremental time periods by end point rate (m/yr) and shoreline cell for Cedar Island, Virginia.....	116
Table 11: Long-term (1852–1998) and short-term (1998–2010) end point and linear regression rates (m/yr) by shoreline cell of Cedar Island .....	117
Table 12: Historical metrics of the Wachapreague Inlet tidal inlet complex .....	135
Table 13: Mean values and linear regression rates ( $\text{m}^2/\text{yr}$ ) of the cross-sectional area changes at Wachapreague Inlet across multiple time periods .....	137

Table 14: Mean values and linear regression rates ( $\text{m}^3/\text{yr}$ ) of tidal prism changes at Wachapreague Inlet across multiple time periods .....	138
Table 15: Mean values and linear regression rates ( $\text{m}^3/\text{yr}$ ) of the ebb-tidal delta volume changes at Wachapreague Inlet across multiple time periods .....	138
Table 16: Temporally portioned shoreline retreat rates of Cedar Island according to Nebel et al. (2012). .....	180
Table 17: Nebel and Trembanis (2010) storminess index values (storms/yr) and Cedar Island retreat rates (m/yr) (top) and storminess and retreat rates over incremental time periods using end point rates (m/yr) (bottom) .....	183



## LIST OF FIGURES

Figure	Page
Figure 1: Extensive tree die-offs strewn along the foreshore of the north-central, non-inlet-influenced, open-ocean shoreline of Parramore Island, April 27, 2006. ....	4
Figure 2: Maritime forest impacts at the transition zone between the southern, washover-dominated, open-ocean shoreline and the north-central, non-inlet influenced, open-ocean shoreline of Parramore Island, April 27, 2007. ....	4
Figure 3: Nearly complete elimination of the maritime forest along the backshore of the north-central, non-inlet-influenced, open-ocean shoreline of Parramore Island, August 31, 2011. Note the dead trees (snags) along the interior relict dune ridges (i.e., Italian Ridge). Image provided by Randolph A. McBride. ....	5
Figure 4: Northern extent of widespread tree die-offs at the transition zone between the north-central, non-inlet-influenced, open-ocean shoreline and the northern, inlet-influenced shoreline, April 22, 2010. Note the large number of dead trees in the interior of Parramore Island. ....	5
Figure 5: Ecogeomorphic changes (e.g., tree die-offs) because of the intrusion of saltwater spray along Italian Ridge (a relict dune) of Parramore Island, April 22, 2010. Note the interspersing of dead trees among the remnants of the living trees in the distance. ....	6
Figure 6: Relict marsh outcropping along the foreshore of the southern, washover-dominated, open-ocean shoreline of Parramore Island, April 27, 2007. ....	7
Figure 7: Relict marsh outcropping along the foreshore of the southern, bay-backed, open-ocean shoreline of Cedar Island, April 25, 2008. ....	7
Figure 8: Large washover fan and exposed relict marsh along the northern, non-inlet-influenced, open-ocean shoreline of Cedar Island, April 21, 2010. ....	8
Figure 9: Large washover fan, exposed relict marsh, and extensive foreshore along the southern, washover-dominated shoreline of Parramore Island, April 22, 2010. ....	8

Figure 10: Location of the most recent Cedar breach that closed in the spring of 2007 along the south-central, bay-backed, open-ocean shoreline. Photo taken August 31, 2011 by Randolph A. McBride.....	9
Figure 11: The “Coast Guard” breach along the northern inlet- and breach-influenced shorelines of Cedar Island, April 21, 2010. ....	9
Figure 12: Three-stage model of runaway transgression (Fitzgerald et al., 2004). ....	11
Figure 13: The Delmarva Peninsula with Delaware Bay to the north, Chesapeake Bay to the west, and the mouth of the Chesapeake Bay to the south (image from Google Earth, July 2010).....	20
Figure 14: Landscape elements of the New Jersey and Delmarva coastal components (Oertel and Kraft, 1994).....	22
Figure 15: Pleistocene and Holocene barrier configurations in the Virginia sector of the Delmarva Peninsula (Demarest and Leatherman, 1985). ....	23
Figure 16: Distribution of barrier island/spit lengths, tidal range, and wave height (McBride, 1999), modified from Fitzgerald (1982).....	24
Figure 17: The Virginia Eastern Shore of the Delmarva Peninsula.....	28
Figure 18: The Parramore-Cedar barrier island and Wachapreague tidal inlet system. Aerial photography courtesy of USDA Aerial Photography Field Office (APFO).....	29
Figure 19: Wachapreague Inlet environs August 15, 2011. Note the large ebb tidal delta and ephemeral Dawson Shoals to the north of the inlet. Aerial photography courtesy of USDA APFO. ....	31
Figure 20: T-sheet 512, Parramore Island’s outer shoreline in 1852. Source: NOAA Coastal Services Center. ....	33
Figure 21: Physical features of the beach. The berm crest was walked during GPS shoreline position surveys on both Parramore and Cedar in order to map the high water line (HWL) as described by Pajak and Leatherman (2002).....	36
Figure 22: The berm crest, the physical shoreline feature surveyed on Parramore and Cedar Islands.....	38
Figure 23: GPS data collection system in use during survey of Parramore Island on April 30, 2011.....	38

Figure 24: Parramore Island shoreline cell reference map. ....	46
Figure 25: Cedar Island shoreline cell reference map. ....	47
Figure 26: Wachapreague Inlet-throat cross-sections from 1852 to 1972 (DeAlteris & Byrne, 1975). ....	50
Figure 27: Top, Tide-gauge locations in the Wachapreague Inlet area. Bottom, Bathymetric surveys across the inlet throat of Wachapreague Inlet, Virginia from 2007 to 2011. Aerial photography courtesy of USDA APFO. ....	52
Figure 28: Schematic and deployment of ADCP in Wachapreague Inlet. Shown are bathymetric survey transects for April 23, 2010 bathymetric profile (landward/west) and August 12, 2010 (Fenster et al., 2011). ....	53
Figure 29: Backbarrier storage volume relative to tidal elevations at town of Wachapreague, Virginia. Mean tide level = 4.36 ft. (Byrnes et al., 1974). ....	55
Figure 30: Tidal prism vs. cross-sectional area: Inlets on Atlantic coast with one or no jetties (Jarrett, 1976). ....	58
Figure 31: Walton and Adams (1976) tidal prism–outer bar storage relationship for tidal inlets. ....	63
Figure 32: Offshore bar/shoal emergence model (from Leatherman, 1982). ....	66
Figure 33: Mainland beach ridge submergence model (from Leatherman, 1982). ....	66
Figure 34: Barrier island formation through spit elongation and island breaching model (from Leatherman, 1982). ....	67
Figure 35: The six elements of a barrier island system (from Oertel, 1985). ....	70
Figure 36: Relationship between wave energy and tidal energy and the effects on barrier island morphology (Davis & Hayes, 1984). ....	71
Figure 37: Hayes (1980) model of morphology of ebb-tidal deltas. ....	74
Figure 38: Primary morphologic features of a flood-tidal delta (Hayes, 1980). ....	75
Figure 39: The drumstick barrier island model demonstrating a local reversal in sediment transport because of wave refraction around the large ebb-tidal delta (Hayes and Kana, 1976). ....	77

Figure 40: Schematic of Wachapreague Inlet sand circulation loop (Bryne et al., 1974).	78
Figure 41: Curray (1964) diagram of the rate of change of relative sea level and rate of net deposition on the transgression (landward) and regression (seaward) movement of a shoreline.	81
Figure 42: Interaction of factors affecting shoreline changes with arrows pointing towards the dependent variables and the number of arrows indicate the relative degree of independence or interaction (Morton, 1977).	82
Figure 43: Temporal growth of Fishing Point, Virginia and the arc of erosion on the southern Delmarva Pensinsula (Galgano, 1998).	86
Figure 44: Historic trend analysis of inlet-induced shoreline behavior demonstrating pre-inlet and post-inlet shoreline trends and determination of the distance downdrift where inlet influences ceases (Galgano, 2009).	86
Figure 45: Storm impact model for barrier islands (Sallenger, 2000).	88
Figure 46: Parramore Island shoreline reference map.	98
Figure 47: Magnitude of change with linear regression rate and trendline of Parramore Island (1852 to 2010) for Cells 3-4 normalized to the 1852 shoreline.	100
Figure 48: Long-term (1852–1998) and short-term (1998–2010) linear regression rates (LRR) of the alongshore change of Cells 3–4 spatially correlated to the compiled historical shorelines of Parramore Island, Virginia. Long-term rates are in blue and short-term rates are in red.	112
Figure 49: Long-term (1852–1998) linear and weighted linear regression rates (LRR and WLR, respectively) of the alongshore change of Cells 3–4 spatially correlated to the compiled historical shorelines of Parramore Island, Virginia.	113
Figure 50: Cedar Island shoreline cell reference map.	115
Figure 51: Magnitude of change with linear regression rate and trendline of Cedar Island (1852–2010) normalized to the 1852 shoreline.	117
Figure 52: Long-term (1852–2007) and short-term (2007–2010) linear regression rates (LRR) of alongshore change of Cells 3–4 with spatially correlated map and graph of Cedar Island, Virginia. The long-term rate is in blue and the short-term rate is in red.	126

Figure 53: Long-term (1852–2007) linear and weighted linear regression rates of alongshore change of Cells 3–4 with spatially correlated map and graph of Cedar Island, Virginia. ....	128
Figure 54: Shoreline changes of Wachapreague Inlet, Virginia from 1852 to 2010 with long-term and short-term changes rates. In general, Wachapreague Inlet has been slowly migrating in a southerly direction over the long term.....	130
Figure 55: Bathymetric profiles of the inlet throat of Wachapreague Inlet, Virginia on April 28, 2007 (Moyer, 2007).....	131
Figure 56: Bathymetric profiles of the inlet throat of Wachapreague Inlet, Virginia on April 23, 2010 (Richardson, 2010). ....	132
Figure 57: Bathymetric profiles of the inlet throat of Wachapreague Inlet, Virginia on April 29, 2011 (Richardson, 2011). ....	133
Figure 58: Cross-sectional area (m <sup>2</sup> ), tidal prism (m <sup>3</sup> ), and ebb-tidal delta volume (m <sup>3</sup> ) at Wachapreague Inlet, Virginia from 1871 to 2011 with linear regression rates and strength of relationship with 15% variability bars.....	139
Figure 59: Tidal prism (m <sup>3</sup> ), ebb-tidal delta volume (m <sup>3</sup> ), and cross-sectional area (m <sup>2</sup> ) at Wachapreague Inlet, Virginia with linear regression rates (1871–2007). The overall trend is a slight decrease from 1871 to 2007. ....	140
Figure 60: Tidal prism (m <sup>3</sup> ), ebb-tidal delta volume (m <sup>3</sup> ), and cross-sectional area (m <sup>2</sup> ) at Wachapreague Inlet, Virginia with linear regression rates (2007–2011). The overall trend is a distinct increase from 2007 to 2011. ....	141
Figure 61: Maximum inlet throat depths (m) and inlet widths (m) of Wachapreague Inlet, Virginia with linear regression rates (1871–2011). ....	143
Figure 62: Cross-sectional area (m <sup>2</sup> ) and maximum inlet throat depth (m) of Wachapreague Inlet, Virginia with linear regression rates (1871–2011). ....	143
Figure 63: End point rate (m/yr) by shoreline cell and incremental time period for Parramore Island, Virginia.....	146
Figure 64: Trendlines of end point rate (m/yr) by shoreline cell and incremental time period for Parramore Island, Virginia. ....	146
Figure 65: End point rate (m/yr) by shoreline cell and incremental time periods of Cedar Island, Virginia. The general trends for cells 2, 3, and 5 show increasing retreat rates through time. ....	148

Figure 66: Trendlines of end point rate (m/yr) by shoreline cell and incremental time period of Cedar Island, Virginia. ....	149
Figure 67: Long-term linear regression retreat rates for Parramore and Cedar Islands along non-inlet-influenced, open ocean shoreline for the entire period of record.....	151
Figure 68: Long-term and short-term (in parentheses) shoreline change rates (m/yr) by geomorphic cell for the entire Parramore–Cedar barrier island system. USDA APFO, 1994.....	152
Figure 69: Satellite image circa 1982 of the southern Delmarva Peninsula showing the large and distinct arc of erosion south of the southern tip of Assateague Island that extends from Chincoteague Inlet, Virginia to Wachapreague Inlet, Virginia. (Photo provided by Duncan FitzGerald.) The white features in the Chesapeake Bay are areas of sea ice.....	165
Figure 70: Oblique aerial photo of Cedar Island Breach in November 2006. (Photo taken by Richard Ayers.) .....	166
Figure 71: Changes in Cedar Island land area (feet/year) over various time intervals and physiographic locations (from Gaunt, 1991). ....	168
Figure 72: Island breaching along the southern portion of Cedar Island, Virginia in 1957 (Byrne et al. 1975). ....	168
Figure 73: Location of a possible emerging breach along the boundary of Cell 4 and Cell 5 on Cedar Island, Virginia in April 2010. The view is westward from the berm crest along the open-ocean shoreline toward the backbarrier bay and the town of Wachapreague, Virginia. ....	170
Figure 74: The Parramore–Cedar Barrier-Island System (1994). Note the opening of the Coast Guard breach along Cedar’s Cell 1 and Cedar Island breach along the bay-backed, open-ocean shoreline of Cedar’s Cell 4. USDA APFO, 1994.....	172
Figure 75: The Parramore–Cedar Barrier-Island System (2004). Note the closure of the Coast Guard breach to the north and the southerly migration, breach widening, and rotation of the throat of Cedar Island breach along Cell 4. USDA APFO, 1994.....	173
Figure 76: The Parramore–Cedar Barrier-Island System (2006). Note the continued closure of the Coast Guard breach along Cell 1 to the north and that the Cedar Island breach along Cell 4 is waning as breach filling begins. USDA APFO, 1994.....	174

Figure 77: The Parramore–Cedar Barrier-Island System (2008). Note the opening of the Coast Guard breach along Cell 1 and the closure of the Cedar breach along Cell 4 that occurred in April 2007. USDA APFO, 1994. ....	175
Figure 78: The Parramore–Cedar Barrier-Island System (2009). Note the continued closure of the Cedar Island breach along Cell 4 and the continuous area of washover along the marsh-backed portion of Cedar Island (Cell 3). USDA APFO, 1994. ....	176
Figure 79: The Parramore–Cedar Barrier-Island System (2011). Note the closure of the Coast Guard breach, the continued closure of the Cedar Island breach, and possibly an emerging breach in the southern spit shoreline (Cell 5). USDA APFO, 1994. ....	177
Figure 80: Histogram of all U.S. East Coast shoreline reversal dates over the long term (Fenster and Dolan, 1994). The average reversal date is 1967 and the modal reversal date is 1968. ....	179
Figure 81: Average long- and short-term retreat rates by section for Cedar Island (Nebel et al., 2012). ....	182
Figure 82: Low-oblique aerial photography of Cedar Island, Virginia on May 21, 2009 (top) and December 4, 2009 (bottom), roughly 2 weeks after Nor’Ida. Image provided by USGS St. Petersburg Coastal and Marine Science Center. The yellow arrows point to the same lo ....	187
Figure 83: Extensive outcropping and eroded pieces of relict marsh along the entire shore of Cedar Island's north-central, marsh-backed, open-ocean shoreline (Cell 3). ....	188
Figure 84: Massive amounts of dead trees along the foreshore of Parramore Island's north-central, open-ocean shoreline (Cell 3). The view is west toward Italian Ridge and the town of Wachapreague, Virginia. Note the high amount of tree die-off along the higher elevation dune ridges in the interior of Parramore Island, Virginia. ....	188
Figure 85: Stage 1 of the six-stage model of coastal change and barrier island system evolution. Stage one was >2000 years ago and displays the original shoreline, the absence of a recurved spit complex, and lack of an arc of erosion. ....	190
Figure 86: Stages of Holocene development of the large recurved spit complex at the southern end of Assateague Island, Virginia-MD (Goettle, 1981). ....	192
Figure 87: Stage 2 of the six-stage model of coastal change and barrier island system evolution. Stage 2 occurred 2000 to 500 years ago and reflects updrift sand trapping, the development of recurved spits, and an arc of erosion initiation. ....	193

Figure 88: Stage 3 of the six-stage model of coastal change and barrier island system evolution. Stage 3 occurred 500–200 years ago. The arc of erosion propagated southward as a series of stages in response to updrift sediment trapping at the large recurved spit complex at the southern end of Assateague Island, Virginia–Maryland. As it propagated southward, the arc of erosion enveloped Cedar Island by the 1850s (end of Stage 4) and enveloped Parramore by the 1950s (end of Stage 5). .....	196
Figure 89: Sparse remnants of the cedar maritime forest on the northern end of Cedar Island, Virginia in April 2010. USGS topographic sheets from the 1950s and 1960s illustrate 10 to 20 foot dune ridges and a fairly extensive forest (Gaunt, 1991).....	197
Figure 90: A thin sand veneer covers the breach closure area on Cedar Island's bay-backed, open-ocean shoreline. April 21, 2010.....	197
Figure 91: View is from beach looking west across the backbarrier marsh along the northern, marsh-backed, open-ocean shoreline (Cell 3) of Cedar Island, Virginia in April 2008. Note the position of the immobile red truck (upper left). .....	198
Figure 92: View is south along the berm crest of Cedar Island, Virginia during a GPS shoreline survey along Cell 3 in April 2010 (~2 years after the previous photo [Fig. 75]). The same red truck is now buried in sand on the active foreshore near the same general area of the previous photo. ....	198
Figure 93: Stage 4 of the six-stage model of coastal change and barrier-island system evolution. Stage 4 was 200 to 150 years before present and demonstrates morphodynamic changes of Cedar Island including the progressive southern extension of the large arc of erosion and transition from mixed-energy, tide-dominated barrier island to a mixed-energy, wave-dominated barrier island. Omega symbol ( $\Omega$ ) represents tidal prism. ....	199
Figure 94: Parramore Island circa 1976. Note the home of a caretaker along the backshore and the broad, extensive, and full tree canopy. Image provided by Stephen Leatherman. ....	201
Figure 95: Low oblique aerial photo of Parramore Island, Virginia taken on October 13, 2003. Note the dune ridge fronting the beach with an extensive stand of trees and vegetation with scattered fallen trees along the foreshore. The trees on Italian Ridge in the background have a full, healthy canopy.....	202
Figure 96: Low oblique aerial photo of Parramore Island, Virginia taken September 21, 2005. Note the area of trees and vegetation fronting the beach have experienced thinning and die-off. A number of dead trees are now apparent decreasing in number in a landward direction. ....	202



Figure 97: Low oblique aerial photo of Parramore Island, Virginia taken on November 28, 2009. Note the areas of overwash and salt marsh inundation with an absence of trees and vegetation fronting the beach. Dead trees are more extensive.....	203
Figure 98: Low oblique aerial photo of Parramore Island, Virginia taken on August 31, 2010. Note the extensive washover fans, large areas of salt marsh inundation fronting Italian Ridge, and rapid retreat of the shoreline.....	203
Figure 99: Stage 5 of the six-stage model of coastal change and barrier island system evolution. Stage 5 was 50 to 40 years before the present and demonstrates the morphodynamics changes of Parramore Island. The arc of erosion reaches Parramore Island and thus begins its transformation from a high-profile, regressive barrier island with a classic drumstick shape to a lower profile transgressive, mixed-energy, wave-dominated barrier island that has become more vulnerable to storm impacts. Omega symbol ( $\Omega$ ) represents tidal prism.....	204
Figure 100: Stage 6 of the six-stage model of coastal change and barrier island system evolution. Stage 6 projects 10–100 years into the future. Parramore Island evolves into a mixed-energy, wave-dominated barrier island and Cedar Island fragments into three segments. Wachapreague Inlet’s tidal prism increases and thereby enlarges the ebb-tidal delta and establishes a flood-tidal delta in the backbarrier bay, which further exacerbates sediment supply shortages by sequestering ever-larger sediment quantities on the inlet shoals. Omega symbol ( $\Omega$ ) represents tidal prism. ....	206
Figure 101: Vertical aerial photograph of Cedar, Parramore, and Hog Islands from the International Space Station, taken on April 16, 2008. ....	208

## LIST OF EQUATIONS

Equation	Page
Equation 1: O'Brien (1969) tidal prism and inlet area relationship.....	56
Equation 2: Jarrett (1976) tidal prism and inlet area relationship.....	57
Equation 3: Metric version of Jarrett (1976), unjettied or single-jettied inlets, inlets on the Atlantic coast. ....	60
Equation 4: Conversion of metric version of Jarrett (1976) unjettied or single-jettied inlets on the Atlantic coast to solve for tidal prism. ....	60
Equation 5: Seminack's equation for the calculation of cross-sectional area at natural unjettied inlets on the Atlantic coast. ....	61
Equation 6: Richardson–McBride–Seminack equation for the calculation of tidal prism in metric units based on cross-sectional area. ....	61
Equation 7: Walton and Adams (1976) equation for calculating outer bar/shoal sand storage volume with tidal prism volume.....	62
Equation 8: Walton and Adams's all inlets equation (English units). ....	62
Equation 9: Fontolan et al. (2007) conversion of Walton and Adams's (1976) all inlets equation (metric units). ....	63

## **ABSTRACT**

MORPHODYNAMIC CHANGES OF THE PARRAMORE-CEDAR BARRIER-ISLAND SYSTEM AND WACHAPREAGUE INLET, VIRGINIA FROM 1852 TO 2011: A MODEL OF BARRIER ISLAND AND TIDAL INLET EVOLUTION ALONG THE SOUTHERN DELMARVA PENINSULA, USA

Trent Michael Richardson, Ph.D.

George Mason University, 2012

Dissertation Director: Dr. Randolph A. McBride

This dissertation is a study of the shoreline and tidal inlet changes of the Parramore–Cedar barrier-island and Wachapreague tidal inlet system through the integration of a variety of geospatial data sets over a range of spatial and temporal scales. Fundamental changes to the historical trends of shoreline and tidal inlet behavior provide a means to quantitatively test the three-stage model of runaway transgression (Fitzgerald et al., 2004). The analysis of a robust set of shoreline data sets demonstrates the pattern of clockwise rotational instability over the long term as documented by Leatherman et al. (1982) has evolved into sustained rapid retreat along the entire outer shoreline of Parramore Island. In addition, Cedar Island has transitioned from in-place narrowing to rapid barrier rollover and landward migration through overwash and inlet processes. The non-inlet-influenced, open-ocean shoreline of Parramore Island experienced a -4.1 m/yr

retreat rate from 1852 to 1998 and a -12.2 m/yr retreat rate from 1998 to 2010, according to a linear regression analysis. Similarly, Cedar Island's non-inlet-influenced, open-ocean shoreline underwent a -5.5 m/yr retreat rate from 1852 to 2007 and a -15.4 m/yr retreat rate from 2007 to 2010, also according to a linear regression analysis. The short-term retreat rates for both islands are nearly triple the long-term rates. These increases in short-term retreat rates constitute a fundamental change in the pattern of historical shoreline movement for the Parramore–Cedar barrier-island system.

The cross-sectional area of an inlet throat is used as a proxy to calculate tidal prism and ebb-tidal delta volume of tidal inlets. The historical cross-sectional areas for Wachapreague Inlet were 1845 m<sup>2</sup> in 1852, 4473 m<sup>2</sup> in 1871, 4737 m<sup>2</sup> in 1911, 4572 m<sup>2</sup> in 1934, 4047 m<sup>2</sup> in 1972, 4398 m<sup>2</sup> in 2007, 4735 m<sup>2</sup> in 2010 (April), 5014 m<sup>2</sup> in 2010 (August), and 5210 m<sup>2</sup> in 2011. Tidal prism and ebb-tidal delta volumes at Wachapreague Inlet fluctuated from 1871 to 2011 with tidal prism ranging between  $4.82 \times 10^7$  m<sup>3</sup> and  $6.09 \times 10^7$  m<sup>3</sup> and ebb-tidal delta volumes ranging between  $1.85 \times 10^7$  m<sup>3</sup> and  $2.46 \times 10^7$  m<sup>3</sup>. From 1871 to 2007, the long-term linear regression rates of change were -2.4 m<sup>2</sup>/yr for cross-sectional area,  $-2.67 \times 10^4$  m<sup>3</sup>/yr for tidal prism, and -1.26 m<sup>3</sup>/yr for ebb-tidal delta volume. However, from 2007 to 2011, the short-term linear regression rates of change switched to high rates of increase with 186.1 m<sup>2</sup>/yr for cross-sectional area,  $2.04 \times 10^6$  m<sup>3</sup>/yr for tidal prism, and  $9.89 \times 10^5$  m<sup>3</sup>/yr for ebb-tidal delta volume. Overall, from 1871 to 2007, cross-sectional area, tidal prism, and ebb-tidal delta volumes were characterized by relative stability to a slight decrease with a distinct increase more recently (2007–2011). This research accounts for the natural variability in tidal prism on

a monthly basis (e.g., neap vs. spring tides, perigee vs. apogee) and a seasonal basis (e.g., potential coastal setup caused by meteorological events, thermal expansion of the water column [steric effect]) by utilizing a 15% natural variability in the tidal-inlet analyses as documented by O'Brien (1969).

These spatial analyses provide insight into how shoreline and bathymetric changes of the Parramore–Cedar barrier-island system are driven by 1) the southern extension of the large arc of erosion located south of Assateague Island in response to sediment trapping at the large recurved spit complex at Fishing Point, Virginia; 2) relative sea level rise along the southern Delmarva Peninsula; 3) updrift barrier-island breaching north of Wachapreague Inlet along Cedar Island and other breaches further north; and 4) increased storminess along the outer barrier islands of the Virginia Eastern Shore. Of these four coastal-change drivers, the southern propagation of the large arc of erosion (i.e., lack of sediment supply) appears to be the primary driver of coastal evolution along the Parramore-Cedar barrier-island system for the past 150 years and potentially for the next 10 to 100 years into the future. Furthermore, this research presents a six-stage model of barrier evolution along the southern Delmarva Peninsula. The six-stage model accounts for changes in sediment supply, relative sea level rise, increased storminess, and the projected consequences to the Parramore–Cedar barrier-island system. The significance of short-term shoreline and bathymetric changes that depart from historical trends is important because these developments may indicate wider patterns of barrier-island change for the entire Virginia Eastern Shore and, perhaps, large expanses of mixed-energy coasts along the entire U.S. Atlantic seaboard.

## **CHAPTER ONE: INTRODUCTION**

### **Statement of the Problem**

The Virginia barrier islands along the southern Delmarva Peninsula exist in a natural state and the effects of sustained human activities upon this coastal environment are largely absent. These circumstances make the area uniquely suited to study the natural oceanographic and geologic processes operating along this coastline without the statistical noise of anthropogenic influences. Moreover, recent studies indicate certain barrier islands along the Virginia Eastern Shore—such as Parramore and Cedar Islands—are experiencing a fundamental adjustment in their pattern of historical shoreline movement (Gaunt, 1991; Richardson & McBride, 2007; Richardson & McBride, 2011; Nebel et al., 2012).

The average erosion rate for the U.S. mid-Atlantic shoreline is between -0.5 and -1.5 m/yr (Dolan et al., 1979; Hapke et al., 2011). In contrast, non-inlet-influenced, open-ocean shorelines of the Parramore–Cedar Island barrier-island system have experienced long-term retreat rates an order of magnitude greater than the average background rate of the U.S. mid-Atlantic coast (Gaunt, 1991; Richardson & McBride, 2007; Richardson & McBride, 2011; Nebel et al., 2012). As a result, these barrier-island shorelines along the southern Delmarva Peninsula stand out as having some of the highest long-term retreat rates along the U.S. mid-Atlantic seaboard. Examining why the southern Delmarva

Peninsula deviates from the average behavior of the U.S. mid-Atlantic coast could provide further insight on why substantial portions of U.S. Atlantic shorelines do not recede at consistent rates over long time periods (Fenster & Dolan, 1994).

The Intergovernmental Panel on Climate Change (IPCC) (2007) reports the global average sea level rose 1.8 mm per year from 1961 to 2003 and up to 3.1 mm per year from 1993 to 2003. The IPCC estimates eustatic sea level will continue to rise between 0.18 and 0.59 m by the end of the 21<sup>st</sup> century. A rise in relative sea level along the U.S. mid-Atlantic coast during the Holocene epoch is a well-documented phenomenon, and rates are projected to increase throughout the 21<sup>st</sup> century (Zervas, 2001; Engelhart et al., 2011). The rate of relative sea-level rise along the southern Delmarva Peninsula ranges from 3.5 mm/yr (1951–2006) at the southern end of the peninsula (Kiptopeke, Virginia) to 5.5 mm/yr (1975–2006) at Ocean City, Maryland (NOAA, 2009).

Leatherman et al. (2000), Leatherman and Douglas (2003), and Zhang et al. (2004) reach the conclusion that a rise in relative sea level is the primary cause of coastal erosion along the U.S. Atlantic coast, and in fact, they minimize the influence of storms upon these coastlines throughout the 20<sup>th</sup> century. However, Zhang et al. (2004) does not include transects of nearly the entire Virginia Eastern Shore in their analysis of the relationship between sea-level rise and beach erosion. In contrast, Fenster and Dolan (1994) conclude that nearly two thirds of the U.S. East Coast shorelines underwent a significant change in the long-term rates of change during the 1960s. Fenster and Dolan (1994) link this adjustment in the long-term rate of shoreline change to a peak in extratropical storm frequency and magnitude that occurred around 1967 or 1968. In

addition, Fenster et al. (2001) demonstrate the frequency and magnitude of storms can influence long-term shoreline changes.

Curry (1964), Morton (1979), and Kraft and Chrzastowski (1985) documented the critical role of sediment supply, a primary factor in driving the landward or seaward migration of barrier islands. Interruptions or fundamental changes in updrift sediment supply affect downdrift islands and may outweigh the effects of relative sea-level rise. It is notable that Cedar Island resides within the large arc of erosion south of Fishing Point, Virginia (Rice and Leatherman, 1983). Sand trapping at the recurved spit complex at the southern end of Assateague Island has captured large quantities of sediment from the regional sediment budget. The spit's growth has resulted in downdrift sediment starvation that over time has resulted in a decreased sediment supply moving from north to south, as discussed by Wikel (2008).

The changes to the Parramore–Cedar barrier-island system are clearly and immediately evident through observing numerous qualitative factors. Particularly striking are the considerable tree die-offs along the backshore and further inland along the interior dune ridges of Parramore Island (Figures 1–4). In fact, the impacts are most noticeable along historically stable portions of Parramore Island's open-ocean shoreline. These eco-geomorphic impacts to the maritime forest of Parramore Island are presumably the result of rapid rates of shoreline retreat with an increase in saltwater intrusion and the landward penetration of salt spray into relict dune ridges from an encroaching ocean (Figure 5). In addition, a lightning strike caused a natural fire on Parramore Island on September 1, 2002 that burned approximately 1,200 acres or 1/3 of the island (Harper, 2002).



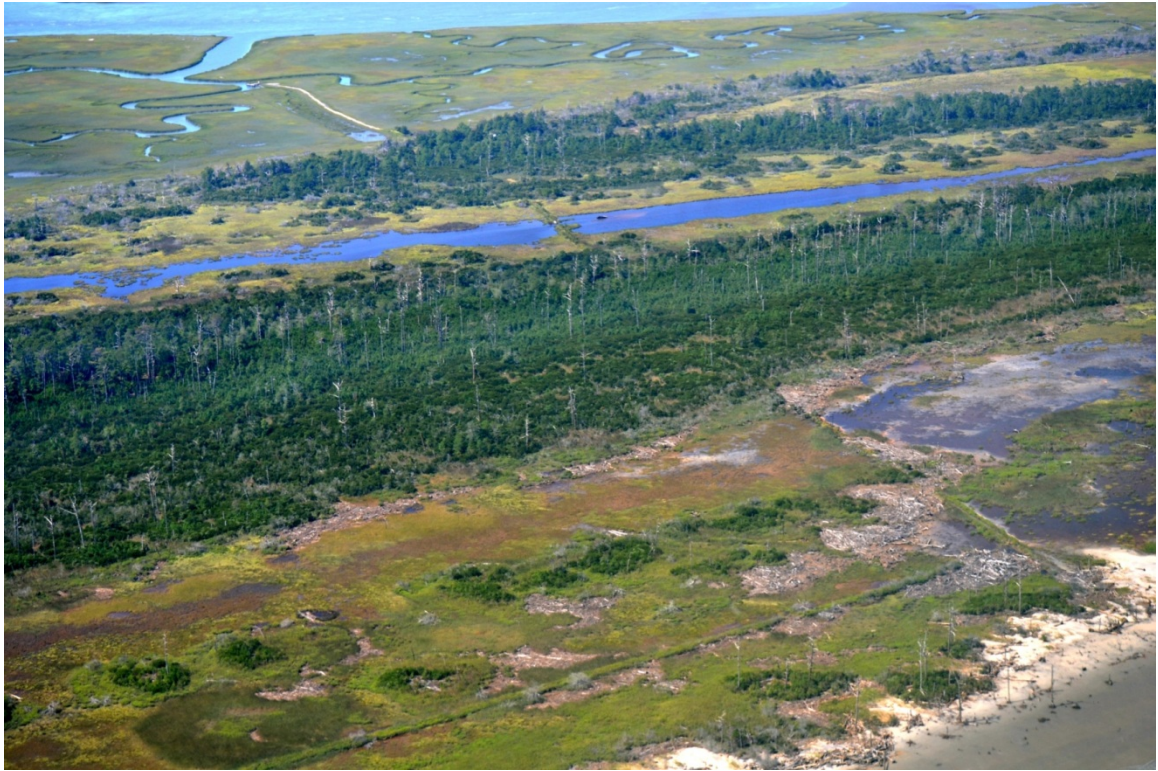


**Figure 1: Extensive tree die-offs strewn along the foreshore of the north-central, non-inlet-influenced, open-ocean shoreline of Parramore Island, April 27, 2006.**



**Figure 2: Maritime forest impacts at the transition zone between the southern, washover-dominated, open-ocean shoreline and the north-central, non-inlet influenced, open-ocean shoreline of Parramore Island, April 27, 2007.**





**Figure 3: Nearly complete elimination of the maritime forest along the backshore of the north-central, non-inlet-influenced, open-ocean shoreline of Parramore Island, August 31, 2011. Note the dead trees (snags) along the interior relict dune ridges (i.e., Italian Ridge). Image provided by Randolph A. McBride.**



**Figure 4: Northern extent of widespread tree die-offs at the transition zone between the north-central, non-inlet-influenced, open-ocean shoreline and the northern, inlet-influenced shoreline, April 22, 2010. Note the large number of dead trees in the interior of Parramore Island.**



**Figure 5: Ecogeomorphic changes (e.g., tree die-offs) because of the intrusion of saltwater spray along Italian Ridge (a relict dune) of Parramore Island, April 22, 2010. Note the interspersing of dead trees among the remnants of the living trees in the distance.**

Additional qualitative factors provide evidence of the rapid and ongoing changes to the Parramore–Cedar barrier-island system. These include expansive areas of relict marsh outcropping along the foreshore of both Parramore and Cedar Islands, especially long stretches along the foreshore of Cedar Island (Figures 6 and 7). In addition, large washover fans are commonplace on both Parramore and Cedar Islands (Figures 8 and 9). Cedar Island is experiencing expansive areas of washover onto backbarrier marsh along its open ocean shoreline and this behavior is indicative of rapid rates of shoreline retreat. Furthermore, Cedar Island is impacted by episodes of island breaching along two distinct areas, and this development leads one to conclude that Cedar Island is in the process of fragmenting into smaller and thinner remnants (Figures 10 and 11).





**Figure 6: Relict marsh outcropping along the foreshore of the southern, washover-dominated, open-ocean shoreline of Parramore Island, April 27, 2007.**



**Figure 7: Relict marsh outcropping along the foreshore of the southern, bay-backed, open-ocean shoreline of Cedar Island, April 25, 2008.**



**Figure 8: Large washover fan and exposed relict marsh along the northern, non-inlet-influenced, open-ocean shoreline of Cedar Island, April 21, 2010.**



**Figure 9: Large washover fan, exposed relict marsh, and extensive foreshore along the southern, washover-dominated shoreline of Parramore Island, April 22, 2010.**





**Figure 10: Location of the most recent Cedar breach that closed in the spring of 2007 along the south-central, bay-backed, open-ocean shoreline. Photo taken August 31, 2011 by Randolph A. McBride.**



**Figure 11: The “Coast Guard” breach along the northern inlet- and breach-influenced shorelines of Cedar Island, April 21, 2010.**

This dissertation will analyze shoreline and tidal inlet changes along the Parramore–Cedar barrier-island and Wachapreague tidal inlet system in order to test Fitzgerald et al.'s (2004) three-stage conceptual model of sand trapping processes at tidal inlets and the long-term response of barrier islands to a diminished sediment supply in a regimen of accelerated sea-level rise (Figure 12). The Fitzgerald et al. (2004) conceptual model is applicable to mixed-energy coasts (such as those along the Virginia Eastern Shore) that are characterized by short, stubby barrier islands, numerous tidal inlets, well-developed ebb-tidal deltas, and backbarrier marsh. The model accounts for the transformation of backbarrier salt marsh to open water and intertidal environments and an associated increase in tidal prism (i.e., the volume of water moving in or out of an inlet during a tidal cycle) between the ocean and estuary in a regimen of accelerated sea-level rise. Essentially, the backbarrier salt marsh is incapable of accreting vertically at the same rate as the rate of relative sea-level rise and thus cannot maintain its areal extent. The progressive decline in salt marsh area enlarges bay area and increases tidal range, the two fundamental variables in the determination of tidal prism. Tidal range in the backbarrier region may increase as salt marsh converts to open water (Fitzgerald et al., 2008). This increase in tidal prism leads to a widening and deepening of the tidal inlet and the growth in both the ebb- and flood-tidal deltas.

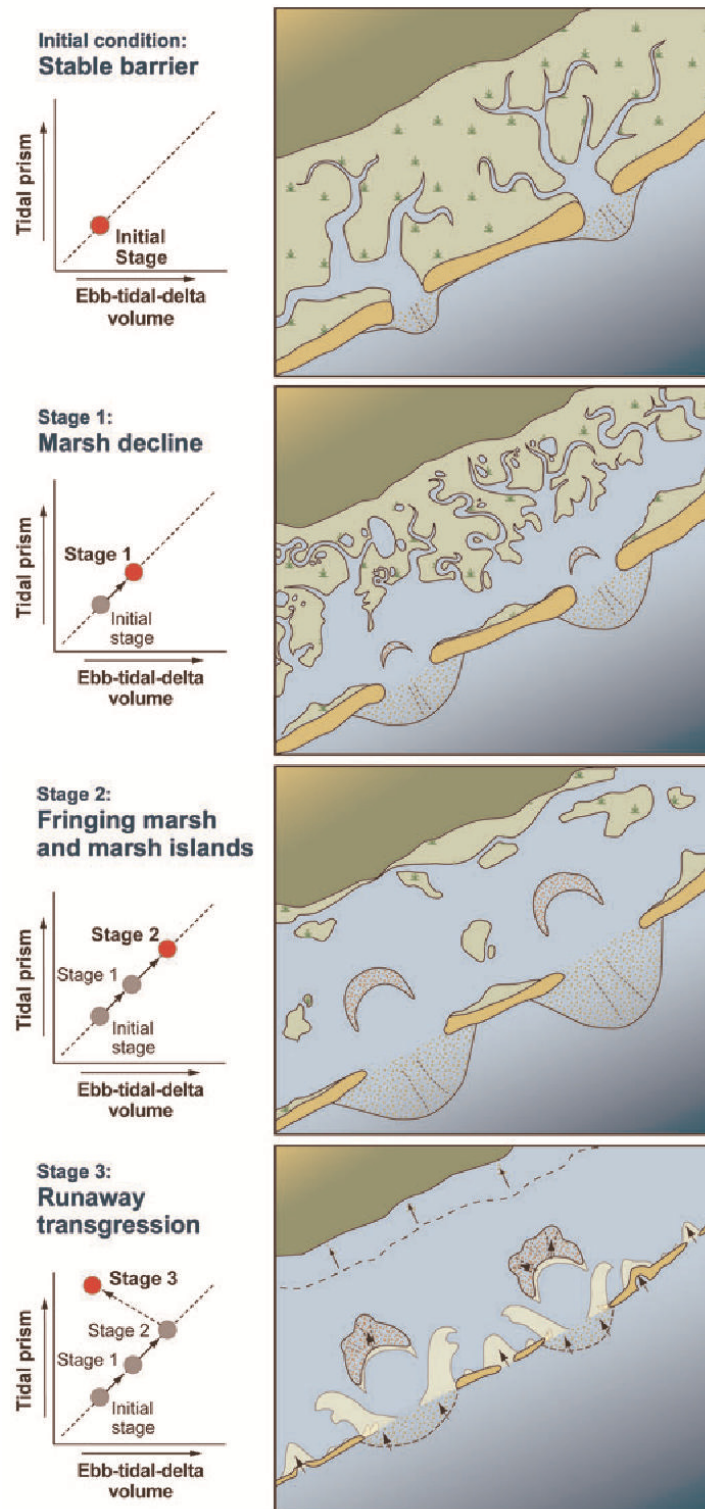


Figure 12: Three-stage model of runaway transgression (Fitzgerald et al., 2004).



The stages of the Fitzgerald et al. (2004) conceptual model include the initial phase of a stable barrier, followed by 1) marsh decline, 2) fringing marsh and marsh islands, and 3) runaway transgression (Figure 12). The initial stable barrier stage is represented as the present or past general configuration of mixed-energy coasts characterized by barrier islands backed with an expansive estuarine marsh system and a network of tidal creeks. Stage 1 is a period in which an accelerated rise in relative sea level converts portions of the estuarine marsh to intertidal and subtidal environments. This transformation increases tidal prism that scours tidal creeks further, enlarges the tidal inlet, and sequesters more sand on the ebb tidal delta. In Stage 2 large expanses of estuarine marsh areas are in rapid decline and increased tidal prism continues to enlarge tidal inlet size and ebb-tidal delta volume. In addition, the inlet hydraulics now favor flood dominance with flood tidal current transporting sand in a net landward direction because of the absence of natural sand flushing by ebb currents. The adjacent barriers thin and breach and new ephemeral and permanent tidal inlets emerge. In Stage 3 (runaway transgression) many new tidal inlets and island breaches develop, the antecedent tidal inlets drown, and barrier-island rollover is an active process during moderate to severe storms. The collapse of ebb-tidal deltas onshore is a result of the multiple new inlets that capture and reduce tidal prism at the former large inlets. This sand reworking from the ebb-tidal deltas temporarily nourishes the drowning barriers. Finally, the mainland suffers from encroaching tidal waters and coastal flooding.

During a sustained regimen of relative sea-level rise, backbarrier marsh is transformed to open water through channel deepening and marsh inundation. This

conversion of the estuarine marsh to open water results in an increased tidal prism. In response, increased tidal prism widens and deepens the tidal inlet through channel scour. In addition, increased tidal prism causes progradation of the ebb-tidal delta and the expansion and retrogradation of the flood-tidal delta. This seaward advance of the ebb-tidal delta results in the sand body capturing more longshore sediment transport and the ever-larger sediment sequestration on the ebb- and flood-tidal deltas. The increased sand capture by the ebb-tidal delta results in barrier degradation because of downdrift sediment starvation (Miner et al., 2007). Consequently, ebb-tidal delta growth diminishes sediment supply along the coast and this leads to barrier starvation, barrier-island fragmentation, onshore migration, and evolution to a transgressive coastal system.

## **Research Questions**

A spatial and temporal analysis of the long-term and short-term shoreline change rates of Parramore and Cedar Islands and the analysis of trends in cross-sectional area at the inlet throat of Wachapreague Inlet may answer a number of queries pertaining to the behavior of the Parramore–Cedar barrier-island system. Specific questions posed are as follows:

- Are the qualitative changes to the Parramore–Cedar barrier-island system observed over the past 15 years explained by the three-stage Runaway Transgression model of FitzGerald et al. (2004)?
- What are the magnitude, direction, and change rates of the outer shorelines of Parramore and Cedar Islands over a range of temporal scales?

- What are the retreat or advance rates of specific geomorphic zones (i.e., shoreline cells), and how do the long-term rates compare to short-term rates?
- What are the changes in cross-sectional area at the inlet throat at Wachapreague Inlet over the historical period of record, and how do the long-term rates compare to the short-term rates?
- Have tidal prism and ebb-tidal delta volumes increased, decreased, or remained fairly stable at Wachapreague Inlet across a range of temporal scales?
- Has the Parramore–Cedar barrier-island system entered the initial stages of the Fitzgerald et al. (2004) three-stage model of runaway transgression?
- What are the primary drivers of change to the Parramore–Cedar barrier-island system, and what's the relative influence of the various individual drivers?
- Has the large arc of erosion south of Assateague Island, Virginia (Fishing Point) extended further southward, and is it now affecting Parramore Island?
- How does storminess affect the current state of the Parramore–Cedar barrier-island system?

## **Multiple Working Hypotheses**

The multiple working hypotheses of this study are based on examining the potential drivers of change to the Parramore–Cedar barrier-island system and developing a model of barrier evolution along the southern Delmarva Peninsula. Coastal processes are not mutually exclusive, but the null and alternative hypotheses are designed to parse out cause and effect with respect to longer- and shorter-term processes and responses.

The following three working hypotheses are intended to help explain the long-term versus short-term changes of the Parramore–Cedar barrier-island system:

1. The Parramore–Cedar barrier-island system is in a state of equilibrium characterized by shoreline change rates that do not depart from historical trends. The tidal prisms and ebb-tidal delta sand volumes at Wachapreague Inlet are consistent throughout the period of record (1852–2011). The stability of the barrier-island system can be attributed to steady and adequate rates of longshore sediment transport from updrift sources and non-fluctuating tidal prism at Wachapreague Inlet. This system behavior would also indicate the Parramore–Cedar barrier-island system is not acutely affected by relative sea-level rise and/or sediment supply fluctuations and is not affected significantly by storm impacts.
2. The Parramore–Cedar barrier islands are experiencing an adjustment in their historical pattern of shoreline movement, whereas the Wachapreague Inlet complex has maintained consistent tidal prism and ebb-tidal delta volumes. The behavior of the system could be explained by the southerly extension of the long arc of erosion south of Assateague Island, updrift island breaching at Cedar Island, and/or an increase in the magnitude and frequency of storm activity. Stable tidal prism values at Wachapreague Inlet indicate the system is not affected by a rise in relative sea level.
3. The Parramore–Cedar barrier-island system is experiencing a fundamental shift in coastal change trends and barrier evolution and an increase in tidal prism with an enlarging ebb-tidal delta at Wachapreague Inlet. The rapid retreat of the barrier

island shorelines and the increase in tidal prism could be attributed to a reduction in net sediment supply (e.g., a southern extension of the large arc of erosion south of Assateague Island) and amplification in tidal prism because of a rise in relative sea level. These results indicate the Parramore–Cedar barrier-island system has potentially entered the initial stages of the three-stage model of runaway transgression and is also affected by increased storm frequency and/or storm magnitude.

## **Overall Goal and Scientific Objectives**

The overall goal of this research is to determine if the Parramore–Cedar barrier-island and Wachapreague tidal inlet system have entered into the initial stage of the three-stage model of runaway transgression proposed by Fitzgerald et al. (2004). This research attempts to accomplish this goal by examining the historical movement of shoreline positions along Parramore and Cedar Islands and the analysis of the changes in tidal prism and ebb-tidal delta volume at Wachapreague Inlet. The results and conclusions of this study provide information to propose a conceptual model of barrier-island evolution along the southern Delmarva Peninsula.

This research addresses the coastal morphodynamics of the Parramore–Cedar barrier-island system and Wachapreague Inlet, Virginia. The three primary objectives of this study are as follows:

1. Quantify the rate, magnitude, and direction of shoreline change along Parramore and Cedar Islands across a range of temporal scales (long term and short term) and geomorphic zones (i.e. shoreline cells).

2. Quantify the cross-sectional area of Wachapreague Inlet over the historical period of record and determine if tidal prism and ebb-tidal volumes at Wachapreague Inlet are stable, increasing, or decreasing over the long term and short term.
3. Test the three-stage model of runaway transgression (Fitzgerald et al., 2004) by relating changes to the Parramore–Cedar barrier-island and Wachapreague tidal inlet system to the characteristics or predicted behaviors of the individual stages of the three-stage model of runaway transgression.

## **Scope of the Study**

This dissertation presents a study on the coastal change and barrier evolution of the Parramore–Cedar barrier-island and Wachapreague tidal inlet system. *Chapter Two* details the regional setting including the geology of the southern Delmarva Peninsula, the coastal geomorphology of the Virginia Eastern Shore, and the coastal processes operating along the Parramore–Cedar barrier-island system. *Chapter Three* presents the shoreline and bathymetric data sets utilized in this research including a review of data sources, selection of proxies, overviews of the various technologies utilized, an accuracy assessment of the data sets, and a summary of methodologies including the statistical methods employed in the various analyses. *Chapter Four* is a literature review of related studies and concepts relevant to this research including barrier island formation and system dynamics, the importance of tidal inlets and sediment supply to the behavior of barrier-island systems, and a review of the potential drivers of change to these systems. *Chapter Five* presents the results of the shoreline data analysis of Parramore and Cedar Islands through the comparison of long-term and short-term shoreline change rates by

geomorphic zones and various temporal scales using a host of statistical measurements.

The cross-sectional area, tidal prism, and ebb-tidal delta volumes at Wachapreague Inlet are also analyzed across a range of temporal scales. The results chapter concludes with a testing of the Fitzgerald et al. (2004) three-stage model of “runaway transgression.”

*Chapter Six* is a discussion of the changes to the Parramore–Cedar barrier-island system, an examination of the primary drivers of change to the system, and the presentation of a model of barrier-island evolution for the Parramore–Cedar barrier-island system. The six-stage model of barrier-island evolution along the southern Delmarva Peninsula synthesizes how the overall coastal depositional system has operated in the past and also draws conclusions on the future of the Parramore–Cedar barrier-island system. *Chapter Seven* summarizes the purpose of the study, presents the conclusions of the findings of the study, and makes recommendations for future research.

## **CHAPTER TWO: REGIONAL SETTING**

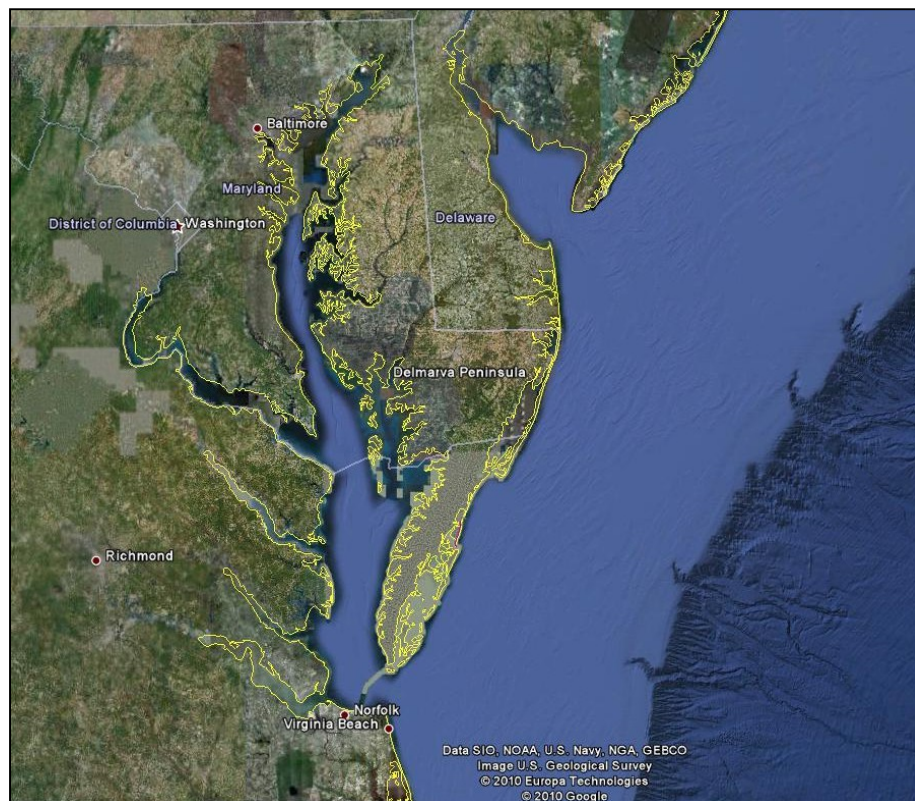
### **Geology of the Southern Delmarva Peninsula**

The Delmarva Peninsula is large and resides within the Atlantic coastal plain found along the mid-Atlantic bight of the eastern United States. The Delaware Bay is to its northeast, the Chesapeake Bay to its west, the Atlantic Ocean to its east, and the mouth of the Chesapeake Bay to its south (Figure 13). The peninsula intersects the areas of three states—Delaware, Maryland, and Virginia—thereby providing its name. The peninsula along its Atlantic coastline is fronted by a relatively wide and flat outer continental shelf. The U.S. Atlantic east coast is an Amero-trailing edge coastline characterized by large drainage systems and substantial sediment supplies that have produced extensive barrier-island systems (Inman & Nordstrom, 1971; Glaeser, 1978). Precursors of the Delmarva barrier islands formed in the late Pleistocene and were located much further eastward (Field & Duane, 1976).

The geology of the Delmarva barrier islands and backbarrier estuaries is strongly influenced by the inherited coastal plain physiography resulting from Pleistocene sea-level change over the past million years (Demarest & Leatherman, 1985). The antecedent topography of the area is overwhelmingly erosional in nature with substantial quantities of unconsolidated or poorly consolidated sediments nourishing the pre-Holocene Delaware River and Chesapeake Bay during the last low stand in sea level (Morton &



Donaldson, 1973; Rice et al. 1976; Belknap & Kraft, 1985). The Delmarva Peninsula's geography is characterized by gently rolling valleys and interfluvies that are primarily Holocene and Pleistocene with elevations ranging from 24 m above sea level in the north-central portion of Delmarva to a near-maximum of 9 m below present sea level over large areas of submerged lowlands in the nearshore environment (Byrnes, 1988). As stated in the Introduction, along the southern Delmarva Peninsula relative sea-level rise ranges from 3.5 mm/yr (1951–2006) at the southern end of the peninsula (Kiptopeke, Virginia) to 5.5 mm/yr (1975–2006) at Ocean City, Maryland (NOAA, 2009).



**Figure 13: The Delmarva Peninsula with Delaware Bay to the north, Chesapeake Bay to the west, and the mouth of the Chesapeake Bay to the south (image from Google Earth, July 2010).**

## **Coastal Geomorphology**

Oertel and Kraft (1994) summarized the coastal geomorphology of the Delmarva Peninsula into four segments moving from north to south: 1) a cusped spit, 2) an eroding headland, 3) barrier spits and long linear barrier islands (wave-dominated barrier islands), and 4) short barrier islands with many inlets (tide-dominated barrier islands). The Virginia section of the Delmarva Peninsula is segmented into two of these major components (wave-dominated barriers and tide-dominated barriers) (Figure 14). The northerly component of the Virginia barrier-island system comprises the long Assateague Island wave-dominated barrier system that terminates at Chincoteague Inlet. A second southerly component is composed of short, stubby, tide-dominated and mixed-energy barrier islands that are separated by numerous tidal inlets. Within this southern compartment the barrier islands are further segmented into the northerly shorelines along a large arc of erosion (Wallops, Assawoman, Metompkin, and Cedar Islands), a middle transitional section exhibiting historical clockwise rotational instability (Parramore, Hog, and Cobb Islands), and a southerly sector with higher levels of tidal influence (Wreck, Ship Shoal, Myrtle, Smith, and Fisherman Islands) (Leatherman et al, 1982).

Along the northern portion of the southern Delmarva Peninsula, Assateague Island is separated from the mainland by Chincoteague Bay and a large compound spit at its southern terminus that serves as a major sediment sink (Goettle, 1981). The barriers southward of the compound spit are characterized by extensive backbarrier estuaries with a network of tidal channels, tidal marshes, and mud flats. These barriers primarily consist of fine-grained sand and frequently experience overwash during storms (Rice et al.,

1976). The linear mainland shoreline landward of the backbarrier lagoon abuts the Pleistocene shoreface that formed 60,000 BP (Demarest & Leatherman, 1985) throughout the entirety of the Delmarva Peninsula (Figure 15).

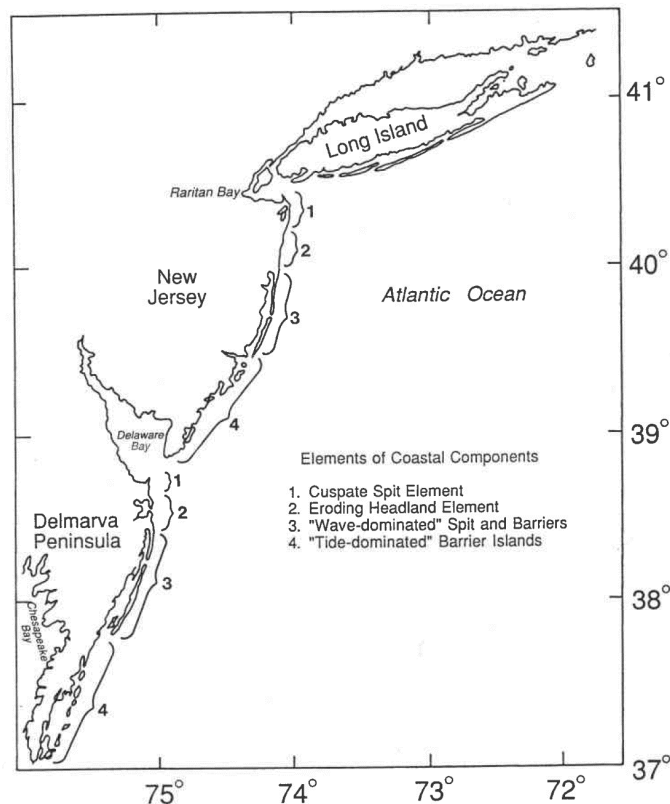
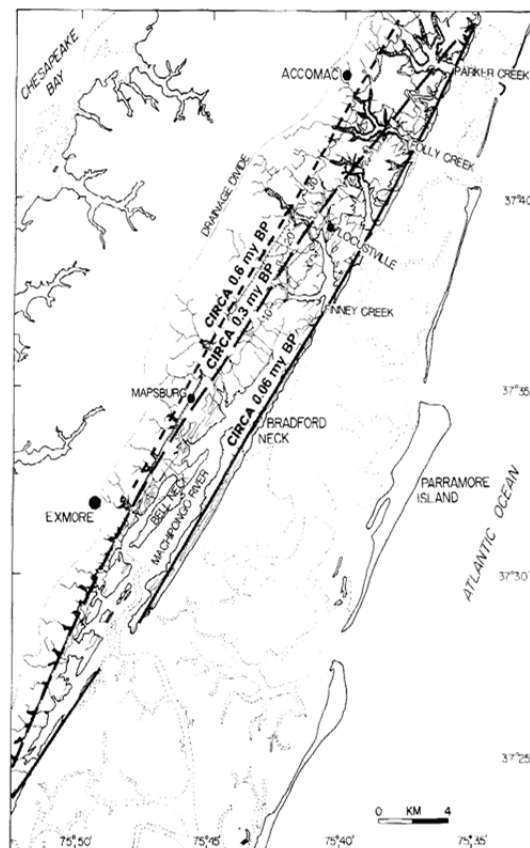


Figure 14: Landscape elements of the New Jersey and Delmarva coastal components (Oertel and Kraft, 1994).

The Holocene barrier-island systems of the Delmarva most likely formed 5,000 to 7,000 years B.P., but the modern landscape features formed within the past several centuries (Oertel & Kraft, 1994). Significant levels of freshwater drainage and corresponding sediment transport into the coastal environment are almost entirely absent from the eastern Delmarva Peninsula. The erosion of headlands and the transport of Holocene and Pleistocene shoreface sediments are the only sediment sources for the

barrier islands (Kraft et al., 1973; Swift, 1975; Belknap & Kraft, 1985). As a result, the primary source of sediment supply feeding the barrier islands system results from net longshore sediment transport along the shoreface. Demarest and Leatherman (1985) postulate that with contemporary transgression rates the barrier islands will continue to migrate landward, estuaries will narrow, wetlands will decrease in area, and the Holocene barrier-island system will eventually fuse to the relict Pleistocene shoreface.



**Figure 15: Pleistocene and Holocene barrier configurations in the Virginia sector of the Delmarva Peninsula (Demarest and Leatherman, 1985).**

The major tidal inlets of the Virginia barrier-island system correspond with the topographic lows of the Pleistocene surface (Morton & Donaldson, 1973). The drumstick shape of the short, stubby, mixed-energy barriers is primarily a function of inlet stability and the local longshore sediment transport reversals because of wave refraction around the ebb-tidal delta. Active and historical inlet information was compiled by McBride (1999) and documented how the spatial and temporal distribution of tidal inlets affects barrier island processes and shoreline evolution along the Delmarva Peninsula. McBride (1999) demonstrated that tides and waves are critical factors controlling inlet behavior, distribution, and density, and he expanded on Fitzgerald (1982) regarding the distribution of barrier island/spit lengths to tidal range and wave height (Figure 16).

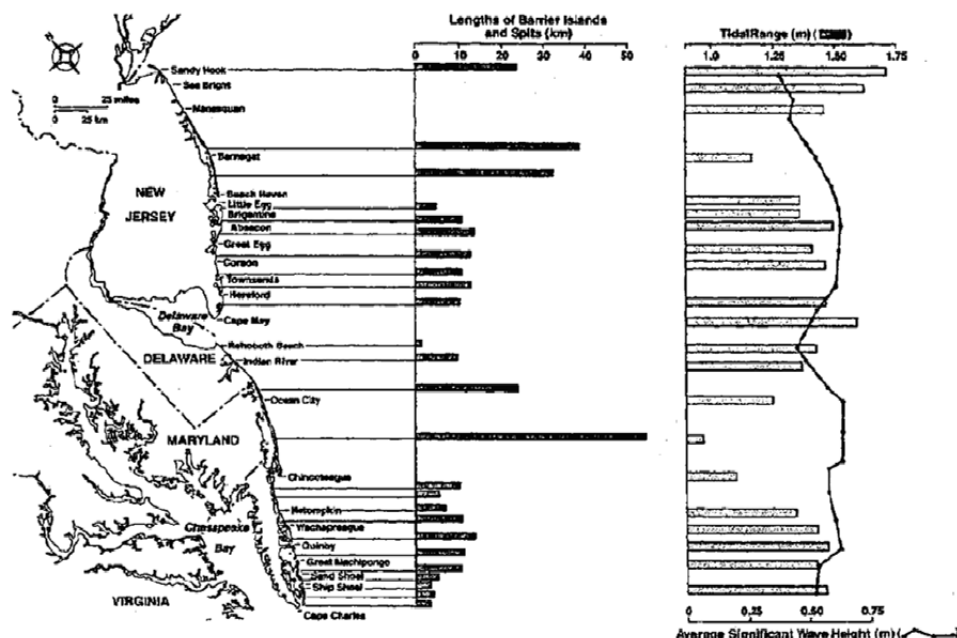


Figure 16: Distribution of barrier island/spit lengths, tidal range, and wave height (McBride, 1999), modified from Fitzgerald (1982).

## **Coastal Processes**

The unconsolidated sandy sediments of the Virginia barrier islands are primarily transported by waves, tides, and wind. In addition, the Virginia coastal zone is also affected by relative sea-level rise and sediment supply. The U.S. Atlantic coast experiences unequal semi-diurnal tides. The tide level along the Virginia barrier islands is classified as low mesotidal with an average spring tidal range of 1.7 m (McBride, 1999). The estuaries of the Virginia barrier islands have tidal ranges nearly equivalent to ocean tides with a lag time of approximately 15 minutes (Oertel & Kraft, 1994). The system experiences moderate wave energy with an average significant wave height of 0.6 m (McBride, 1999). Waves are typically from the southeast during the summer and from the northeast during the winter. Net longshore sediment transport is to the south because of seasonal weather systems that move an average of 160,000 m<sup>3</sup> of sand per year (Byrnes, 1988; Oertel & Kraft, 1994).

The Delmarva coast is affected by two distinct weather system patterns during the course of a year. The most frequent systems are low-pressure, anticyclone cold fronts (i.e., northeasters) that occur from the fall to the spring and less frequent are the cyclone tropical systems that move into the region from the south during the summer and early fall months. These weather systems can generate substantial short-term changes to the shorelines of the Virginia barrier islands, but typically northeasters have the most significant impacts because they are higher in frequency and larger in magnitude (Davis & Fox, 1974; Davis et al., 1993; Zhang et al., 2002). The storm waves generated by a

northeaster move in a southerly direction and produce strong south-flowing longshore currents that can move large quantities of sediment.

## **Area of Investigation**

The Parramore–Cedar barrier-island system is located mid-way between southern Assateague Island and the mouth of the Chesapeake Bay along the Virginia Eastern Shore of the Delmarva Peninsula (Figure 17). Parramore and Cedar Islands are two of fourteen undeveloped barrier islands constituting The Nature Conservancy’s “Virginia Coast Reserve” (Figure 18). The reserve is intended to protect coastal wilderness including thousands of acres of salt marshes, tidal mudflats, shallow bays, and forested uplands (The Nature Conservancy, 2010). In addition, the islands provide habitat for more than 250 species of raptors, songbirds, and shorebirds. The reserve is the longest expanse of coastal wilderness remaining on the eastern seaboard of the United States.

## **Parramore Island**

Parramore Island is the largest island of the Virginia Coast Reserve and is considered its crown jewel. The island is an undeveloped, mixed-energy, tide-dominated barrier island with a classic “drumstick” shape. Large ebb-tidal deltas characterize the tidal inlets at either end at Wachapreague and Quinby Inlets. Parramore Island’s outer shoreline is approximately 12.7 km in length and may be segmented into three primary geomorphic zones: 1) the high-profile, inlet-influenced northern end; 2) the north-central segment characterized by the truncation of high-profile, tree-lined beach ridges; and 3) the southern portion, which is a low-profile, washover-dominated barrier and barrier spit

(a more thorough description of Parramore's geomorphic zones will follow in the Methods chapter). Wachapreague Inlet and Cedar Island are to the north and Quinby Inlet and Hog Island are to the south. In recent years, the open-ocean shoreline of Parramore Island has retreated at a rapid rate as indicated by numerous qualitative factors, such as massive tree die-offs along interior dune ridges, extensive numbers of fallen trees across the foreshore, outcropping of relict marsh along the beachface, and exposure of a historical shipwreck on the beach.

### **Cedar Island**

Cedar Island lies directly north of Parramore Island. Although primarily owned by The Nature Conservancy, it does contain a few privately owned land parcels and dwellings and land parcels controlled by the U.S. Fish and Wildlife Service. Cedar Island was previously developed for vacation homes, but rapid rates of shoreline retreat eventually forced these owners to abandon their property and homes. Cedar Island is 10.8 km in length with an average width of 191 m (Gaunt, 1991). It is characterized as low profile (highest elevations approaching 3 m) with few dunes and is washover dominated (Gaunt, 1991). Although mean spring tidal range is 1.7 m, the morphology of Cedar Island reflects a mixed-energy, wave-dominated barrier island. In addition, the northern two thirds of the island are backed by estuarine wetlands, whereas the southern third is primarily backed by open water. Remnant cedar and pine forest have been nearly eliminated by island retreat and washover processes.



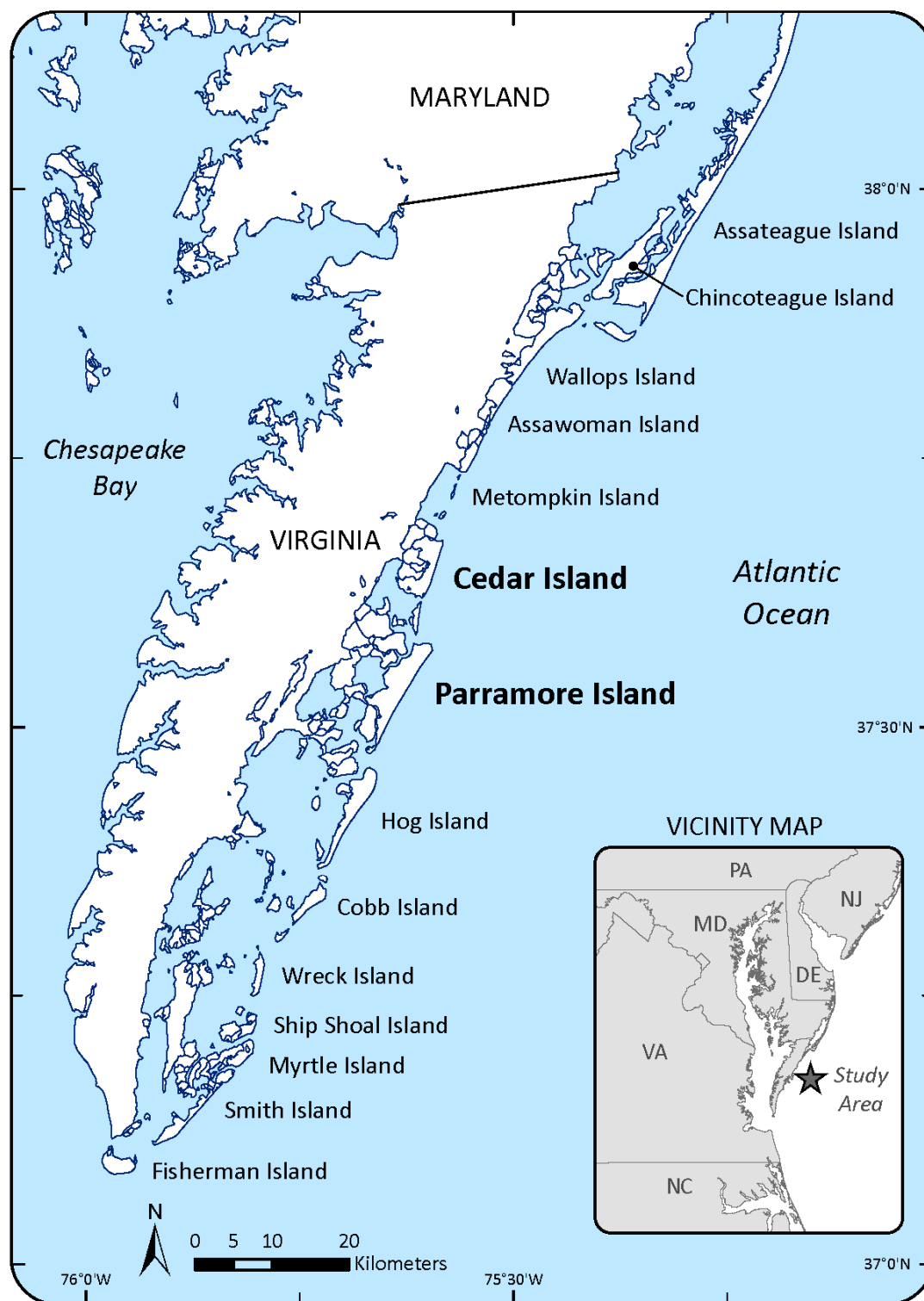


Figure 17: The Virginia Eastern Shore of the Delmarva Peninsula.

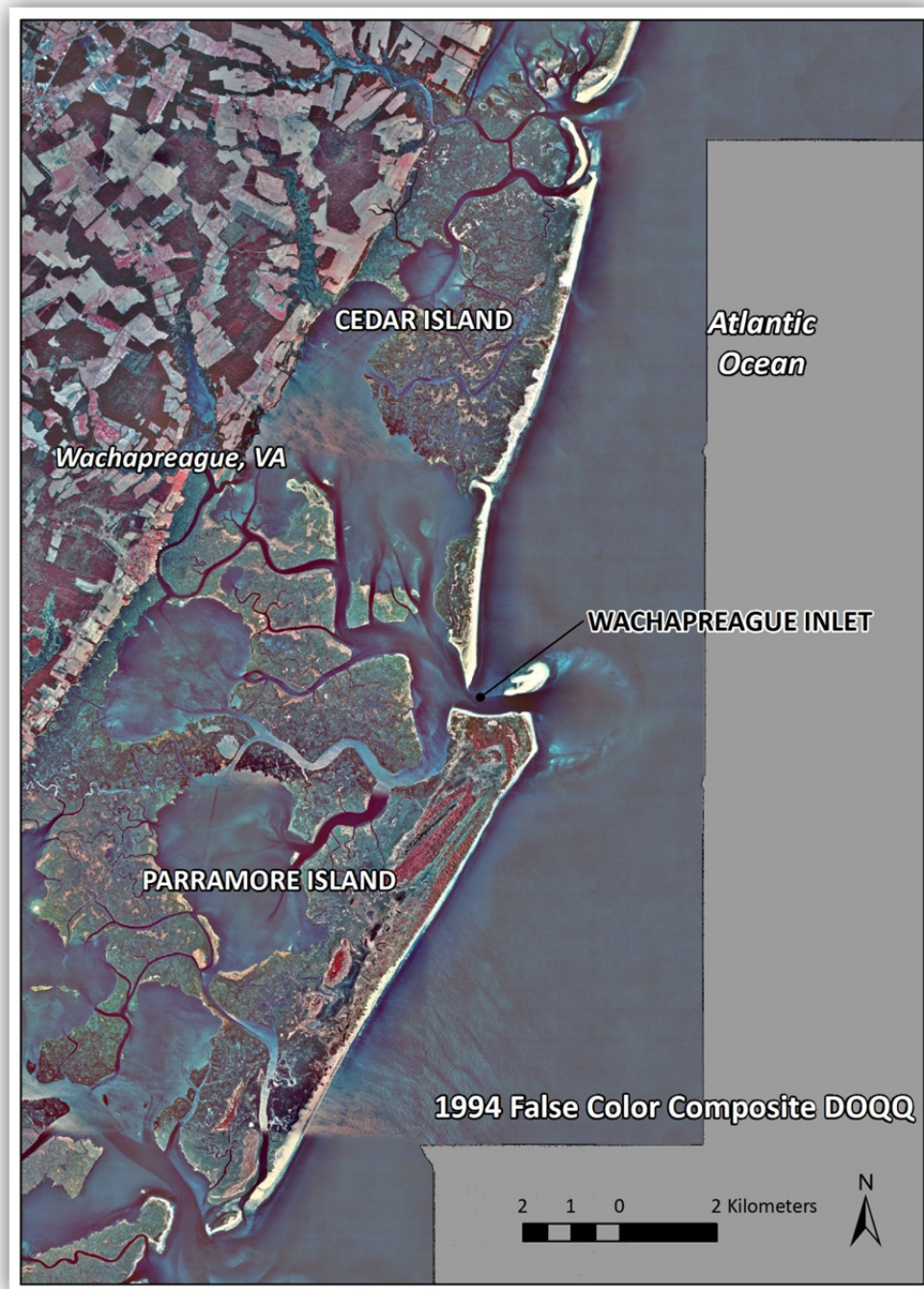


Figure 18: The Parramore-Cedar barrier island and Wachapreague tidal inlet system. Aerial photography courtesy of USDA Aerial Photography Field Office (APFO).

Cedar Island was positionally stable throughout large portions of the 20<sup>th</sup> century but narrowed at increasing rates after 1962 as a result of updrift interruptions in the sediment transport caused by the ephemeral island breaching of southern Metompkin Island and attendant sand trapping in Metompkin Bay (Gaunt, 1991). In addition, Cedar Island breached three times within the past 50 years along its southern, bay-backed portion (Moyer, 2007; Hanley & McBride, 2011). The most recent breach was open for approximately 9 years and closed in April 2007. Recent field investigations support the qualitative assessment that the island continues to narrow and rollover with a thin sand veneer covering increasing areas of saltwater marsh.

### **Wachapreague Inlet**

Wachapreague Inlet is a natural downdrift offset tidal inlet located between Cedar Island to the north and Parramore Island to the south. The tide-dominated inlet system is composed of a deep and narrow main channel at the inlet throat, a large crescent-shaped ebb-tidal delta directly to the east, a poorly developed flood-tidal delta, and extensive salt marsh and tidal channels in its backbarrier estuary to the west (Figure 19). In cross-section, the shape of the inlet is asymmetrical with the channel floor on the north side characterized by a gradual slope and an average inclination of 5 degrees, whereas the channel floor on the south side has an average slope of 15 degrees and a maximum slope of 45 degrees (DeAlteris & Byrne, 1975). Wachapreague Inlet is anchored in a Pleistocene stream valley and has been relatively stable throughout the Holocene. The inlet has a well-defined channel with a historical migration to the south. Wachapreague's

natural ebb-dominance is the result of differential hydraulic properties between ebb and flood tides (Byrne et al., 1974; DeAlteris & Byrne, 1975).



**Figure 19: Wachapreague Inlet environs August 15, 2011. Note the large ebb tidal delta and ephemeral Dawson Shoals to the north of the inlet. Aerial photography courtesy of USDA APFO.**

## **CHAPTER THREE: DATA SETS AND METHODS**

This chapter describes the shoreline data sets compiled and used in the study including a review of data sources, selection of shoreline proxies, the utilization of global positioning system (GPS) technology, and an accuracy assessment of the data. Other topics include a thorough review regarding the methods of shoreline-change analysis with a description of the establishment of shoreline cells and the statistical methods employed in the analysis. The second portion of this chapter is a review of the bathymetric data sets compiled and used including a review of data sources, previous research, survey methods, and an overview of tidal prism and ebb-tidal delta equation conversions and calculations.

### **Shoreline Data Sets**

Using U.S. Coast and Geodetic Survey and National Ocean Service (NOS) topographic sheets (T-sheets) and GPS shoreline-position surveys, historical shoreline changes of Parramore Island and Cedar Island are quantified between 1852 and 2010 to address both long-term and short-term trends in shoreline movement. T-sheets are a critical source of historical shoreline data, and the accuracy of these shoreline positions makes them an indispensable source of data to quantify the historical patterns, magnitudes, and rates of barrier-island change. A T-sheet representing the 1852 shoreline of Parramore Island is provided as an example in Figure 20. This study also utilizes high-





1:1 for the GPS surveys is indicative of the scale at which the data was collected, i.e. walking a shoreline feature. The T-sheet shorelines were acquired in standard GIS format (ESRI shapefiles) from the National Oceanic and Atmospheric Administration's Coastal Services Center (CSC). The data sets were thoroughly reviewed for positional, attribute, and metadata accuracy. Quality control processes included comparing the digitized shoreline positions to the source scanned raster (image) versions of the T-sheets, a systematic qualitative visual inspection of shoreline integrity, coordination with NOS and CSC regarding datum transformations from U.S. Standard Datum (1856–1857) to North American Datum 1983 (NAD83), and comprehensive metadata review including scale checks.

**Table 1: Parramore Island shoreline data sets (NOS T-sheets and GPS shoreline position surveys)**

<b>Parramore Island Shoreline Datasets</b>			
<b>Year</b>	<b>Scale</b>	<b>Max. Error</b>	<b>Source</b>
1852	1:10000	25.0m	T-Sheet
1871	1:10000	25.0m	T-Sheet
1910	1:10000	20.0m	T-Sheet
1942	1:20000	10.2m	T-Sheet
1962	1:10000	8.5m	T-Sheet
1998	1:1	4.0m	GPS
1999	1:1	4.0m	GPS
2000 (2)	1:1	4.0m	GPS
2002	1:1	4.0m	GPS
2005	1:1	4.0m	GPS
2006	1:1	4.0m	GPS
2007	1:1	4.0m	GPS
2010	1:1	4.0m	GPS

**Table 2: Cedar Island shoreline data sets (NOS T-sheets and GPS shoreline position surveys)**

<b>Cedar Island Shoreline Datasets</b>			
<b>Year</b>	<b>Scale</b>	<b>Max. Error</b>	<b>Source</b>
1852	1:10000	25.0m	T-Sheet
1871	1:10000	25.0m	T-Sheet
1910	1:10000	20.0m	T-Sheet
1933	1:10000	20.0m	T-Sheet
1942	1:20000	10.2m	T-Sheet
1962	1:10000	8.5m	T-Sheet
2007	1:1	4.0m	GPS
2008	1:1	4.0m	GPS
2009	1:1	4.0m	GPS
2010	1:1	4.0m	GPS

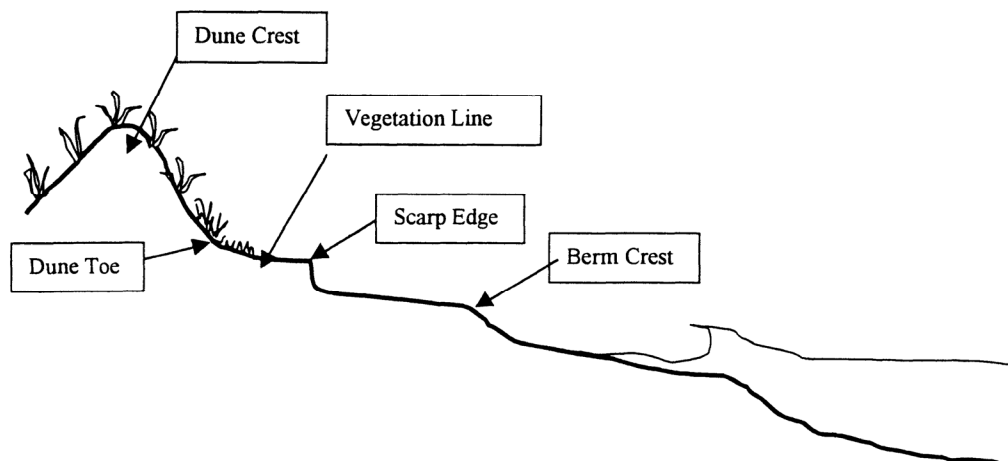
### **Data Sources, Proxies, and GPS**

T-sheets were first compiled in the mid-1800s by the National Ocean Service (formerly U.S. Coast and Geodetic Survey). The accuracy of these maps has been extensively analyzed and their accuracy errors commonly fall well within the magnitude of change experienced by a barrier island over the course of many decades or hundreds of years (Anders & Byrnes, 1991; Crowell et al., 1991). Early T-sheets (mid-1800s to early 1940s) were compiled in the field by surveyors mapping the high water line (HWL) “by noting the vegetation, driftwood, discoloration of rocks, or other visible signs of high tides” (Shalowitz, 1964). Analyses of these early T-sheets collected prior to the age of aerial photography have a total maximum positional error ranging from 20-25 m (Shalowitz, 1964; Ellis, 1978; Anders & Byrnes, 1991; Byrnes et al., 1991; Crowell et al., 1991). T-sheets produced after 1941 with the aid of aerial photography were intended to



meet National Map Accuracy Standards (NMAS). NMAS standards dictate the maximum allowable error for 90% of points are 8.5 m at 1:10,000 scale and 10.2 m at 1:20,000 scale (Ellis, 1978).

Monitoring the HWL enables the longest possible record of shoreline position (~160 years) for determining shoreline change rates as opposed to other shoreline proxies (Byrnes et al., 1991; Moore, 2000; Honeycutt et al., 2001; Pajak & Leatherman, 2002; Boak & Turner, 2005). This study also utilizes GPS shoreline surveys to map the HWL by visibly identifying the berm crest or the base of the active dune scarp (Figure 21) during the beach surveys (i.e., walking the berm crest) on Parramore and Cedar Islands. The berm crest is a physical feature on the beach that represents the high tide line plus wave run-up. In essence, it is the transition point between the foreshore and backshore and represents an excellent indicator of the HWL (Boak and Turner, 2005) (Figure 22).



**Figure 21: Physical features of the beach. The berm crest was walked during GPS shoreline position surveys on both Parramore and Cedar in order to map the high water line (HWL) as described by Pajak and Leatherman (2002).**

GPS shoreline position surveys are a rapid, low-cost, large-scale, and highly accurate means to map a shoreline. The GPS system used in this research was a Trimble XR Pro receiver, a Trimble Nomad handheld data collector with Trimble GPS Controller software (or TSC1 Asset Surveyor), and Trimble Terrasync software (Figure 23). The accuracy of a GPS survey largely depends on the knowledge and competency of the surveyor, the choice of shoreline indicator, and post-processing techniques (e.g., differential correction [office] or real-time kinematic corrections [field]). The survey positions were differentially corrected in the office through standard post-processing procedures that utilized base station files from a Continuously Operating Reference Station (CORS) at the Virginia Institute of Marine Science (VIMS) in Wachapreague, Virginia, located approximately 7 to 14 km from Parramore and Cedar Islands, respectively. Pajak and Leatherman (2002) conclude that mapping a shoreline with GPS is more accurate than using aerial photography to delineate specific shoreline features because of the inability to accurately map and distinguish discrete shoreline proxies from aerial photography or satellite imagery. The accuracy of the GPS surveys for this study is estimated at 4.0 m based on two primary error components: 1) delineating the high water line feature in the field (1–2 m) and 2) GPS positional accuracy following post-processing (1–2 m).



**Figure 22: The berm crest, the physical shoreline feature surveyed on Parramore and Cedar Islands.**



**Figure 23: GPS data collection system in use during survey of Parramore Island on April 30, 2011.**

## **Shoreline Accuracy Assessment**

An accuracy assessment of the shoreline data is critical to document the inherent errors associated with the T-sheet and GPS shoreline surveys. The accuracy assessment helps to determine whether the shoreline changes fall within an acceptable error range. The quantification of shoreline change and the confidence in the measurements are dependent on the measurement of maximum inherent and operator errors. More specifically, the errors associated with these shoreline surveys are primarily positional errors related to the data source and survey technique. Without this error quantification, it is difficult to judge the significance of the measured change.

A root-mean-square (RMS) method is a well-established practice (Merchant, 1987; Byrnes et al., 1991) and is used to generate an assessment of the total potential error of the shoreline data sets. Error is additive when comparing shoreline historical shoreline positions. Fundamentally, RMS is the square root of the mean of the squares of the values. The technique is particularly useful for measuring the magnitude of a varying quantity. The RMS approach can provide an assessment of combined potential errors. Table 3 (Parramore Island) and Table 4 (Cedar Island) are summaries of the maximum RMS potential error in regards to both magnitude (m) and rate (m/yr). The results are organized by year and the positional accuracy of the data source and maximum potential error. Specifically, in certain circumstances shorelines are combined into the same category when they share common maximum errors in order to concisely demonstrate the changes in RMS throughout the periods of record. The results indicate a low rate of

potential error (0.1 m) for both island's data sets across the entire historical period of record.

**Table 3: Maximum root-mean-square (rms) shoreline change error (Parramore Island, Virginia)**

**Maximum Root-Mean-Square (rms) Potential Error**  
Parramore Island Shoreline Change Analysis

Date	1910	1942	1962	1998/2010
1852/71	23.5 <sup>1</sup>	21.2	19.4	12.1
	(± 0.4-0.6) <sup>2</sup>	(± 0.2-0.3)	(± 0.2)	(± 0.1)
1910		16.6	14.3	7.9
		(± 0.5)	(± 0.3)	(± 0.1)
1942			9.4	5.4
			(± 0.5)	(± 0.1)
1962				5.1
				(± 0.1)

<sup>1</sup> Magnitude of potential error associated with high-water shoreline position change (m).

<sup>2</sup> Rate of potential error associated with high-water shoreline position change (m/yr).

**Table 4: Maximum root-mean-square (rms) shoreline change error (Cedar Island, Virginia)**

**Maximum Root-Mean-Square (rms) Potential Error**  
Cedar Island Shoreline Change Analysis

Date	1910/33	1942	1962	2007/2010
1852/71	22.7 <sup>1</sup>	20.9	19.5	15.4
	(± 0.3-0.6) <sup>2</sup>	(± 0.2-0.3)	(± 0.2)	(± 0.1)
1910/33		17.7	15.9	11.7
		(± 0.3-2.0)	(± 0.3-0.5)	(± 0.1-0.2)
1942			9.4	6.4
			(± 0.5)	(± 0.1)
1962				5.9
				(± 0.1)

<sup>1</sup> Magnitude of potential error associated with high-water shoreline position change (m).

<sup>2</sup> Rate of potential error associated with high-water shoreline position change (m/yr).

## **Shoreline Analysis Methodology**

The principal methodological approach of the shoreline analysis compares the horizontal position of the T-sheet and GPS shorelines using the Digital Shoreline Analysis System (DSAS) that is freely available through the United States Geological Survey (USGS) Woods Hole Science Center (Thieler et al., 2008). DSAS is an ESRI ArcGIS software extension that computes rate-of-change statistics for a time series of vector shoreline positions. It uses shoreline positions and a baseline(s) to generate transects and shoreline intersections. The DSAS transects for this study are plotted perpendicular to the shoreline at 50-m intervals in order to calculate the magnitude and rates of change. The DSAS analyses are able to generate a host of shoreline statistics including end point rate, linear regression rate, weighted linear regression rate, least median of squares, and corresponding error statistics. These statistics are then evaluated to assess the long- and short-term responses to natural coastal processes across a wide range of temporal scales.

## **Shoreline Change Statistics**

The shoreline-change results for Parramore and Cedar Island are reviewed by examining individual shoreline cells with various statistical measures. Net shoreline movement (NSM) calculates the distance between two shorelines, the most recent and the oldest. NSM is different than the shoreline change envelope (SCE). SCE is the greatest distance between all shorelines. The total distance between the youngest and oldest shorelines (NSM) is divided by the number of years between to derive the end point rate (EPR). EPR is commonly used to measure shoreline movement over time because of its

ease of computation and the need for only two shoreline positions. However, the technique ignores additional shoreline data and thus is less robust regarding changes in the pattern of shoreline movement, magnitude of events, or cyclical trends (Crowell et al., 1997; Dolan et al., 1991).

A linear regression rate (LRR) is a regression analysis that calculates a rate of change statistic and not a simple report of distance over time. An LRR is determined by fitting a least-squares regression line among all sample data points. The regression line is determined by minimizing the sum of the squared residuals, and subsequently, the LRR is the slope of the line. The advantages of an LRR are four-fold: 1) all data are used, 2) the method is purely computational, 3) the rate is grounded in accepted statistical concepts, and 4) the method is easy to utilize (Dolan et al., 1991). The primary disadvantage to an LRR is that it can be influenced by data outliers and can thus overestimate or underestimate the rate of change (Dolan et al., 1991). Error analysis statistics generated by the Digital Shoreline Analysis System (DSAS) measure the strength of the linear relationship, and associated errors include the standard error of the estimate (LSE), the standard error of the slope (LCI), and the R-squared value (LR2).

A weighted linear regression (WLR) calculation is a derivative of the LRR, but in this case, more reliable data are given greater weight when calculating a best-fit line. The weight is placed proportionally on data points that have lower values of positional uncertainty. The weight is calculated through the use of an uncertainty equation that determines the uncertainty of the measurements. Similar to the LRR, a standard error of

the estimate (WSE), the standard error of the slope (LCI), and the R-squared value (WR2) are also calculated with the DSAS.

The least median of squares (LMS) method contrasts to the ordinary and weighted least-squares regression calculation by using the median value—not the mean—of the squared residuals to determine the best-fit line. This method minimizes the influence of data outliers on the regression equation, but in fact, it follows the same process and logic for calculating the rate of change as a linear regression rate. In other words, linear regression places equal influence on all data points, a weighted linear regression places additional weight on more trusted or accurate data, and the least median of squares reduces the influence of data points with larger offsets.

For the purposes of this study, the end point rate (EPR) and linear regression rate (LRR) are the two primary statistical methods presented in the analysis of shoreline changes. EPR is utilized because of its simplicity, widespread scientific use, and ability to examine shoreline changes with incremental time periods (i.e., one shoreline date to another shoreline date). With a rich series of shorelines such as Parramore and Cedar Islands, trends and even distinct switches in shoreline movement can be tracked to a specific time period with the use of EPR. LRR is selected because it utilizes all the data as a result of the low RMS of positional error, the extensive acceptance of the technique in the coastal research community, and the lack of clear data outliers especially in the long-term data. The LRR is also a useful technique when comparing long-term and short-term trends across the historical period of record and also provides insight into tidal inlet behavior over time. The WLR and LMS statistics are utilized and discussed in the Results



section to reinforce or highlight trends or distinct changes in shoreline movement or behavior.

### **Shoreline Cells**

Parramore Island and Cedar Island shoreline change results are calculated and analyzed in detail by geomorphic zone (i.e., shoreline cells) because these individual barrier island segments react differently to various coastal processes. These shoreline cells are established to analyze, summarize, and arrive at conclusions regarding the patterns of coastal changes along these distinct areas of the islands. In other words, a clearer picture of the overall behavior of a barrier island can emerge by initially examining the geomorphic zones in relative isolation. The results for the shoreline cells of both Parramore and Cedar Islands are presented sequentially by moving from north to south (i.e., Cell 0 to 5) for the sake of consistency and ease of comparison. The complete shoreline change results for Parramore and Cedar Islands are contained in Appendix A and B, respectively. The appendices are organized in table format by shoreline cell and present the results across a range of temporal timeframes.

A number of similarities exist in both the consistency of the numbering system employed in this research and the corresponding geomorphic characteristics of the shoreline cells of Parramore and Cedar Islands. Specifically, Cells 1, 2, and 5 are inlet-influenced shorelines and Cells 3 and 4 are the open-ocean, non-inlet-influenced shorelines. A primary difference between Parramore and Cedar cells is the influence of breaches along Cedar Island; specifically, Cell 1 and 2 of Cedar are influenced by the “Coast Guard breach” and Cell 4 also contains a bay-backed breach zone. However,

every attempt has been made to correlate overriding geomorphic characteristics where possible so that cell-by-cell comparisons can be made between the islands where appropriate.

As shown in Figure 24, Parramore Island's shoreline is segmented into six shoreline cells—Cell 0: the northern, bay-side shoreline; Cell 1: the northern, Wachapreague Inlet-throat shoreline; Cell 2: the northern, inlet-influenced, open-ocean shoreline; Cell 3: the north-central, open-ocean shoreline; Cell 4: the southern, washover-dominated, open-ocean shoreline; and Cell 5: the southern spit shoreline. Of note, the dynamic and changing shoreline orientation of Cell 2 necessitated the creation of a nested sub-cell to adequately sample the 1852 and 1871 shorelines.

As shown in Figure 25, Cedar Island's shoreline is segmented into six shoreline cells—Cell 0: the northern, Metompkin Inlet-influenced shoreline; Cell 1: the Coast Guard breach shoreline; Cell 2: the northern, inlet-influenced, open-ocean shoreline; Cell 3: the north-central, marsh-backed, open-ocean shoreline; Cell 4: the south-central, bay-backed, open-ocean shoreline; and Cell 5: the southern spit shoreline.

## Shoreline Cell Reference Map

Parramore Island, Virginia

### Shoreline Cell Description

- Cell 0: Northern, bay-side
- Cell 1: Wachapreague Inlet-throat
- Cell 2: Northern, inlet-influenced
- Cell 3: North-central, open-ocean
- Cell 4: Southern, washover-dominated, open-ocean
- Cell 5: Southern spit

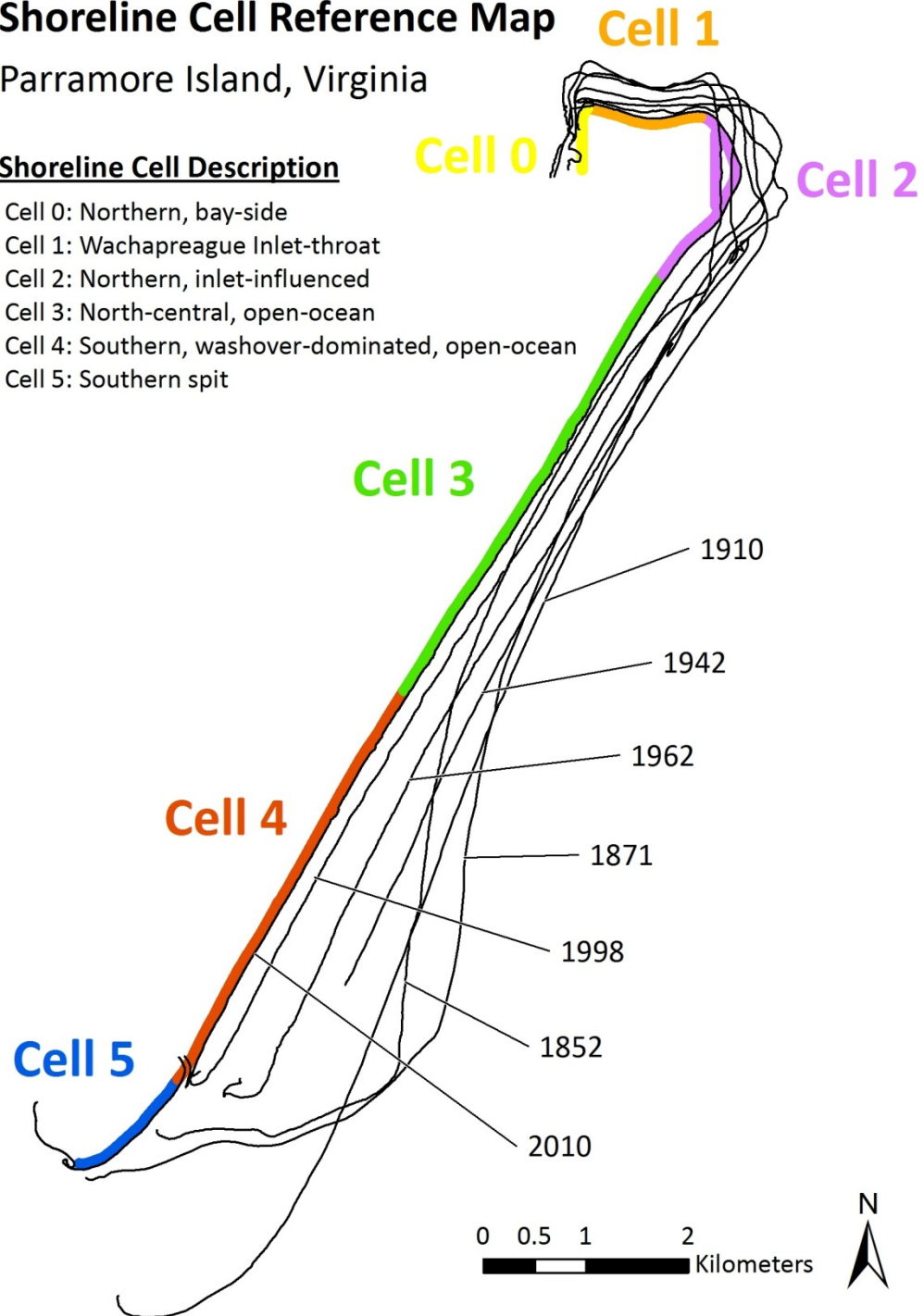


Figure 24: Parramore Island shoreline cell reference map.

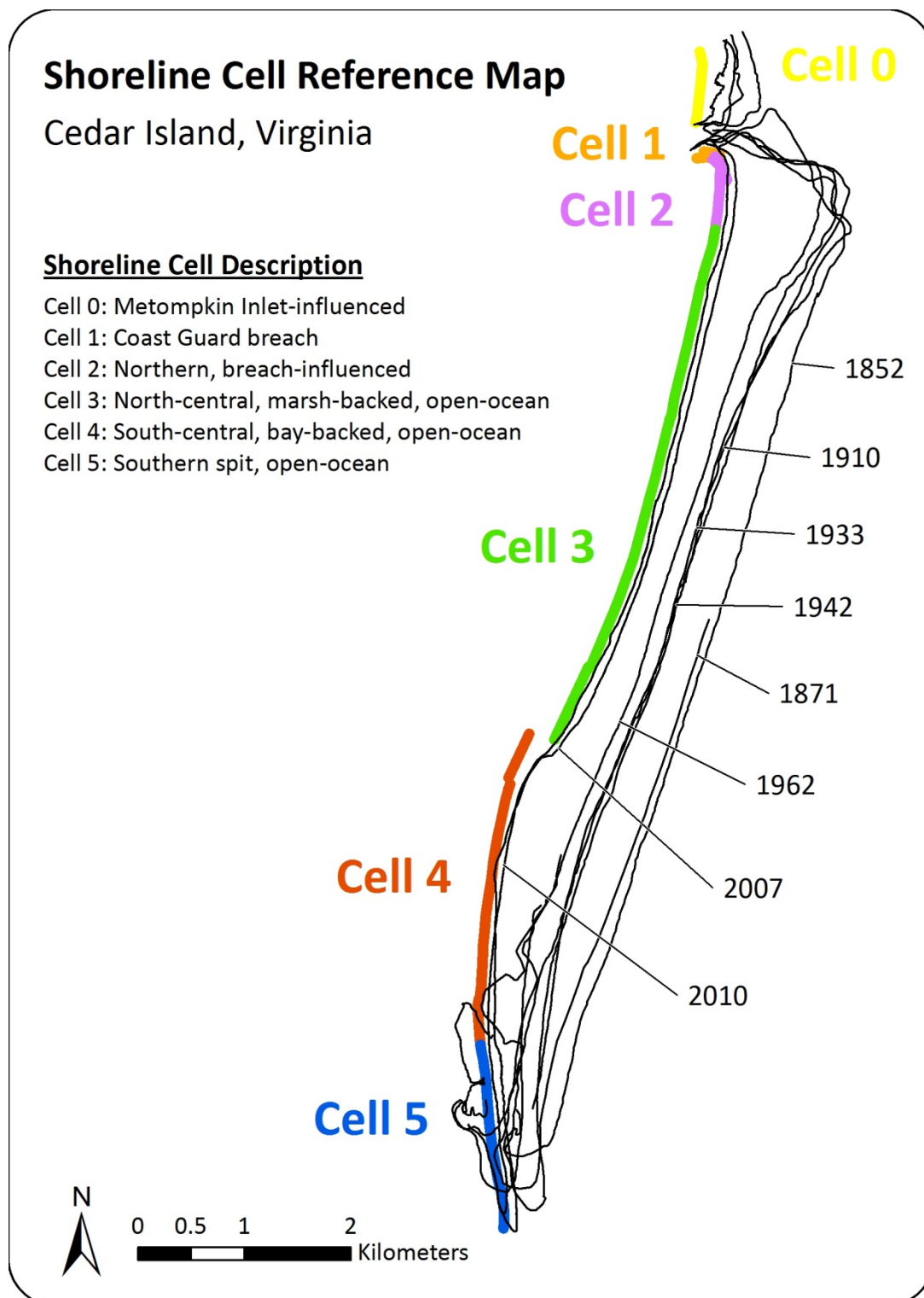


Figure 25: Cedar Island shoreline cell reference map.

## **Bathymetric Data Sets**

A number of diverse data sources are used to analyze the historical and contemporary changes of cross-sectional area at the inlet throat of Wachapreague Inlet. Available bathymetric data sets include hydrographic sheets (H-sheets) from 1852 to 1934 compiled and analyzed by DeAlteris and Byrne (1975) and the five in situ inlet surveys of Wachapreague Inlet from 1972 to 2011 by a number of researchers (Table 5). The configuration and bathymetric profiles of Wachapreague Inlet from 1852 to 1972 were compiled and contoured by DeAlteris and Byrne (1975) in their paper “The Recent History of Wachapreague Inlet” (Figure 26). The authors documented changes in cross-sectional area of the tidal inlet by using H-sheets from 1852, 1871, 1911, and 1934. In addition, the authors also conducted a detailed bathymetric survey of the entire inlet complex in 1972 to map and quantify the cross-sectional area of Wachapreague Inlet. The 1972 survey established range lines at intervals of 200 meters for a total of 10 range lines collected during repetitive surveys over the course of 13 months (Byrne et al., 1974).

## ***In Situ* Inlet Survey Methodology (2007–2011)**

The collection of multiple cross-sectional areas over several years allows for the comparison of historical cross-sectional areas to the contemporary time period. *In situ* tidal inlet surveys of Wachapreague Inlet were conducted in 2007, 2010, and 2011 to calculate the cross-sectional area of the inlet throat. These surveys and resulting comparisons more fully document changes to the Wachapreague Inlet bathymetric complex. The cross-sectional areas were collected by bathymetric sounders with the assistance of personnel from the Virginia Institute of Marine Science’s Eastern Shore

Laboratory. For the years 2007, 2010, and 2011 the methods included collecting multiple profiles from the southern tip of Cedar Island to waypoints on Parramore Island.

Soundings were collected with a Garmin GPSmap 178 Sounder on a 24-foot Carolina skiff and were recorded every 10 seconds (Moyer, 2007) or 5 seconds (Richardson, 2010 and 2011) at an approximate speed of 5 knots and with GPS locations (Figure 26).

**Table 5: Wachapreague Inlet bathymetric data sets (H-sheets and bathymetric surveys)**

<b>Wachapreague Inlet Datasets</b>		
<b>Year</b>	<b>Scale</b>	<b>Source</b>
1852	1:10000	H-Sheet
1871	1:10000	H-Sheet
1911	1:10000	H-Sheet
1934	1:10000	H-Sheet
1972	1:1	DeAlteris <sup>1</sup>
2007 (Apr)	1:1	Moyer <sup>2</sup>
2010 (Apr)	1:1	Richardson <sup>3</sup>
2010 (Aug)	1:1	Fenster <sup>4</sup>
2011 (Apr)	1:1	Richardson <sup>3</sup>

<sup>1</sup> DeAlteris, J.T. & Byrne, R.J., 1975. The recent history of Wachapreague Inlet, Virginia. In L.E. Cronin, ed. *Estuarine Research*. New York, NY: Academic Press. pp. 167-181.

<sup>2</sup> Moyer, K.S., 2007. *An assessment of an ephemeral breach along Cedar Island, Virginia*. Master's Thesis. Environmental Science and Policy, George Mason University, p. 101.

<sup>3</sup> Bathymetric surveys at tidal inlet throat (located at the southern tip of Cedar Island) with soundings occurring at a five second sampling interval.

<sup>4</sup> Fenster, M.S., et al., 2011. A field test of the theoretical evolution of a mixed-energy barrier coast to a regime of accelerated sea-level rise. *Proceedings of Coastal Sediments '11*, ASCE, pp. 216-229.

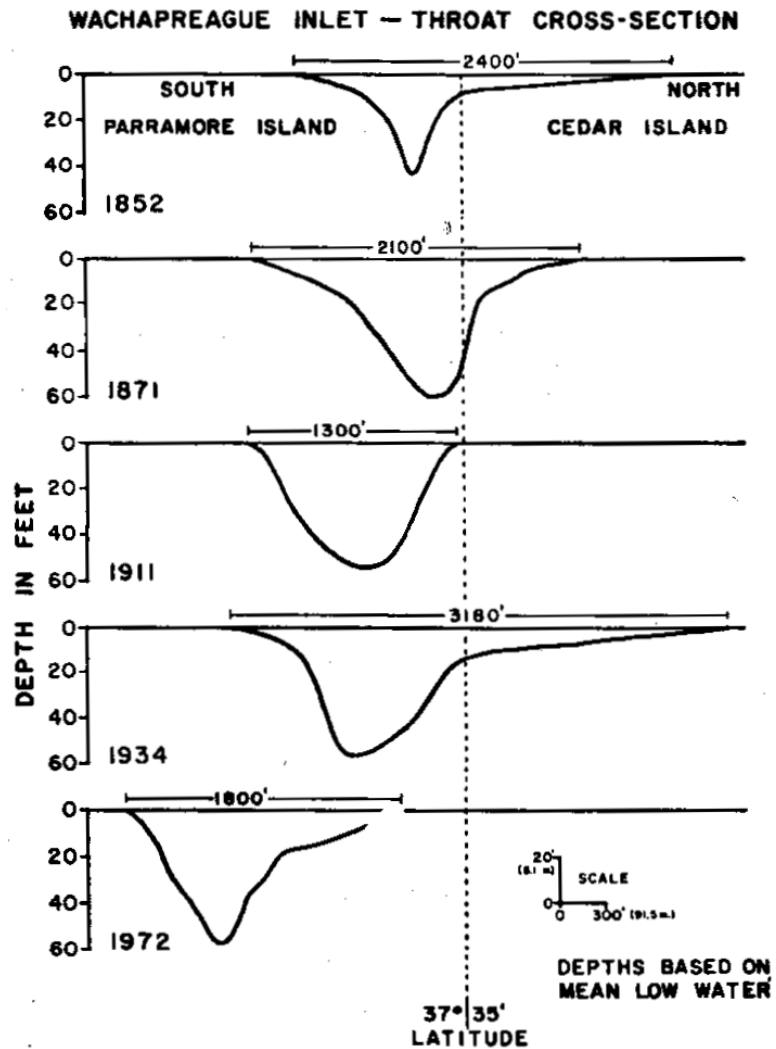


Figure 26: Wachapreague Inlet-throat cross-sections from 1852 to 1972 (DeAlteris & Byrne, 1975).

For the Moyer (2007) and Richardson (2010, 2011) surveys, the methods to tidally correct the sounding data to mean sea level involved collecting the actual tide levels recorded at Wachapreague Channel (WC) and relating them to the tide level at Wachapreague Inlet (WI) (Figure 27, top). The time and tide level corrections were then compared to the reference station at Ocean City, Maryland. The results revealed the high

tide at WI is 36 minutes before high tide at WC and is 0.983 times the tide level at WC. Furthermore, low tide at WI is 24 minutes before low tide at WC and is 1.18 times the tide level at WC. Both Moyer (2007) and Richardson assumed a linear relationship between tide levels at WC and the soundings at each transect at WI because of the small difference between the correction factors for high and low tides. The cross-sectional areas of the inlet were calculated by measuring the depth and distance between soundings and then calculating an interpolated area along the entire length of a survey transect. The cross-sectional areas of the discrete transects (four in 2007, two in 2010 and 2011) were then averaged to determine the mean cross-sectional area of the tidal inlet survey (Figure 27, bottom).

An additional data point included in this research is from the work of Fenster et al. (2011). Specifically, Fenster et al. (2011) obtained current velocity data using Teledyne RDI and Nortek AWAC, bottom-mounted and upward-looking Acoustic Doppler Current Profile (ADCP) systems deployed in the main ebb channel of Wachapreague Inlet (Figure 28). The deployment period spanned 8 days from August 9 to 16, 2010. In addition, they acquired current velocity data using a vessel-mounted downward-looking TRDI Workhorse Monitor 1200 kHz ADCP across each of three tidal inlets (Metompkin, Wachapreague, and Quinby) over a complete semi-diurnal tidal cycle. A vessel mounted single-beam fathometer was also used to determine swath bathymetry across the inlet and the cross-sectional area of the inlet throat. Integrating the bathymetric data with the measured tidal current data allowed Fenster et al. (2011) to determine dynamic tidal discharges and tidal prisms for each inlet.



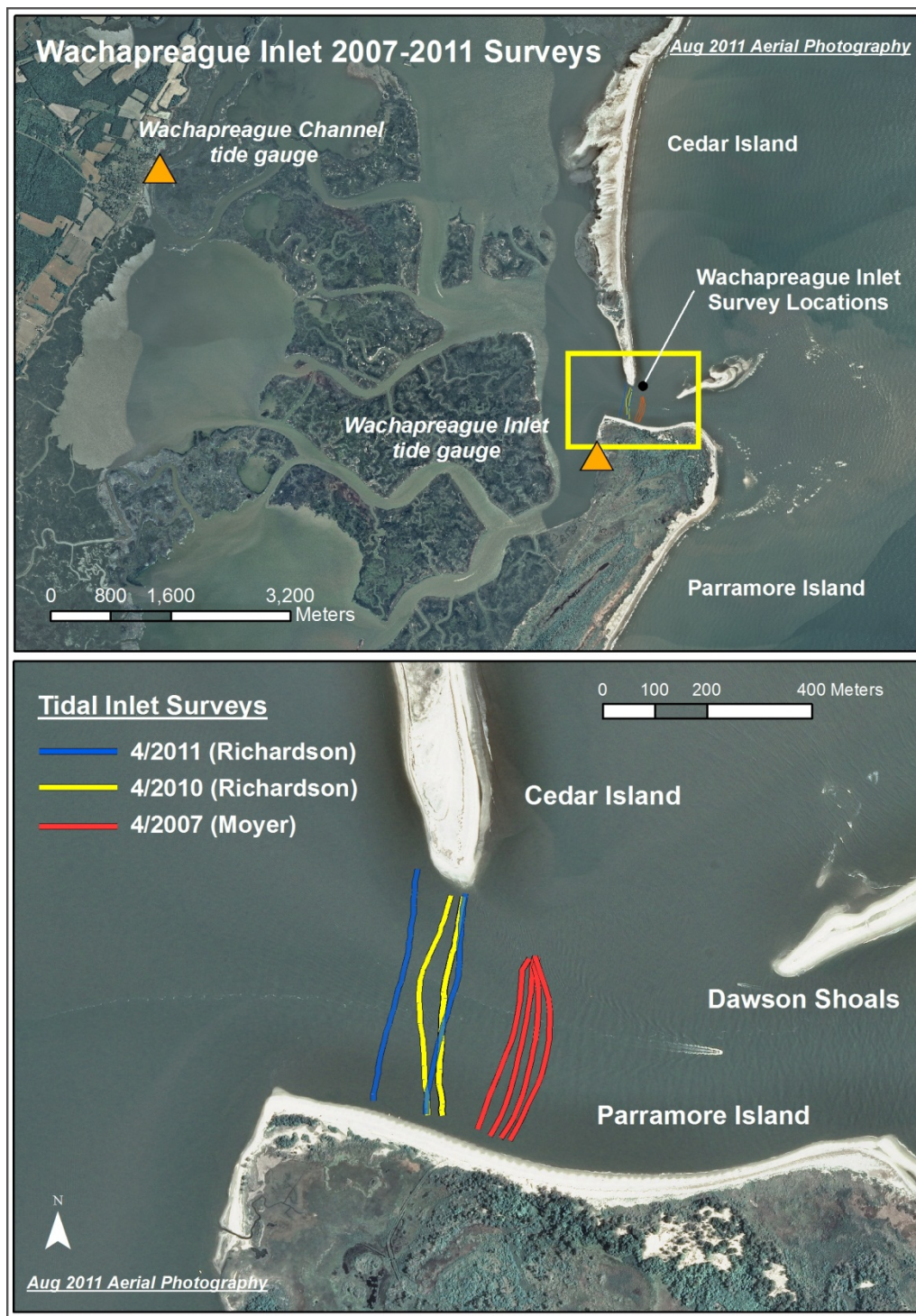


Figure 27: Top, Tide-gauge locations in the Wachapreague Inlet area. Bottom, Bathymetric surveys across the inlet throat of Wachapreague Inlet, Virginia from 2007 to 2011. Aerial photography courtesy of USDA APFO.

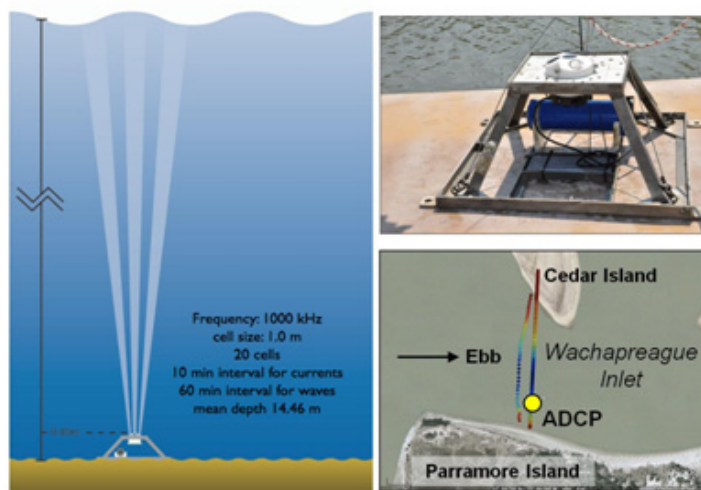


Figure 28: Schematic and deployment of ADCP in Wachapreague Inlet. Shown are bathymetric survey transects for April 23, 2010 bathymetric profile (landward/west) and August 12, 2010 (Fenster et al., 2011).

## Bathymetric Data Set Errors

The errors associated with the calculation of cross-sectional areas and tidal prism fall into two primary categories: 1) seasonal/yearly differences and 2) changes in tidal prism between neap and spring tides, and 3) measurement errors. In regard to seasonal/yearly differences, Byrne and DeAlteris (1974:1594) report that “mean tide level shows significant variations in absolute level during the year as a result of steric fluctuations and atmospheric pressure patterns. An analysis of Wachapreague tides for a three year period showed mean tide levels are lowest in January and February, whereas the highest occur in September, October, and November. Calculations using the storage relationship between mean tide level and volume of water storage at Wachapreague, Virginia indicate the October tidal prism is 18% larger than January” (Figure 29).

In regard to differences between neap and spring tides, O'Brien's (1969:44) appraisal of inlet data to quantify flow area and tidal prism states the relationship is "accurate within  $\pm 10\%$  in flow area and  $\pm 15\%$  in tidal prism." Jarrett (1976:15) builds upon this analysis by stating, "[W]here possible, current observations made during spring tides were used to compute tidal prisms. If observations were not available for spring tide conditions, the spring tidal prism was estimated by a ratio of the bay tidal range during spring conditions to the bay tidal range at the time of the current observations." Furthermore, Seabergh (2007:27) states regarding coastal inlet hydraulics that "[n]atural inlet area can have a reasonable variation in magnitude (plus or minus 10%) over a short period of time due to variation in tide range, variation in wave activity, and storms." Taken as a whole, these observations of natural variability associated with the calculation of tidal prism lead this author to conclude that a magnitude of 15% is an appropriate measurement of natural variability for the Parramore–Cedar barrier-island system. Variability bars associated with this conclusion are applied in the exhibits in the Results chapter and discussed further in the Discussion chapter.

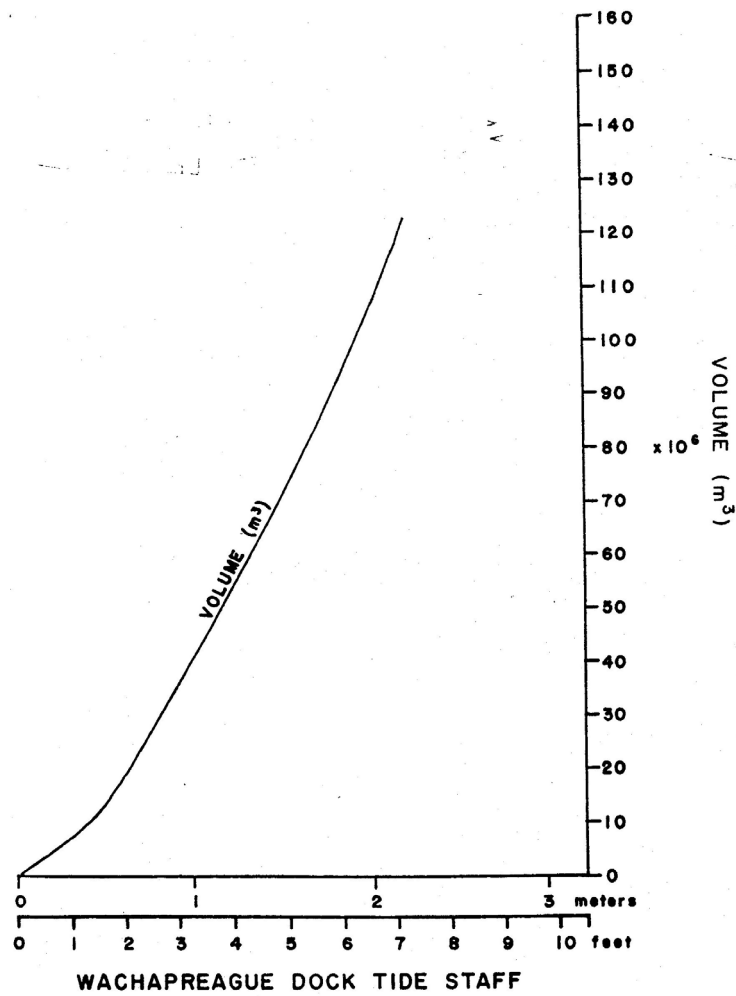


Figure 29: Backbarrier storage volume relative to tidal elevations at town of Wachapreague, Virginia. Mean tide level = 4.36 ft. (Byrnes et al., 1974).

## Tidal Prism Calculations

Tidal prism in the context of a barrier-island system such as the Parramore–Cedar mixed-energy environment is the volume of water moving in or out of a tidal inlet during one tidal cycle (e.g., from mean high tide to mean low tide or from mean low tide to mean high tide), excluding any freshwater input. This water exchange from ocean to bay

and vice versa is strongly correlated to inlet size. The inlet cross-sectional area is defined as inlet width at its narrowest point adjoining the adjacent barrier islands (i.e., inlet throat) versus inlet depth across this same span. O'Brien (1931, 1969) quantified this relationship by plotting cross-sectional area of the inlet throat at mean sea level against tidal prism during spring tidal conditions (Equation 1). This equation is calculated with (A) serving as the cross-sectional area and (P) as spring tidal prism:

**Equation 1: O'Brien (1969) tidal prism and inlet area relationship.**

$$A = 2.0 \times 10^{-5} P$$

The O'Brien relationship was further modified by Jarrett (1976) when he quantified tidal prism and inlet area relationships for inlets on sandy coasts across a range of coastlines along the United States. Jarrett used 162 data points and 108 inlets to group coasts into three main categories: 1) all inlets, 2) unjettied or single-jettied inlets, and 3) inlets with two jetties. In addition, he also segmented these three categories into the following: A) inlets on all three coasts, B) inlets on the Atlantic coast, C) inlets on the Gulf coast, and D) inlets on the Pacific coast. A regression analysis performed by Jarrett (1976) demonstrated a strong relationship with high  $R^2$  values that resulted in the following equation with (A) as the cross-sectional area, (P) as spring tidal prism, (C) as a correlation coefficient, and ( $n$ ) as a power function (Equation 2):

Equation 2: Jarrett (1976) tidal prism and inlet area relationship.

$$A = CP^n$$

The full suite of regression equations of P versus A in the form of the previous equations are contained in Table 6. The categories selected for the Wachapreague Inlet calculations are “unjettied or single-jettied inlets” and “inlets on the Atlantic coast.” The strength of the linear relationship is demonstrated in Figure 30.

Table 6: Jarrett (1976) regression equations of tidal prism and cross-sectional area

Regression Equations of P Versus A ; Form of Equations $A = CP^n$						
Equation	95% Confidence Limits of C		95% Confidence Limits of n		Width of 95% Confidence Limits of A for Mean P Natural Logarithms	Number of Data Points
	Lower	Upper	Lower	Upper		
1. All Inlets						
a. Atlantic, Gulf, and Pacific coasts						
$A = 5.74 \times 10^{-5} P^{0.95}$	$5.36 \times 10^{-5}$	$6.13 \times 10^{-5}$	0.91	1.00	1.70615	162
b. Atlantic coast						
$A = 7.75 \times 10^{-6} P^{1.05}$	$7.14 \times 10^{-6}$	$8.41 \times 10^{-6}$	0.99	1.12	1.46894	79
c. Gulf coast						
$A = 5.02 \times 10^{-4} P^{0.84}$	$4.25 \times 10^{-4}$	$5.93 \times 10^{-4}$	0.73	0.95	2.03012	36
d. Pacific coast						
$A = 1.19 \times 10^{-4} P^{0.91}$	$1.07 \times 10^{-4}$	$1.32 \times 10^{-4}$	0.86	0.97	1.45688	47
2. Unjettied or Single-Jettied Inlets						
a. Atlantic, Gulf, and Pacific coasts						
$A = 1.04 \times 10^{-5} P^{1.03}$	$9.47 \times 10^{-6}$	$1.13 \times 10^{-5}$	0.97	1.10	1.78570	96
b. Atlantic coast						
$A = 5.37 \times 10^{-6} P^{1.07}$	$4.86 \times 10^{-6}$	$5.92 \times 10^{-6}$	0.99	1.16	1.40610	50
c. Gulf coast						
$A = 3.51 \times 10^{-4} P^{0.86}$	$2.97 \times 10^{-4}$	$4.16 \times 10^{-4}$	0.73	0.99	1.86524	30
d. Pacific coast						
$A = 1.91 \times 10^{-6} P^{1.10}$	$1.57 \times 10^{-6}$	$2.32 \times 10^{-6}$	0.99	1.21	1.61031	16
3. Inlets with Two Jetties						
a. Atlantic, Gulf, and Pacific coasts						
$A = 3.76 \times 10^{-4} P^{0.86}$	$3.44 \times 10^{-4}$	$4.11 \times 10^{-4}$	0.81	0.92	1.44345	66
b. Atlantic coast						
$A = 5.77 \times 10^{-5} P^{0.95}$	$4.98 \times 10^{-5}$	$6.69 \times 10^{-5}$	0.81	1.09	1.61274	29
c. Gulf coast						
Insufficient data for regression analysis						
d. Pacific coast						
$A = 5.28 \times 10^{-4} P^{0.85}$	$4.96 \times 10^{-4}$	$5.23 \times 10^{-4}$	0.81	0.88	0.71289	31

## Jarrett Equation Modifications

As stated previously, Jarrett (1976) builds upon the tidal prism and inlet area relationships for inlets on sandy coasts established by O'Brien (1931, 1969). However, the units of measurement in the Jarrett (1976) equations are expressed in English units, whereas modern science reports data and points in metric. Furthermore, the variables contained in the Jarrett (1976) equations are converted to metric because the shoreline and bathymetric data have been processed, collected, analyzed, and presented in metric units. As a result, the Jarrett (1976) equation requires a conversion from feet to meter units for the proper calculation of distance, area, and volume.

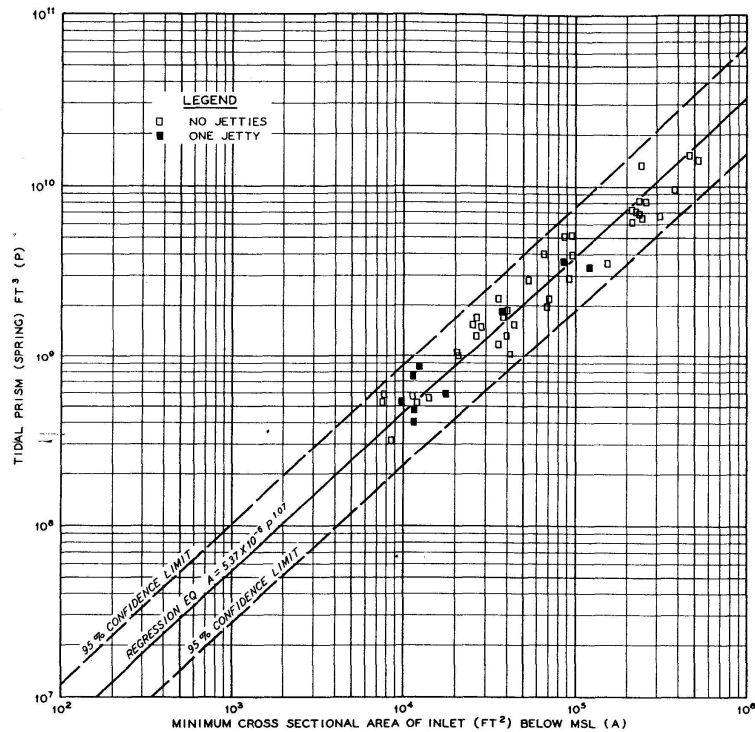


Figure 30: Tidal prism vs. cross-sectional area: Inlets on Atlantic coast with one or no jetties (Jarrett, 1976).

The steps to calculate spring tidal prism based on cross-sectional areas using the Jarrett (1976) equation with a conversion from English to metric units and the determination of a metric correlation coefficient and power function are as follows:

1. If necessary, convert cross-sectional area from square feet to square meters.
2. Match the study area's inlet setting to the geographic area and inlet type in Jarrett (1976). In the context of this study, the proper Jarrett equation is “inlets on the Atlantic coast” and “unjettied or single-jettied inlets” (Table 6).

$$A = 5.37 \times 10^{-6} P^{1.07}$$

$$P = \sqrt[1.07]{(A / 5.37 \times 10^{-6})}$$

3. The change in dimension from feet to meters is not built into the root equation so the correlation coefficient must be changed to reflect this change in dimension. Convert the correlation coefficient to account for a change in unit by replacing feet with “number of feet in a meter,”

$$C (\text{meters}) = C (\text{feet}) * [(3.28084)^{(3 * n (\text{feet}))}] / (3.28084)^2$$

$$C (\text{meters}) = 5.37 \times 10^{-6} * [(3.28084)^{(3 * 1.07)}] / (3.28084)^2$$

$$C (\text{meters}) = 2.26 \times 10^{-5}$$

4. The resulting modified Jarrett equation for “unjettied or single-jettied inlets” and “inlets on the Atlantic coast” in metric units is the following (Equation 3):



**Equation 3: Metric version of Jarrett (1976), unjettied or single-jettied inlets, inlets on the Atlantic coast.**

$$A = 2.26 \times 10^{-5} P^{1.07}$$

However, in the application of this research, the reverse is performed—namely, calculating the tidal prism from the cross-sectional area. Rearranging the previous equation to solve for P includes deriving a new power function (friction coefficient) by dividing the power function by 1. The resulting equation for the calculation of tidal prism is as follows (Equation 4):

**Equation 4: Conversion of metric version of Jarrett (1976) unjettied or single-jettied inlets on the Atlantic coast to solve for tidal prism.**

$$P = (A/2.26 \times 10^{-5})^{0.93}$$

5. As a further refinement to the metric version of Jarrett (1976) unjettied or single-jettied inlets on the Atlantic coast, Seminack (personal communication, 2011) conducted an analysis of the relationship between cross-sectional area and tidal prism of only the natural unjettied inlets of Jarrett's (1976) Atlantic data set. More specifically, Seminack analyzed a total of 34 unjettied Atlantic inlets in Jarrett (1976) and calculated an equation with a high level of confidence ( $R^2 = 0.94$ ) for unjettied inlets on the Atlantic coast. This additional refinement of unjettied or single-jettied inlets on the Atlantic coast removed the influence of single-jettied

data points on the calculation of tidal prism and produced the following metric equation for natural unjettied inlets on the Atlantic coast (Equation 5):

**Equation 5: Seminack’s equation for the calculation of cross-sectional area at natural unjettied inlets on the Atlantic coast.**

$$A = 2.04*10^{-5} P^{1.08}$$

6. The reformulation of this equation, hereafter referred to as the “Richardson–McBride–Seminack equation,” was then used to calculate the tidal prism from the measured cross-sections at Wachapreague Inlet (Equation 6).

**Equation 6: Richardson–McBride–Seminack equation for the calculation of tidal prism in metric units based on cross-sectional area.**

$$P = (A/2.04*10^{-5})^{0.926}$$

## **Ebb-Tidal Delta Calculations**

In addition to an inlet cross-sectional area and tidal prism relationship, an ebb-tidal delta volume and tidal prism relationship also exists. Walton and Adams (1976) determined that the sand volume contained in an ebb-tidal delta is closely related to tidal prism. In essence, the sand volume constituting an ebb-tidal delta is largely the function of ebb discharge. In other words, larger tidal prisms generate larger ebb-tidal deltas and

vice versa on sandy shores. Specifically, the Walton and Adams (1976) equation, with (V) representing sand volume stored, (P) as tidal prism, and (a, b) as correlation coefficients, is expressed as follows (Equation 7):

**Equation 7: Walton and Adams (1976) equation for calculating outer bar/shoal sand storage volume with tidal prism volume.**

$$V = a P^b$$

Walton and Adams (1976) separated their data set into three inlet categories: 1) high-wave energy coasts, 2) moderate-wave energy coasts, and 3) low-wave energy coasts. Walton and Adams's (1976) categorization by wave energy takes into account the role of waves to transport sand back onshore and thereby reduce the sand volume of an ebb-tidal delta. The examination of the Wachapreague Inlet data sets utilizes the "all inlets" Walton and Adams (1976) category because of the high confidence of the correlation coefficient and extensive application by coastal scientists (Equation 8). The strength of the linear relationship is illustrated in Figure 31. Human factors such as offshore borrow sites, jetties, and inlet and backbarrier dredging are discounted because of the lack of anthropogenic activities along the Virginia coast.

**Equation 8: Walton and Adams's all inlets equation (English units).**

$$V = 1.07 \times 10^4 P^{1.23}$$

As with the Jarrett (1976) equation, the English units of the Walton–Adams (1976) relationship also require a conversion from English to metric units. A similar methodology was employed to convert the Walton and Adams (1976) equation. However, the major exception to the process is the generation of a new coefficient based on a volume-to-volume relationship (tidal prism to ebb-tidal delta volumes) and not an area-to-volume relationship (cross-sectional area to tidal prism volume) (Equation 9).

Equation 9: Fontolan et al. (2007) conversion of Walton and Adams's (1976) all inlets equation (metric units).

$$V = 6.56 \times 10^{-3} P^{1.23}$$

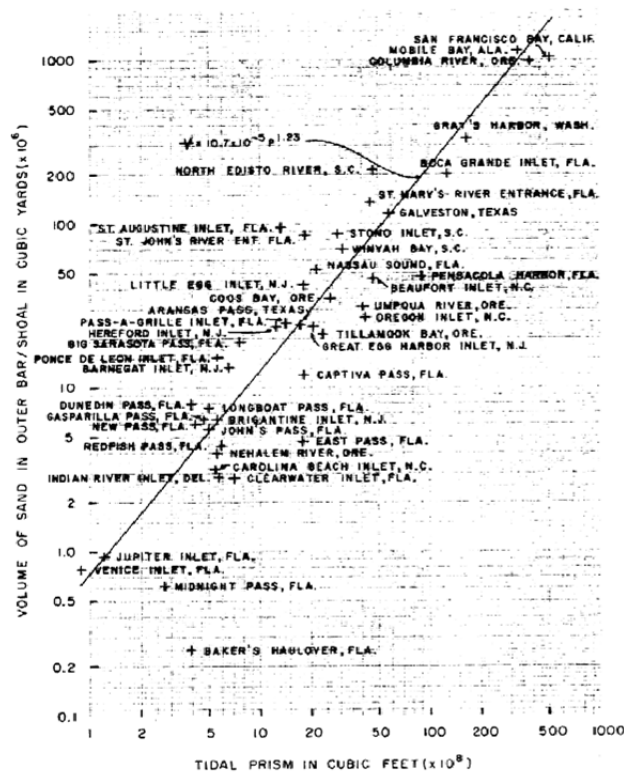


Figure 31: Walton and Adams (1976) tidal prism–outer bar storage relationship for tidal inlets.

## **CHAPTER FOUR: RELATED STUDIES AND CONCEPTS**

Chapter Four is a review of related studies and concepts connected to this research. The chapter includes an overview of the relevant research pertaining to barrier-island formation, barrier-island system dynamics, and the influence of tidal inlets and sediment supply on the behavior of barrier-island systems. Additional topics include an examination of the potential drivers of change to the barrier-island system such as a rise in relative sea level, alterations in sediment supply, and storminess. The concepts are related to coastal morphodynamics with an emphasis on the southern Delmarva Peninsula. Finally, other applicable research is reviewed pertaining to the proposed methods, related issues, and similar problems found elsewhere in other research.

### **Barrier-Island Formation**

The origin and evolution of barrier islands may result from several but different key methods of formation. These methods of barrier island formation have been debated and modeled since the 19<sup>th</sup> century, and coastal scientists have coalesced around three primary theories (Hoyt, 1967; Fisher, 1968; Otvos, 1970; Schwartz, 1973). Leatherman (1982) summarizes these primary models of barrier island formation: 1) offshore bar/shoal emergence (De Beaumont, 1845; Otvos, 1970), 2) coastal ridge submergence (McGee, 1890; Hoyt, 1967), and 3) spit elongation (Gilbert, 1885; Fisher, 1968). Offshore bar emergence or shoal emergence starts with the formation of an offshore

shoal, and over time the shoal captures more sand, grows vertically, and eventually emerges from the sea (Figure 32). Coastal ridge submergence or the dune drowning model is based on a relative rise in sea level during which a mainland beach and its dune complex are flooded by an encroaching ocean and thereby create an estuary or marsh that separates the barrier beach from the mainland (Figure 33). Spit elongation is the growth of sand spits at coastal headlands as a result of longshore sediment transport, the breaching of these spits during storms, and the eventual detachment and separation of the spit from the mainland by a tidal inlet (Figure 34).

Swift (1975) studied barrier-island genesis along the central Atlantic shelf of the eastern United States and concluded that most barrier systems likely retreated into their present positions from seaward positions along the outer continental shelf in response to the post-Wisconsin transgression (landward movement of the shoreline). The barriers along the mid-Atlantic bight of North America do not contain drowned barriers; rather, they developed through spit progradation or mainland-beach ridge detachment. In general, Swift (1975) believed the barriers along the Delmarva Peninsula retreated into a series of progressively landward locations from their preceding seaward position.

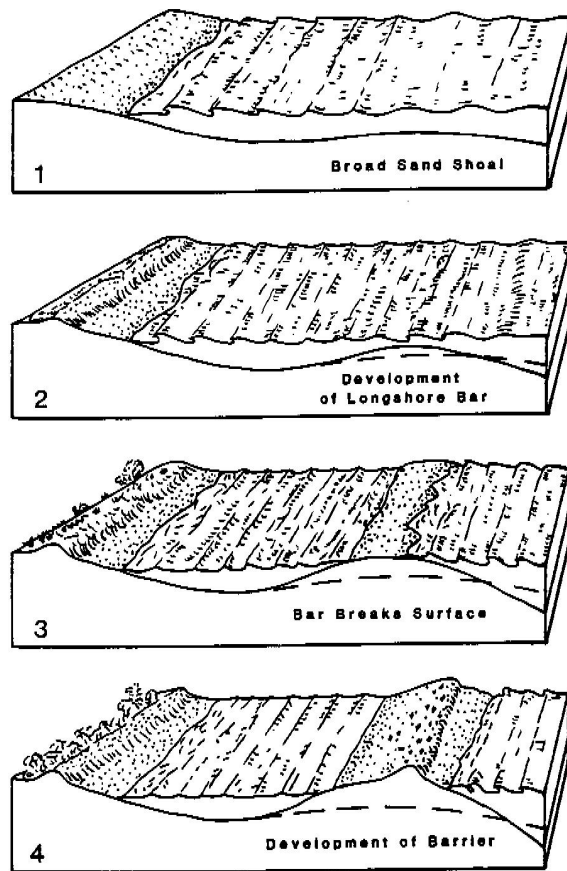


Figure 32: Offshore bar/shoal emergence model (from Leatherman, 1982).

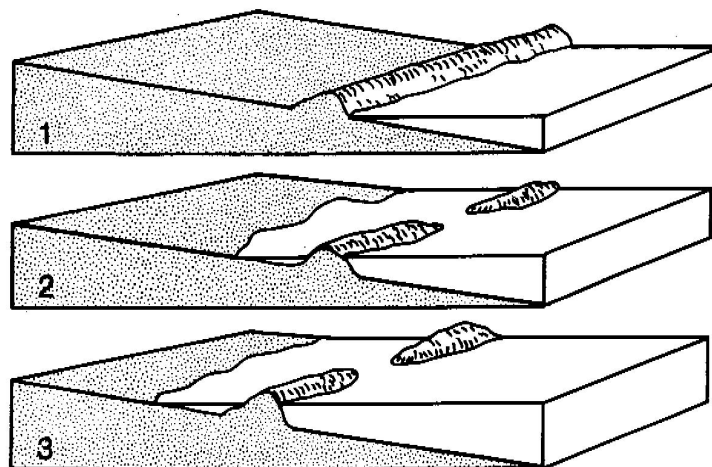
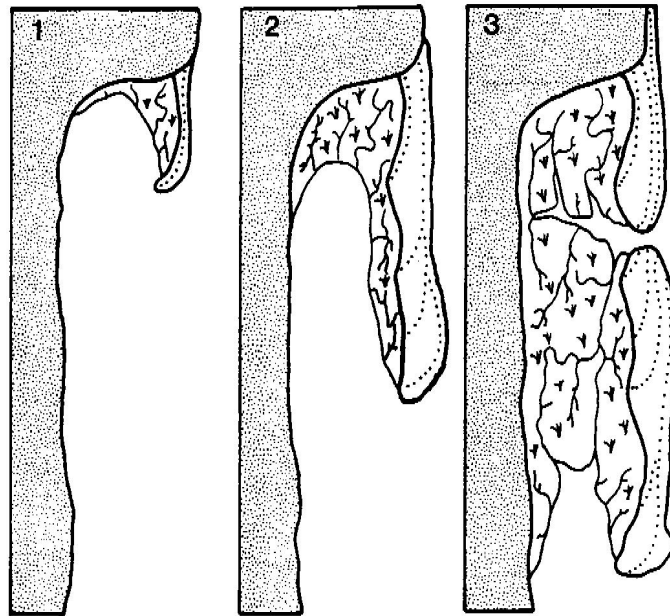


Figure 33: Mainland beach ridge submergence model (from Leatherman, 1982).



**Figure 34: Barrier island formation through spit elongation and island breaching model (from Leatherman, 1982).**

Demarest and Leatherman (1985) studied the Delmarva Peninsula and concluded the present-day configuration of the barrier islands and backbarrier bays of the Delmarva Peninsula are the product of wave climate, tidal energy, sediment texture, Pleistocene sediments, and antecedent topography. However, the morphology of the Delmarva Peninsula is significantly affected by Pleistocene sea-level change over the past million years, and Demarest and Leatherman identified several distinct transgressive events during interglacial high sea level from more than 1 million years to 60,000 years before the present day. The mainland shoreline closely corresponds to the location of Pleistocene beaches, and the authors believe the southern Delmarva barrier islands will



weld to the Pleistocene beach shoreline because of barrier rollover facilitated by a relative rise in sea level.

Furthermore, Oertel et al. (1989) examined the anatomy of the barrier platform of the outer barrier lagoon of the southern Delmarva Peninsula. A series of vibracores revealed a thick layer (7–9 m) of fine-grained sediment below the floor of the barrier lagoons. These sediments provide a platform of topographic highs composed of silt and clay for landward retreating barrier islands to roll over upon in response to overwash processes. Furthermore, the backbarrier lagoonal mud is dominantly pre-Holocene with marine microfauna, confirming the deposition occurred in a marine environment. In other words, Oertel (1989) demonstrates the importance of multiple transgressive events and their role in lagoonal development and barrier-island retreat along the southern Delmarva coast.

### **The Barrier-Island System**

A barrier-island system is a highly dynamic unit and must contain the following six interactive components: mainland, estuary, barrier islands, tidal inlets and deltas, barrier island platform, and shoreface (modified from Oertel, 1985). Oertel (1985:2) states the mainland “establishes an island as a barrier and is a necessary requirement for the designation of barrier island. Three major characteristics determine how the mainland interacts with the barrier island system: lithology, slope, and drainage.” An estuary is a backbarrier body of water that is a “depositional environment that separates the barrier island and associated inlets from the mainland.” A barrier island is the “subaerial expression of an accumulation of sediment between two inlets, and between the shoreface

and the backbarrier [estuary].” Komar (1976:13) defines a barrier island as “an unconsolidated elongated body of sand or gravel lying above the high-tide level and separated from the mainland by a lagoon or marsh.”

Oertel (1985:7) states that tidal inlets are “channels laterally adjacent to barrier islands that separate one island element from another or from a laterally adjacent mainland element” and deltas are “accumulations of sediment on the seaward (ebb-tidal delta) or landward (flood-tidal delta) side of inlets. The barrier island platform is “the stratigraphic substructure of a barrier island...and is primarily related to the origin and evolution of the barrier island system.” The shoreface is “the shore zone of ocean flood beyond the low tide line and is divided into two distinct zones.... [The] upper shoreface is dominated by shoaling and breaking waves and extends beyond the break point of storm waves while the lower shoreface is influenced by the combination of wave orbital current and inner shelf currents.” The evolution of one of these elements affects the adjacent environments, which in turn affects the entire coastal system. These six interactive elements have unique morphologic, sedimentologic, and stratigraphic characteristics and connections to the barrier island and the larger barrier-island system (Figure 35).

The strength and relative dominance of tidal energy versus wave energy greatly influences the morphology of barrier islands, the number and spacing of tidal inlets, and the foremost type of inlet delta located near the tidal inlet (Hayes, 1979; Hayes, 1980; Davis and Hayes, 1984; Hayes, 1994) (Figure 36). Hayes observed that shorelines with moderate wave energy exhibited fundamental differences in morphology because of

different tidal ranges. The approximate limit of barrier island formation on Figure 36 marks the line where macrotidal processes dominate and thus prevent the formation of barriers due to the predominance of strong tidal currents in a shore normal orientation.

Hayes developed a tidal range classification system, as follows:

- Microtidal: 0–1 m (e.g., Outer Banks, North Carolina)
- Low mesotidal: 1–2 m (e.g., Delmarva Peninsula)
- High mesotidal: 2–3.5 m (e.g., Georgia Bight)
- Low macrotidal: 3.5–5 m (e.g., German Bight)
- Macrotidal: >5 m (e.g., Bay of Fundy)

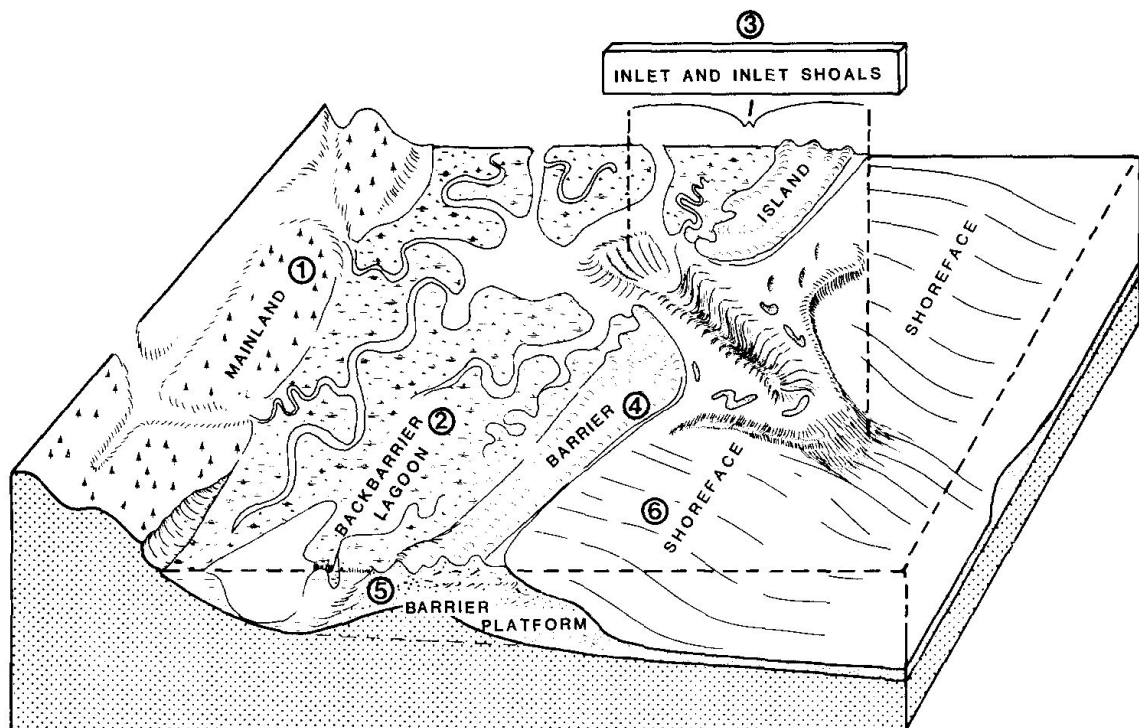


Figure 35: The six elements of a barrier island system (from Oertel, 1985).

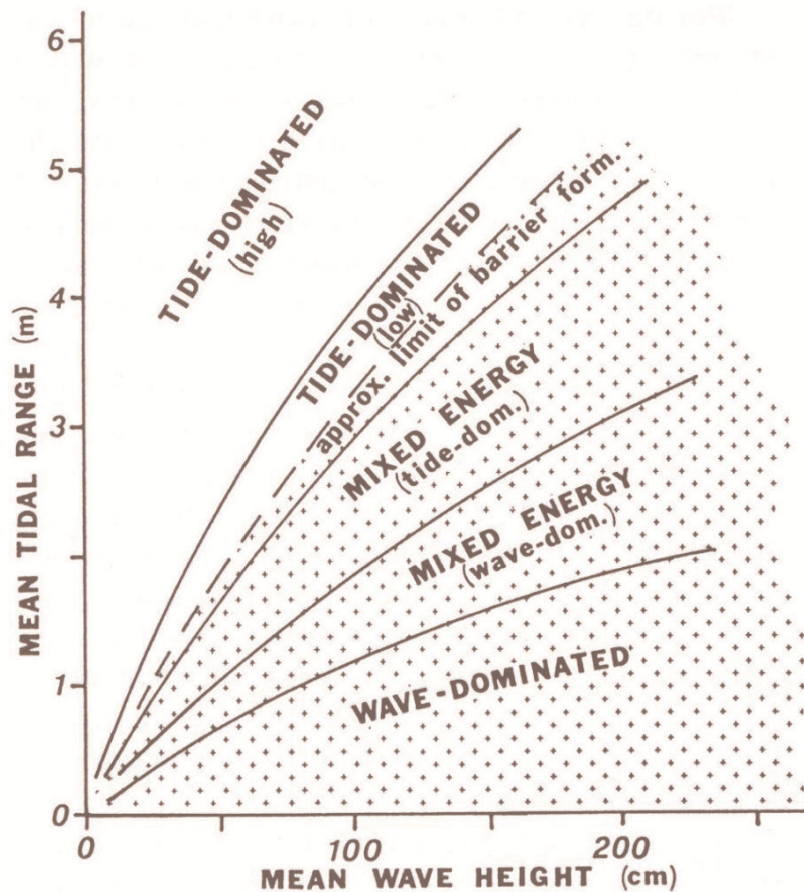


Figure 36: Relationship between wave energy and tidal energy and the effects on barrier island morphology (Davis & Hayes, 1984).

Higher tidal ranges and/or lower significant wave heights will produce tide-dominated conditions. In contrast, lower tidal ranges and/or higher significant wave heights will produce wave-dominated conditions. Tide-dominated barrier islands are short and wide with numerous and closely spaced tidal inlets. Wave-dominated barrier islands are long and narrow with few and widely spaced tidal inlets. The barrier islands along the southern Delmarva Peninsula exist in a mixed-energy environment with wave-dominated conditions prevailing to the north and tide-dominated conditions dominating

to the south (Oertel & Kraft, 1994). Barrier islands can also be classified as either high-profile or low-profile depending on the elevation of key shore features such as dune ridge height (Morton & Miller, 2005). Oertel and Kraft (1994) also demonstrate the influence of mainland topography on the location of coastal compartments with regional divides creating headland coasts, intermediate divides creating coastal lagoon systems, and small drainage divides determining the location of tide-dominated barriers; the former river channels/valleys (i.e., topographic lows) determine the locations of tidal inlets.

In the context of the Delmarva Peninsula, the coast is fronted by a wide, gently sloping continental shelf with the tidal cycle moving from north to south. The volume of water exchanged through a tidal inlet during each cycle is the same. However, a difference can exist between the amount of time necessary for the flood versus the ebb currents to flow. Along the southern Delmarva Peninsula, longer times equate to slower flow velocities (flood) and shorter times result in faster flow (ebb). The mean difference between rising and falling tides produces a mean ebb discharge along the southern Delmarva Peninsula, and as a result, the shorelines to the south have larger tidal ranges than the shorelines to the north (Leatherman et al., 1982).

## **Tidal Inlets and Tidal Deltas**

Tidal inlets are the primary channels separating barrier islands in a barrier-island system. The inlets are conduits for water and sediment between the estuary and the ocean. The dominant factors affecting tidal inlet morphology are tidal range, tidal prism, significant wave height, and the storage and geometry of the backbarrier bay (Fitzgerald & Fitzgerald, 1977; Nummedal & Fischer, 1978). Oertel and Kraft (1994) and Rice and Leatherman (1983) document the key role of tidal inlets in the configuration of the coastline along the Virginia barrier islands. The Parramore–Cedar barrier-island system is a mixed-energy, tide-dominated system resulting in the formation of large ebb shoals that store large amounts of sand along the oceanside margins of inlets.

Hayes (1979, 1980) and Boothroyd (1985) studied the general morphology and sediment patterns in tidal inlets, particularly the morphology of ebb- and flood-tidal deltas. Ebb-tidal deltas are seaward shoals, and flood-tidal deltas are landward shoals. An ebb-tidal delta is composed of a main ebb channel with channel margin linear bars along its flanks and a terminal lobe at the seaward end with a swash platform on both sides of the main channel (Figure 37). A flood-tidal delta is a fan-shaped sand body located immediately landward of a tidal inlet. A flood-tidal delta is composed of a flood ramp and bifurcating flood channels on the seaward side and ebb-oriented bedforms on the landward side (Hayes, 1980) (Figure 38). A flood-tidal delta is largely nonexistent at Wachapreague Inlet; however, anecdotal observations indicate the estuary landward of Wachapreague Inlet may be experiencing some infilling and shoaling (VIMS, 2011).

An ebb-tidal delta largely results from the interaction of tidal currents and waves. The concept of ‘time-velocity asymmetry of tidal currents’ plays an integral role in the development of an ebb-tidal delta’s morphology (Hayes 1980; Fitzgerald, 1982). Essentially, the maximum ebb current occurs late in the tidal cycle near low water, but as the water level rises, flood currents seek a path around the strong ebb currents. As a result, the flood currents travel along the marginal flood channels to begin flooding the backbarrier bay, as demonstrated in Figures 36 and 37. In addition, Fitzgerald (1988) showed that the size of an ebb-tidal delta and the absence of flood-tidal delta result from a large tidal range and small waves heights and the ratio of open water to marsh in an estuary.

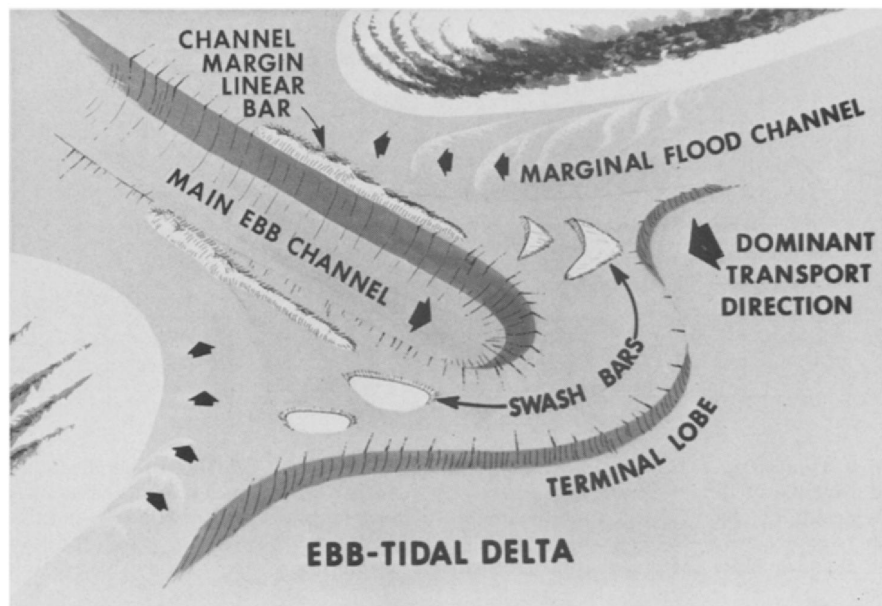
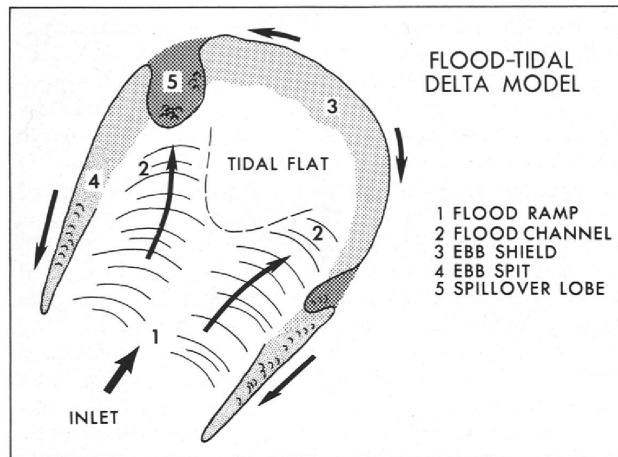


Figure 37: Hayes (1980) model of morphology of ebb-tidal deltas.



**Figure 38: Primary morphologic features of a flood-tidal delta (Hayes, 1980).**

Through a study of the sediment distribution and evolution of the tidal deltas of Wachapreague Inlet, Morton and Donaldson (1973) synthesized the factors exerting the greatest influence on tidal delta formation along the Eastern Shore, which are relatively stable, non-migratory inlets; erosional shorelines; a rise in relative sea level; a 1.3-m tidal range; and little freshwater input into the coastal system. Unlike many areas along the Atlantic coast of the United States where sediment originates from mainland drainage or local erosion, the sediment along the Virginia Eastern Shore is supplied by the Holocene barrier islands themselves and is reworked through longshore transport and tidal inlet processes. In addition, sediment borings of the ebb- and flood-tidal deltas of Wachapreague Inlet reveal the inlet has been relatively stable throughout the Holocene (Morton and Donaldson, 1973), and the primary tidal inlets are located in Pleistocene stream valleys (Halsey, 1979).

Inlets and their associated ebb- and flood-tidal deltas can have significant effects on adjacent barrier shorelines by affecting the distribution of wave energy and the storage

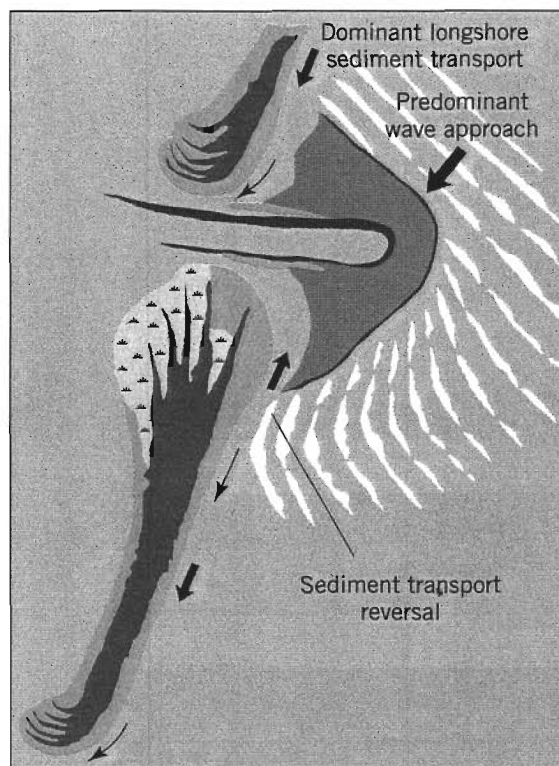


of sizable sediment reservoirs that are similar in volume to their bordering barrier islands (Fitzgerald, 1988; Fenster & Dolan, 1996; Fitzgerald et al., 2003; Davis, 2004; Fitzgerald et al., 2004). Sediment bypassing studies have shown sediment deposited on either ebb- or flood-tidal deltas originate from littoral sand entering a tidal inlet from an adjacent barrier island (Bruun & Gerritsen, 1959, Fitzgerald, 1982, Fitzgerald, 1988, Fenster & Dolan, 1996). In addition, relative sea-level rise, through the expansion of tidal prism, can restrict sediment supply to an adjacent barrier by trapping large amounts of sediment on ebb-tidal deltas (Fitzgerald et al., 2004; Miner et al., 2007; Fitzgerald et al., 2007). Furthermore, the dynamics of the ebb-tidal delta can produce substantial swings in shoreline position because of wave refraction, a local reversal in longshore sediment transport, and seasonal onshore/offshore sediment transport (Fitzgerald et al., 1984).

A local reversal in longshore sediment transport caused by wave refraction around the ebb-tidal delta creates the geomorphic response of rotational instability (Hayes & Kana, 1976) (Figure 39). Rotational instability describes a barrier island that rotates around a stable mid-point in response to advance and retreat at the other end of the island (McBride et al., 1995). Rotational instability is used to describe the net effects of retreat and advance in changing the shape and orientation of an island and not an actual physical rotation of the island. In other words, rotational instability is the product of net advance at one end of a barrier island and net shoreline retreat at the opposite end of a barrier island.

McBride (1999) studied the spatial and temporal distribution of historical and active tidal inlets along the Delmarva Peninsula and New Jersey. He clarified that the main factors controlling inlet behavior, distribution, and densities along the Delmarva

Peninsula are tidal range, wave energy (height), wave direction (littoral drift), tidal prism, and storm frequency and magnitude. McBride also further determined that the location and characteristics of a tidal inlet are also influenced by antecedent geology (Halsey, 1979; Boon and Byrne, 1981). Wachapreague Inlet is strongly influenced by tide-dominated processes and the antecedent geology naturally stabilizes the inlet.



**Figure 39: The drumstick barrier island model demonstrating a local reversal in sediment transport because of wave refraction around the large ebb-tidal delta (Hayes and Kana, 1976).**

Wachapreague Inlet conveys water to and from a system of backbarrier bays, salt marsh, and tidal channels behind Parramore and Cedar Islands. Wachapreague Inlet is characterized by a single, stable, deep channel and one of the largest ebb-tidal deltas of

the Delmarva Peninsula. Byrne et al. (1974) conducted a detailed multi-year study of the Wachapreague Inlet complex and determined the following: 1) direct wave activity affects the short-term cross-sectional area and ratio of ebb-tidal power to wave power, 2) the inlet is ebb dominant and possesses a strong natural flushing ability, and 3) the ebb-tidal delta delivers significantly more sand volumes to the inlet channel than estimated longshore sediment transport. A model of the dominant sand circulation loop between the channel and the ebb-tidal delta and flow characteristics of the inlet channel are represented in Figure 40. The results of the study also reinforced the importance of considering local sand circulation between an ebb-tidal delta system and the tidal inlet channel.

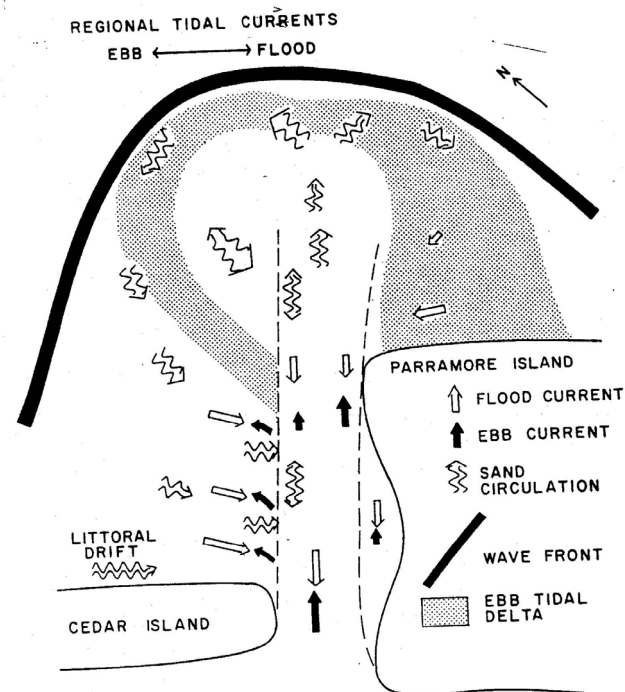


Figure 40: Schematic of Wachapreague Inlet sand circulation loop (Byrne et al., 1974).

## **Coastal Morphodynamics and Drivers of Shoreline Change**

The drivers (forcing mechanisms) of coastal change such as a rise in relative sea level, changes in sediment supply, and storm impacts are prominent subjects among scientists, engineers, and the various stakeholders in coastal communities. Identifying the signal of an individual driver of change in isolation among the noise of the other factors affecting a coastline and its larger impacts to the barrier-island system is challenging, especially over increasingly short time periods (Leatherman et al., 2000). In addition, the drivers of change that potentially contribute to coastal change operate at a variety of spatial and temporal scales. Many of the drivers of change act in concert or are affected by each other.

Long-term phenomenon such as relative sea-level rise or changes in sediment supply may occur over decades or hundreds of years, whereas short-term processes such as storm impacts may affect the coast ranging from hours to days to years. Rising sea level may affect large swaths of a coastline, whereas an individual storm may affect more severely discrete areas. The drivers of change affecting the barrier island system may function independently, but in reality, these separate but connected processes interact and influence each other to produce coastal change (Zhang et al., 2004).

### **Sediment Supply**

The long-term trends and behaviors of barrier island systems are intricately tied to regional sediment budgets (Curry, 1964; Fenster et al., 1993; Oertel & Kraft, 1994; Byrnes & Hiland, 1995). A sediment budget quantifies sediment sources, sinks, and pathways in a regional setting and helps to understand the large-scale dynamics of a

coastal system. An interruption in the updrift sediment supply in the longshore transport system may produce considerable impacts on downdrift barrier islands and inlet deltas (Fitzgerald et al., 2004, 2007, 2008). The Curray (1964) diagram (Figure 41) is significant in the context of potential drivers of change to a barrier-island system because it demonstrates shoreline movement is based on rates of net deposition and relative sea level. The Curray diagram visually outlines the conditions where a shoreline will either undergo transgression (landward shoreline movement) or regression (seaward shoreline movement) regardless of the forcing mechanism (e.g., sediment budget, relative sea-level changes, storm impacts). The vertical dashed line signifies a stable sea level and the diagonal solid line represents a stationary shoreline (no movement or dynamic equilibrium). The intersection of these two lines represents a stable relative sea level and a stationary shoreline position.

Erosion refers to the removal of material from one place and its transport to another location with a net sediment loss at the place of origin. Coastal erosion is a three-dimensional process that involves redistributing sediment throughout the various components of a coastal system (Rosati, 2005). In the case of a barrier island, for example, sediment may be transported to the landward side of the island because of storm-generated overwash processes. This situation represents shoreline retreat because the sediment stays within the barrier island system. However, if the sediment is removed from the beach and carried a significant distance offshore or along the shore, then this sediment is considered lost from the system.

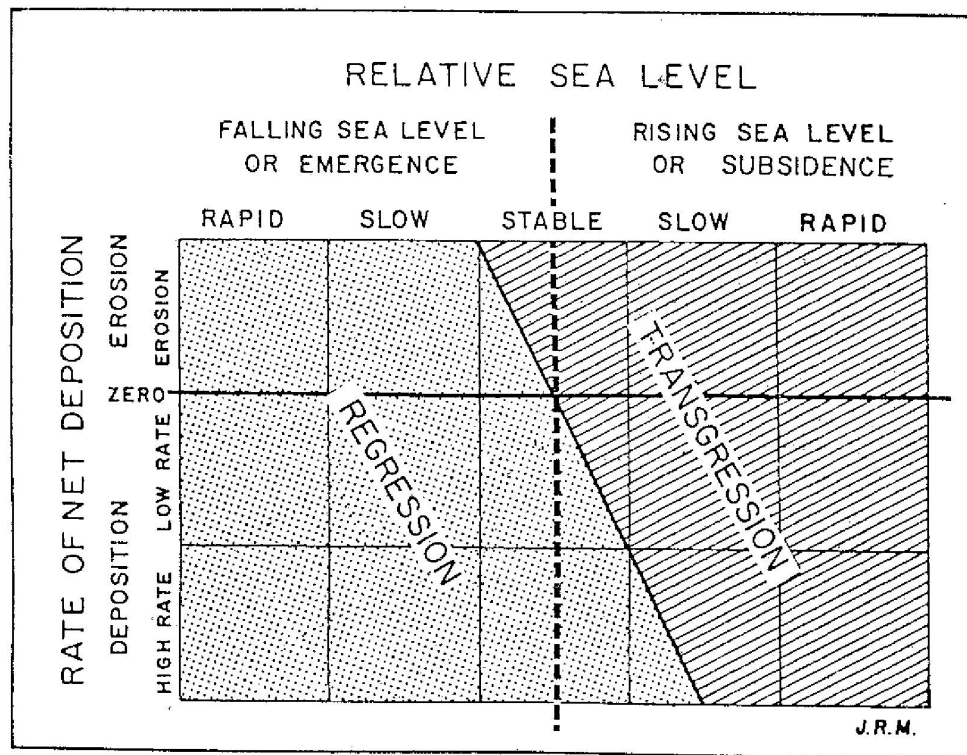
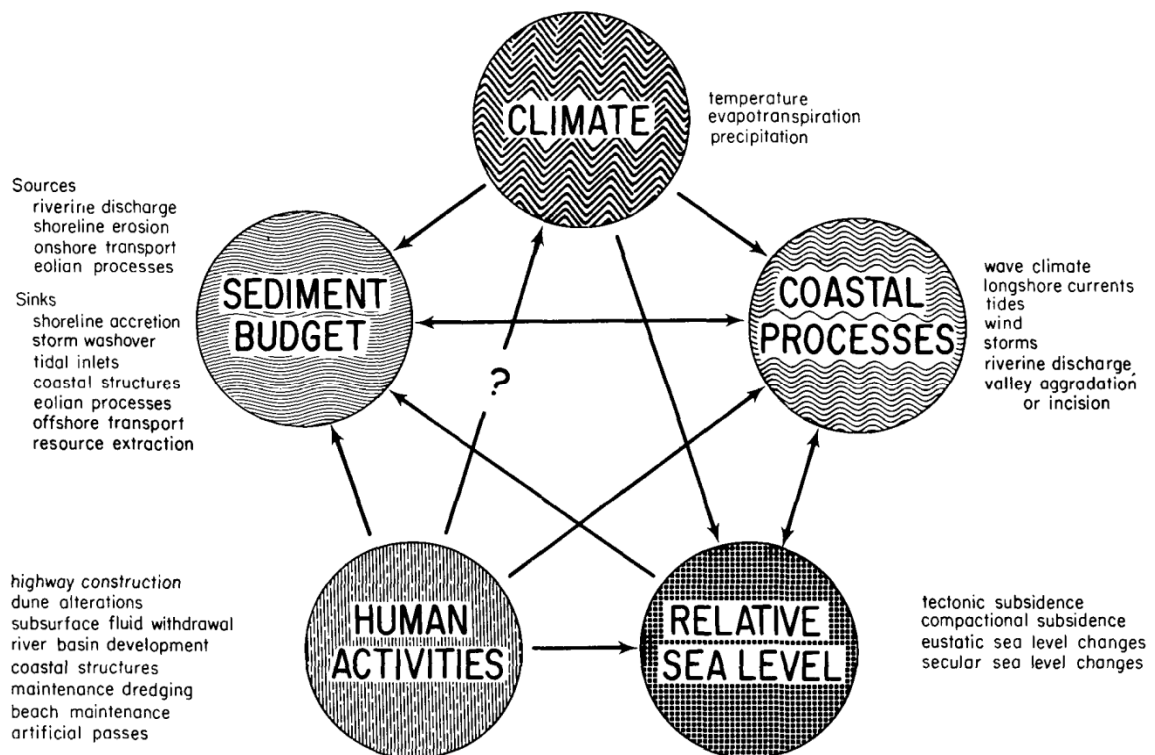


Figure 41: Curray (1964) diagram of the rate of change of relative sea level and rate of net deposition on the transgression (landward) and regression (seaward) movement of a shoreline.

Morton (1977) documented the temporal and spatial variations in the historical shoreline changes of the Texas Gulf Coast and their causes through sequential shoreline monitoring. Morton (1977) showed that shoreline erosion is caused by the interaction of factors that were grouped into several dependent variables; specifically, climate, coastal processes, relative sea level, human activities, and sediment budget (Figure 42). Moreover, Morton (1977) also established that jettied inlets and navigation channels serve as the greatest sediment sink and major shoreline changes are frequently the result of human impacts. Morton (1979) built upon this earlier work and demonstrated natural processes such as decreased sediment supply and relative sea-level rise are the primary

drivers of long-term shoreline retreat whereas short-term shoreline changes may reflect long-term trends, but they also reflect secular sea-level variations and human activities. In addition, Morton (1979) added further evidence that shoreline erosion is largely the result of decreases in sediment supply and relative sea-level rise and that the more short-term (historical) increases in shoreline erosion are likely related to an increased rise in relative sea level. However, Morton (1979) also added the acceleration of coastal erosion may signal the crossing of equilibrium where other factors such as human activities may play a more important role in system behavior.



**Figure 42: Interaction of factors affecting shoreline changes with arrows pointing towards the dependent variables and the number of arrows indicate the relative degree of independence or interaction (Morton, 1977).**

Kraft and Chrzastowski (1985) further developed an understanding of the processes of change that affect a shoreline area and listed the factors that most importantly influence a shoreline configuration and the characteristics of the coastal features (Table 7). It is difficult, if not impossible, to precisely isolate and quantify the relative influence of each factor upon a system, but Kraft and Chrzastowski (1985) demonstrate a full range of factors must be considered when attempting to determine the forces and processes affecting a shoreline. In other words, there is an overwhelming need to consider a full range of factors impinging upon the shoreline area and potential responses in contrast to analyzing form or response based only on one set of parameters.

Galgano (1998) conducted a geomorphic analysis of U.S. East Coast shoreline behavior and the influence of tidal inlets on coastal configuration in an attempt to establish the spatial extent of inlet influence on adjacent shorelines and arcs of erosion. Galgano (2009) further defined an arc of erosion as a mobile platform with a short initial arc of erosion with very high rates of erosion, and as the arc of erosion extends, the erosion rates are attenuated but the area of change remains constant. As such, over time the arc of erosion expands downdrift affecting progressively more shoreline to inlet-induced erosion and shoreline modifications extend downdrift indefinitely.



Table 7: Processes of coastal change (Kraft and Chrzastowski, 1985).

- A. Local tectonism
  - possibility of short-term emergence or submergence
- B. Regional tectonism
  - the possibility of complete emergence of the basin or possibility of continuous or discontinuous submergence of the entire basin
- C. Eustatic change
  - world's sea-level fluctuation which, in its most simple form, will lead to direct transgression or regression of the marine environment
- D. Tectonism in the hinterland
  - uplift or downwarp and its effect on increasing or decreasing amount of erosion
- E. Climatic change in the hinterland
  - effect on erosion and transportation of sedimentary products out of the area to the shoreline
- F. Climatic change in the depositional area
  - effect on the ability of deposition to take place in "normal" process forms and the potential for rapid alteration of the depositional product
  - in the tropics, the possibility of carbonate depositional forms; in the Arctic, severe alteration of process forms
  - the strong possibility of altering the vegetational forms that may control deposition in the shoreline area
- G. The overall tectonic-depositional setting
  - geosynclinal basin—length, width and thickness
  - Compaction rates
  - Geologic history of the basin
- H. Ocean currents and wave regime
  - the most important single factor in the formation of a shoreline is the imposition of waves and their form as they come in contact with shallow marine areas and modify their form and energy toward the shoreline
  - the nature and frequency of high-intensity events, such as hurricanes
  - the possibility of directed current, such as oceanic currents, impinging on the shoreline area
  - tidal effect, tidal currents, tidal range frequencies, etc.
- I. Source and type of sediment
  - Distance from detrital sediment source
  - Transportation energies and types
  - Contribution source—is it direct from the continent or is it indirect and by reformation of other nearby shoreline elements of the same geologic age and time event?
  - No terrigenous sediments available—biogenic and chemical precipitants only available source
- J. Man's intrusion into the shoreline zone
  - Man's alteration of the hinterland and changes in the sedimentary erosion, transportation, and depositional patterns

Galgano (1998) determined that tidal inlets strongly affect shoreline trends and behavior, and in fact, shoreline changes are unremarkable outside of the influence of tidal inlets and seldom exceed  $\pm 1.0$  m/yr. In addition, Galgano (1998) correlated the age of an inlet and the volume of net longshore transport to the spatial extent of an arc of erosion. The findings from his study showed that an arc of erosion has no downdrift termination temporally and the length of the arc expands at a non-linear rate. Furthermore, the arc of erosion creates specific geomorphic and sedimentary response types and areas within the arc of erosion are predisposed to inlet breaching.

Galgano (2007) built upon this previous research to study beach erosion anomaly areas (EAAs) and how stabilized tidal inlets create perhaps the most spatially extensive and destructive hotspots. Galgano (2007) classified the Virginia barrier islands as a prime example of an EAA occurring over a millennia time scale along a large (25–100+ km), natural, coastal compartment (Figure 43). Furthermore, Galgano (2007) identified that the absence of an adequate sediment supply interrupts large-scale behaviors within a coastal compartment and subsequently causes downdrift sediment starvation. In other words, sediment supply is the key variable for the creation of an EAA when other variables remain unchanged over long periods of time. And finally, Galgano (2007) proposed a classification scheme for the Eastern U.S. coast and defined an erosion anomaly area as “a segment of beach that is eroding at least two times the rate of adjacent beaches within the same geographic unit.” Furthermore, Galgano (2009) used an historical trend analysis of long-term shoreline change data to determine the temporal and spatial behavior of beaches adjacent to tidal inlets (Figure 44).

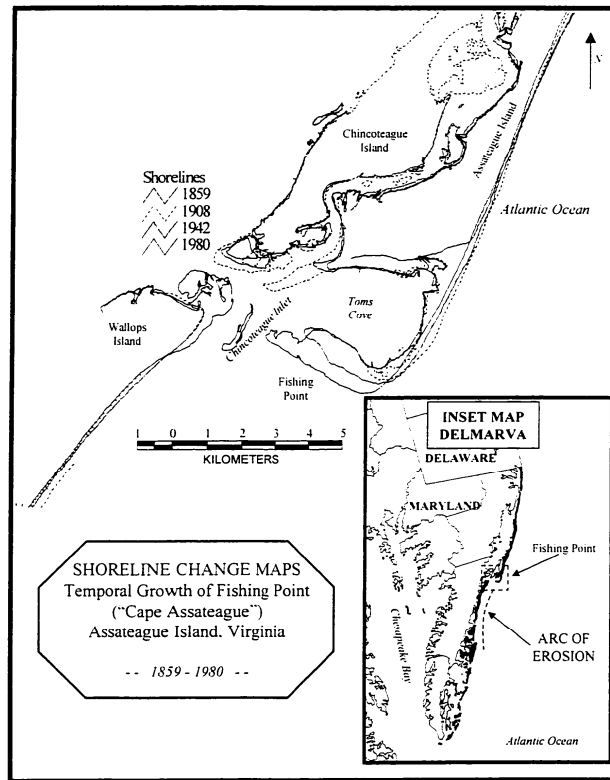


Figure 43: Temporal growth of Fishing Point, Virginia and the arc of erosion on the southern Delmarva Peninsula (Galgano, 1998).

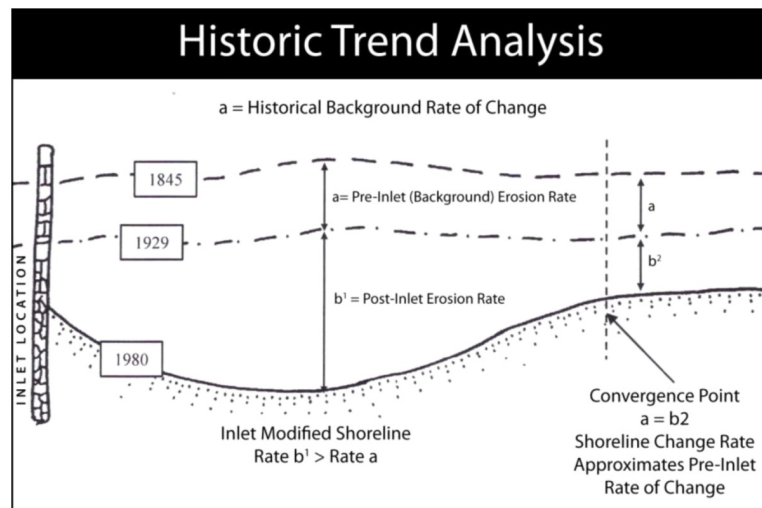


Figure 44: Historic trend analysis of inlet-induced shoreline behavior demonstrating pre-inlet and post-inlet shoreline trends and determination of the distance downdrift where inlet influences ceases (Galgano, 2009).

## **Storminess**

Storms can play a major role in coastal morphology and also cause significant coastal change because of beach and dune erosion, overwash processes, and the opening of new tidal inlets. The high-energy conditions that characterize a storm—large waves, elevated water level, and strong longshore currents—may cause a significant movement of sediment through the following: 1) landward washover, 2) offshore transport, and/or 3) longshore transport (Sallenger, 2000). In fact, a sandy coast may lose sediment through all these processes during a storm. In addition, strong winds may cause a rise in water level along a shoreline. During a storm, the piling up of water along a shoreline because of strong onshore winds is commonly termed storm surge.

The two primary types of coastal storms are extratropical cyclones and tropical cyclones. The southern Delmarva Peninsula is squarely situated in the mid-latitudes and is affected by both of these storm types during a year. Extratropical storms are often referred to as northeasters because the onshore winds are from the northeast in response to the counterclockwise rotation of the winds in the northern hemisphere. The U.S. mid-Atlantic coast typically encounters dozens of cold fronts per year with the strongest storms occurring in late winter and early spring. Northeasters are a more important change agent than tropical storms because of their longer duration, large geographic extent, and higher occurrence frequency (Dolan and Davis, 1992; Zhang et al., 2001). The spatial configuration of an affected coastal area is also a factor in the extent and type of impacts resulting from these storms.

Sallenger (2000) developed a storm impact model for barrier islands that categorizes storm-induced patterns and magnitudes of net erosion and accretion on barrier islands by representing thresholds where processes and magnitudes of impacts change progressively (Figure 45). The greater potential hazard progressively increases over four distinct regimes: 1) swash, 2) collision, 3) overwash, and 4) inundation. The various stages of the model account for dune erosion, onshore transport through overwash processes, and onshore transport through inundation. Post-storm beach surveys and profiles can quantify the net change produced by a storm.

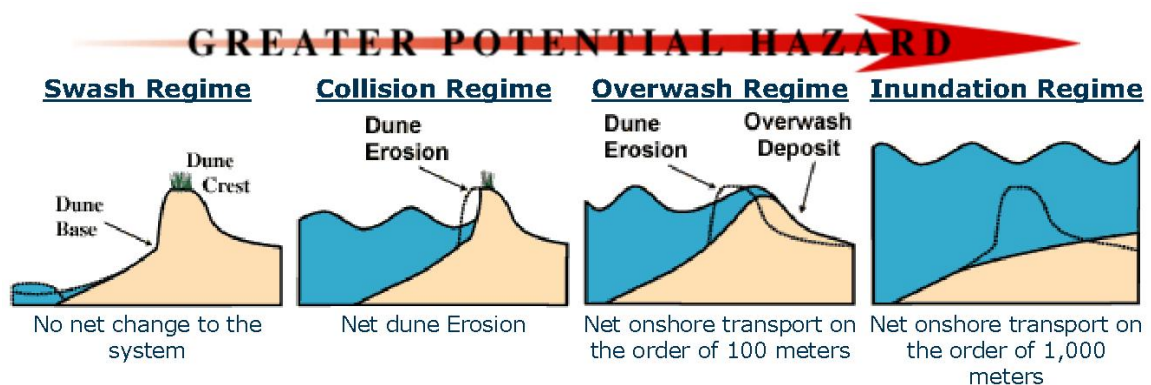


Figure 45: Storm impact model for barrier islands (Sallenger, 2000).

### Relative Sea-Level Rise versus Storm Activity as Principal Drivers

Leatherman et al. (2000) and Zhang et al. (2004) suggest that relative sea-level rise is the primary enabler of long-term coastal erosion and the problem will only increase with further global warming. A rising relative sea level in itself does not generate significant coastal erosion, but a heightened sea level enables storms and their

associated waves to reach further inshore and thereby force the landward movement (transgression) of a shoreline (Bruun, 1962; Leatherman et al., 2000; Leatherman & Douglas, 2003; Zhang et al., 2004; Fitzgerald et al., 2007; Fitzgerald et al., 2008). A global rise in sea level has occurred over the past century, and more specifically, sea level has risen 20–40 cm along the U.S. East Coast in the past 100 years (Douglas, 1991).

Zhang et al. (1997, 2002) and Zhang (1998) conclude no significant long-term trend of increased storm activity occurred along the U.S. Atlantic coast during the 20<sup>th</sup> century. Zhang et al. (2001), with the development of a storm erosion potential index, conclude that storm impacts are strongly dependent on storm tide (astronomical tide and storm surge). These two observations (importance of storm tides and relative sea-level rise) strongly suggest that even with the absence of an increase in storm activity, a rise in relative sea level can alone create the conditions for increased erosion and washover on barrier islands. This hypothesis is supported by Bruun (1962), who states the rate of coastal erosion can be many multiples even over 100 times the rate of relative sea-level rise because a rising sea level allows storm tides and waves to affect ever greater reaches of the backshore. Furthermore, Zhang et al. (2001) also demonstrate with a storm erosion potential index that the Delmarva coast is one of the most highly vulnerable regions to storm-induced erosion along the U.S. Atlantic coast due to the impacts from northeasters.

Many researchers such as Leatherman et al. (2000a) and Zhang et al. (2004) reached the conclusion that a long-term rise in relative sea-level is the predominant cause of shoreline erosion along the U.S. Atlantic coast. However, Pilkey et al. (2000), Sallenger et al. (2000) and Galvin (2000) reach different conclusions specifically related

to the use of the Bruun Rule, techniques of subsetting data, and perceived subjective correlations. Furthermore, much of this research does not address storms and, more specifically, Fenster and Dolan (1994) concluded that nearly two thirds of the U.S. Atlantic shoreline underwent a significant change in the long-term change rates during the 1960s. Fenster and Dolan (1994) link this adjustment in the long-term rate of shoreline change to a peak in extratropical storm frequency and magnitude that occurred around 1967–1968. Short-term events such as storms are cyclic and low frequency and have been traditionally considered as noise in the long-term trend. In contrast, Fenster et al. (2001) demonstrate that the frequency and magnitude of storms influence long-term shoreline changes. As a result, storms can contribute to the signal of shoreline movement and do not represent data outliers. However, Douglas et al. (2002) conclude that the analysis of Fenster et al. (2001) was based on an unrealistic definition of a storm-influenced shoreline and thus an incorrect analysis of their data.

The debate between Douglas et al. (2002) and Fenster et al. (2001) on whether to include or exclude storm-influenced data in a shoreline change analysis centers on the issue of whether storms contribute to long-term shoreline behavior (signal) or if they are merely short-term fluctuations (noise) in the long-term trend. Honeycutt et al. (2001), Douglas and Crowell (2000), and Leatherman et al. (2000a) analyzed past trends to predict future shoreline positions based on a subset of shoreline positions (non-storm-influenced data). However, Fenster et al. (2001, 2003) selected an approach that incorporated storm-influenced data points in a shoreline analysis in an attempt to quantify the influence of storms upon long-term shoreline trends. The results of these various

studies show that no single “correct” approach exists for treating post-storm data because of the variability in storm response along the U.S. mid-Atlantic coast.

The lack of a single approach for treating post-storm data is a critical point because a comprehensive model that couples physical processes to shoreline responses does not exist as a result of the inherent difficulties associated with modeling the real-world complexities of the shoreline process-response system (Fitzgerald et al., 2008). Existing shoreline change studies use time as a proxy for all the processes that produce shoreline responses. Dolan et al. (1991) state that shoreline rate-of-change statistics are expected to reflect a cumulative summary of the processes that have affected the coast through time. Of course, the main problem with this approach is what has occurred in the past may not accurately model current or future conditions. In addition, data collected by happenstance rather than through a systematic sampling program may be too noisy to be useful. I conclude that the decision whether to include or exclude storm-influenced shoreline data from an assessment of historical shoreline change or predictions of future shoreline positions should be made on a case-by-case basis. The shorelines observed during the course of this study were not surveyed immediately following a high-magnitude storm event. However, the vast majority of the shorelines were collected in late spring where the cumulative effects of the multiple northeasters or perhaps an individual storm may have affected the barrier island from late fall to early spring.

## **Coastal Change Studies**

The quantity of case studies and the wide range of research pertaining to barrier islands and tidal inlet change, and more specifically the Parramore–Cedar barrier-island



system, are much too large to fully review in this short amount of space. Several key studies have been conducted on similar barrier-island environments and serve as the solid building blocks of this research. Noteworthy studies of the southern Delmarva Peninsula and the Parramore–Cedar barrier-island system not stated previously include, but are certainly not limited to, the following.

Davis and Fox (1974) examined the process-response patterns in beach and nearshore sedimentation on Cedar Island and discovered the absence of nearshore sand bars allows wave energy to be imparted on the beach. In addition, patterns of accretion and erosion are related to barometric pressure and wave refraction with storms causing upper beach erosion, lower beach deposition, and swell waves generating widespread foreshore erosion. Boon (1975) examined the tidal discharge asymmetry of the salt marsh drainage system near Wachapreague and determined a pronounced asymmetry in curves of discharge and current speed through time. An apparent difference in flood and ebb flows may have a systematic, long-term influence on the net transport of sediment entering and leaving the backbarrier bay. Rice et al. (1976) developed a thorough and well-documented historical and environmental review of The Nature Conservancy's Virginia Coast Reserve. The report examines the land-use history, climate and soils, geology, flora, and fauna of the Virginia barrier islands. Dolan et al. (1979) developed a shoreline mapping technique, analyzed shoreline erosion rates along the middle Atlantic coast of the United States, and predicted the development of cape-like features along the Virginia shoreline. The analysis of his data shows that the average rate of shoreline recession is -1.5 m/yr with rates as much as 10 m/yr for the Virginia barrier islands.

Goettle (1981) documented the geological development of the southern portion of Assateague Island and proposed a model of progressive spit elongation and the growth of a series of spits during the late Holocene. The research documented all but the youngest spit (e.g., Fishing Point) has been eroded to some degree by landward migration of the barrier, by inlet formation, and by tidal currents. Leatherman et al. (1982) conducted a reappraisal of the Virginia barrier-island configuration model and concluded a smoother shoreline configuration of Virginia shorelines can be anticipated in the future.

Leatherman et al. (1982) divided the 12 Virginia barrier islands into three groups based on historical retreat rates and characteristics and disagreed with the conclusions of Dolan et al. (1979) in regard to the development of cape-like features.

Belknap and Kraft (1985) studied the influence of antecedent geology on stratigraphic preservation potential land evolution of Delaware's barrier systems. Byrnes (1988) developed a shoreline response model for low-profile barrier systems based on the Holocene geology and migration of Metompkin Island. Gaunt (1991) studied the evolution and potential causal mechanisms of Cedar Island from 1852 to 1986 in an effort to clarify barrier-island response to sea-level rise and also examined the events on Metompkin Island in an attempt to clarify Cedar Island changes. Gaunt's (1991) analysis shows Cedar Island was positionally stable while thinning at varying rates with an increase after 1962.

Harris (1992) studied the historical geomorphology of Hog Island through an analysis of historical shoreline charts, aerial photography, juxtaposition of landforms, and the physical characteristics of the island. Harris (1992) also examined larger trends on the

Virginia barrier islands, noting system-wide changes around 1871. Coastal change studies that utilize geospatial datasets and technology have the ability to examine coastal landforms and quantify morphological processes at various spatial and temporal scales using a variety of techniques, as documented by several studies (e.g., Byrnes et al., 1995; McBride & Byrnes 1997; and Morton & Miller, 2005). McBride et al. (1995) identified geomorphic response types for barrier coastlines based on quantitative documentation of historical changes in shoreline position over a period of nearly 150 years. Eight primary geomorphic response-types were classified including 1) lateral movement, 2) advance, 3) dynamic equilibrium, 4) retreat, 5) in-place narrowing, 6) landward rollover, 7) breakup, and 8) rotational instability. This megascale study illuminated important form/process relationships in coastal depositional systems and reinforced that rates of relative sea-level rise and sediment supply are major factors in controlling the occurrence of geomorphic response types. Parramore and Cedar Islands demonstrate a wide range of these geomorphic response types over the historical period of record, as will be demonstrated in this study.

Studies of coastal environments are generally hampered by the limited accurate datasets, but historical data sets such as NOS T-sheets, H-sheets, and aerial photographs provide critical sources of quantitative data about past coastal environments and can serve as a baseline for future projections, as analyzed and discussed by Anders and Byrnes (1991), Crowell et al. (1991), Crowell et al. (1993), and Byrnes et al. (2003). Fenster and Dolan (1996) assessed the impact of tidal inlets on adjacent barrier island shorelines, and one of the study areas was Wachapreague Inlet. The research quantified

the maximum distance of inlet influence extends 6.8 km updrift and 5.4 km downdrift of inlets along the Virginia barrier islands. In addition, shoreline changes can be dominated by inlet processes to a maximum distance of 4.3 km.

Honeycutt and Krantz (2003) studied the influence of the geologic framework on spatial variability in long-term shoreline change from Cape Henlopen to Rehoboth Beach, Delaware. Although outside the area of this study, it does provide important insights into regional behavior. The ability to study coastal change has continued to improve with the maturation of geospatial technology and wider access to geographic data—specifically, the development of geographic information systems (GIS), global positioning systems (GPS), airborne Light and Detection and Ranging (LIDAR) technology, and high-resolution bathymetric surveys (Boak & Turner, 2005). Moore et al. (2006) compared mean high water and high water line and how the selection of a proxy affects a shoreline change analysis. The research illustrated the complexity associated with mapping the high water line and calls into question the use of a wetted bound or high tide marks as a high water line proxy; however, shoreline change rates themselves are not likely to be significant. Hobbs et al. (2008) provide a broad overview and summary of the coastal processes and offshore geology of Virginia and advance the understanding of the interactions of waves, tidal currents, sea-level rise, and antecedent geology on the coastal geology of the Virginia barrier islands. Finally, Richardson and McBride (2007) conducted a shoreline change analysis of Parramore Island and subsequently followed up with a shoreline change analysis of Cedar Island (Richardson & McBride, 2011).

## **CHAPTER FIVE: RESULTS**

Chapter Five presents the findings of the shoreline change analysis of Parramore and Cedar Islands and the morphodynamic changes at Wachapreague Inlet. The long-term and short-term shoreline change rates are compared and contrasted by geomorphic zones and various time periods using a host of statistical measurements. An in-depth analysis of individual shoreline cells and, in particular, the non-inlet-influenced open-ocean shorelines and the tidal inlet shorelines are studied in greater detail. This chapter also reviews the historical and contemporary changes in cross-sectional area of the inlet throat at Wachapreague Inlet and their relation to spring tidal prism and ebb-tidal delta sand volumes.

### **Parramore Island**

Figure 46 is a reference map of the historical shorelines used in the Parramore Island shoreline analysis. More specifically, the shoreline dates are from the years 1852, 1871, 1910, 1942, 1962, 1998, and 2010). As mentioned in the Methods chapter, Parramore Island's shoreline is segmented into six shoreline cells—Cell 0: the northern, bay-side shoreline; Cell 1: the northern, Wachapreague Inlet-throat shoreline; Cell 2: the northern, inlet-influenced shoreline; Cell 3: the north-central, open-ocean shoreline; Cell 4: the southern, washover-dominated, open-ocean shoreline; and Cell 5: the southern spit shoreline. Table 8 compiles end point rates by shoreline cell throughout a series of six

incremental time periods: 1852–1871, 1871–1910, 1910–1942, 1942–1962, 1962–1998, and 1998–2010. The table is organized by incremental time periods to eliminate the weighting of historical data points on the rates of progressively more modern time periods. This approach highlights shoreline change rates during distinct time periods within the entire period of record and helps to define switches in the trend of shoreline migration.

Additional shoreline change statistics such as the linear regression rate are also used in the cell by cell analysis. Specifically, the long-term (1852–1998) and short-term (1998–2010) end point and linear regression rates (m/yr) by shoreline cell are presented in Table 9. This table allows for the easy comparison of EPR and LRR rates for individual shoreline cells across the long-term and short-term time periods. Particular attention is paid to the non-inlet-influenced, open-ocean shoreline (Cells 3–4). Figure 47 shows the overall linear regression rate of Cells 3–4 and includes a chart with a trendline that demonstrates the magnitude of change over the entire period of record. Finally, the long-term and short-term linear regression rates of the alongshore changes of Cells 3–4 are spatially correlated to the compiled shorelines of Parramore Island in Figure 48. Using the same spatially correlated map/graph template, the long-term linear regression and the long-term weighted linear regression rates are compared in Figure 49.

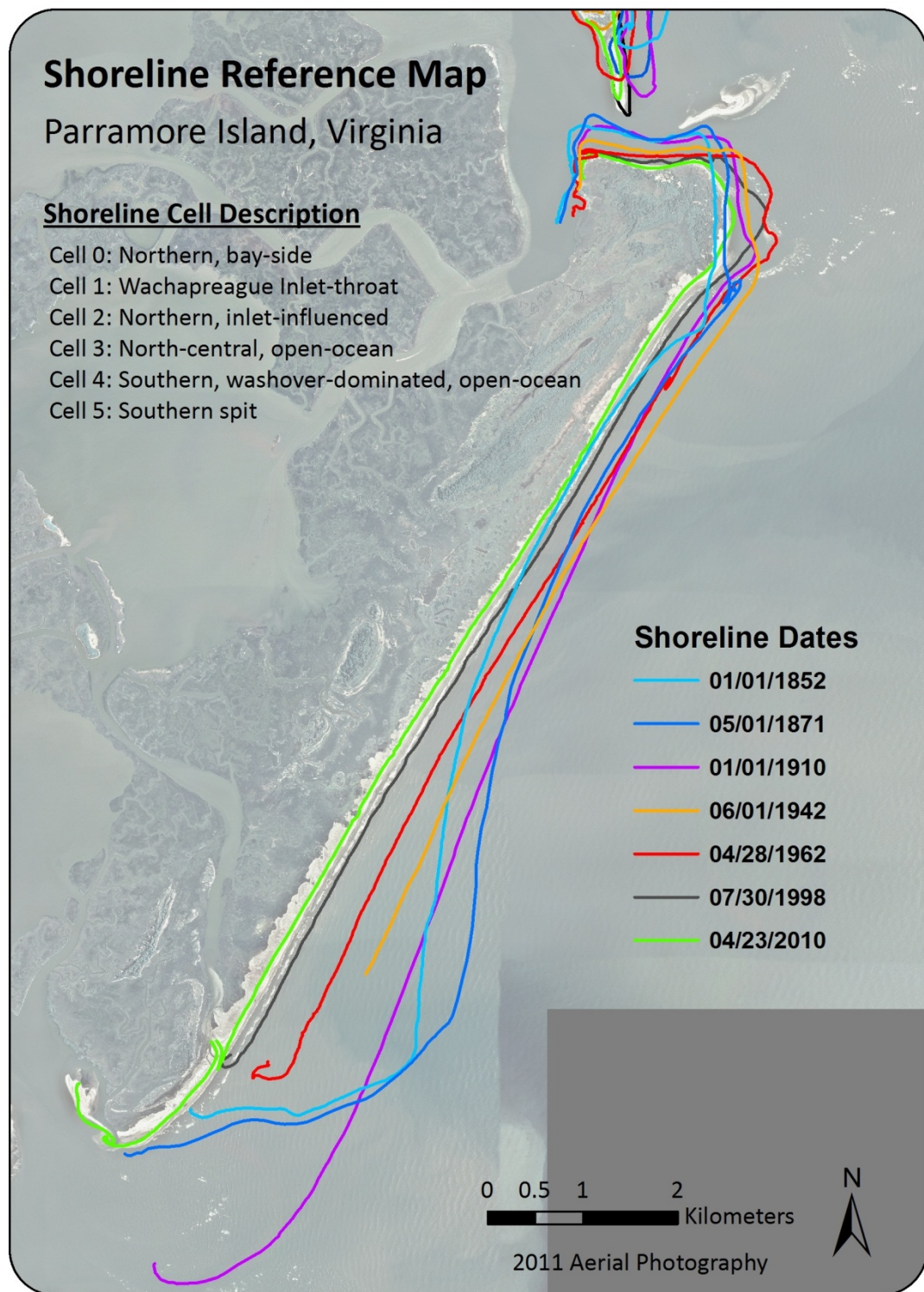


Figure 46: Parramore Island shoreline reference map.

**Table 8: Comparison of long-term incremental time periods by end point rate (m/yr) and shoreline cell of Parramore Island, Virginia**

**Shoreline Change Summary of Parramore Island, Virginia**  
Comparison of Long-Term Incremental Time Periods by  
End Point Rate (m/yr) and Shoreline Cell

Shoreline Cell	1852-1871	1871-1910	1910-1942	1942-1962	1962-1998	1998-2010
0	-1.9	-1.8	-0.3	1.0	x	x
1	1.4	-0.7	-4.1	-3.4	-1.2	-3.6
2	7.5	1.8	4.2	-1.2	-4.7	-16.2
3	15.4	1.8	0.2	-7.5	-6.7	-12.5
4	16.8	-7.3	-9.8	-14.9	-10.5	-14.6
5	11.4	30.7	x	x	x	x
3-4	16.1	-2.5	-3.5	-10.2	-8.5	-13.5

**Cell Definitions**

Cell 0: Northern, bay-side

Cell 1: Wachapreague Inlet-throat

Cell 2: Northern, inlet-influenced, open-ocean

Cell 3: North-central, open-ocean

Cell 4: Southern, washover-dominated, open-ocean

Cell 5: Southern spit

Cells 3-4: Non-inlet influenced, open-ocean

(-) sign indicates shoreline retreat and a positive integer signals advance.

(x) sign indicates no data is available for specified time period.



Table 9: Long-term (1852–1998) and short-term (1998–2010) end point and linear regression rates (m/yr) by shoreline cell of Parramore Island

### Shoreline Change Summary of Parramore Island, Virginia

Long-Term (1852-1998) and Short-Term (1998-2010)  
End Point and Linear Regression Rates (m/yr) by Shoreline Cell

Shoreline	1852-1998		1998-2010	
	EPR	LRR	EPR	LRR
Cell 0*	-0.7	-0.7	-1.5	-1.3
Cell 1	-1.7	-2.0	-3.6	-3.9
Cell 2	1.1	1.4	-16.2	-11.6
Cell 3	-0.1	-0.3	-12.5	-11.4
Cell 4	-7.0	-8.3	-14.6	-13.2
Cell 5**	19.6	20.2	-17.5	-18.2

\* Date ranges for Cell 0 are 1852-1962 and 1999-2010 due to an absence of data in 1998.

\*\* Date ranges for Cell 5 are 1852-1910 and 2005-2010 due to an absence of data in 1998.

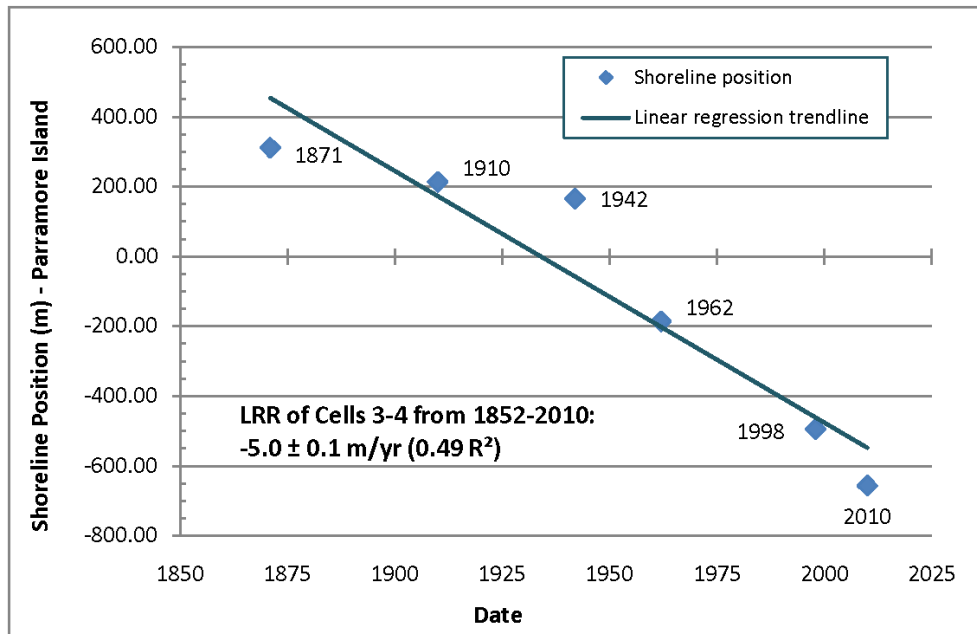


Figure 47: Magnitude of change with linear regression rate and trendline of Parramore Island (1852 to 2010) for Cells 3-4 normalized to the 1852 shoreline.

### **Cell 0: Northern, Bay-Side Shoreline**

Cell 0 is the northern, bay-side shoreline. Cell 0 is not the focus of the study because it is a bay-side shoreline, but the results are reported. The incremental end point rates show the northern, bay-side shoreline switched from a low retreat rate to a low advance rate during the historical period of record. From 1852 to 1871 the shoreline migrated -1.9 m/yr, and from 1871 to 1910, the rate was similar at -1.8 m/yr. The rate slows to -0.3 m/yr from 1910 to 1942 and then switches direction by advancing at 1.0 m/yr from 1942 to 1962.

Observations of the 1962 to 1998 and 1998 to 2010 time periods are not possible because of an absence of data in 1998. However, the end point rate of -1.5 m/yr is available from 1999 to 2010. The long-term EPR from 1852 to 1962 is -0.7 m/yr and the LRR for the same time period is also -0.7 m/yr (0.58  $R^2$ ). The short-term LRR from 1999 to 2010 is -1.3 m/yr (0.80  $R^2$ ). It is notable that the short-term EPR of -1.5 m/yr covering the entire short-term period of record (1999 to 2010) closely corresponds to the historical shoreline change rates evident in the incremental time period end point rates. Hence, little variation occurs in the shoreline change rate across the period of record and the results from the long-term and short-term calculations are in the same order of magnitude.

### **Cell 1: Wachapreague Inlet-Throat Shoreline**

Cell 1 is the Wachapreague Inlet-throat shoreline. The end point rates demonstrate the cell migrated to the north at 1.4 m/yr from 1852 to 1871 but then switched to a sustained pattern of southerly migration throughout the remainder of the time periods. The lowest rate of southerly migration from 1871 to 1910 immediately follows the only

time period of northerly migration (1852 to 1871). The highest rate of southerly inlet movement, -4.1 m/yr, occurs from 1910 to 1942. The migration rate for the following two time periods shows a slowing of the southern migration rate with -3.4 m/yr from 1942 to 1962 and -1.2 m/yr from 1962 to 1998. However, the 1998 to 2010 time period is the second highest southern migration rate among all incremental time periods at -3.6 m/yr.

The overall EPR of Cell 1 over the long-term record (1852 to 1998) is -1.7 m/yr and the LRR is -2.0 m/yr ( $0.87 R^2$ ). The highest final LRR across all time periods within the long-term record occurs from 1910 to 1962; -3.9 m/yr ( $0.99 R^2$ ) (Appendix A). The WLR and LMS values of -2.0 m/yr closely correspond to the EPR and are identical to the LRR. However, an examination of the short-term record (1998 to 2010) highlights differences between the long-term and short-term records.

Over the entire short-term record, the EPR is -3.6 m/yr, the LRR is -3.9 m/yr ( $0.83 R^2$ ), and the LMS is -3.4 m/yr (Appendix A). The highest rates of shoreline migration in the short-term occur from 05/2000 to 2010 with an EPR and LRR rate of -4.7 m/yr ( $0.88 R^2$ ).

The shoreline change results from Cell 1 show the Wachapreague-Inlet throat shoreline has migrated to the south at a generally consistent rate throughout the vast portion of the historical record. It is noteworthy that a shift occurred from northern to southern movement between the time periods of 1852–1871 to 1871–1910, and this trend of southerly migration continues today. In addition, the shoreline migrated to the south at higher rates during large segments of the 20<sup>th</sup> century when compared to the overall EPR, LRR, WLR, and LMS rates from 1852 to 1998. In other words, the data from 1852 to

1871 and 1871 to 1910 weigh the data in a manner that obscures contemporary trends in shoreline movement.

Essentially, the Wachapreague-Inlet throat shoreline has migrated consistently to the south throughout the short-term time periods with an EPR of -3.6 m/yr and an LRR of -3.9 m/yr. However, it is also notable that these contemporary rates from 1998 to 2010 represent a threefold increase from the 1962–1998 EPR of -1.2 m/yr.

## **Cell 2: Northern, Inlet-Influenced Shoreline**

Cell 2 is the northern, inlet-influenced shoreline. The results show the shoreline advanced throughout a considerable portion of the historical period of record, 1852 to 1942. The highest advance rate is 7.5 m/yr from 1852 to 1871, but it slows to 1.8 m/yr from 1871 to 1910 and then recovers to 4.2 m/yr from 1910 to 1942. Starting with the 1942–1962 time period, Cell 2 experiences a fundamental reversal in its shoreline change pattern or trend from rates of advance to retreat. From 1942 to 1962, the shoreline retreats -7.5 m/yr and experiences a similar retreat rate of -6.7 m/yr from 1962 to 1998. Furthermore, the retreat rate increases substantially to -16.2 m/yr from 1998 to 2010. The range in change rate from the initial period of 1852–1871 (7.5 m/yr of advance) to the final period of 1998–2010 (-16.2 m/yr of retreat) results in a net difference of 23.7 m/yr in the rate of shoreline movement.

The overall EPR for Cell 2 over the long-term record (1852–1998) is -0.4 m/yr and the LRR is 0.1 m/yr (0.20  $R^2$ ). The highest LRR of advance occurs from 1852 to 1942 at 3.0 m/yr (0.69  $R^2$ ) and the highest LRR of retreat occurs from 1962 to 2010 at -6.9 m/yr (0.89  $R^2$ ) (Appendix A). Additional statistics also demonstrate the variability for

Cell 2. Specifically, the WLR from 1852 to 1998 is -0.3 m/yr ( $0.36 R^2$ ), whereas the LMS for the same time period records 1.5 m/yr of advance. Over the short-term record, the overall EPR and LRR document rapid retreat rates when compared to the long-term record. The EPR from 1998 to 2010 is -16.2 m/yr and the LRR for the same period is -11.6 m/yr ( $0.66 R^2$ ).

The inherent dynamics of the inlet-influenced shoreline have strongly influenced the results of Cell 2. Considerable variation occurs in the end point rates for Cell 2 across the time periods, but markedly, the shoreline is characterized by a distinct switch from moderate advance rates (7.5 m/yr from 1852 to 1871) to rapid retreat rates (-16.2 m/yr from 1998 to 2010) (Appendix A). The overall long-term calculations that record low rates of shoreline advance—such as the LRR of 1.4 m/yr from 1852 to 1998—mask the spatial and temporal variability of shorelines associated with a tidal inlet.

The results for Cell 2 could lead one to conclude the shoreline demonstrates spatial consistency. However, this is not true upon a closer inspection of the data. The shoreline change results for Cell 2 clearly mark a distinct shift from shoreline advance to retreat during the period of record. The Cell 2 shoreline is strongly influenced by tidal inlet processes and the associated ebb-tidal delta fronting Wachapreague Inlet. The dynamics of the ebb-tidal delta can produce substantial swings in shoreline position because of wave refraction, the local reversal in longshore sediment transport, sand bar welding, and seasonal onshore/offshore sediment transport.

### **Cell 3: North-Central, Open-Ocean Shoreline**

Cell 3 is the north-central, open-ocean shoreline. This shoreline cell from 1852 to 1871 is marked by a high rate of shoreline advance; 15.4 m/yr. The rate of shoreline advance slows substantially to 1.8 m/yr from 1871 to 1910 and then reaches nearly a steady state at 0.2 m/yr from 1910 to 1942. From this incremental time period moving forward, Cell 3 experiences shoreline retreat. The rate from 1942 to 1962 is -7.5 m/yr and the rate from 1962 to 1998 is similar at -6.7 m/yr. However, the rate jumps to -12.5 m/yr from 1998 to 2010. The net change in rate from the initial time period of 1852–1871 to the final time period of 1998–2010 totals a 27.9 m/yr change in the shoreline movement pattern.

The EPR for Cell 3 over the long-term record (1852–1998) is -0.1 m/yr and the LRR is -0.3 m/yr ( $0.07 R^2$ ). It is notable that the R-squared of LRR is quite low and the lack of strength in the linear relationship is reflective of the profound shift from moderate/high rates of shoreline advance to moderate/high rates of shoreline retreat. The highest LRR of advance occurs from 1852 to 1910 at 5.7 m/yr ( $0.69 R^2$ ) and the highest LRR of retreat occurs from 1962 to 2010 at -7.8 m/yr ( $0.98 R^2$ ) (Appendix A). Additional statistics also demonstrate the variability of results for Cell 3. Specifically, the WLR from 1852 to 1998 is -2.8 m/yr ( $0.42 R^2$ ), whereas the LMS for the same time period records -0.6 m/yr of retreat. The higher WLR of -2.8 m/yr is the result of more confidence in the more recent datasets that are dominated by shoreline retreat rates.

The short-term data (1998–2010) illuminate the trend of increasing shoreline retreat rates along the north-central, open-ocean shoreline of Parramore Island. The

overall EPR from 1998 to 2010 is -12.5 m/yr and the LRR is -11.4 m/yr. However, these results only tell a portion of the story because a closer inspection of the data reveals generally ever-increasing shoreline retreat rates in the short term along Cell 3. In particular, the EPR from 2007 to 2010 is -19.9 m/yr and an even higher EPR is recorded from 2006 to 2010: -22.7 m/yr (Appendix A). In fact, the LRRs also support the validity of the EPR calculations. Specifically, the LRR from 2002 to 2010 is -17.4 m/yr ( $0.96 R^2$ ) and then increases to -19.8 m/yr from 2005 to 2010 and increases once again to -22.1 m/yr from 2006 to 2010. The LMS values for the same time periods are also in close agreement.

The north-central, open-ocean shoreline should be the most stable of all the outer shoreline barrier island segments because of the lack of tidal inlet processes and adequate updrift sediment supply. However, Cell 3 is marked by a pronounced reversal from moderate/high levels of shoreline advance in the earlier portions of the historical record to rapid retreat rates in the contemporary time period. The total net difference in LRR shoreline change rates from 1852 to 1998 to 1998 to 2010 is 17.1 m/yr.

Clearly, a distinctive change from shoreline advance to retreat has steadily occurred over the historical period of record for Cell 3, but the modern trend represents a new period of sustained and rapid retreat. The results for the critical north-central, open-ocean shoreline of Parramore lead one to a host of hypotheses to explain these notable changes including a reduction in updrift sediment supply, the effects of a rise in relative sea level, or higher frequency and larger magnitude storms.

#### **Cell 4: Southern, Washover-Dominated, Open-Ocean Shoreline**

Cell 4 is the southern, washover-dominated, open-ocean shoreline. Cell 4 records the highest rate of shoreline advance of any shoreline cell during the 1852 to 1871 time period at 16.8 m/yr, but this advance rate quickly shifts to a significant retreat rate in the following time period, -7.3 m/yr from 1871 to 1910. This retreat rate continues to increase in the next two time periods: -9.8 m/yr from 1910 to 1942 and then -14.9 m/yr from 1942 to 1962. The rate slows to -10.5 m/yr from 1962 to 1998 but then experiences an increase to -14.6 m/yr from 1998 to 2010. In total, the net shoreline movement for Cell 4 from 1852 to 2010 is more than 1.5 km (Appendix A).

The overall EPR of Cell 4 over the long-term record (1852–1998) is -7.0 m/yr and the LRR is -8.3 m/yr (0.78  $R^2$ ). The highest LRR across all the time periods within the long-term record occurs during the 1910 to 2010 timeframe with a retreat rate of -12.2 m/yr (1.00  $R^2$ ) and the lowest retreat rate is -0.4 m/yr (0.32  $R^2$ ) from 1852 to 1910 (Appendix A). The WLR and LMS statistics support the high retreat rates evident along Cell 4. The WLR from 1852 to 1998 is -9.5 m/yr (0.92  $R^2$ ) and an LMS of -10.6 m/yr for the same time period, both of which are higher retreat rates than the EPR and LRR calculations and the high R-squared value for the WLR is notable.

Over the short term, the overall EPR and LRR calculations reflect even higher retreat rates compared to the long-term record. Specifically, the EPR from 1998 to 2010 is -14.6 m/yr and the LRR is -13.2 m/yr (0.94  $R^2$ ). A comparison between the long-term and short-term EPR and LRR calculations reveal a marked increase in the retreat rate for Cell 4 over the short term. The EPR rate from 1852 to 1998 more than doubles (-7.0 to -



14.6 m/yr) and the LRR incurs a total increase of 4.9 m/yr (-8.3 to -13.2 m/yr). In addition, the short-term results also show even higher retreat rates within the short-term record—specifically, LRRs of -19.7 m/yr (0.95  $R^2$ ) from 2005 to 2010—and an even higher rate of -22.5 m/yr (0.98  $R^2$ ) from 2006 to 2010 (Appendix A).

Cell 4 is marked by a distinct change from shoreline advance to retreat throughout the entire historical period of record. Unlike Cell 3, however, the switch from advance to retreat occurs much earlier in the historical record. This shoreline change pattern is consistent with the concept of barrier island rotational instability as described by Leatherman et al. (1982). It is notable that Cell 4 has the highest retreat rate among all the shoreline cells during the most recent time period (LRR of -13.2 m/yr from 1998 to 2010). These results indicate the shoreline retreat pattern for Cell 4 is fairly consistent throughout large portions of the historical record. However, the shoreline is characterized by rapid shoreline retreat throughout the long-term record but suffers from even higher retreat rates in the short term.

#### **Cell 5: Southern Spit Shoreline**

Cell 5 is the southern spit shoreline. Only limited datasets are available for this shoreline cell—specifically, the years 1852, 1871, 1910, and 2010 over the long term and 2005, 2006, 2007, and 2010 over the short term. As such, the summary of incremental time periods offers little information. However, the shoreline change rates toward the beginning of the historical record are quite high. The shoreline advance rate is 11.4 m/yr during the 1852 to 1871 timeframe and increases to a high rate of 30.7 m/yr during the 1871 to 1910 timeframe. The overall long-term EPR from 1852 to 1910 is 19.6

m/yr of advance and an LRR of 20.2 m/yr ( $0.97 R^2$ ). The overall short-term EPR from 2005 to 2010 is -17.5 m/yr of retreat and an LRR of -18.2 m/yr ( $0.74 R^2$ ).

Cell 5 is heavily influenced by sand transport and deposition processes from updrift sources. In addition, the southern spit shoreline is also affected by tidal inlet processes at Quinby Inlet. The lengthening and shortening of Cell 5 and the rapid change rates are indicative of shorelines in proximity to inlet processes. However, it is notable that a substantial swing occurs from high advance rates early in the historical record (1852–1910) to high retreat rates toward the end of the historical record (2005–2010).

#### **Cells 3–4: Non-Inlet Influenced, Open-Ocean Shoreline**

The non-inlet-influenced, open-ocean shoreline of Parramore Island is defined as Cell 3 (the north-central, open-ocean shoreline) and Cell 4 (the southern, washover-dominated, open-ocean shoreline), hereafter referred to as “Cells 3–4.” The results from Cells 3 and 4 are combined into this larger cell in order to more clearly illuminate the trend and pattern of shoreline movement along the entire length of Parramore’s non-inlet-influenced, open-ocean shoreline. The linear regression rate of shoreline change for Cells 3–4 over the entire period of record is -5.0 m/yr ( $0.49 R^2$ ) (Figure 48).

The low  $R^2$  value results from the considerable variability in change rates for Cells 3–4 across the entire period of record. The variability in the results is illuminated by the rates of advance and retreat documented in the incremental end point rates. From 1852 to 1871 the shoreline advanced at a rate of 16.1 m/yr, but from 1871 to 1910 the rate reversed to a sustained shoreline retreat at a rate of -2.5 m/yr. The retreat rate continues an increase to -3.5 m/yr from 1910 to 1942 and then jumps to -10.2 m/yr from

1942 to 1962. The retreat rate slows slightly to -8.5 m/yr from 1962 to 1998. However, the retreat rate increases once again to a record high of -13.5 m/yr from 1998 to 2010.

The linear regression rate of retreat over the entire period of record can be further analyzed, and more importantly trends can be illuminated, by spatially correlating the linear regression rates of the alongshore changes of Cells 3–4 to the compiled shorelines of Parramore Island. Figure 48 compares the long-term (1852–1998) rates to the short-term rates (1998–2010) and the results are striking. Specifically, the long-term LRR is -4.1 m/yr (0.41  $R^2$ ) and the short-term rate LRR is -12.2 m/yr (0.91  $R^2$ ). Moreover, Figure 48 graphically demonstrates low advance rates or low retreat rates over the long term for the Cell 3 shoreline. Standing in contrast are the moderate to high retreat rates of Cell 4 over the long term with a shoreline curve that visually represents the changes in shoreline position. Over the short term, high retreat rates occur throughout the entire shoreline length of Cells 3 and 4. In short, the results demonstrate a pronounced reversal from shoreline advance to shoreline retreat then to more rapid retreat rates for Cells 3–4.

In Figure 49 the long-term linear regression rates are compared to the weighted linear regression rates of the alongshore changes of Cells 3–4. The long-term WLR is -6.0 m/yr (0.66  $R^2$ ), which represents an increase of 1.9 m/yr of shoreline retreat over the LRR of -4.1 m/yr (0.41  $R^2$ ). Most notable in this calculation is the higher confidence in the strength of linear relationship when using WLR. As stated in the Methods chapter, a WLR calculation is a derivative of the LRR, but in this case, more reliable data are given greater weight when calculating a best-fit line. The weight is placed proportionally on data points that have higher values of positional certainty. In other words, the more recent

shorelines of Parramore Island that generally demonstrate higher retreat rates—when compared to the earlier portions of the historical record—are given more weight in the WLR calculation. Hence, the WLR of -6.0 m/yr is perhaps an elevated number, as shown by retreat rates throughout the entire shoreline length of Cells 3–4 when the results have shown that Cell 3 has exhibited low to moderate advance rates during periods of the historical record.

The results indicate a fundamental change has occurred regarding the behavior of Parramore Island's non-inlet-influenced, open-ocean shoreline (Cells 3–4). Specifically, the short-term LRR of -12.2 m/yr is nearly triple the retreat rate when compared to the long-term LRR of -4.1 m/yr. A tripling of the retreat rate is evidenced during an on-site survey of Parramore Island where substantial eco-geomorphic changes, such as massive pine tree die-offs along the backshore and ubiquitous areas of relict marsh outcropping along the foreshore, are prevalent. Parramore Island has undergone a distinct change from rotational instability, as documented by Leatherman et al. (1982), to sustained and increasing retreat rates across the length of Parramore's non-inlet-influenced, open-ocean shoreline. These patterns of shoreline movement could signify important changes for the Virginia Coast Reserve as a whole and should not be viewed in isolation.

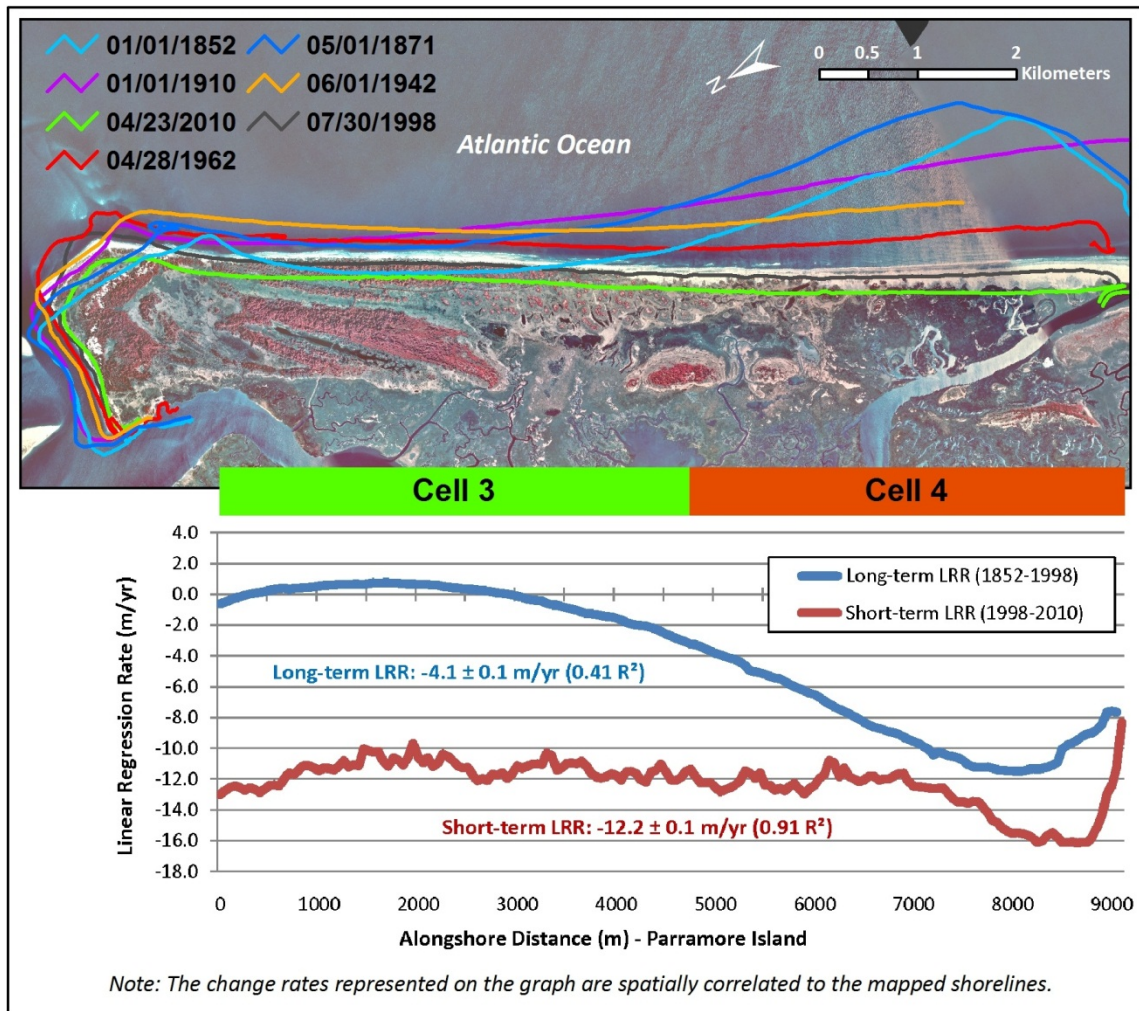


Figure 48: Long-term (1852–1998) and short-term (1998–2010) linear regression rates (LRR) of the alongshore change of Cells 3–4 spatially correlated to the compiled historical shorelines of Parramore Island, Virginia. Long-term rates are in blue and short-term rates are in red.

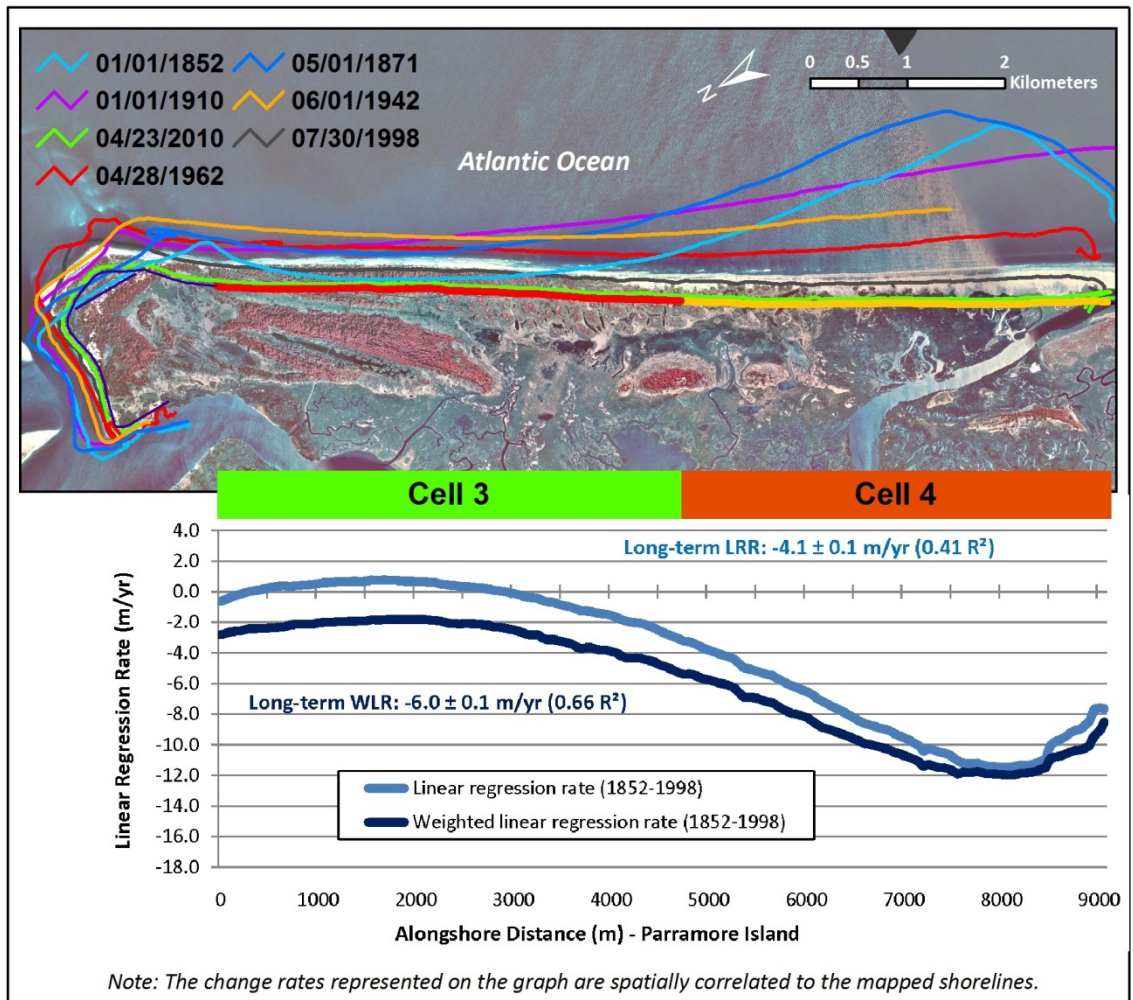


Figure 49: Long-term (1852–1998) linear and weighted linear regression rates (LRR and WLR, respectively) of the alongshore change of Cells 3–4 spatially correlated to the compiled historical shorelines of Parramore Island, Virginia.

## **Cedar Island**

Figure 50 is a reference map of the historical shorelines used in the Cedar Island shoreline analysis. More specifically, the shoreline dates are from the years 1852, 1871, 1910, 1933, 1942, 1962, 2007, and 2010). As mentioned in the Methods chapter, Cedar Island is segmented into shoreline cells based on its distinguishing geomorphic characteristics and the shoreline change results are examined by discrete time periods and various statistical measures. Cedar Island has six shoreline cells numbered sequentially from north to south; Cell 0: the Metompkin Inlet-influenced shoreline; Cell 1: the Coast Guard breach shoreline; Cell 2: the northern, breach-influenced shoreline; Cell 3: the north-central, marsh-backed, open-ocean shoreline; Cell 4: the south-central, bay-backed, open-ocean shoreline; and Cell 5: the southern spit shoreline.

End point rates are segmented by incremental time periods across the historical period of record in Table 10. Specifically, the time periods are 1852–1871, 1871–1910, 1910–1942, 1942–1962, 1962–2007, and 2007–2010. Second, the long-term (1852–2007) and short-term (2007–2010) end point and linear regression rates (m/yr) by shoreline cell are presented in Table 11. Figure 51 shows the overall linear regression rate of Cells 3–4 and includes a chart with a trendline that demonstrates the magnitude of change over the entire period of record. Finally, the long-term and short-term linear regression rates of the alongshore changes of Cells 3–4 are spatially correlated to the compiled shorelines of Cedar Island in Figure 52. Using the same spatially correlated map/graph template, the long-term linear regression and the long-term weighted linear regression rates are compared in Figure 53.



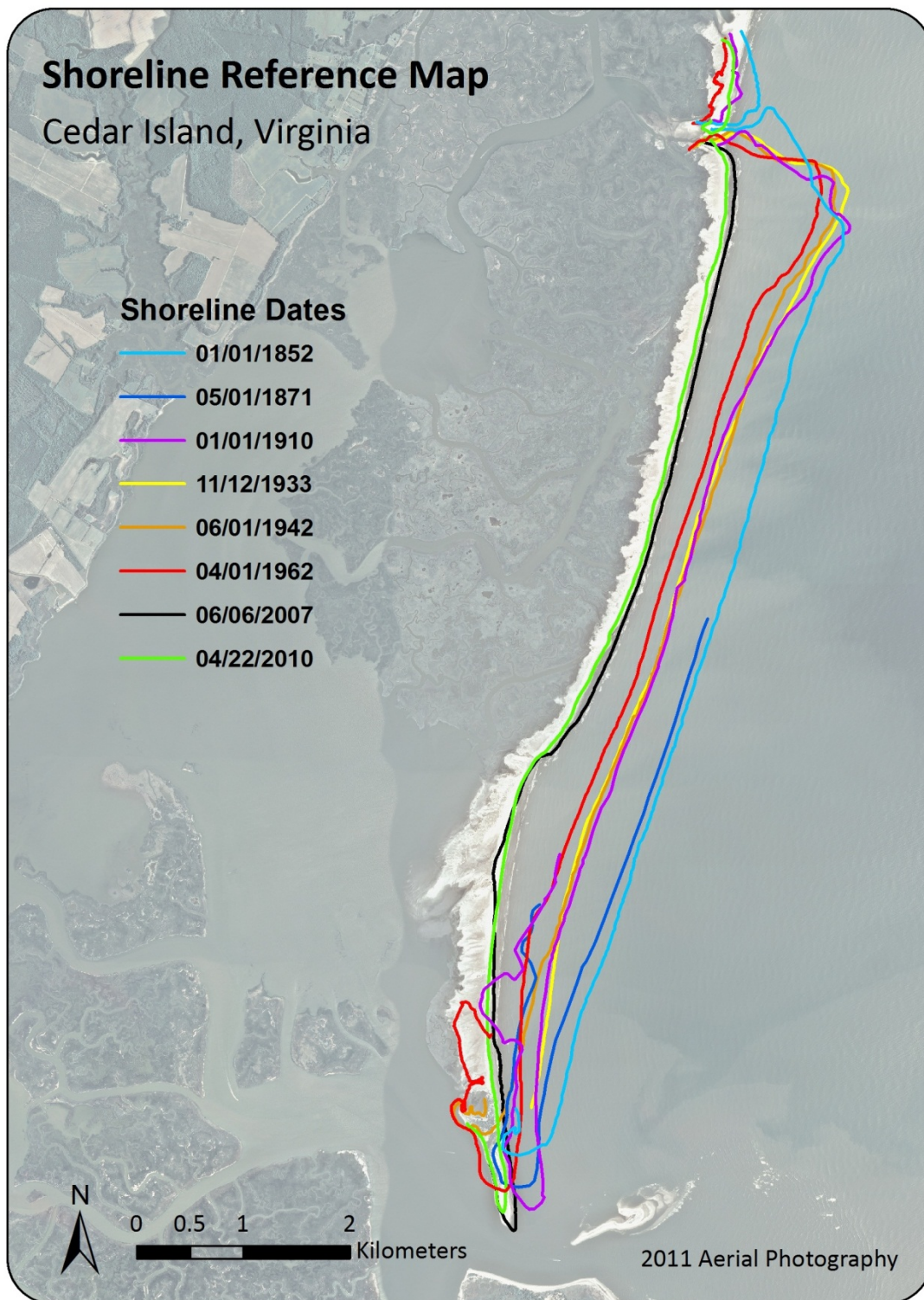


Figure 50: Cedar Island shoreline cell reference map.



**Table 10: Comparison of long-term incremental time periods by end point rate (m/yr) and shoreline cell for Cedar Island, Virginia**

**Shoreline Change Summary of Cedar Island, Virginia**  
Comparison of Long-Term Incremental Time Periods by  
End Point Rate (m/yr) and Shoreline Cell

Shoreline Cell	1852-1871	1871-1910	1910-1942	1942-1962	1962-2007	2007-2010
0	x	x	x	x	x	x
1	x	x	2.4	0.6	-1.7	4.7
2	x	x	-0.6	-5.6	-11.5	-23.3
3	-3.6	-8.6	-0.7	-7.8	-7.4	-23.0
4	-5.7	-8.7	-2.0	-7.4	-9.8	-2.3
5	-8.3	-1.2	-7.4	4.0	-3.0	-26.0
3-4	-5.0	-8.7	-1.1	-7.7	-8.3	-15.3

**Cell Definitions**

Cell 0: Metompkin Inlet and Coast Guard breach-influenced

Cell 1: Coast Guard breach-throat

Cell 4: South-central, bay-backed, open-ocean

Cell 2: Northern, inlet-influenced, open-ocean

Cell 5: Southern spit, open-ocean

Cell 3: North-central, marsh-backed, open-ocean

Cells 3-4: Non-inlet influenced, open-ocean

(-) sign indicates shoreline retreat and a positive integer signals advance.

(x) sign indicates no data is available for specified time period.

**Cell 0: Metompkin Inlet and Coast Guard Breach-Influenced Shoreline**

Cell 0 is the Metompkin Inlet and Coast Guard breach-influenced shoreline.

Incremental time period results as defined in Table 10 are not available for this cell because of the limited dataset of this segment of Cedar Island. As such, the EPR from 1852 to 1962 is -2.8 m/yr and this is identical to the LRR of -2.8 m/yr (0.99 R<sup>2</sup>). The shoreline then switches to advance at 2.6 m/yr from 1962 to 2010. The LRR over the entire period of record is -1.4 m/yr (0.57 R<sup>2</sup>) (Appendix B).

Table 11: Long-term (1852–1998) and short-term (1998–2010) end point and linear regression rates (m/yr) by shoreline cell of Cedar Island

**Shoreline Change Summary of Cedar Island, Virginia**  
Long-Term (1852-2007) and Short-Term (2007-2010)  
End Point and Linear Regression Rates (m/yr) by Shoreline Cell

Shoreline	1852-2007		2007-2010	
	EPR	LRR	EPR	LRR
Cell 0*	-2.8	-2.8	2.6	x
Cell 1	-1.0	-0.9	4.7	7.6
Cell 2	-4.7	-4.3	-23.3	-22.1
Cell 3	-5.5	-5.3	-23.0	-22.0
Cell 4	-7.1	-6.7	-2.3	0.7
Cell 5	-3.7	-3.5	-26.0	-24.6

\*Date ranges for Cell 0 are 1852-1962 & 1962-2010 due to an absence of data in 2007.

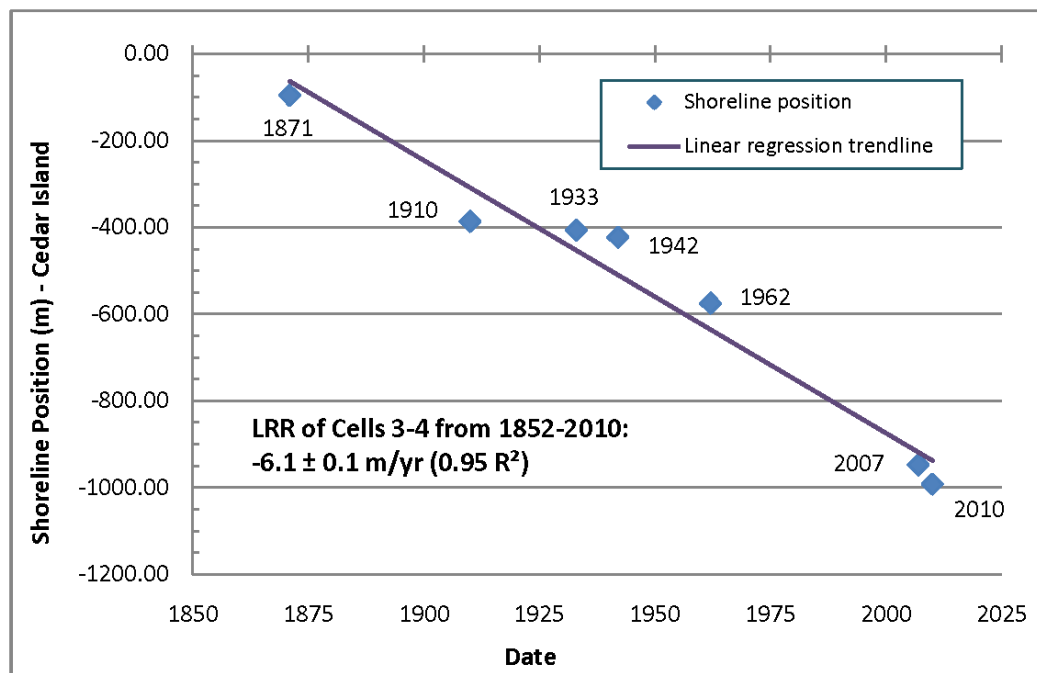


Figure 51: Magnitude of change with linear regression rate and trendline of Cedar Island (1852–2010) normalized to the 1852 shoreline.

### **Cell 1: Coast-Guard Breach-Throat Shoreline**

Cell 1 is the Coast Guard breach-throat shoreline. The end point rate results demonstrate variability in the rate of shoreline migration across the available historical period of record (1910–2010). The rate from 1910 to 1942 shows shoreline migration in a northerly direction at 2.4 m/yr. The rate of northerly movement reduces to 0.6 m/yr from 1942 to 1962. The 1962 to 2007 time period switches to a southerly migration direction at a rate of -1.7 m/yr. The most recent time period from 2007 to 2010 records the highest rate of northerly migration at 4.7 m/yr. The linear regression rate (-0.9 m/yr, 0.71  $R^2$ ) and end point rate (-1.0 m/yr) over the long term (1852–2007) indicate a gradual southerly shoreline movement. However, over the short term (2007–2010), the shoreline migrates northerly at a linear regression rate of 7.6 m/yr (0.39  $R^2$ ).

Cell 1 is dominated by processes governing the opening and closing of ephemeral breaches. Whereas the long-term record is dominated by low rates of southerly migration, the short-term record ranges from rapid southerly migration (-21.3 m/yr EPR from 2007 to 2008) to rapid northerly migration (28.8 m/yr EPR from 2008 to 2009) (Appendix B). In short, this shoreline is located along the pathway of shortest and least resistance between bay and ocean during tidal exchange. As such, Cell 1 is subject to the extremes of shoreline migration as evident in the short-term results. However, the LRR of -0.9 m/yr (0.75  $R^2$ ) over the entire period of record (1910–2010) is indicative of the dominant behavior of Cell 1 (i.e., a sustained but low rate of southerly migration).

## **Cell 2: Northern, Breach-Influenced Shoreline**

Cell 2 is the northern, breach-influenced shoreline. As with Cell 1, data are not available for the 1852–1871 and 1871–1910 time periods, but data are available for the remainder of the incremental time periods. Results from Cell 2 demonstrate progressively higher retreat rates over the long term. From 1910 to 1942, the shoreline retreats slowly at -0.6 m/yr but then increases to -5.6 m/yr from 1942 to 1962. The pattern of increasing retreat rates continues with a more than two-fold increase in retreat to -11.5 m/yr from 1962 to 2007. Between 2007 and 2010, the shoreline retreat rate roughly doubles to -23.3 m/yr compared to the preceding time period (1962–2007).

The shoreline change rates increase from a moderate retreat rate over the long term to a severe retreat rate over the short term. Specifically, the end point and linear regression rates from 1852 to 2007 are -4.7 and -4.3 m/yr, respectively. However, the linear regression rate over the short term jumps to -22.1 m/yr ( $0.81 R^2$ ) from 2007 to 2010. This increase in the rate of retreat represents a five-fold increase from -4.3 m/yr ( $0.67 R^2$ ) during the 1852–2007 timeframe. The rapid retreat rate in the short-term record is also reflected in the long-term record because the highest linear regression rate occurs during the 1962 to 2010 timeframe: -11.9 m/yr ( $0.98 R^2$ ).

Cell 2 is experiencing rapid retreat rates in the short-term and in the latter portions of the long-term record. Cell 2 illustrates a sustained pattern of severe and rapid retreat despite the shoreline being influenced by the northern breach zone and accompanying tidal forces of Cell 1. Clearly, the long-term results indicate an increasing level of retreat

throughout the historical record and the short-term results magnify the rapid retreat rates along Cell 2.

### **Cell 3: North-Central, Marsh-Backed, Open-Ocean Shoreline**

Cell 3 is the north-central, marsh-backed, open-ocean shoreline. From 1852 to 1871, the shoreline retreated at -3.6 m/yr. The retreat rate increased to -8.6 m/yr from 1871 to 1910. The retreat rate of -0.7 m/yr from 1910 to 1942 is the lowest retreat rate across all incremental time periods. However, the rate increases to -7.8 m/yr from 1942 to 1962 and then maintains a similar rate of -7.4 m/yr from 1962 to 2007. The rate from 2007 to 2010 is the highest retreat rate at -23.0 m/yr.

Cell 3 is marked by a profound change from moderate retreat rates over the long term to extremely high retreat rates over the short term. The short-term rates of -23.0 m/yr (EPR) and -22.0 m/yr (0.83  $R^2$ ) (LRR) represent a four-fold increase over the long-term rates of -5.5 m/yr (EPR) and -5.3 m/yr (0.93  $R^2$ ) (LRR), respectively. It is notable the most recent short-term measurement from April 2009 to April 2010 records an end point rate of -47.7 m/yr (Appendix B). This is the highest retreat rate in either the short-term or long-term record. The severe retreat rate indicates that Cedar Island was strongly affected by significant meteorological events (e.g., impact of NorIda in November 2009) during that timeframe. By comparison, the highest linear regression rate in the long-term record is -7.5 m/yr (0.99  $R^2$ ) from 1942 to 2007. This long-term rate is further supported by an identical rate of -7.5 m/yr as witnessed by weighted linear regression and least median of square rate calculations (Appendix B).

Cell 3 is critically important to understanding the behavior of Cedar Island because the shoreline migration patterns are not as heavily influenced by factors such as inlet processes and breaching episodes. Hence, the results from Cell 3 offer perhaps the clearest signal of the primary processes affecting Cedar Island. The retreat rates indicate Cedar has experienced moderate retreat rates throughout the historical record that have ranged between -7.4 and -8.6 m/yr for large portions of the historical record. However, the linear regression rate jumps to -23.0 m/yr from 2007 to 2010. The end point rates within the short-term record (-10.0 m/yr from 2007 to 2009) signal a more moderate increase in the retreat rate. In other words, the storms of 2009–2010 (e.g., NorIda in November 2009) had a pronounced impact on the shorelines that further magnified ongoing changes that cannot be easily reversed, possibly because of limited sediment supplies along the Virginia Eastern Shore.

#### **Cell 4: South-Central, Bay-Backed, Open-Ocean Shoreline**

Cell 4 is the south-central, bay-backed, open-ocean shoreline. The shoreline cell exhibits retreat throughout all incremental time periods. From 1852 to 1871, the shoreline retreated at -5.7 m/yr and the rate increased to -8.7 m/yr from 1871 to 1910. Similar to the shoreline change pattern for Cell 3, the retreat rate slows notably to -2.0 m/yr from 1910 to 1942 and then experiences an increase to -7.4 m/yr from 1942 to 1962. The rate continues to increase to -9.8 m/yr in the following time period of 1962 to 2007. The rate then moderates to -2.3 m/yr in the subsequent time period of 2007 to 2010.

The long-term and short-term trends of Cell 4 stand in contrast to the results of the other open-ocean shorelines of Cedar Island. The long-term end point rate is -7.1 m/yr

and the linear regression rate is -6.7 m/yr from 1852 to 2007 ( $0.96 R^2$ ). The highest retreat rates are recorded during the 1942 to 2007 timeframe with retreat rates ranging from -9.1 to -9.3 m/yr for the LRR, WLR, and LMW rates (Appendix B). However, the short-term results from 2007 to 2010 indicate a low linear regression rate of shoreline advance at 0.7 m/yr ( $0.47 R^2$ ). In other words, Cell 4 demonstrates a lower rate of retreat (or advance) over the short term when compared to the long-term results, whereas Cells 2, 3, and 5 have pronounced higher rates of short-term shoreline retreat when compared to the long-term results.

Cell 4 is characterized by frequent island breaching (Moyer 2007). Cell 4 has the lowest end point rate of retreat (and the only linear regression rate of advance) among any open-ocean shoreline cell from 2007 to 2010. And the results from 2007 to 2010 reflect a breaching event in a unique way. In Figure 52, the large spike in shoreline advance that spatially corresponds to the bay-backed portion of Cedar Island is representative of shoreline recovery (i.e., advancement) following the most recent breach closure in April 2007 of Cedar Island breach (Moyer 2007). In addition, the rapid advance rate dampens the overall retreat rate of Cell 4 from 2007 to 2010. It is notable that Cell 4 switches back to retreat during the 2009 to 2010 timeframe (i.e., NorIda impact in November 2009), as witnessed by the end point rate of -26.1 m/yr.

### **Cell 5: Southern Spit Shoreline**

Cell 5 is the southern spit shoreline. From 1852 to 1871, Cell 5 retreated at the highest rate of any of the shoreline cells: -8.3 m/yr. Notably, the rate slows to -1.2 m/yr from 1871 to 1910 and this constitutes the lowest retreat rate among any of the shoreline

cells for this period. The retreat rate increases to -7.4 m/yr from 1910 to 1942 and this represents the highest retreat rate of all the shoreline cells for this time period. Between 1942 and 1962, the change rate reverses to 4.0 m/yr of shoreline advance. The shoreline advance for this time period constitutes the only period of advance for the outer shoreline of Cedar Island among all the shoreline cells and time periods. The cell returns to the prevailing pattern of shoreline retreat at -3.0 m/yr from 1962 to 2007. Cell 5 retreats at -26.0 m/yr from 2007 to 2010, the highest retreat rate of all shoreline cells and incremental time periods.

The results for Cell 5 closely reflect the patterns for Cells 2 and 3—specifically, low to moderate retreat rates over the long term and highly elevated retreat rates in the short term. From 1852 to 2007, the end point rate is -3.7 m/yr and the linear regression rate is -3.5 m/yr ( $0.89 R^2$ ). The linear regression rates over the long-term record (1852–2007) range from -3.3 m/yr ( $0.79 R^2$ ) to -4.5 m/yr ( $0.84 R^2$ ) of retreat (Appendix B). However, from 2007 to 2010, the linear regression rate is -24.6 m/yr ( $0.83 R^2$ ) and this rate is reinforced by the high end point rate of -26.0 m/yr for the same time period. It is notable that the -54.9 m/yr of retreat evidenced along Cell 5 from 2009 to 2010 represents the highest retreat of any of the cells during this timeframe. The linear regression rate during the short-term time period when excluding the 2010 data point is -9.3 m/yr ( $0.90 R^2$ ) from 2007 to 2009 (Appendix B).

Cell 5 demonstrates volatility in shoreline movement as a result of sediment being intermittently supplied to the shoreline most likely because of storm impacts and the morphodynamics of the Wachapreague Inlet complex. Specifically, this southern spit



shoreline is affected by intense overwash processes (e.g., NorIda in November 2009 and other northeasters) and sand bar welding originating from the Dawson's Shoals associated with Wachapreague Inlet. Unlike the other shoreline cells, Cell 5 demonstrates a brief period of shoreline advance from 1942 to 1962 (4.0 m/yr, EPR). Despite this sand bar welding onto the beach face, the southern spit still experiences retreat rates over the long term (1852–2007). In fact, it suffers from the highest retreat rate over the short term (2007–2010).

### **Cells 3–4: Non-Inlet-Influenced, Open-Ocean Shoreline**

The non-inlet-influenced, open-ocean shoreline of Cedar Island is defined as Cell 3 (the north-central, marsh-backed, open-ocean shoreline) and Cell 4 (the south-central, bay-backed, open-ocean shoreline), referred to here as “Cells 3–4.” The results are combined into this larger cell to illuminate more fully the trend and pattern of shoreline movement along the entire length of the outer open-ocean shoreline. The linear regression rate of shoreline change for Cells 3–4 over the entire period of record (1852–2010) is -6.1 m/yr (0.95  $R^2$ ) (Figure 52).

The high  $R^2$  value is because of the lack of variability in change rates for Cells 3–4 across the entire period of record. The incremental time period results demonstrate that shoreline retreat rates have been within the same order of magnitude during large portions of the historical record for Cells 3–4. From 1852 to 1871, the retreat rate is -5.0 m/yr and increases to -8.7 m/yr from 1871 to 1910. The retreat rate slows to -1.1 m/yr from 1910 to 1942 but then rebounds to a higher retreat rate of -7.7 m/yr. The rate then increases to -8.3 m/yr from 1962 to 2007. Finally, the retreat rate nearly doubles to -15.3

m/yr from 2007 to 2010. As with Parramore Island, the linear regression rate of retreat over the entire period of record of Cedar Island can be further examined by spatially correlating the linear regression rates of the alongshore changes of Cells 3–4 to the compiled shorelines of Cedar Island. Figure 52 compares the long-term (1852–2007) rates to the short-term rates (2007–2010). The long-term linear regression rate is -5.5 m/yr ( $0.93 R^2$ ) from 1852 to 2007 and the short-term linear regression rate is -15.4 m/yr from 2007 to 2010 ( $0.72 R^2$ ). As with Parramore Island, this short-term increase represents nearly a three-fold increase to the long-term LRR. Figure 52 also demonstrates consistent retreat rates over the long-term over the entire length of Cells 3–4. However, the short-term results display two entirely different stories. The retreat rates for Cell 3 typically range between -15 and -30 m/yr, whereas the results for Cell 4 peak at more than 30 m/yr of shoreline advance. The boundaries of these results represent more than 60 m difference in change rate.

As stated previously, the large spike in shoreline advance spatially corresponds to the bay-backed portion of Cedar Island. These results strongly suggest shoreline recovery has occurred along this shoreline cell in response to the most recent breach closure in April 2007 (Moyer 2007). In summary, the results reveal a switch from consistently low to moderate retreat rates for Cells 3–4 over the long term and a noticeable increase in retreat rates over the short term. In addition, the effects of long-term processes are masked by the short-term processes of sediment renourishment as evidenced by the closure and filling of the ephemeral breach along Cells 3–4.

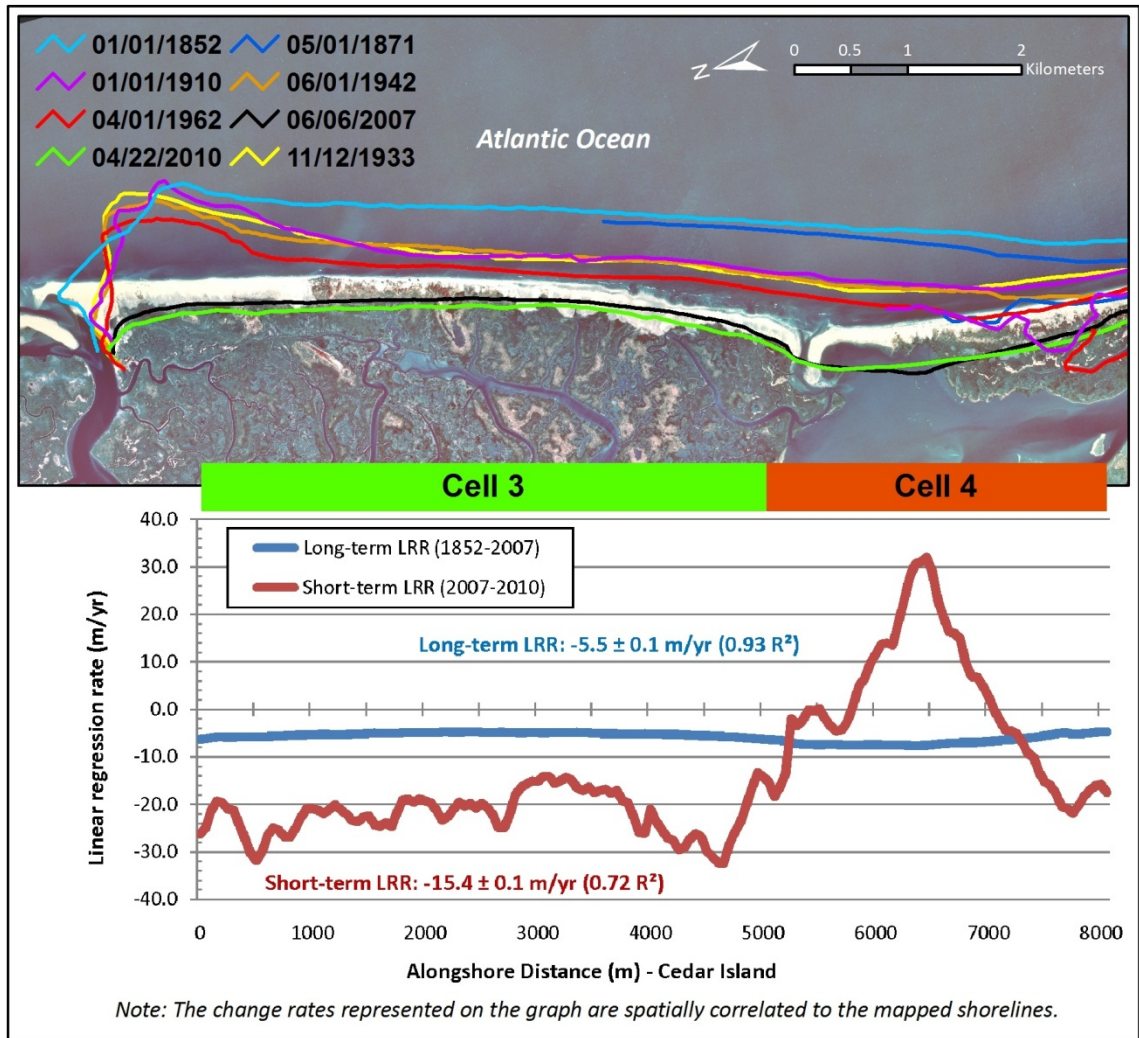


Figure 52: Long-term (1852–2007) and short-term (2007–2010) linear regression rates (LRR) of alongshore change of Cells 3–4 with spatially correlated map and graph of Cedar Island, Virginia. The long-term rate is in blue and the short-term rate is in red.

In Figure 53 the long-term linear regression rates are compared to the weighted linear regression rates of the alongshore changes of Cells 3–4. The long-term weighted linear regression rate for Cells 3–4 is  $-6.3$  m/yr ( $0.96 R^2$ ), which represents an increase of  $0.8$  m/yr of shoreline retreat over the LRR of  $-5.5$  m/yr ( $0.93 R^2$ ). Compared to the

Parramore Island analysis, only a minor difference exists in the confidence of the LRR and WLR calculations. However, most notable is the difference in shoreline behavior at the bay-backed portion of Cell 4 over the long term versus the short term.

Specifically, Figure 53 shows that the bay-backed portion of Cell 4 generally experiences higher retreat rates over the long term than any other segment of Cells 3–4. These results stand in direct contrast to the rapid advance rates demonstrated along this section of shoreline in Figure 52. These results reinforce that the open-ocean, bay-backed portion of Cedar Island has been subject to frequent breaching episodes over the historical period of record. After the breach closes because of its hydraulic inefficiency and inability to capture tidal prism from Wachapreague Inlet, the shoreline recovers.

The results demonstrate a pronounced shift from moderate retreat rates over the long term to high or even severe retreat rates over the short term for Cells 3–4. The short-term retreat rates are noticeably different between the approximate boundaries of Cells 3 and 4. The results indicate the geomorphology of Cedar Island has evolved from low to moderate retreat rates over the long term to a mixed-energy, wave-dominated system experiencing sustained and increasingly higher retreat rates in the short term. In other words, Cedar Island is experiencing a change in its historical pattern of shoreline migration and has transitioned from in-place narrowing to rapid barrier rollover and landward migration through overwash and inlet processes.

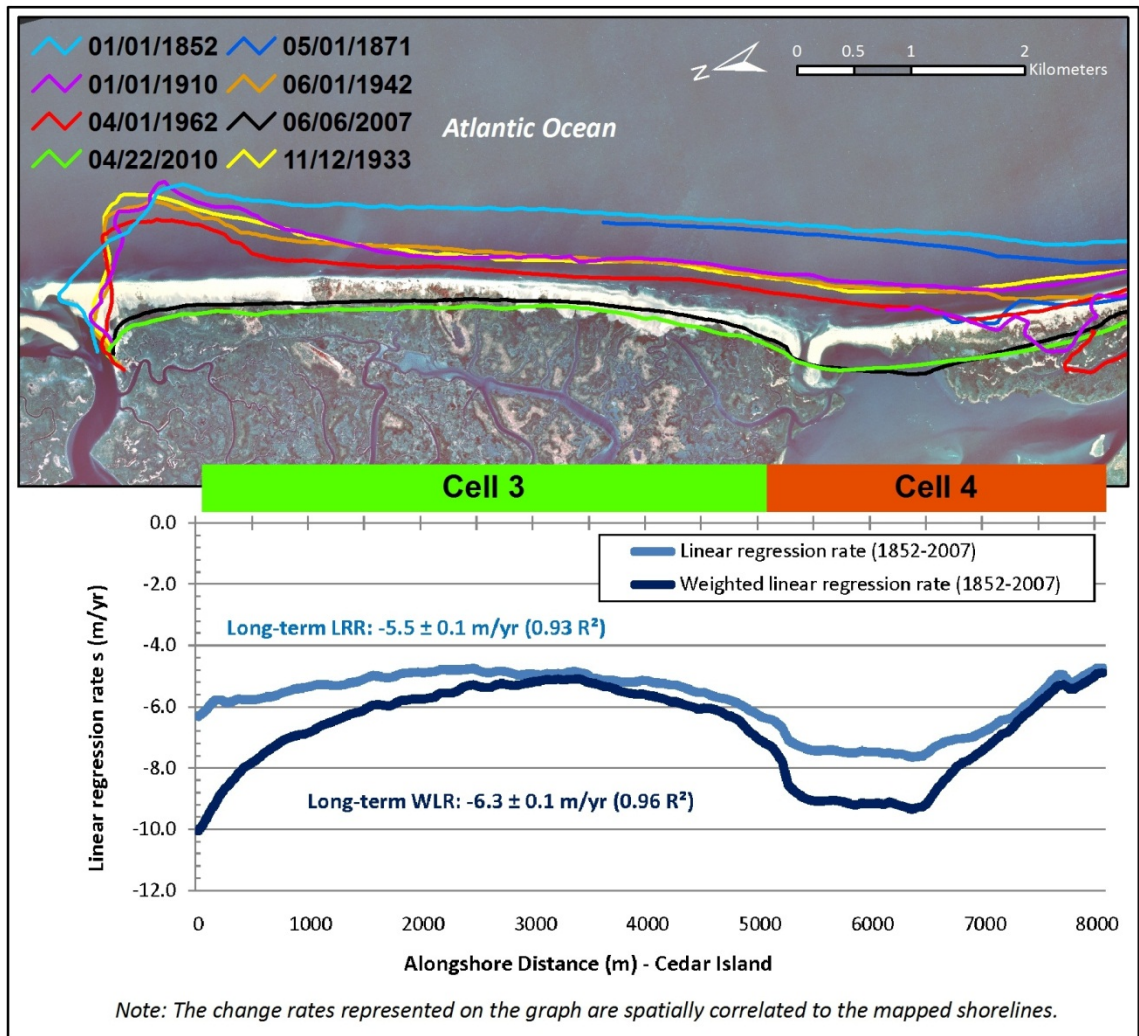


Figure 53: Long-term (1852–2007) linear and weighted linear regression rates of alongshore change of Cells 3–4 with spatially correlated map and graph of Cedar Island, Virginia.

## **Wachapreague Inlet**

### **Shoreline Changes of Wachapreague Inlet: 1852 to 2010**

The southern tip of Cedar Island and the inlet throat shoreline of northern Parramore Island displayed consistent movement patterns over the long term. Over the short term, however, the shoreline movement trend deviated from the historical record of behavior for the Wachapreague Inlet-influenced shorelines of Cedar and Parramore Islands. Specifically, the southern tip of Cedar migrated in a southerly direction at a linear regression rate of +0.9 m/yr (0.01  $R^2$ ) over the long term (1852–2007). However, the southern tip of Cedar Island migrated in a northerly direction at 83.8 m/yr (0.82  $R^2$ ) over the short term (2007–2010). In other words, the southern tip of Cedar Island had a general trend of southerly migration throughout most of the historical period of record, but in the short term, the southern tip of Cedar Island experienced a high rate of northerly migration. Northern Parramore Island demonstrated slow to moderate rates of southerly migration over the long-term period at a rate of -2.0 m/yr from 1852 to 1998. However, the short-term rate of southerly migration of -3.9 m/yr from 1998 to 2010 is nearly double the long-term rate. The various Wachapreague Inlet shorelines of Cedar and Parramore Islands and corresponding southerly migration rates are presented in Figure 54. Overall, Wachapreague Inlet has been slowly migrating in a southerly direction from 1852 to 2010.



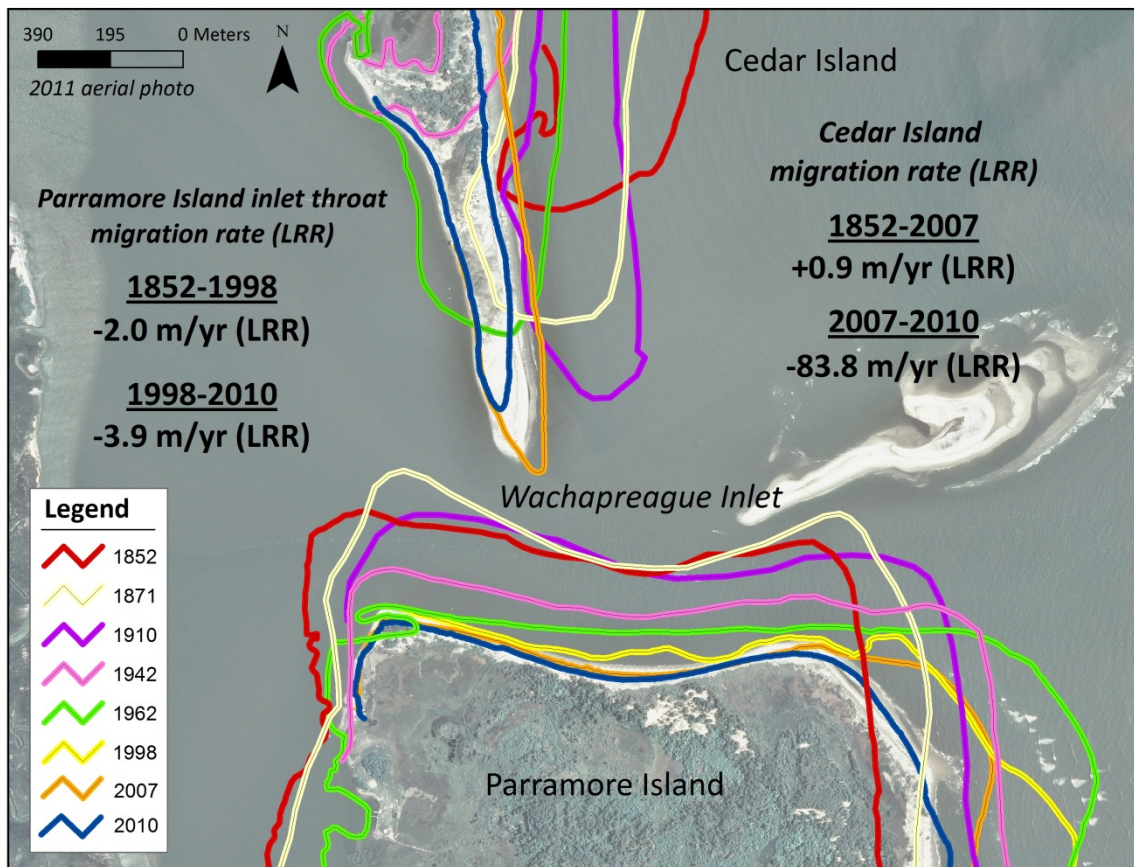


Figure 54: Shoreline changes of Wachapreague Inlet, Virginia from 1852 to 2010 with long-term and short-term changes rates. In general, Wachapreague Inlet has been slowly migrating in a southerly direction over the long term.

### Wachapreague Inlet Bathymetric Surveys (2007–2011)

Moyer (2007) conducted a bathymetric survey of Wachapreague Inlet on April 28, 2007 and collected four transects across the inlet throat (Figure 55). The weather conditions were fair with winds from the northwest at 6 mph, temperature of 17° C, and a trace of precipitation. The lunar phase was waxing gibbous with 88% of the moon's visible disk illuminated. The surveys occurred approximately at the beginning of a falling tide with a high tide of 1.2 m and a low of 0.1 m above mean lower low water. The

maximum depth of any transect was 20.6 m and an average inlet width was 374 m. The four transects ranged from a low of 4275 m<sup>2</sup> to a high of 4598 m<sup>2</sup> with an average value of 4398 m<sup>2</sup>. The four transects when overlaid on Figure 55 reveal spatial consistency of the inlet system.

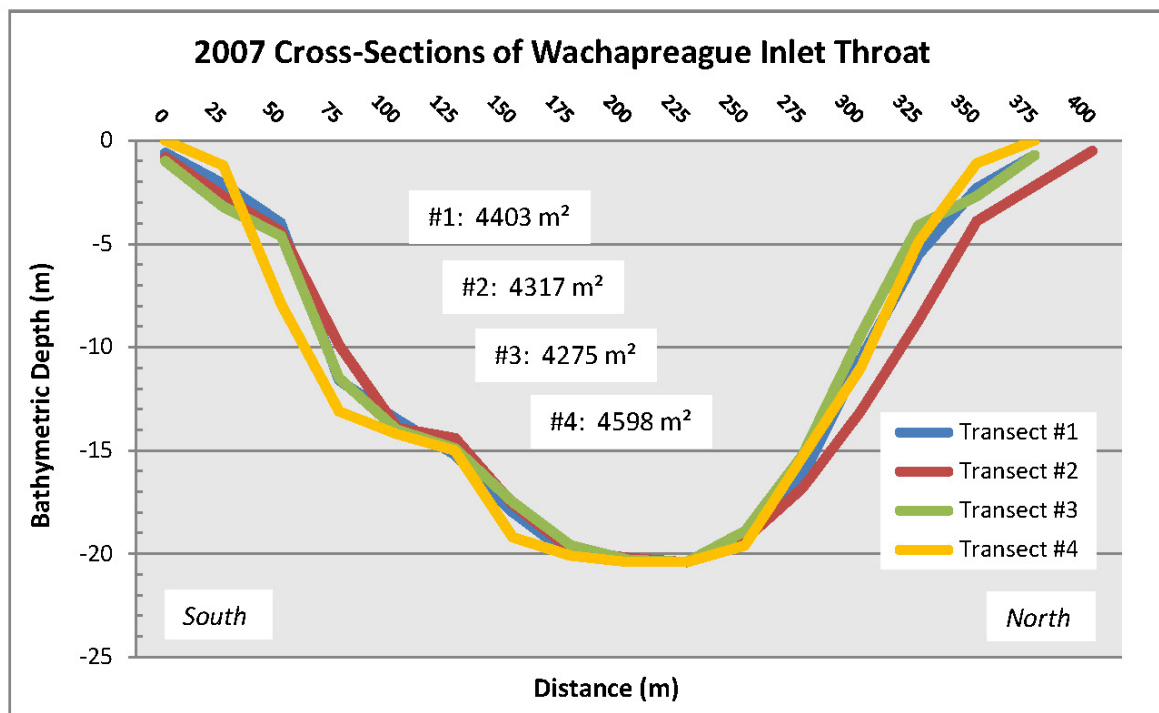


Figure 55: Bathymetric profiles of the inlet throat of Wachapreague Inlet, Virginia on April 28, 2007 (Moyer, 2007).

Richardson (2010) conducted a bathymetric survey of Wachapreague Inlet on April 23, 2010 and collected two transects across the inlet throat (Figure 56). The weather conditions were fair with winds from the south at 6 mph, temperature of 14° C, and no precipitation. The lunar phase was waxing gibbous with 71% of the moon's visible disk



illuminated. The surveys occurred during a rising tide with a high of a 1.3 m and a low of 0.1 m above mean lower low water. The maximum inlet depth was 20.2 m and the average inlet width was 429m. The two transects ranged from a low of 4668 m<sup>2</sup> to a high of 4802 m<sup>2</sup> with an average cross-section of 4735 m<sup>2</sup>. The two transects when overlaid demonstrate spatial consistency of the surveys with close alignment to the south and some variability evident to the north.

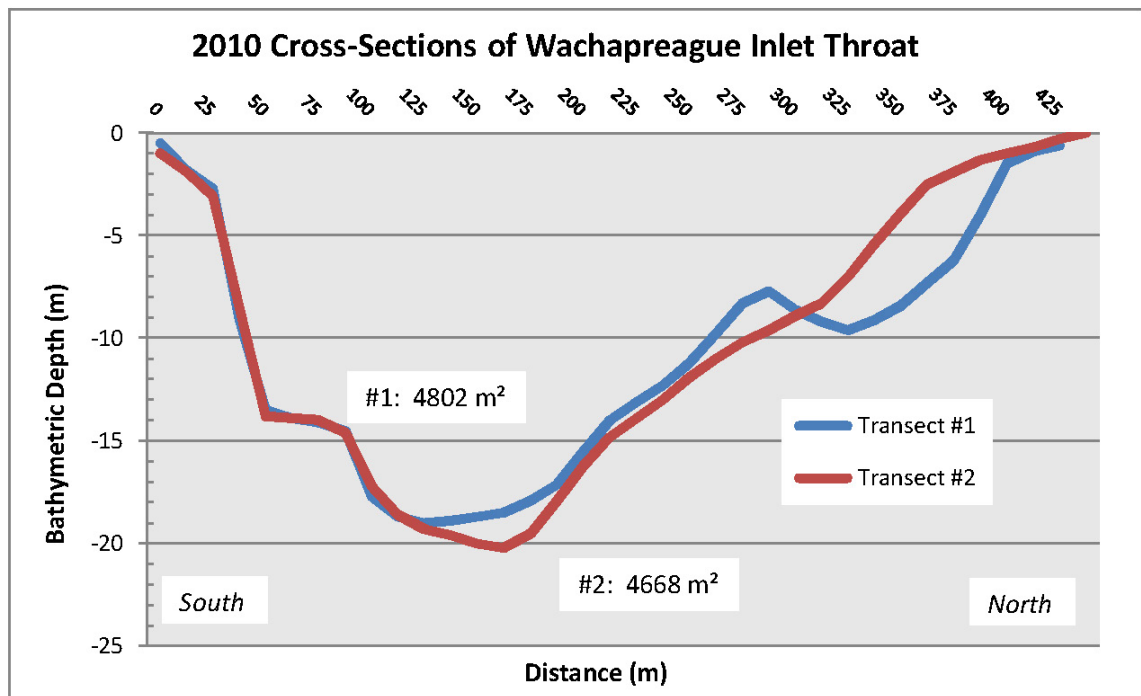


Figure 56: Bathymetric profiles of the inlet throat of Wachapreague Inlet, Virginia on April 23, 2010 (Richardson, 2010).

Richardson (2011) also conducted a bathymetric survey of Wachapreague Inlet on April 29, 2011 and collected two transects across the inlet throat (Figure 57). The weather

conditions were fair with winds from the northwest at 8 mph, temperature of 17° C, and no precipitation. The lunar phase was waning crescent with 12% of the moon's visible disk illuminated. The surveys occurred during mid-cycle of a rising tide with a high of a 1.4 m and a low of 0.1 m above mean lower low water. The maximum inlet depth was 20.9 m and the inlet width was 445 m. The two transects ranged from a low of 5176 m<sup>2</sup> to a high of 5244 m<sup>2</sup> with an average cross-section of 5210 m<sup>2</sup>. The two transects when overlaid also show spatial consistency, but the transects also demonstrate the most variability of the three inlet surveys from 2007 to 2011.

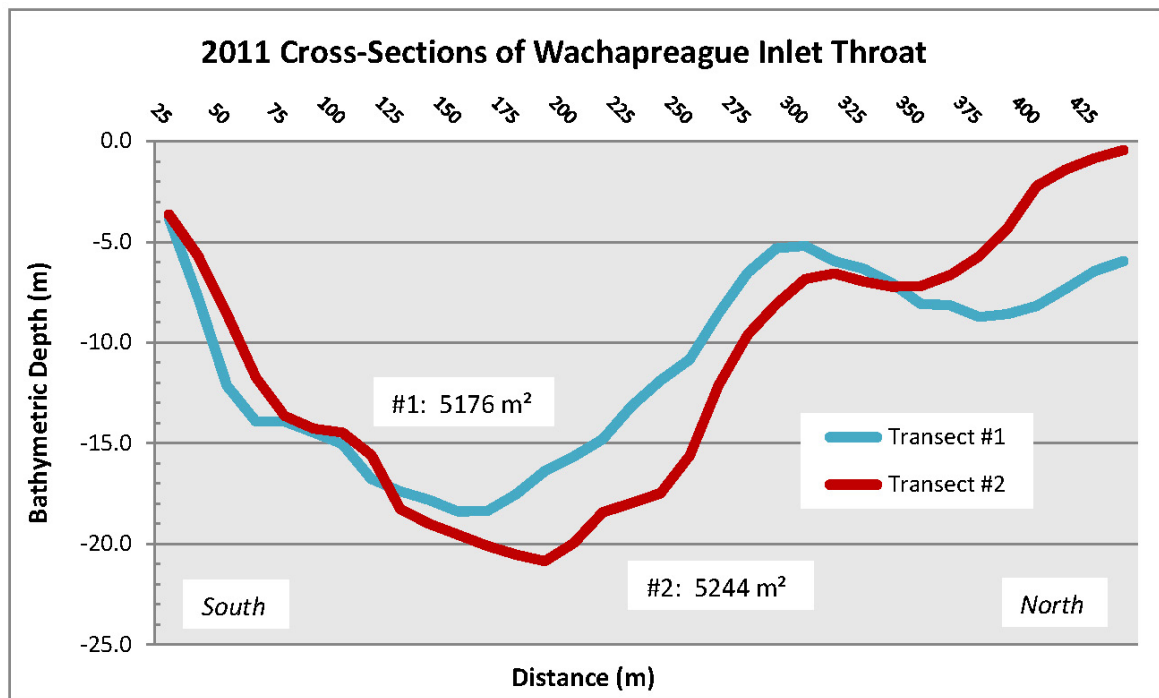


Figure 57: Bathymetric profiles of the inlet throat of Wachapreague Inlet, Virginia on April 29, 2011 (Richardson, 2011).

### **Historical Tidal Inlet Bathymetric Surveys (1852–1972)**

As stated in the Methods chapter, DeAlteris and Byrne (1975) compiled bathymetric profiles of Wachapreague Inlet from 1852 to 1972 (Figure 26). According to DeAlteris and Byrne, the maximum inlet depth in 1852 was 14.0 m with an inlet width of 732 m and a cross-sectional area of 1845 m<sup>2</sup>. In 1871 the maximum inlet depth increased to 18.3 m but with an inlet width that decreased to 640 m and a cross-sectional area that increased to 4473 m<sup>2</sup>. In 1911 the maximum depth slightly decreased to 17.0 m and was accompanied by a smaller inlet width of 396 m. However, the inlet still produced a larger cross-sectional area of 4737 m<sup>2</sup>. In 1934 the maximum depth slightly increased to 17.7 m with an inlet width that greatly expanded to 969 m, but the inlet generated a smaller cross-sectional area of 4572 m<sup>2</sup>. In 1972 the maximum inlet depth increased to 18.2 m with a narrower inlet width of 549 m and a smaller cross-sectional area of 4047 m<sup>2</sup>. Of note, maximum inlet depths were determined upon a close visual inspection of the exhibit, not a calculation using inlet width and cross-sectional area.

### **Historical Metrics of Wachapreague Inlet**

Table 12 organizes the historical metrics of Wachapreague Inlet across the entire period of the record by displaying the survey year, maximum inlet throat depth, inlet width, cross-sectional area, tidal prism (calculated with modified Jarrett [1976] equation [Equation 6]), and ebb-tidal volumes (calculated with modified Walton & Adams [1976] formula [Equation 9]). The results described in the narrative from this point forward largely exclude the data point from 1852 from the analysis. The 1852 cross-sectional area

when qualitatively compared to all other data points appears as an outlier and potentially obfuscates inlet behavior. In addition, DeAlteris and Byrne (1975) suggest the “historical evidence indicates that the configuration of the interior marsh-lagoon system has changed little since 1852.

**Table 12: Historical metrics of the Wachapreague Inlet tidal inlet complex**

<p style="text-align: center;"><b>Wachapreague Inlet</b> Historical Metrics of the Inlet Complex</p>					
<b>Year (Month)</b>	<b>Maximum Depth (m)</b>	<b>Inlet Width (m)</b>	<b>Cross-Sectional Area (m<sup>2</sup>)</b>	<b>Tidal Prism (m<sup>3</sup>) <sup>a</sup></b>	<b>Ebb Tidal Delta Volume (m<sup>3</sup>) <sup>b</sup></b>
1852	14.0	732	1845	$2.33 \times 10^7$	$7.55 \times 10^6$
1871	18.3	640	4473	$5.29 \times 10^7$	$2.07 \times 10^7$
1911	17.0	396	4737	$5.57 \times 10^7$	$2.21 \times 10^7$
1934	17.7	969	4572	$5.39 \times 10^7$	$2.12 \times 10^7$
1972	18.2	549	4047	$4.82 \times 10^7$	$1.85 \times 10^7$
2007 (Apr)	20.6	374	4398 <sup>c</sup>	$5.20 \times 10^7$	$2.03 \times 10^7$
2010 (Apr)	20.2	429	4735 <sup>d</sup>	$5.57 \times 10^7$	$2.21 \times 10^7$
2010 (Aug)	--	--	5014 <sup>e</sup>	$5.88 \times 10^7$	$2.36 \times 10^7$
2011 (Apr)	20.9	445	5210 <sup>d</sup>	$6.09 \times 10^7$	$2.46 \times 10^7$

<sup>a</sup> Jarrett (1976) formula, Unjettied, Atlantic coast (Richardson-McBride-Seminack conversion)

<sup>b</sup> Walton & Adams (1976) formula, All Inlets (Fontolan conversion)

<sup>c</sup> Bathymetric soundings (10 second sample interval) with four transects at inlet throat

<sup>d</sup> Bathymetric soundings (5 second sample interval) with two transects at inlet throat

<sup>e</sup> Survey at inlet throat with current velocity data obtained with ADCP system

The changes at Wachapreague Inlet are further analyzed across the historical period of record (1871–2011), the long term (1871–2007), and the short term (2007–2010) in Tables 13–15. These tables present the mean values and linear regression rates

( $\text{m}^2/\text{yr}$ ) of cross-sectional area ( $\text{m}^2$ ), tidal prism ( $\text{m}^3$ ), and ebb-tidal delta volume ( $\text{m}^3$ ), respectively. The presentation of the information in this manner allows for the comparison of cross-sectional changes across a range of time periods. The tidal prism and ebb-tidal delta volumes are calculated with metric derivatives of the modified Jarrett (1976) and Walton and Adams (1976) equations (Equations 6 and 9, respectively), and as such, the calculated volumes correlate to cross-sectional area. Of particular importance, this research accounts for the natural variability in tidal prism on a monthly basis (e.g., neap vs. spring tides, perigee vs. apogee) and a seasonal basis (e.g., potential coastal setup caused by meteorological events, thermal expansion of the water column [steric effect]) by utilizing a 15% natural variability in the tidal-inlet analyses (see Chapter 3, Bathymetric Data Set Errors). The 15% variability bars are used in Figures 58–60 to demonstrate inlet natural variability potentially centering around the recorded values.

From 1871 to 2011 the cross-sectional area of the inlet throat ranged from a minimum of  $4047 \text{ m}^2$  in 1972 to a maximum of  $5210 \text{ m}^2$  in 2011 with an average value of  $4648 \text{ m}^2$ . The linear regression change rate across this historical period of record demonstrated a low expansion rate of  $2.2 \text{ m}^2/\text{yr}$  (0.11) (Table 13). The inlet's cross-sectional area during the earlier portions of the historical record are larger than the low of 1972 and more closely match the historical average as evidenced by the values of  $4473 \text{ m}^2$  in 1871,  $4737 \text{ m}^2$  in 1911, and  $4572 \text{ m}^2$  in 1934. Across the long-term time period of 1871–2007 the mean cross-sectional area was  $4445 \text{ m}^2$  and a linear regression change rate of  $-2.4 \text{ m}^2/\text{yr}$  (0.25) (Table 13). Over the short-term, cross-sectional areas show a steady but consistent increase from  $4398 \text{ m}^2$  in 2007 to  $5210 \text{ m}^2$  in 2011. This change over a

four-year period represents a total increase of 812 m<sup>2</sup> in cross-sectional area at the inlet throat. Cross-sectional area experienced a distinct change from a low reduction rate over the long term to a high expansion rate over the short term. From 2007 to 2011 the mean cross-sectional area was 4839 m<sup>2</sup> with a linear regression change rate of 186.1 m<sup>2</sup>/yr (0.87). Finally, the mean area of 4839 m<sup>2</sup> from 2007 to 2011 is 191 m<sup>2</sup> higher than the historical average of 4648 m<sup>2</sup> (1871–2011) (Figure 58).

**Table 13: Mean values and linear regression rates (m<sup>2</sup>/yr) of the cross-sectional area changes at Wachapreague Inlet across multiple time periods**

**Cross-Sectional Area Changes at Wachapreague Inlet**  
Period of Record (1871-2011), Long-Term (1871-2007),  
and Short-Term (2007-2011) Time Periods  
Mean Values and Linear Regression Rates (m<sup>2</sup>/yr)

	<b>1871-2011</b>	<b>1871-2007</b>	<b>2007-2011</b>
Mean	4648.3	4445.4	4839.3
St. Dev.	363.6	256.3	352.9
Change Rate	2.2	-2.4	186.1
R <sup>2</sup>	0.11	0.25	0.87
St. Error	370.6	256.8	153.8

**Table 14: Mean values and linear regression rates (m<sup>3</sup>/yr) of tidal prism changes at Wachapreague Inlet across multiple time periods**

**Tidal Prism Changes at Wachapreague Inlet**  
Period of Record (1871-2011), Long-Term (1871-2007),  
and Short-Term (2007-2011) Time Periods  
Mean Values and Linear Regression Rates (m<sup>3</sup>/yr)

	<b>1871-2011</b>	<b>1871-2007</b>	<b>2007-2011</b>
Mean	5.48 x 10 <sup>7</sup>	5.25 x 10 <sup>7</sup>	5.69 x 10 <sup>7</sup>
St. Dev.	3.98 x 10 <sup>6</sup>	2.79 x 10 <sup>6</sup>	3.88 x 10 <sup>6</sup>
Change Rate	2.40 x 10 <sup>4</sup>	-2.67 x 10 <sup>4</sup>	2.04 x 10 <sup>6</sup>
R <sup>2</sup>	0.11	0.26	0.87
St. Error	4.06 x 10 <sup>6</sup>	2.78 x 10 <sup>6</sup>	1.69 x 10 <sup>6</sup>

**Table 15: Mean values and linear regression rates (m<sup>3</sup>/yr) of the ebb-tidal delta volume changes at Wachapreague Inlet across multiple time periods**

**Ebb Tidal Delta Volume Changes at Wachapreague Inlet**  
Period of Record (1871-2011), Long-Term (1871-2007),  
and Short-Term (2007-2011) Time Periods  
Mean Values and Linear Regression Rates (m<sup>3</sup>/yr)

	<b>1871-2011</b>	<b>1871-2007</b>	<b>2007-2011</b>
Mean	2.16 x 10 <sup>7</sup>	2.06 x 10 <sup>7</sup>	2.27 x 10 <sup>7</sup>
St. Dev.	1.92 x 10 <sup>6</sup>	1.33 x 10 <sup>6</sup>	1.87 x 10 <sup>6</sup>
Change Rate	1.18 x 10 <sup>4</sup>	-1.26 x 10 <sup>4</sup>	9.89 x 10 <sup>5</sup>
R <sup>2</sup>	0.11	0.25	0.88
St. Error	1.95 x 10 <sup>6</sup>	1.33 x 10 <sup>6</sup>	8.10 x 10 <sup>5</sup>

From 1871 to 2007, tidal prism ranged fluctuated between  $4.82 \times 10^7$  m<sup>3</sup> (1972) and a high of  $5.57 \times 10^7$  m<sup>3</sup> (1911) with a mean of  $5.25 \times 10^7$  m<sup>3</sup> (Tables 12 and 14). Ebb-tidal delta volumes ranged between  $1.85 \times 10^7$  m<sup>3</sup> (1972) and  $2.21 \times 10^7$  m<sup>3</sup> (1911) (Tables 12 and 15). The long-term linear regression rates of change (1871–2007) at

Wachapreague Inlet were  $-2.67 \times 10^4 \text{ m}^3/\text{yr}$  for tidal prism and  $-1.26 \text{ m}^3/\text{yr}$  for ebb-tidal delta volume (Figure 59). Overall from 1871 to 2007, tidal prism and ebb-tidal delta volumes have demonstrated fluctuations throughout the long-term time period. As with cross-sectional area, tidal prism and ebb-tidal delta values are higher in the earlier portions of the historical record prior to 1972. In addition, tidal prism and ebb-tidal delta volumes in 2007 represent a net increase of  $3.8 \times 10^6 \text{ m}^3$  in tidal prism and  $1.8 \times 10^6 \text{ m}^3$  in ebb tidal delta volumes when compared to the values from 1972.

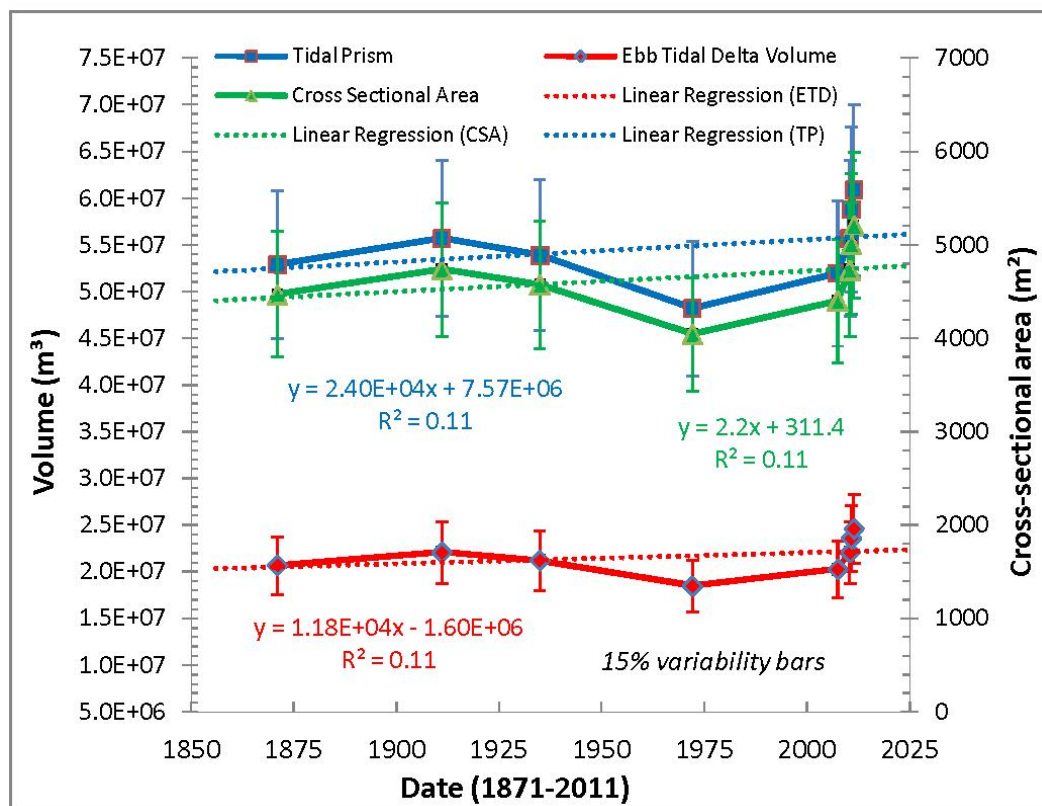


Figure 58: Cross-sectional area (m2), tidal prism (m3), and ebb-tidal delta volume (m3) at Wachapreague Inlet, Virginia from 1871 to 2011 with linear regression rates and strength of relationship with 15% variability bars.



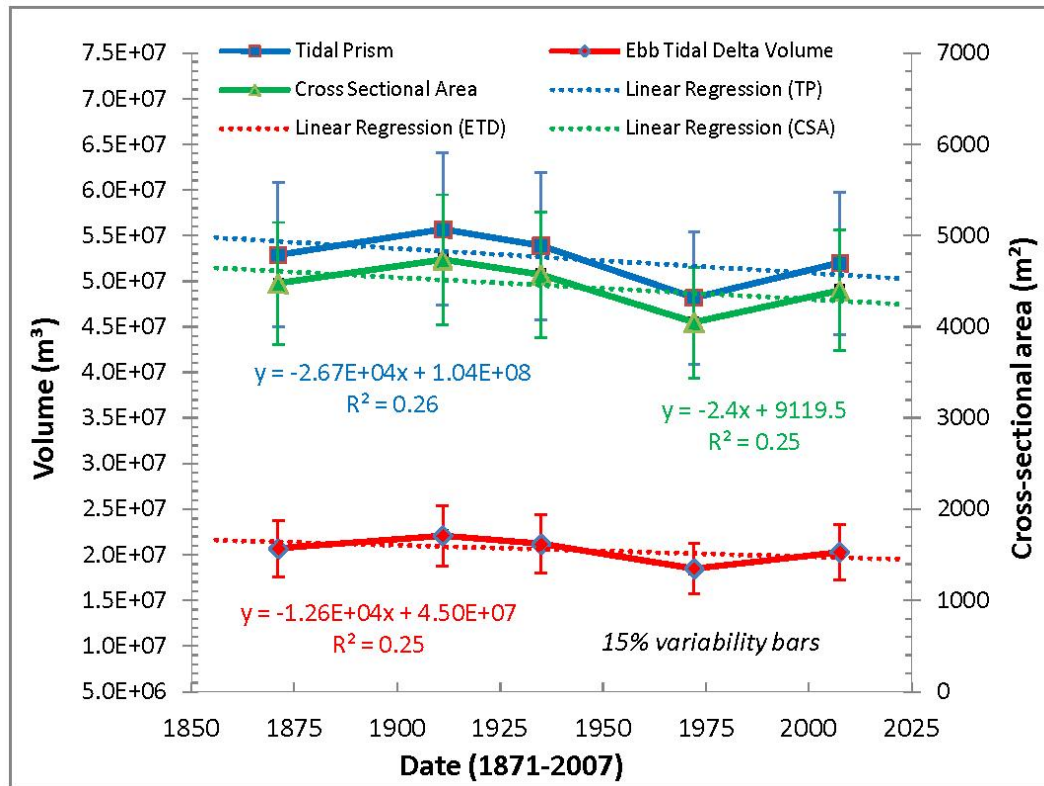


Figure 59: Tidal prism (m<sup>3</sup>), ebb-tidal delta volume (m<sup>3</sup>), and cross-sectional area (m<sup>2</sup>) at Wachapreague Inlet, Virginia with linear regression rates (1871–2007). The overall trend is a slight decrease from 1871 to 2007.

Over the short-term (2007–2011), tidal prism progressively increases from  $5.20 \times 10^7$  m<sup>3</sup> in 2007 to  $6.09 \times 10^7$  m<sup>3</sup> in 2011; similarly, ebb-tidal delta volumes also progressively increase from  $2.03 \times 10^7$  m<sup>3</sup> in 2007 to  $2.46 \times 10^7$  m<sup>3</sup> in 2011 (Table 12). The changes from 2007 to 2011 represent an increase of 71 m<sup>2</sup>/yr in cross-sectional area,  $8.9 \times 10^6$  m<sup>3</sup> in tidal prism, and  $4.3 \times 10^6$  m in ebb-tidal volume over the course of just 4 years. Furthermore, the mean tidal prism over the short term (2007–2011) is  $5.69 \times 10^7$  m<sup>3</sup> and this value is  $2.1 \times 10^6$  m<sup>3</sup> higher than the average long term mean (1871–2007) of  $5.48 \times 10^7$  m<sup>3</sup>. Furthermore, the mean ebb-tidal delta volume from 2007 to 2011 is  $2.27 \times$

$10^7 \text{ m}^3$ , which is  $1.1 \times 10^6 \text{ m}^3$  higher than the average of  $2.38 \times 10^7 \text{ m}^3$  (1871–2007). In addition, from 2007 to 2011 the short-term linear regression rates of change switch to a high rate of increase with  $2.04 \times 10^6 \text{ m}^3/\text{yr}$  for tidal prism and  $9.89 \times 10^5 \text{ m}^3/\text{yr}$  for ebb-tidal delta volume (Figure 60).

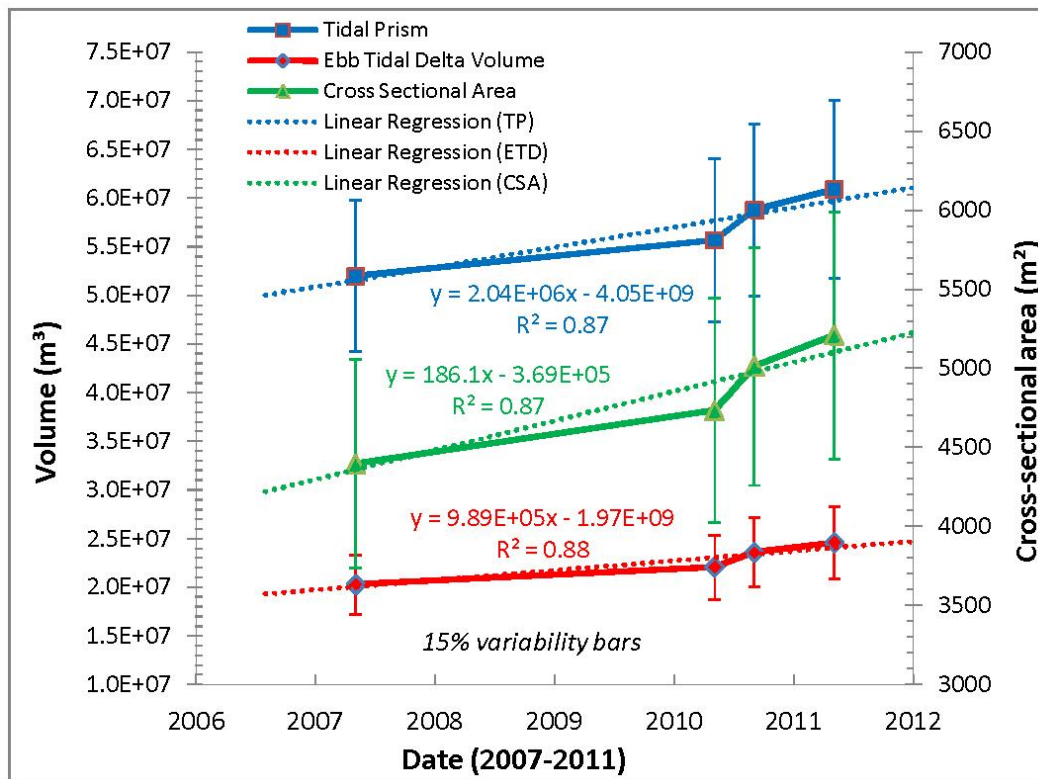


Figure 60: Tidal prism (m<sup>3</sup>), ebb-tidal delta volume (m<sup>3</sup>), and cross-sectional area (m<sup>2</sup>) at Wachapreague Inlet, Virginia with linear regression rates (2007–2011). The overall trend is a distinct increase from 2007 to 2011.

Additional metrics measuring tidal inlet behavior include maximum depth and inlet width (Figures 61 and 62). From 1871 to 2011, the maximum inlet throat depth ranged from 17.0 m in 1911 to 20.9 m in 2011 with an average value of 19.0 m. This represents an increase of 3.1 m in maximum inlet throat depth over the course of an entire century. In addition, the maximum depths showed a steady and consistent increase beginning in 1911. The inlet width results are not as consistent. The minimum width was 396 m in 1911 and the maximum width was 969 m in 1934 with an average of 551 m. Furthermore, inlet widths fluctuated substantially from 1871 to 1972. However, in the short-term record, inlet widths were more stable with a minimum of 429 m in 2007 to a maximum of 445 m in 2011. As with maximum depths, a small but consistent increase in inlet width occurred in the short-term record. In summary, inlet dimensions during the earlier portions of the historical record generally showed a wider and shallower inlet throat with the tidal inlet developing a deeper and narrower inlet throat, especially over the short term.

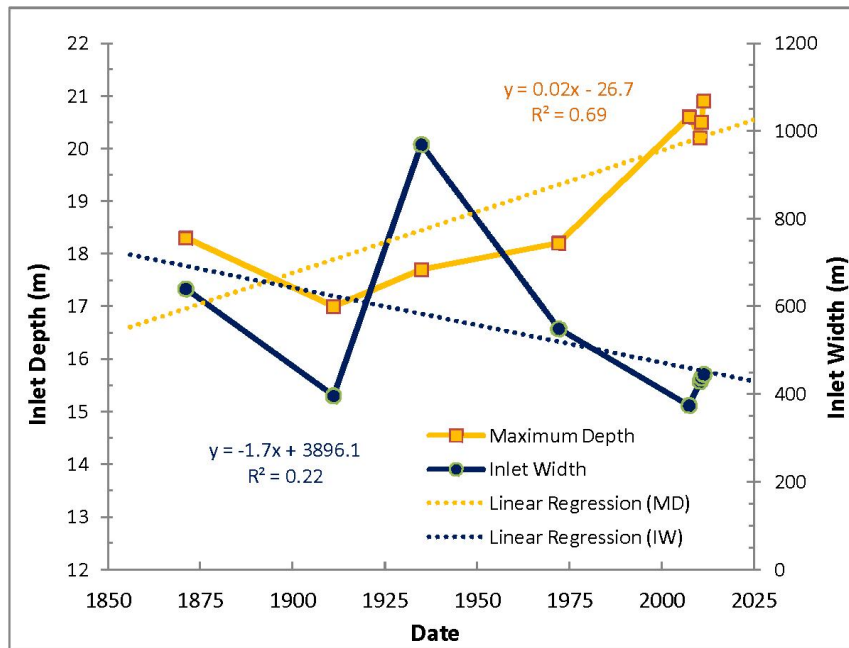


Figure 61: Maximum inlet throat depths (m) and inlet widths (m) of Wachapreague Inlet, Virginia with linear regression rates (1871–2011).

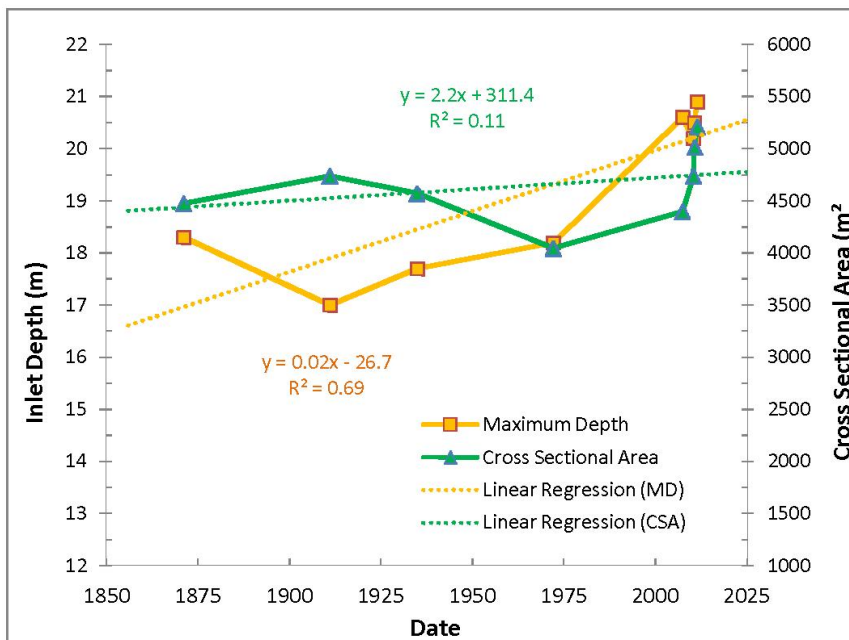


Figure 62: Cross-sectional area (m²) and maximum inlet throat depth (m) of Wachapreague Inlet, Virginia with linear regression rates (1871–2011).

## Parramore Island Summary

Parramore is a classic mixed-energy, tide-dominated barrier island with a historical record of shoreline advance that is now experiencing rapid retreat along its non-inlet-influenced, open-ocean shoreline. Along the entire outer shoreline (Cells 3–4), the results indicate that shoreline behavior of Parramore Island has evolved from clockwise rotational instability over the long term as described by Leatherman et al. (1982) to continuous rapid retreat over the short term. Specifically, Parramore's outer shoreline (Cells 3–4) experienced a linear regression retreat rate of -4.1 m/yr ( $0.41 R^2$ ) over the long term (1852–1998) and -12.2 m/yr ( $0.91 R^2$ ) over the short term (1998–2010).

Parramore Island has undergone a fundamental adjustment in its pattern of shoreline behavior among nearly all its shoreline cells. Specifically, Figure 63 shows the end point rates (m/yr) by shoreline cell and incremental time periods and Figure 64 builds upon this exhibit by overlaying trendlines to more clearly illustrate patterns. Both figures clearly show increases in the retreat rate in every shoreline cell of Parramore Island (aside from Cell 1). In short, the shoreline cells have experienced a distinct switch from moderate and high advance rates in the earlier portions of the historical record to moderate and high retreat rates in the latter portions of the historical record.

The north-central open-ocean shoreline (Cell 3) exhibited moderate to high advance rates during substantial portions of its past: 15.4 m/yr (1852–1871) and 1.8 m/yr (1871–1910) (Table 8). However, Cell 3 experiences high linear regression and end point retreat rates of -11.4 m/yr and -12.5 m/yr, respectively, over the short term (1998–2010). These short-term rates help to explain the extensive tree die-offs along interior relict dune

ridges and the large number of fallen trees across the foreshore of Parramore Island. Moreover, the southern washover-dominated shoreline (Cell 4) experienced the highest retreat rates among all the Parramore shoreline cells with nearly 1.2 km in net shoreline movement over the entire historical period of record (1852–2010). Furthermore, the retreat rate along Cell 4 increased from -8.3 m/yr (LRR) over the long term (1852–1998) to -13.2 m/yr (LRR) over the short term (1998–2010), signifying large areas of washover and even higher rates of rapid shoreline retreat, especially when compared to long-term patterns of behavior (Table 9).

The northern inlet-influenced shoreline (Cell 2) is the only shoreline to show advance over the long term (1852–1998) albeit a low linear regression rate of 1.4 m/yr. However, the short-term rate of Cell 2 switches markedly to a high retreat rate of -11.6 m/yr over the short term (1998–2010). The long-term trend of shoreline advance nearest the inlet demonstrates the role of swash bar attachment on mixed-energy barrier islands. The reversal to retreat rates over the long term begins approximately 4.5 km south of Wachapreague Inlet, and this reveals the location of an inlet-influenced node and the southernmost extent of inlet-influenced processes. These alongshore long-term rates indicate the control of shorter-term inlet dynamics, such as ebb-tidal delta breaching, outer channel shifting, or sediment supply changes on the adjacent shorelines (FitzGerald, 1982, 1988; Fitzgerald et al., 1984). In contrast, high retreat rates occur along the entire length of Cell 2 over the short term.

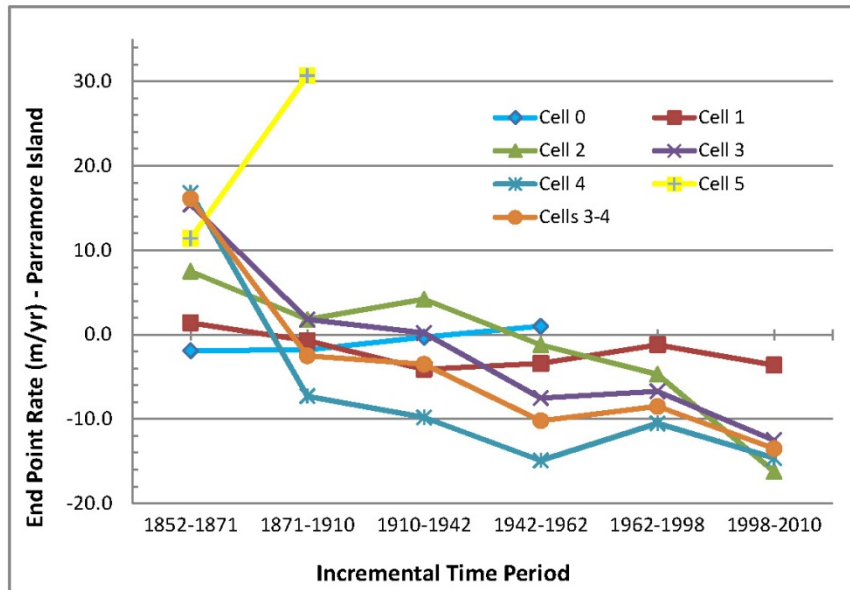


Figure 63: End point rate (m/yr) by shoreline cell and incremental time period for Parramore Island, Virginia.

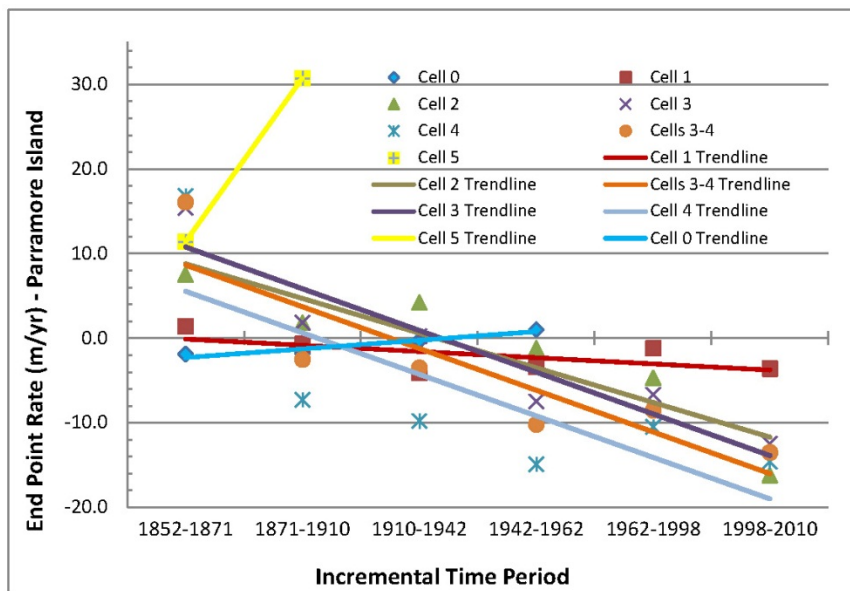


Figure 64: Trendlines of end point rate (m/yr) by shoreline cell and incremental time period for Parramore Island, Virginia.

## **Cedar Island Summary**

Cedar Island has evolved from a mixed-energy, tide-dominated barrier island with low and moderate retreat rates during earlier portions of the historical record to a mixed-energy, wave-dominated barrier island with high retreat rates over the latter portion of the historical record and severe retreat rates over the short term. Cedar Island's non-inlet-influenced, open-ocean shoreline experienced a retreat rate of -5.5 m/yr over the long term (1852–2007) and -15.4 m/yr over the short term (2007–2010). This represents nearly a three-fold increase in the retreat rate of the non-inlet-influenced, open ocean shoreline. Cedar Island has effectively transitioned from in-place narrowing to rapid barrier rollover and landward migration by overwash and inlet processes. The results demonstrate that Cedar Island has experienced sustained retreat across the entire period of record. However, retreat rates have increased markedly over the short term.

In regard to the results and discussion of this research, Figure 65 shows the end point rates (m/yr) by shoreline cell and incremental time periods and Figure 66 builds upon this exhibit by overlaying trendlines to more clearly illustrate patterns. In short, several shoreline cells have experienced a marked increase from low to moderate retreat rates in the earlier portions of the historical record to moderate and high retreat rates in the latter portions of the historical record. In other words, a clear pattern of retreat rates exists with incremental increases in the retreat rate throughout the period of record. Perhaps most interesting is the trendline of Cell 4, as explained in the Results chapter. The low retreat rate of Cell 4 from 2007 to 2010 is because of shoreline recovery following breach closure. The same phenomenon also largely explains the behavior and



trendline of Cell 1. A further discussion of cell dynamics follows with the use of linear regression rates to further illustrate the behavior of Cedar Island.

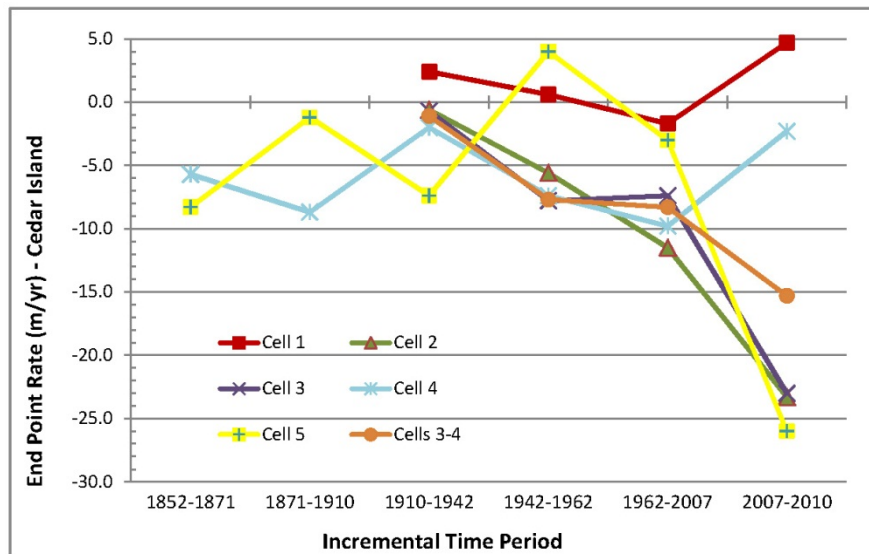
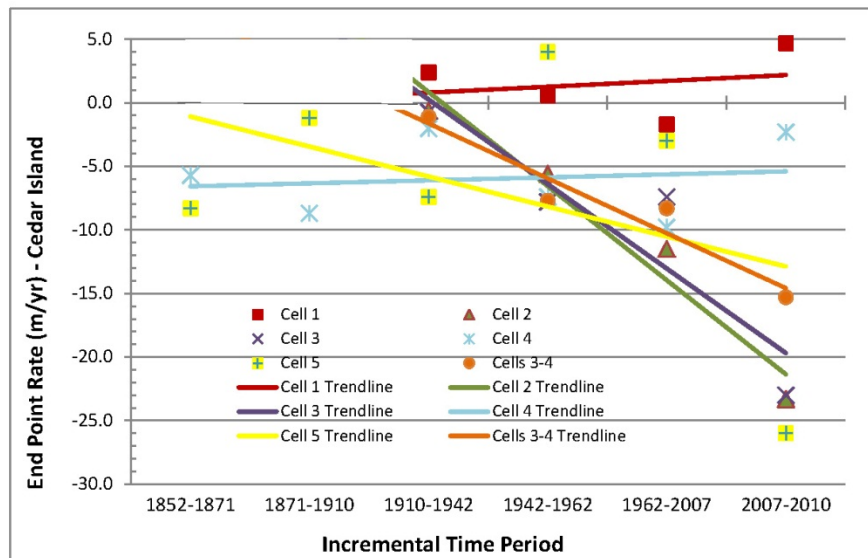


Figure 65: End point rate (m/yr) by shoreline cell and incremental time periods of Cedar Island, Virginia. The general trends for cells 2, 3, and 5 show increasing retreat rates through time.

The results from Cell 3, the north-central, marsh-backed, open-ocean shoreline, offer perhaps the clearest signal of the primary processes affecting Cedar Island because the shoreline migration patterns are the least influenced by factors such as inlet processes and breaching episodes. The end point and linear regression retreat rates indicate Cell 3 experienced moderate retreat for large portions of the historical record, specifically -5.5 m/yr and -5.3 m/yr, respectively (Table 11). However, the retreat rate jumps to -23.0 m/yr (EPR) and 22.0 m/yr (LRR) from 2007 to 2010 (Table 11). This rapid increase in the Cell 3 retreat rate points toward the effects of storm impacts and reduced sediment supply

upon Cedar's outer shoreline. Storm impacts are clearly represented in the shoreline record from 2009 to 2010 with Cell 3 experiencing a retreat rate of -47.7 m following an active season of northeasters in fall 2009 and winter 2010.



**Figure 66: Trendlines of end point rate (m/yr) by shoreline cell and incremental time period of Cedar Island, Virginia.**

Frequent episodes of island breaching characterize Cell 4, the south-central bay-backed shoreline (Moyer 2007). Cell 4 experienced a retreat rate of -7.1 m/yr (EPR) and -6.7 m/yr (LRR) from 1852 to 2007 and an advance rate of 0.7 m/yr (LRR) or -2.3 m/yr (EPR) of retreat from 2007 to 2010. However, as stated in the Results chapter, the rate from 2007 to 2010 reflects a breaching event in a unique way. The large spike in shoreline advance that spatially corresponds to the bay-backed portion of Cedar Island is representative of shoreline recovery (i.e., shoreline advancement) following the most

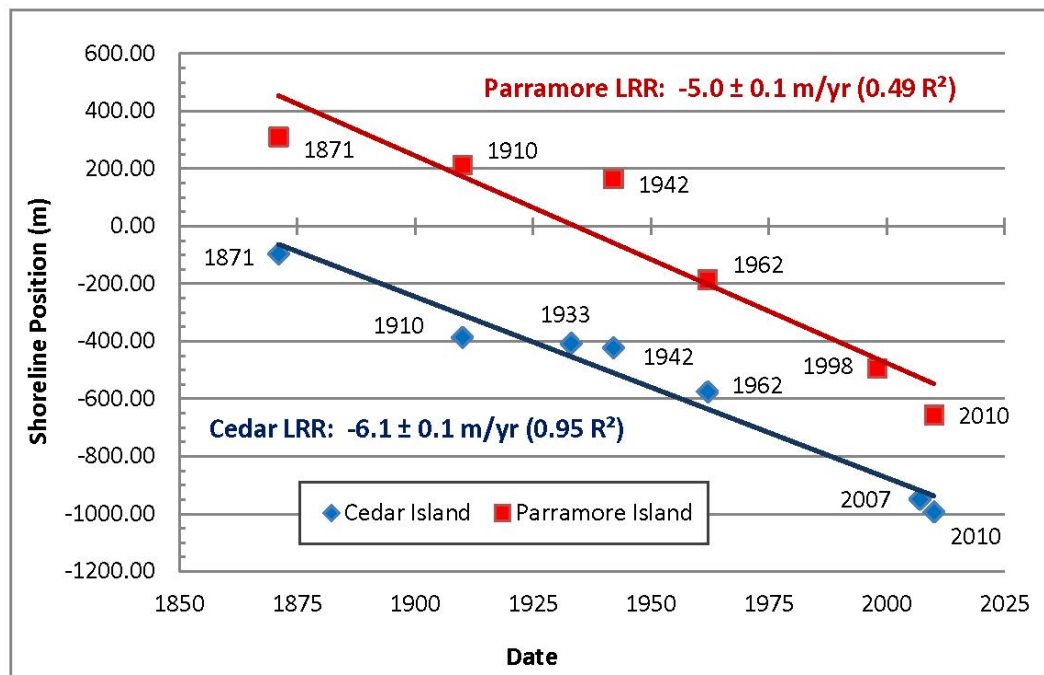
recent closure of the Cedar Island breach in early 2007 (Moyer, 2007; Hanley & McBride, 2011) (Figure 10). The rapid advance rate evident from 2007 to 2009 (10.5 m/yr, 0.53  $R^2$ ) dampens the historical retreat rate across the entire period of record and thus masks the prevailing shoreline behavior of Cell 4 (i.e., moderate retreat rates).

Cell 5, the southern spit open-ocean shoreline, demonstrates volatility in shoreline movement because of sediment intermittently supplied to the shoreline. Unlike other shoreline cells, Cell 5 demonstrated a brief period of moderate shoreline advance from 1942 to 1962 (4.0 m/yr) (Table 10). Despite this episodic sediment supply, the southern spit still experiences retreat at -3.5 m/yr (LRR) over the long term (1852–2007); in fact, Cell 5 suffers the highest short-term retreat rate at -24.6 m/yr (LRR) from 2007 to 2010.

Finally, processes governing the opening and closing of ephemeral breaches dominate the Coast Guard breach shoreline (Cell 1). Cell 1 is located at the closest proximity between estuary and ocean during tidal exchange. As a result, Cell 1 retreats at only -0.9 m/yr (0.75  $R^2$ ) from 1852 to 2007 but shows a moderate advance rate at 7.6 m/yr (0.39  $R^2$ ) from 2007 to 2010. Cell 2, the northern, breach-influenced, open-ocean shoreline, suffers from a trend of sustained and rapid retreat. Although Cell 2 is influenced by the northern breach zone and accompanying tidal processes of Cell 1, it also illustrates a pattern of severe and rapid retreat characteristic of Cedar's other open-ocean shorelines with retreat rates of -4.3 m/yr (0.67  $R^2$ ) from 1852 to 2007 and -22.1 m/yr (0.81  $R^2$ ) from 2007 to 2010.

As shown in Figure 67, the non-inlet-influenced, open-ocean shorelines of both Parramore and Cedar Islands are retreating at -5.0 m/yr (0.49  $R^2$ ) and -6.1 m/yr (0.95  $R^2$ ),

respectively, when measured across the entire period of record (1852–2010). The shoreline positions evident in the figure were determined by the magnitude of change from the 1852 shoreline. Furthermore, the comparison of long-term (top) versus short-term (bottom) shoreline change rates by geomorphic cell evident in Figure 68 demonstrates substantial increases in the shoreline retreat rate for both Parramore and Cedar Islands. The results clearly indicate that a fundamental adjustment in the behavior of the Parramore–Cedar barrier island system has occurred, where Parramore Island has experienced a reversal from net advance to net retreat that is accelerating and Cedar Island has experienced more rapid retreat rates.



**Figure 67: Long-term linear regression retreat rates for Parramore and Cedar Islands along non-inlet-influenced, open ocean shoreline for the entire period of record.**



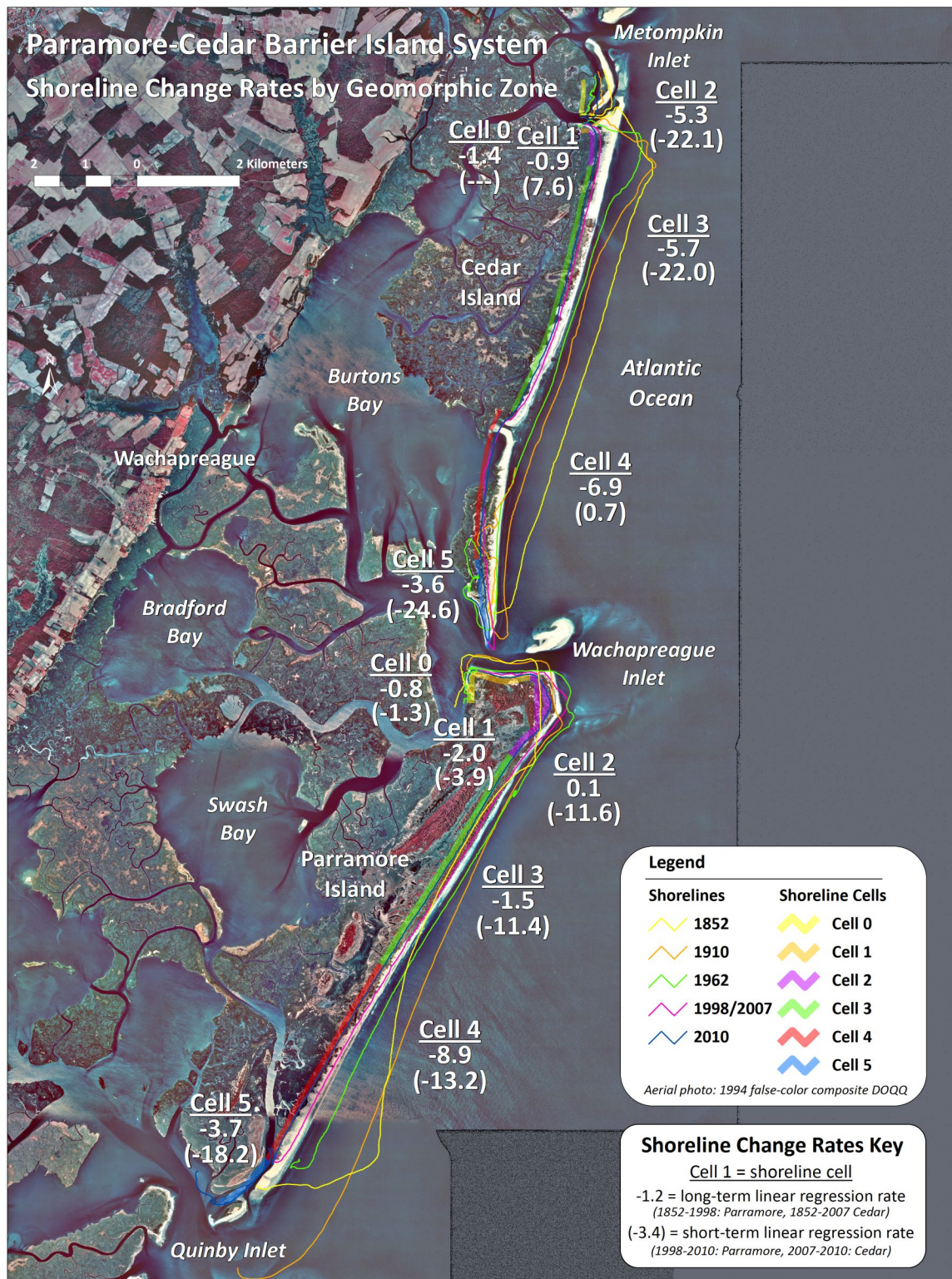


Figure 68: Long-term and short-term (in parentheses) shoreline change rates (m/yr) by geomorphic cell for the entire Parramore-Cedar barrier island system. USDA APFO, 1994.

## Wachapreague Inlet Summary

As presented in Figure 54, the Wachapreague Inlet-throat shoreline of Parramore Island (Cell 1) migrated in a southerly direction at 2.0 m/yr from 1852 to 1998 but nearly doubled its southerly migration rate to 3.9 m/yr from 1998 to 2010. In addition, the southern tip of Cedar Island also demonstrated notable behavior across the entire period of record with a trend of southerly migration throughout large segments of the historical period of record. However, from 2007 to 2010, the southern tip of Cedar Island experienced a rapid rate of northerly migration at 66.7 m/yr (end point rate [EPR]) and -83.8 m/yr (linear regression rate [LRR]). This increase in the southerly migration of Parramore Island's Cell 1 and the short-term northerly migration of the southern tip of Cedar Island may indicate the tidal inlet shorelines are migrating in a southerly and northerly direction in order to accommodate increased tidal prism at Wachapreague Inlet (i.e., expansion of cross-sectional area). Last, the bayside shoreline of Parramore Island (Cell 0) retreated at the lowest rate of all shoreline segments because of its protection from open-ocean processes. However, the bayside shoreline also experienced a small increase in its retreat rate from -0.8 m/yr (1852–1999) to -1.3 m/yr (1999–2010), which could potentially foreshadow future in-place narrowing of the barrier island.

The inherent dynamics of Wachapreague Inlet also have strongly influenced the results of the northern inlet-influenced shoreline of Parramore Island (Cell 2). Considerable variation exists in the end point rates for Cell 2 across the time periods, but markedly, the shoreline is characterized by a distinct switch from moderate advance rates (7.5 m/yr from 1852 to 1871) to rapid retreat rates (-16.2 m/yr from 1998 to 2010). The

overall long-term calculations that record low advance rates—such as the LRR of 1.4 m/yr from 1852 to 1998—mask the spatial and temporal variability of shorelines associated with a tidal inlet as demonstrated by the incremental time periods as measured by the end point rate. The shoreline change results for Cell 2 clearly mark a distinct shift from shoreline advance to retreat during the period of record. In summary, tidal inlet processes and the ebb-tidal delta fronting Wachapreague Inlet strongly influenced Cell 2. Ebb-tidal delta dynamics can produce substantial swings in shoreline position because of wave refraction, the local reversal in longshore sediment transport, sand bar welding, and seasonal onshore/offshore sediment transport (see FitzGerald, 1982; Fitzgerald et al., 1984; Fitzgerald, 1988).

Perhaps most important, the southern tip of Cedar Island does provide Wachapreague Inlet the ability to expand its cross-sectional area if needed over time. The southern bank and the base of the inlet throat of the inlet channel are impinging upon more-resistant Pleistocene deposits and possibly older units, thus making it difficult for the tidal prism to expand in those directions. However, the northern bank of the inlet channel (i.e., spit at southern end of Cedar Island) is characterized by unconsolidated Holocene sediment because of the southern inlet migration of inlet over time as stated above. Consequently, Wachapreague Inlet is not totally locked in non-erodible banks and could expand its cross-sectional area horizontally (i.e., to the north) if needed in response to increasing tidal prism through time. The recent behavior of the southern terminus of Cedar Island supports this hypothesis.

As a qualitative observation, this shoreline migration of the shoreline in a northerly direction corresponds to the increasing tidal prism from 2007 to 2011. Of note, the southern shoreline migrated further southward from 1852 to 1910, migrated northward in 1962, and once again had moved in a southerly direction by 2007. This most recent migration northward from 2007 to 2010 is especially interesting because it demonstrates that Wachapreague Inlet does have the ability to expand its cross-sectional area if needed. In addition, the maximum depth of Wachapreague Inlet has also slightly increased from 2007 to 2011. In other words, at least over the short-term Wachapreague Inlet is both widening and deepening and both of these processes are symptomatic of inlet response to increasing tidal prism over the short term.

As discussed in detail in the Methods chapter, cross-sectional area is a proxy for calculating tidal prism; furthermore, Table 14 shows that tidal prism at Wachapreague Inlet was relatively stable over the span of 136 years with fluctuations above and below the long-term (1871–2007) mean of  $5.25 \times 10^7 \text{ m}^3$ . These results corroborate the conclusions of DeAlteris and Byrnes (1975) that since 1871 the inlet has migrated south at a rate of 1 m/yr and that the inlet has had a stable cross-section of about  $4400 \text{ m}^2$ . They also point out that the changes in inlet cross-section are distinct, as evidenced by the amount of variability quantified in the study. As a result of this variability, it is important to monitor the inlet over time to obtain a true equilibrium value of inlet cross-section. In addition, their interpretative shallow seismic trace and core data show the existence of resistant strata.



The long-term (1871–2007) linear regression change rate in tidal prism is  $-2.67 \times 10^4 \text{ m}^3$  ( $0.26 R^2$ ) at Wachapreague Inlet (Table 14). This low change rate may indicate cross-sectional area at Wachapreague Inlet could be limited in its ability to expand because the inlet might be locked in non-erodible bank material (i.e., Pleistocene hard grounds or deposits). Consequently, the tidal prism at Wachapreague Inlet could be increasing over time without being reflected in historical cross-sectional changes. However, the short-term cross-sectional area results indicate that tidal prism has increased from 2007 to 2011 when compared to long-term trends. Specifically, tidal prism increased from  $5.20 \times 10^7 \text{ m}^3$  in 2007 to  $6.09 \times 10^7 \text{ m}^3$  in 2011 and this change amounts to a linear regression rate of  $2.04 \times 10^6 \text{ m}^3/\text{yr}$  ( $0.87 R^2$ ). In addition, the shoreline change results of the inlet-influenced geomorphic cells of Parramore and Cedar Islands (i.e., along Wachapreague Inlet) also indicate pronounced changes in behavior and migration patterns when compared to long-term trends (see Figure 54).

## **CHAPTER SIX: DISCUSSION**

Chapter Six is a discussion of the changes to the Parramore–Cedar barrier island system, an examination of the drivers of change to the system, and the presentation of a model of coastal change and barrier evolution for the Parramore–Cedar barrier-island system. The discussion focuses on four primary potential drivers of coastal change: a rise in relative sea level, the southerly extension of the large arc of erosion (i.e., deficit in sediment supply creating an anomalous erosion zone) south of Assateague Island, updrift island breaching, and increased storminess. Finally, a six-stage model of coastal change and barrier-island evolution along the southern Delmarva Peninsula is presented to clarify the processes affecting the Parramore–Cedar barrier-island system and to draw conclusions on the future of the system.

Changes in shoreline and tidal inlet behavior that depart from historical trends along the Parramore–Cedar barrier island system are important because these changes may signal a fundamental switch in the behavior of the Virginia Eastern Shore and, perhaps, large expanses of mixed-energy coasts along the entire U.S. Atlantic seaboard. These shoreline changes along the non-inlet-influenced, open-ocean shorelines of Parramore and Cedar Islands are an order of magnitude greater than the U.S. mid-Atlantic background rate of -1.5 m/yr and the short-term retreat rates stand out as

representing some of the highest retreat rates along the U.S. Atlantic coast (Dolan et al., 1979).

### **Drivers of Change to the Barrier-Island System**

As demonstrated, notable changes are occurring to the Parramore–Cedar barrier-island system, particularly over the short term. The shoreline and bathymetric changes experienced by the Parramore-Cedar barrier island system are most likely a response to one or more potential drivers of barrier-island system change. Specifically:

- 1) Relative sea-level rise, which increases tidal prism, promotes ebb-tidal delta growth, and degrades the marsh and adjacent barrier islands as postulated by the three-stage runaway transgression model presented by FitzGerald et al. (2004).
- 2) The large arc of erosion south of the well-developed recurved spit complex on the southern end of Assateague Island is extending further southward beyond Cedar Island, thus exacerbating downdrift sediment starvation and now causing barrier-island degradation to Parramore Island (Figure 69).
- 3) Updrift island breaching (e.g., the southern breach zone of Cedar Island and other updrift breaches further north) has captured a certain amount of longshore sediment transport, thus decreasing sediment supply downdrift.
- 4) Increased storminess from the 1950s to 1970s with a peak in 1967 (Fenster & Dolan, 1994) and the impact of significant meteorological events such as the 1962 Ash Wednesday storm and others (e.g., Hurricane Gloria in 1985, Nor’Ida in 2009) have resulted in increased washover deposition and/or offshore-directed

sediment transport, thus causing sediment loss from the littoral drift system along the southern Delmarva Peninsula.

### **Relative Sea-Level Rise and the Three-Stage Model of Runaway Transgression**

Fitzgerald et al. (2004) introduced a three-stage conceptual model of sand trapping processes at tidal inlets and the long-term response of adjacent barrier islands to a diminished sediment supply in a regimen of accelerated relative sea-level rise (Figure 12). The model is applicable to mixed-energy coasts (such as those along the Virginia Eastern Shore) that are characterized by short, stubby barrier islands; numerous tidal inlets; well-developed ebb-tidal deltas; and backbarrier marsh. The model accounts for the transformation of backbarrier salt marsh to open water and intertidal environments and the associated increase in tidal prism in a regimen of accelerated sea-level rise. This change in the hydraulic regimen results in an increased tidal prism that leads to growth in both the ebb- and flood-tidal deltas, a subsequent reduction in sediment supply along the coast, and fragmentation of the barrier-island system.

The stages of the conceptual model include: a) stable barrier, b) marsh decline, c) fringing marsh and marsh islands, and d) runaway transgression. The initial stable barrier stage is represented as the present general configuration of mixed-energy coasts characterized by barrier islands backed with an expansive estuarine marsh system and a network of tidal creeks. Stage 1 is a period where portions of the estuarine marsh are converted to intertidal and subtidal environments. This conversion increases tidal prism that scours tidal creeks further, enlarges the tidal inlet, and sequesters more sand on the ebb tidal delta. In Stage 2 estuarine marsh areas are in rapid decline and increased tidal

prism continues to enlarge tidal inlet size and ebb-tidal delta volume. In Stage 3 (runaway transgression) long-term existing tidal inlets have drowned and many new island breaches have developed. Also, barrier-island rollover is an active process. The multiple new inlets capture and reduce tidal prism at the former large inlets, causing the collapse of their ebb-tidal deltas onshore. In other words, during a sustained regimen of accelerated relative sea-level rise, backbarrier marsh is converted to open water through channel deepening and marsh inundation. This conversion of the estuarine marsh to open water results in an increased tidal prism. In response, increased tidal prism widens and deepens the tidal inlet through channel scour. In addition, increased tidal prism causes progradation of the ebb-tidal delta. This seaward advance of the ebb-tidal delta results in the sand body capturing more longshore sediment transport. The increased sand capture by the ebb-tidal delta results in adjacent barrier degradation because of downdrift sediment starvation (Miner et al., 2007). Consequently, ebb-tidal delta growth diminishes sediment supply along the coast that leads to barrier starvation, barrier-island fragmentation, and evolution to a transgressive coastal system.

The behavior of the Parramore and Cedar shorelines and the inlet throat at Wachapreague Inlet strongly suggest the system is entering Stage 1 of the Fitzgerald et al. (2004) three-stage model of runaway transgression. Clearly, the system no longer contains stable barriers and tidal prism has been increasing over the short term. The system appears to display positive feedback through the process of increasing tidal prism enlarging the ebb-tidal delta, which subsequently captures more sediment from the system and thus exacerbates a sediment shortage in the system. An important additional

point is that if erosion of the channel section is not substantially influenced by the geologic framework and has remained fairly constant during the period of record, then perhaps the hypsometry of the backbarrier has not changed substantially either.

The three-stage model of runaway transgression is based on morphologic, sedimentologic, and hydrodynamic responses to accelerated relative sea-level rise. The time factor has not been determined because each system will have its own value dependent on sediment availability, sedimentation processes, marsh growth (below grown biomass addition), rate of sea-level rise, storm frequency, and other factors. Ultimately, these factors and others control the hypsometry of the backbarrier, which in turn control bay tidal prism, flood versus ebb tidal current dominance, and accommodation space. When these various factors are taken as a whole it points to the particular need for additional research on the backbarrier of the Parramore–Cedar barrier-island system. However, the short-term increase in tidal prism at Wachapreague Inlet, the degradation of the adjacent barrier islands, and the distinct change to increased shoreline retreat rates support the hypothesis that the Parramore–Cedar barrier-island system could be entering or has entered Stage 1 of the runaway transgression model of FitzGerald et al. (2004) within the past 10 to 40 years.

### **Southern Extension of Large Arc of Erosion**

As Curray (1964) documented, the rate of relative sea-level rise and sediment supply largely drive the landward or seaward migration of barrier islands. Barrier-island chains operate as an interconnected system and thus individual islands cannot be studied in isolation. Furthermore, interruptions or fundamental changes in updrift sediment

supply will eventually—and perhaps significantly—affect downdrift islands and outweigh the effects of relative sea-level rise. It is notable that Cedar Island resides within the long arc of erosion south of Assateague Island (i.e., Fishing Point, Virginia) (Figure 69) that extends from Chincoteague Inlet, Virginia to Wachapreague Inlet, Virginia (Galgano, 1998). As a result, Cedar Island is sand-starved, as revealed in the pattern of sustained shoreline retreat across the entire period of record versus a record of shoreline advance along Parramore Island during the earlier portions of the historical record.

Effective sand trapping at the large recurved spit complex at the southern end of Assateague Island has captured massive sediment quantities from the regional sediment budget. The growth of this large recurved spit complex has resulted in downdrift sediment starvation that over time has resulted in a decreased sediment supply moving from north to south during the period of record. In other words, the sediment captured at the recurved spit complex would have otherwise gradually migrated downdrift to nourish the southerly shorelines.

As demonstrated in the results, Cedar Island is suffering from a decreased sediment supply in response to the large arc of erosion south of the recurved spit complex on the southern end of Assateague Island extending further southward. The marsh-backed portions of Cedar Island will likely continue to experience rapid barrier rollover, whereas the bay-backed segment of the island will breach more frequently and may eventually lead to island fragmentation and breakup because of a poor sediment supply and increased storm frequency (storms will be discussed in greater detail later). More

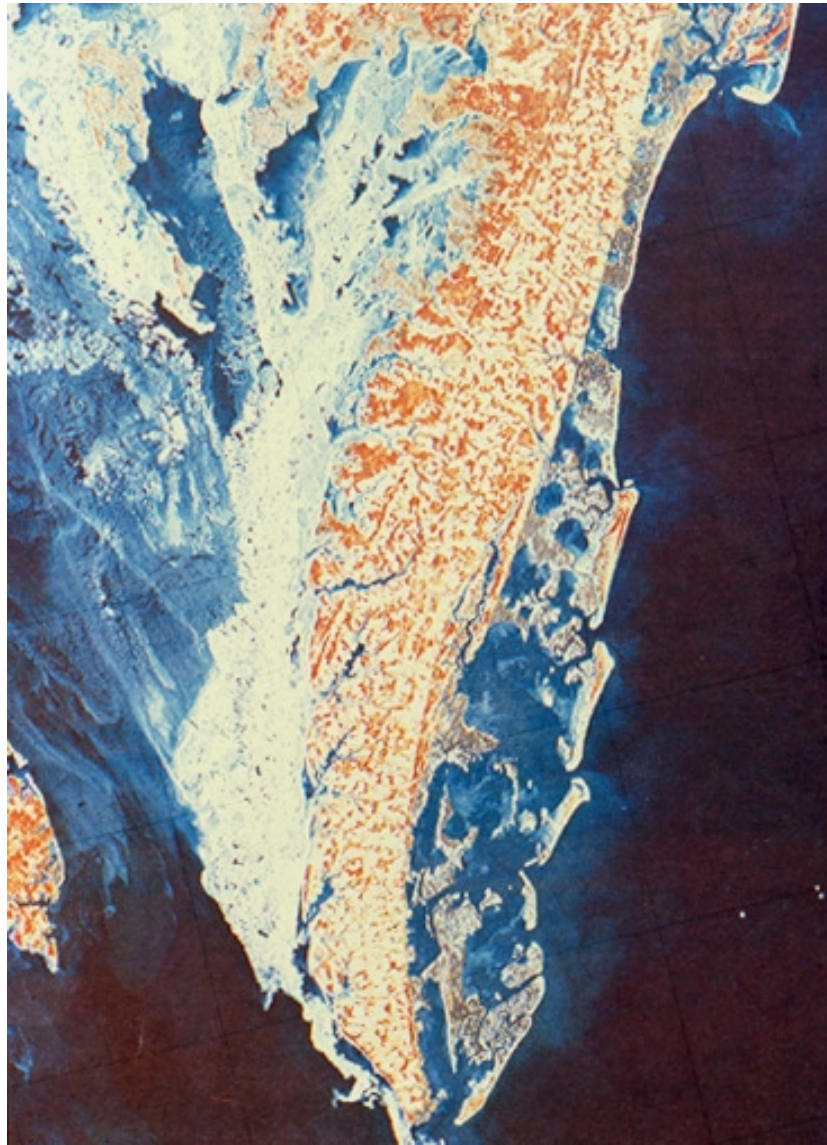
important, however, is that now it appears the large arc of erosion has extended further southward and now affects Parramore Island, as established by the distinct switch from shoreline advance to rapid retreat.

A change from shoreline advance to retreat over the entire period of record marks Parramore Island's southern, washover-dominated shoreline (Cell 4), but unlike Cell 3, the switch from advance to retreat occurs much earlier in the historical record (Table 8). For example, Cell 3 records a shoreline advance rate until the 1942–1962 time period, whereas Cell 4 records its first and ongoing retreat rate starting in the 1871–1910 time period. This pattern of shoreline movement is consistent with the concept of barrier-island rotational instability, as described by Leatherman et al. (1982). It is also notable that Cell 4 has the highest retreat rate among all the shoreline cells from 1998 to 2010 with a linear regression rate of -13.2 m/yr (0.94  $R^2$ ). These results indicate the pattern of shoreline retreat for Cell 4 is fairly consistent throughout large portions of the historical record. However, Cell 4 does experience even higher retreat rates in the short term even when compared to the rapid shoreline retreat throughout the majority of the long-term record. In other words, Cell 4 is experiencing rapid and sustained retreat over the short term, much like the results of Cell 3.

The sum of these long-term and short-term behaviors of Parramore and Cedar Islands strongly suggest the barrier-island system is suffering from lack of sediment supply. The large arc of erosion south of Assateague Island has extended further southward and is now affecting Parramore Island. The support for this hypothesis is the pronounced and distinct change from shoreline advance to retreat for Parramore Island as



compared chronologically to Cedar Island. As documented in the results, Cedar Island has experienced sustained retreat rates for the past 160 years, back to 1852, which is long before Parramore Island experienced a distinct reversal from rotational instability to sustained shoreline retreat, which started sometime in the 1950s or 1960s. In other words, the large arc of erosion has affected Cedar Island throughout its historical record, whereas Parramore Island started to experience sustained retreat rates along its entire outer shoreline subsequent to Cedar Island at least 100 years later. Hence, a relative geomorphic chronology of the alongshore impact and southern propagation of the arc of erosion is determined where Cedar Island was first affected (around or before 1852) followed by Parramore Island (circa 1950s or 1960s). Thus, the sustained Cedar Island retreat rates for its entire historical record (1852–2010) as compared to the distinct change from rotational instability to sustained retreat rates for Parramore Island occurred subsequently in the 1950s or 1960s (i.e., relative geomorphic chronology of the alongshore impact of the arc of erosion) support the hypothesis that the southern extension of the large arc of erosion is now affecting Parramore Island.



**Figure 69:** Satellite image circa 1982 of the southern Delmarva Peninsula showing the large and distinct arc of erosion south of the southern tip of Assateague Island that extends from Chincoteague Inlet, Virginia to Wachapreague Inlet, Virginia. (Photo provided by Duncan FitzGerald.) The white features in the Chesapeake Bay are areas of sea ice.

### **Updrift Island Breaching**

Another probable cause of the deficit in the sediment budget of the Parramore–Cedar barrier-island system is the frequent updrift breaching (e.g., Cedar Island breach

and other updrift breaches further north). For example, Cedar Island has breached three times within the past 50 years along the bay-backed, open-ocean shoreline (Moyer, 2007; Hanley & McBride, 2011) (Figure 70). The most recent breach and the longest lasting episode occurred over the course of 9 years (1998–2007). Moyer (2007:1) goes on to state, “[D]uring its lifetime, the breach rapidly migrated in the direction of net littoral transport [south], continued to lose its relatively small tidal prism, rotated its throat, and closed shortly before April 2007. The breach exhibited characteristics of a flood-dominated inlet and trapped relatively large volumes of sediment, effectively stabilizing the barrier island, at least temporarily. The existing tide-dominated inlet in the system, Wachapreague, showed virtually no effects.”



**Figure 70: Oblique aerial photo of Cedar Island Breach in November 2006. (Photo taken by Richard Ayers.)**

In other words, the breaching of Cedar Island further exacerbates sediment supply issues along the barrier-island system because the breaches and the subsequent shoreline recovery processes capture large quantities of sediment from the system. Fundamentally, Cedar Island breaches serve as sediment sinks that capture a certain percentage of sediment from the system and thus restrict supplies for the barrier-island system.

Gaunt (1991) demonstrates that Cedar Island has experienced in-place narrowing at varying rates throughout the long-term record and the outer ocean shoreline retreat rate was -4.4 m/yr from 1910 to 1986. Gaunt (1991) shows the overall thinning rate from 1910 to 1986 was 2.1 m/yr with the most notable thinning occurring after 1962. Specifically, the island thinning rate increases from approximately 0.6 m/yr from 1910 to 1962 to 4.0 m/yr from 1962 to 1986. Moreover, the data show that Cedar Island lost approximately 295 acres or 32% of its 1910 size from 1910 to 1986.

The spatial variations in island thinning or widening trends over the 1910–1986 time period are presented in Figure 71. The results show the northern, marsh-backed portion of Cedar Island suffered the most land loss because of thinning. The ocean-side shoreline retreat rates for the marsh-backed portion were historically lower than those of the bay-backed portion. In addition, the southern, bay-backed portion of Cedar Island experienced land gain because of the island breaching in 1957 and the subsequent shoreline recovery process (Figure 72). Consequently, these different retreat rates caused a progressively more pronounced offset along the outer shoreline at the boundary between the marsh- and bay-backed portions of the island.

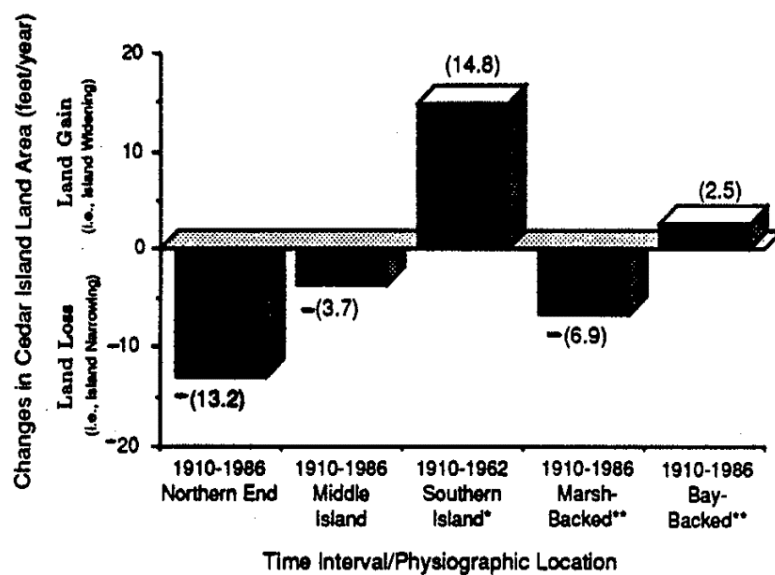


Figure 71: Changes in Cedar Island land area (feet/year) over various time intervals and physiographic locations (from Gaunt, 1991).



Figure 72: Island breaching along the southern portion of Cedar Island, Virginia in 1957 (Byrne et al. 1975).

Gaunt (1991) placed particular emphasis on the effects of island breaching on both Metompkin Island and Cedar Island and the downdrift impacts on sediment supplies. However, Gaunt's focus on the effects of updrift breaching is slightly misplaced because the breaches are more a consequence—not a cause—of the fundamental sediment supply issues along the Parramore–Cedar barrier-island system. In other words, the breaches serve as a local sediment sink that will inevitably supply sediment to the Parramore–Cedar barrier-island system as the islands transgress toward the Pleistocene mainland. Furthermore, Cedar and Metompkin Islands may fuse similar to the updrift barrier islands of Assawoman and Wallops Islands demonstrated in 1988 (Gaunt, 1991).

As a final observation, an emerging but possibly ephemeral breach was noticed at the boundary of Cell 4 and Cell 5 of Cedar Island during the GPS shoreline survey in April 2010 (Figure 73). In addition, the aerial photography from 2011 shows that the open-ocean shoreline (Cells 3 and 4) has experienced significant washover since 2009. These two observations, continued barrier breaching and significant areas of washover, lead one to conclude that Cedar Island may fragment into smaller barriers in the presence of restricted sediment supply. Furthermore, this barrier fragmentation also lends credence to and support of the FitzGerald et al. (2004) model of runaway transgression because barrier thinning and fragmentation are characteristic of Stages 2 and 3. These conditions warrant a further discussion in the fourth and final potential driver of change to the barrier-island system: storminess.

In summary, Cedar Island shows a history of breaching, developing small tidal prism at the breaches, and capturing potentially significant sediment volumes in the form



of flood-tidal deltas and once the breach closes through shoreline recovery. The ability of the breaches to capture sediment is revealed by the shoreline advance of Cell 4 following the closure of the Cedar breach in 2007. Cell 4 experiences rapid advance rates with 10.5 m/yr ( $0.53 R^2$ ) of shoreline migration from 2007 to 2009. Furthermore, portions of Cell 4 even record rates of more than 30 m/yr. In addition, Cell 1 also registers rapid advance rates following the closure of the Coast Guard breach at 16.7 m/yr ( $0.75 R^2$ ) from 2008 to 2010. Clearly, the dynamic breaches along Cedar Island over time have the ability to influence downdrift sediment supplies because of the process of sediment trapping (e.g., flood-tidal delta development, breach closure, and shoreline recovery).



**Figure 73:** Location of a possible emerging breach along the boundary of Cell 4 and Cell 5 on Cedar Island, Virginia in April 2010. The view is westward from the berm crest along the open-ocean shoreline toward the backbarrier bay and the town of Wachapreague, Virginia.

The following series of aerial photographs dating from 1994 to 2011 (Figures 74–79) qualitatively documents the opening and closing of breaches along Cedar Island over the past 17 years. On closer inspection, they also provide valuable insights into the behavior of the shorelines and the tidal inlet system. In 1994 the “Coast Guard breach” (located along the northern segment of Cedar Island) is open, as is the “Cedar Island breach” that Moyer (2007) investigated in detail (Figure 74). In 2004 the Coast Guard breach is closed and the Cedar Island breach has further opened, rotated its throat, and migrated southward (Figure 75). Two years later in 2006, the Coast Guard breach continues to be closed and the Cedar Island breach is in the process of infilling and closing (Figure 76). In 2008 the Coast Guard breach has opened and the Cedar Island breach has fully closed (Figure 77), and in 2009 the same situation applies (Figure 78). In the most recent aerial photograph from 2011, the Coast Guard breach has reopened and the Cedar Island breach remains closed (Figure 79).



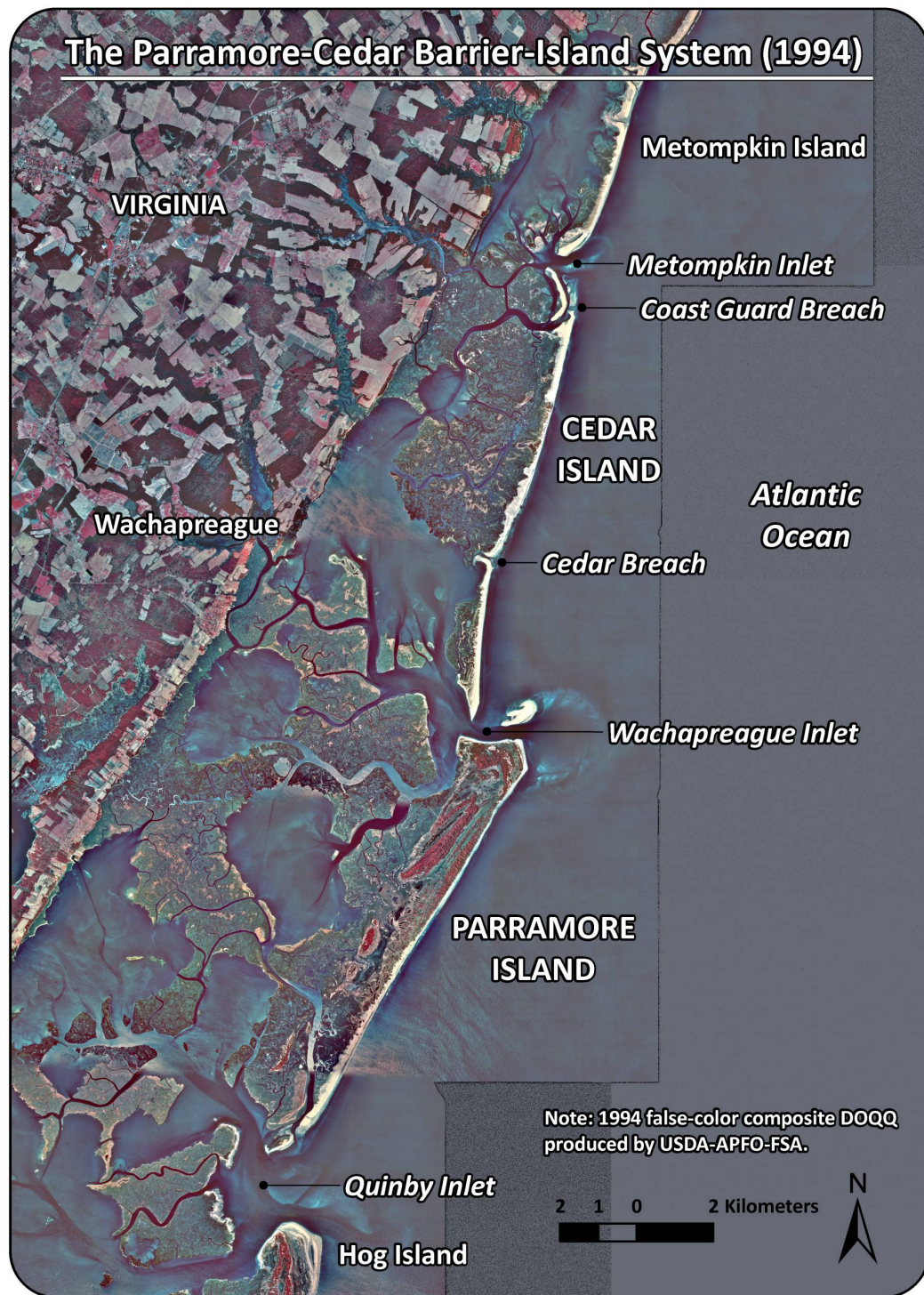


Figure 74: The Parramore–Cedar Barrier-Island System (1994). Note the opening of the Coast Guard breach along Cedar’s Cell 1 and Cedar Island breach along the bay-backed, open-ocean shoreline of Cedar’s Cell 4. USDA APFO, 1994.



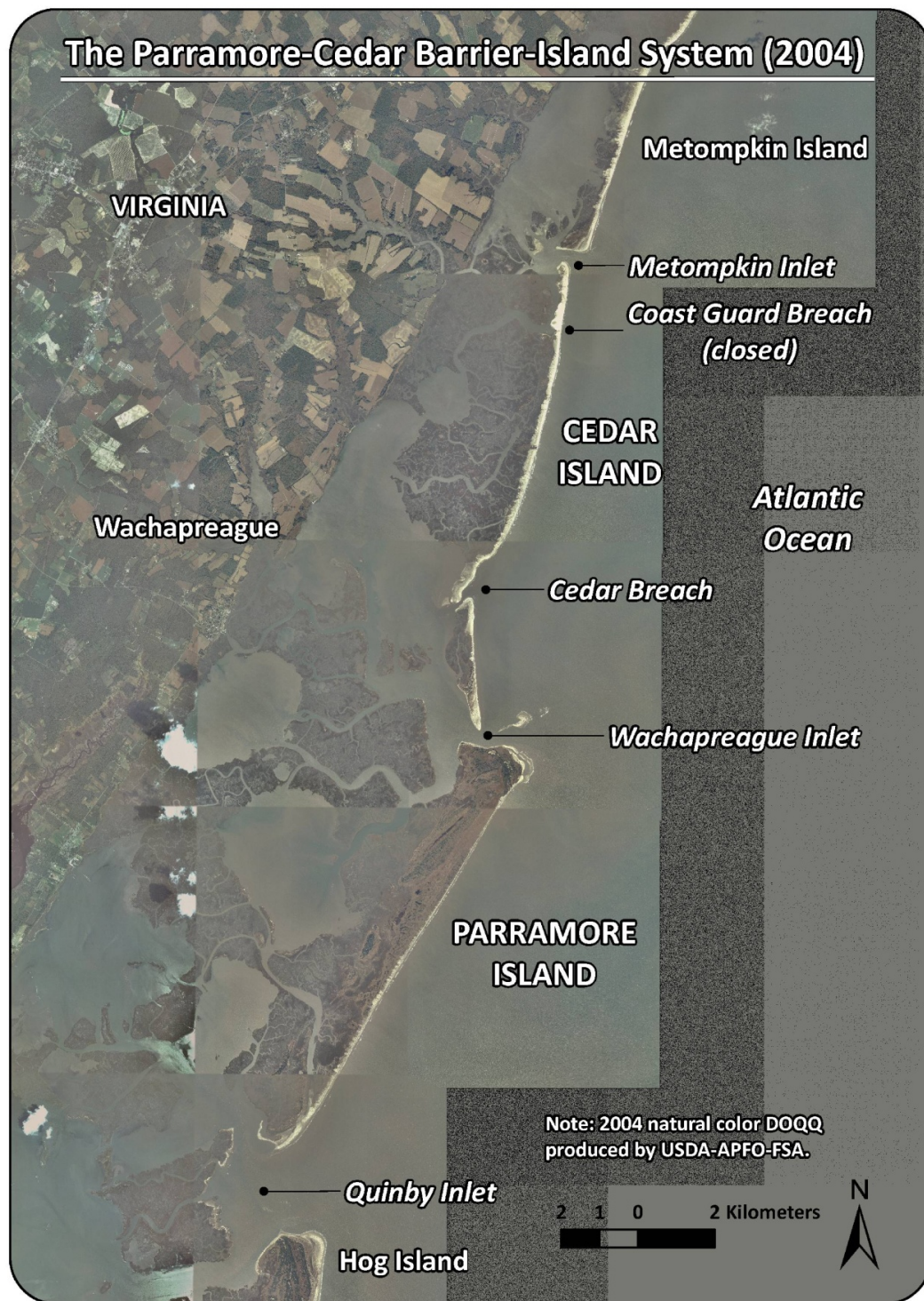


Figure 75: The Parramore–Cedar Barrier-Island System (2004). Note the closure of the Coast Guard breach to the north and the southerly migration, breach widening, and rotation of the throat of Cedar Island breach along Cell 4. USDA APFO, 1994.



**Figure 76: The Parramore–Cedar Barrier-Island System (2006).** Note the continued closure of the Coast Guard breach along Cell 1 to the north and that the Cedar Island breach along Cell 4 is waning as breach filling begins. USDA APFO, 1994.



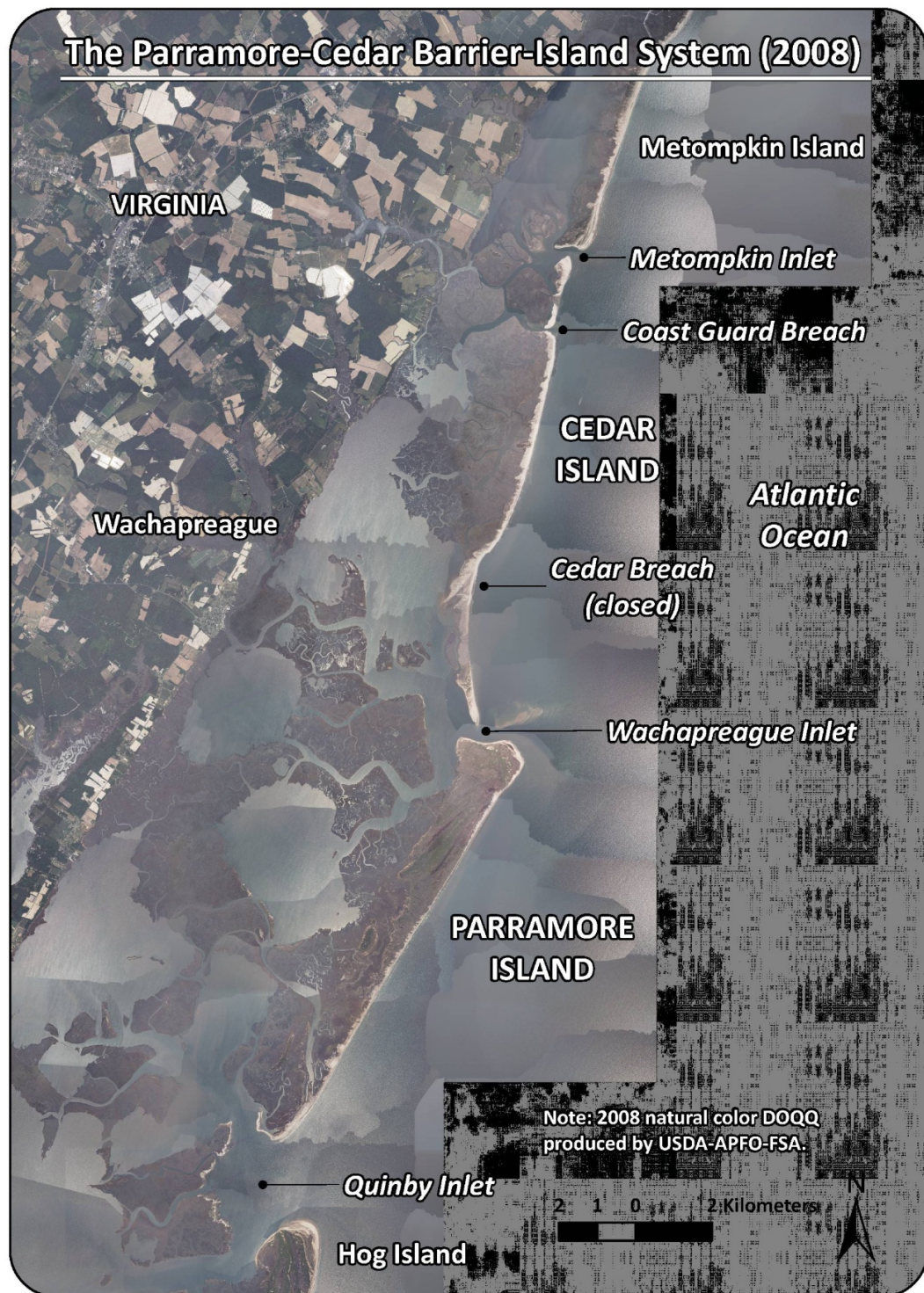


Figure 77: The Parramore–Cedar Barrier-Island System (2008). Note the opening of the Coast Guard breach along Cell 1 and the closure of the Cedar breach along Cell 4 that occurred in April 2007. USDA APFO, 1994.





Figure 78: The Parramore–Cedar Barrier-Island System (2009). Note the continued closure of the Cedar Island breach along Cell 4 and the continuous area of washover along the marsh-backed portion of Cedar Island (Cell 3). USDA APFO, 1994.



Figure 79: The Parramore–Cedar Barrier-Island System (2011). Note the closure of the Coast Guard breach, the continued closure of the Cedar Island breach, and possibly an emerging breach in the southern spit shoreline (Cell 5). USDA APFO, 1994.

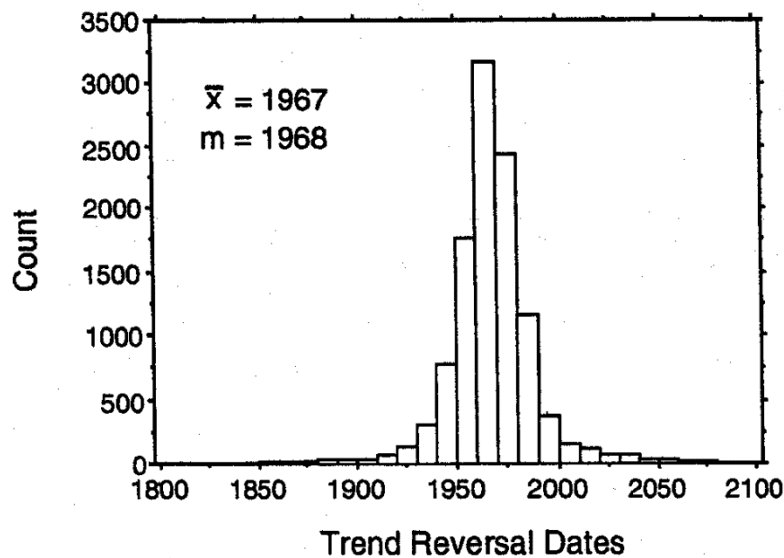


## **Increased Storminess**

The final potential driver of change to the Parramore–Cedar barrier-island system is increased storminess. Fenster and Dolan (1994) documented a period of increased storminess along the U.S. Atlantic coast from the 1950s to 1970s with a peak in 1967 (Figure 80). Also according to Fenster and Dolan (1994), the average reversal date (switch in the pattern of shoreline movement) for the Virginia barrier islands was 1977 and the modal date was 1972 in contrast to 1967-68 for all East Coast shorelines. Furthermore, 60% of this region became more erosional or less accretional. Fenster and Dolan (1994) also demonstrate that 76.3% of the Virginia barrier islands have undergone a change from accretion to erosion, acceleration in the erosion rate, or a deceleration in the accretion rate. Finally, their research asserts a series of powerful storms may have produced a system state change involving large-scale sediment redistributions. Rice et al. (1976) surmise that large storms such as the Ash Wednesday Nor'easter (March 1962) may have caused increased tidal discharge through Wachapreague Inlet, thereby eroding Parramore Island.

A time range between 1967 and 1977 is slightly later but generally corresponds to the incremental time period when the open-ocean shoreline of Parramore Island documented in this dissertation research switched from low/moderate advance rates or low retreat rates to sustained moderate to high retreat rates. For example, when examining the incremental time periods using end point rates along Parramore Island, a noticeable increase of -3.5 m/yr (1910–1942) to -10.2 m/yr (1942–1962) occurs and then a slight decrease to -8.5 m/yr (1962–1998) is seen. Even more granular, the north-central

open-ocean shoreline of Parramore (Cell 3)—the most stable of the shoreline cells—has 0.2 m/yr of advance between 1910 and 1942 and then experiences a switch to -7.5 m/yr of retreat between 1942 and 1962.



**Figure 80:** Histogram of all U.S. East Coast shoreline reversal dates over the long term (Fenster and Dolan, 1994). The average reversal date is 1967 and the modal reversal date is 1968.

Nebel et al. (2012) examined the decadal trends of shoreline movement on Cedar Island from 1852 to 2007 using similar methods as the ones employed in this research. Nebel et al. (2012) also reach similar conclusions to this study on Cedar Island’s long-term (1852–2007) and short-term (1994–2007) shoreline change rates, such as the near tripling of short-term retreat rates. However, their methods also contain noticeable differences, such as the definition of long term and short term, the segmentation of geomorphic zones, the segregation of tidally influenced shoreline data, the selection of an alternate high water line proxy, and an emphasis on end point and not linear regression



rates. Most notably perhaps, the results presented in this dissertation extend the shoreline analysis past 2007 to 2010 and the intervening years.

Nebel et al. (2012) document an alongshore average of -4.1 m/yr over the long term (1852–2007) with an increase in the short term (1994–2007) to -12.6 m/yr. These values are within the same order of magnitude as the linear regression results presented in this research—more specifically, -5.5 m/yr (1852–2007) and -15.4 m/yr (2007–2010). Table 16 reports the temporally portioned shoreline retreat rates of Nebel et al. (2012), showing the end point rates moving from -4.1 m/yr (1852–1910) to -3.0 m/yr (1910–1962) to -7.7 m/yr (1962–2007). In addition, Figure 81 graphically demonstrates the variability along the various Cedar Island shoreline sections and the differences between the long-term and short-term rates. The results of Nebel et al. (2012) documented the northern portion of the island immediately to the south of the “Coast Guard breach” retreated at the highest short-term rate (-24.6 m/yr) with the southern bay-backed shoreline sections also retreating at high rates (-23.0 m/yr and -23.3 m/yr).

**Table 16: Temporally portioned shoreline retreat rates of Cedar Island according to Nebel et al. (2012).**

Time Period	Years Elapsed	EPR (m/y)	LRR
1852–1910	58	–4.1	Not calculated
1910–1962	52	–3.0	Not calculated
1962–2007	45	–7.7	–7.15 m/y

The results and conclusions of Nebel et al. (2012) are insightful, but several nuances exist between their research and the discussion in this study. Nebel et al. (2012) trace an acceleration of Cedar Island shoreline retreat rates within the years 1980 to 1994 and this observation roughly corresponds to the conclusion of Gaunt (1991) that Cedar Island began to thin and narrow at higher rates during the 1962–1986 timeframe. Nebel et al. (2012) go on to conclude that Cedar Island has transitioned from parallel beach retreat to dual counterclockwise shoreline rotation (Figure 81). However, the counterclockwise rotation observation implies shoreline advance along one of the segments while another section suffers from retreat. However, the research presented in this dissertation clearly shows only limited shoreline advance along Cedar Island over the short term and this is because of shoreline recovery following the closure of an ephemeral breach along the southern bay-backed shoreline (i.e., Cedar Island breach). The shoreline advances were short lived and any breach-influenced shorelines will most likely return to the long-term prevailing pattern and suffer from the high retreat rates evident along the entirety of Cedar’s open-ocean shoreline. In other words, Cedar Island may not be rotating in a dual counterclockwise rotation, but rather experiencing rapid barrier rollover and landward migration through overwash and inlet processes with some zones of island breaching.

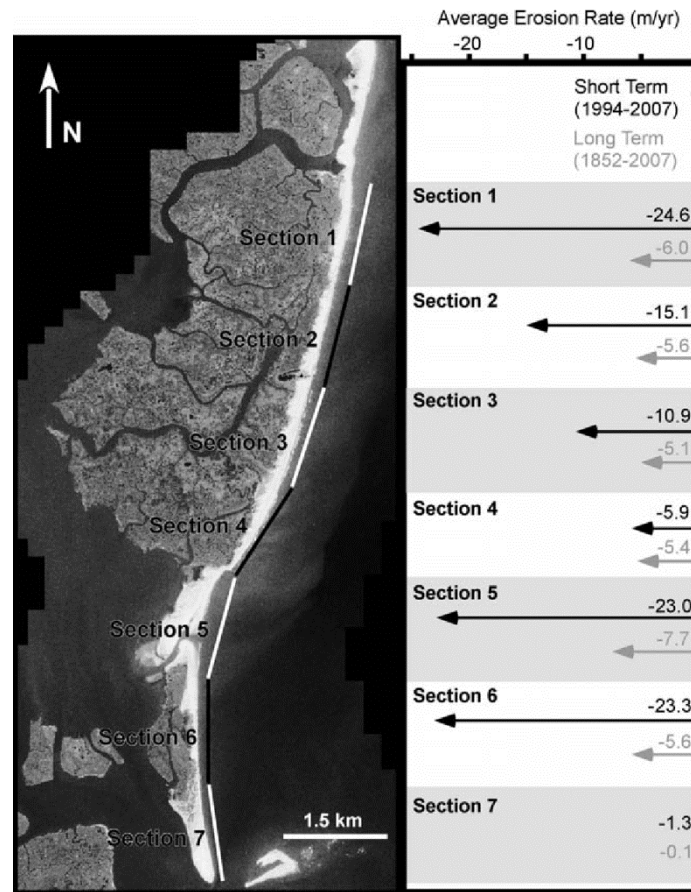
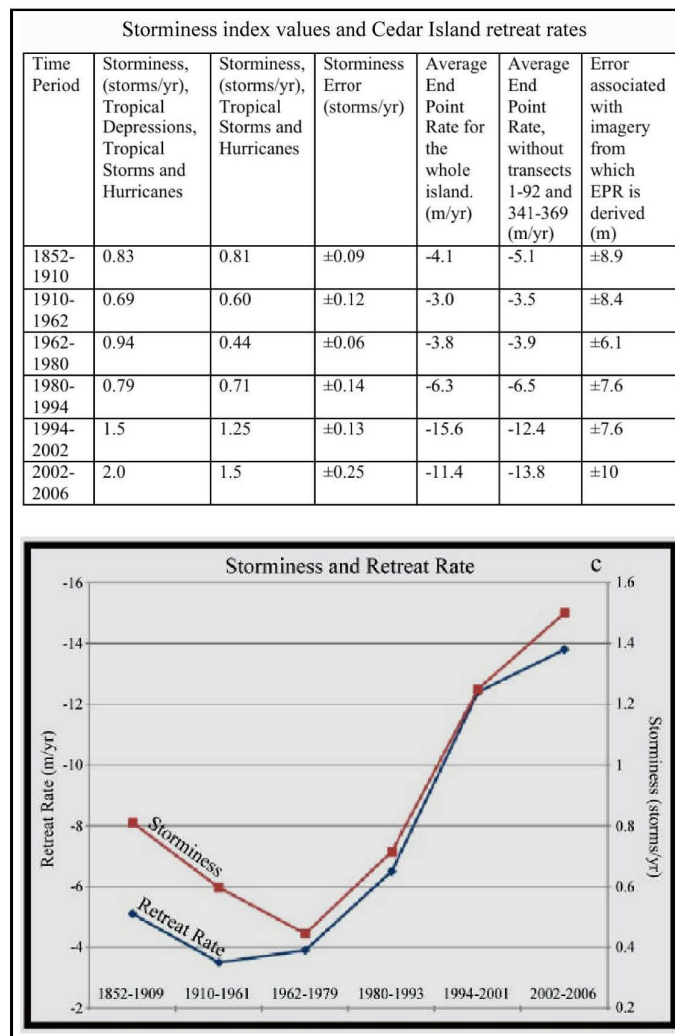


Figure 81: Average long- and short-term retreat rates by section for Cedar Island (Nebel et al., 2012).

A closer examination of more contemporary events also illustrates the impacts of increased storminess on the barrier-island system. Nebel and Trembanis (2010) suggest acceleration in shoreline erosion that began in the 1980s occurs contemporaneously with an increase in tropical storm and hurricane frequency. They also generated a storminess index (storms per year) based on the number of tropical depressions, tropical storms, and hurricanes across a range of time periods. The storminess index was then compared to the average end point rate of the entire island and the non-inlet-influenced, open-ocean

shoreline of Cedar Island (Table 17). Nebel et al. (2012) discovered that the retreat rate of the open-ocean shoreline of Cedar Island moved in close proximity to the storminess index, thus demonstrating a potential relationship between increased storm frequency and higher retreat rates.

**Table 17: Nebel and Trembanis (2010) storminess index values (storms/yr) and Cedar Island retreat rates (m/yr) (top) and storminess and retreat rates over incremental time periods using end point rates (m/yr) (bottom)**



Of course, large magnitude storms—and not just the increased frequency of storms—may also produce distinct changes upon the Parramore–Cedar barrier-island system. In November 2009, Tropical Storm Ida merged with a high pressure system located over the Northeast United States. This created a major northeaster storm later named Nor’Ida. The system affected the mid-Atlantic region for several days with waves exceeding 4.5 m and storm surge generating elevated water levels over several tidal cycles (USGS, 2011). The USGS Hurricanes and Extreme Storms Group collected aerial video, still photography, and laser altimetry surveys of post-storm conditions. Figure 82 is a result of this work and shows extensive washover deposits associated with the impact of Nor’Ida upon a portion of the south-central, bay-backed, open-ocean shoreline of Cedar Island (Cell 4). The significant erosion, absence of the beach, large areas of washover deposition, exposure of underlying relict marsh, and the missing house in the December 2009 photos suggest Cedar Island was inundated during a period of the Nor’Ida event (USGS, 2011).

The shoreline survey results of April 2010 further clarify the effects of Nor’Ida on the shorelines of Parramore and Cedar Islands. The conditions that are documented with the oblique aerial photography continued to exist during the GPS shoreline surveys of 2010 (i.e. the barrier island had experienced significant shoreline impacts and washover from large storms during the fall and winter of 2010–2011) (see Figure 82). The open-ocean shorelines of Cedar Island experienced severe retreat rates between April 2009 and April 2010—specifically rates of -45.4 m/yr (Cell 2), -47.7 m/yr (Cell 3), -26.1 (Cell 4), and -54.9 m/yr (Cell 5). Unfortunately, a 2009 pre-storm shoreline of Parramore Island

does not exist. However, the retreat rate from June 2007 to April 2010 is also high. The end point rates of the open-ocean shorelines of Parramore Island show retreat rates—specifically rates of -27.1 m/yr (Cell 2), -19.9 m/yr (Cell 3), and -21.5 m/yr (Cell 4). Clearly, pronounced changes occurred along the outer shorelines of Parramore and Cedar Islands as a result of storm activity as identified by the highest retreat rates within the entire period of record.

Byrne et al. (1974:1594) discovered that increased storminess also has an effect on tidal prism at Wachapreague Inlet:

“Mean tide level shows significant variations in absolute level during the year as a result of steric fluctuations and atmospheric pressure patterns. An analysis of Wachapreague tides for a three year period showed mean tide levels are lowest in January and February while the highest occur in September, October, and November. Mean tide levels for the survey period are shown in Fig. 8...noted that the October level is 0.3m higher than the January level. The importance of this phenomenon in complex storage systems is evident if a spring tide range (1.43m) is considered at these times. Calculations using the storage relationship indicate the October prism is 18% larger than January. Thus the period of enhanced prisms coincides with the advent of the northeast storm season on the east U.S. coast. During these months the largest longshore drift may be expected as the seasonal reduction in beach volumes occur. Were it not for the enhanced prisms occurring simultaneously more severe inlet shoaling would occur.”

In other words, increased tide levels during the initial months of the northeast storm season enhance a storm's ability to produce change, demonstrated by Nor'Ida in November 2009. This phenomenon also demonstrates the ability of a rise in relative sea level to have a greater impact on a coastline (i.e., enhanced levels of water flow upon the shoreface over time statistically).

Increased storminess appears to have influenced both the long-term and short-term shoreline retreat rates of Parramore and Cedar Islands. The fundamental switch in shoreline behavior for Parramore Island generally corresponds to a documented increase in storminess. The qualitative correlation of storminess to increased retreat rates shows that the increased storm frequency and large-magnitude events have the ability to generate significant changes along the open-ocean shorelines of the system. In addition, the shoreline surveys of 2010 clearly show the effects of Nor'Ida upon the open-ocean shorelines of both Cedar and Parramore Islands (Figures 83 and 84).

In summary, the four potential drivers of change—a rise in relative sea level, the southern extension of the large arc of erosion, updrift island breaching, and increased storminess—all play a role in producing change in the Parramore–Cedar barrier-island system. This research does not quantify the relative weight and influence of each of these factors on producing change but recognizes the combined and complementary effects of these four primary factors in driving the overall changes observed in the Parramore–Cedar barrier-island system. Most important, this research does document fundamental and distinct changes in shoreline movement and a short-term increase in tidal prism. The investigation and discussion of the potential drivers lead to the proposal of a six-stage

model of coastal change and barrier-island evolution that synthesizes the roles of the enlarging arc of erosion, relative sea-level rise, updrift island breaching, and increased storminess.



**Figure 82: Low-oblique aerial photography of Cedar Island, Virginia on May 21, 2009 (top) and December 4, 2009 (bottom), roughly 2 weeks after Nor'Ida. Image provided by USGS St. Petersburg Coastal and Marine Science Center. The yellow arrows point to the same lo**





**Figure 83: Extensive outcropping and eroded pieces of relict marsh along the entire shore of Cedar Island's north-central, marsh-backed, open-ocean shoreline (Cell 3).**



**Figure 84: Massive amounts of dead trees along the foreshore of Parramore Island's north-central, open-ocean shoreline (Cell 3). The view is west toward Italian Ridge and the town of Wachapreague, Virginia. Note the high amount of tree die-off along the higher elevation dune ridges in the interior of Parramore Island, Virginia.**

## **A Six-Stage Model of Coastal Change and Barrier-Island Evolution**

The following section presents a six-stage model of barrier-island evolution along the southern Delmarva Peninsula. The conceptual model is based on findings of this study; previous research within the area of interest; and, of course, reasonable conclusions informed by the discussion presented in this body of research. Fundamentally the model describes the regional processes affecting the Parramore–Cedar barrier-island system. The six stages of the model include: 1) updrift sediment trapping and development of recurved spit complex, 2) arc of erosion development, 3) southern extension of arc of erosion, 4) updrift barrier island changes, 5) downdrift barrier island changes, and 6) future barrier island evolution.

### **Stage 1 ( $\geq 2,000$ Years B.P.): Original Shoreline**

The original shoreline of the Virginia barrier islands approximately 2,000 years before the present is characterized as a healthy mixed-energy, tide-dominated barrier island system with a tidal regime and wave climate similar to existing conditions. The barrier islands comprising the Virginia coastline are aligned in a long linear line with short, stubby barrier and numerous tidal inlets to service tidal prism at near equilibrium (Figure 85). The barrier island chain is backed by a wide and large expanse of salt marsh intertwined with tidal creeks. Inlets along the coast are fronted by mature, well-developed ebb-tidal deltas. The system has not yet developed a recurved spit complex at the southern end of Assateague Island or the arc of erosion.

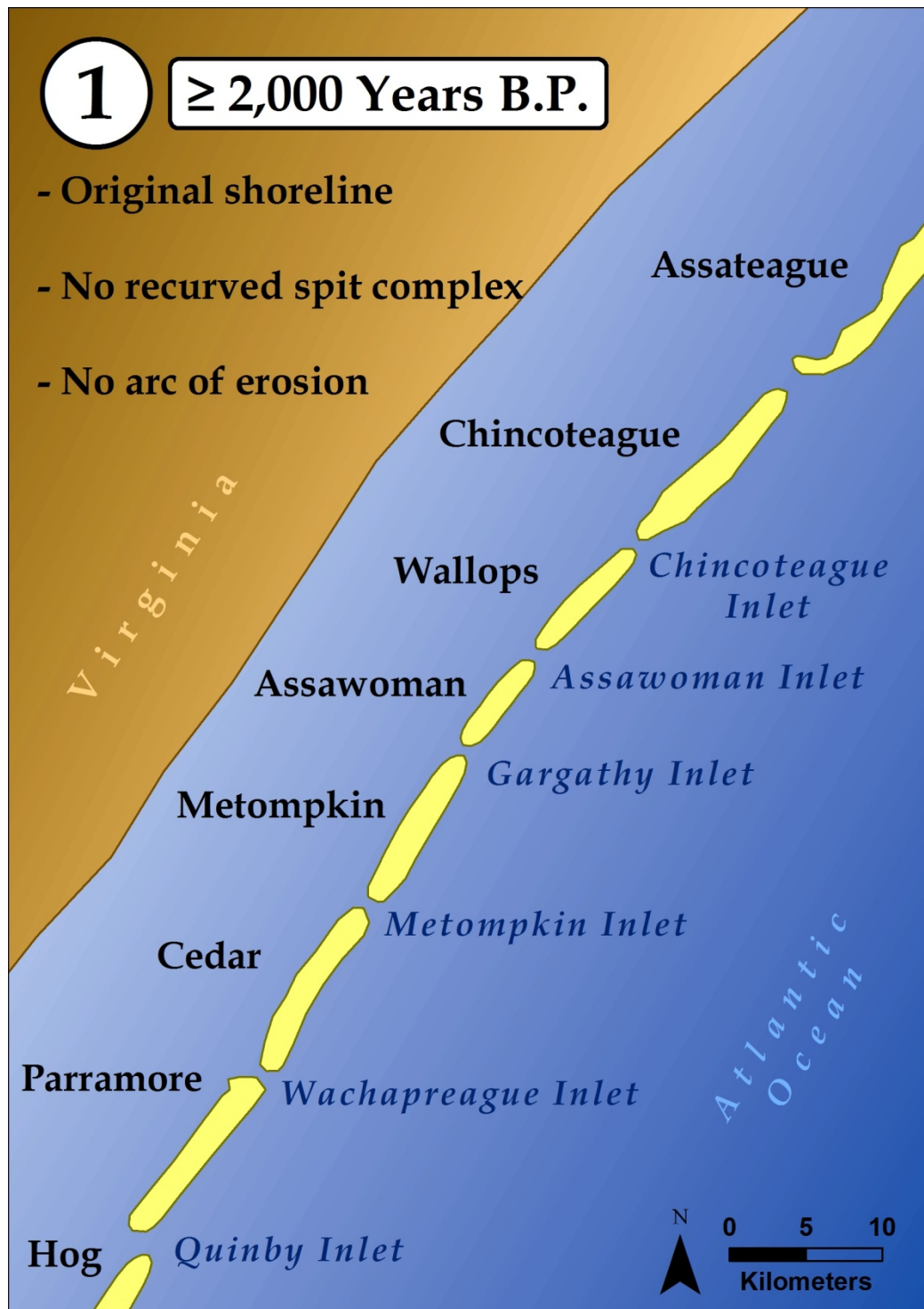


Figure 85: Stage 1 of the six-stage model of coastal change and barrier island system evolution. Stage one was >2000 years ago and displays the original shoreline, the absence of a recurved spit complex, and lack of an arc of erosion.

## **Stage 2 (2000 to 500 Years B.P.): Updrift Sediment Trapping and Recurved Spit and Arc of Erosion Development**

Assateague Island formed 2000+ years before the present. Through time, a series of recurved spits at the south end of Assateague Island continued to extend in a southerly direction because of the net southerly longshore sediment transport. The island gradually prograded to the south through spit accretion and eventually accreted in front of Chincoteague Island, thus sheltering it from open-ocean waves of the Atlantic Ocean. Updrift sediment trapping at the large recurved spit complex located at the southern end of Assateague Island captured large sediment quantities from the littoral drift system starting about 2000 years ago or less. In fact, only 5% of longshore sediment bypasses this system, thus inhibiting downdrift nourishment of the barrier islands (Moffat & Nichol Engineers, 1986).

Sediment trapping at southern Assateague Island during the Holocene over the past 2000 years is described by Goettle (1981) in Figure 86. The recurved spit complex consists of at least five primary paleospits or modern spits known sequentially from oldest to youngest as follows: 1) Morris Island, 2) Piney Island, 3) Lighthouse Ridge, 4) Assateague Point, and 5) Fishing Point. Incident waves refract around the existing recurved spit leading to steady and incremental extension of the shoreline and the accumulation of significant sediment quantities.

The immediate effects of downdrift sediment starvation are readily apparent along the downdrift barrier islands. A natural erosional shadow (arc of erosion) developed to the south of Chincoteague Inlet, Virginia, approximately 2000 to 500 years ago because of the capture of these vast sediment quantities at the recurved spit complex (Figure 87).

The recurved spit complex in effect begins to starve the downdrift barrier-island shorelines of the Virginia Eastern Shore. In Figure 87, the barrier islands immediately south of the recurved spit at southern Assateague Island begin to transgress toward the mainland because of an inadequate sediment supply to maintain the morphology dictated by a marginally mixed-energy, tide-dominated environment. The islands retreat rapidly through overwash and inlet processes and also create eco-geomorphic changes in the interior of the island. The arc of erosion enveloped Wallops, Assawoman, and Metompkin Islands in a gradual progression from north to south over the course of approximately 1500 years.

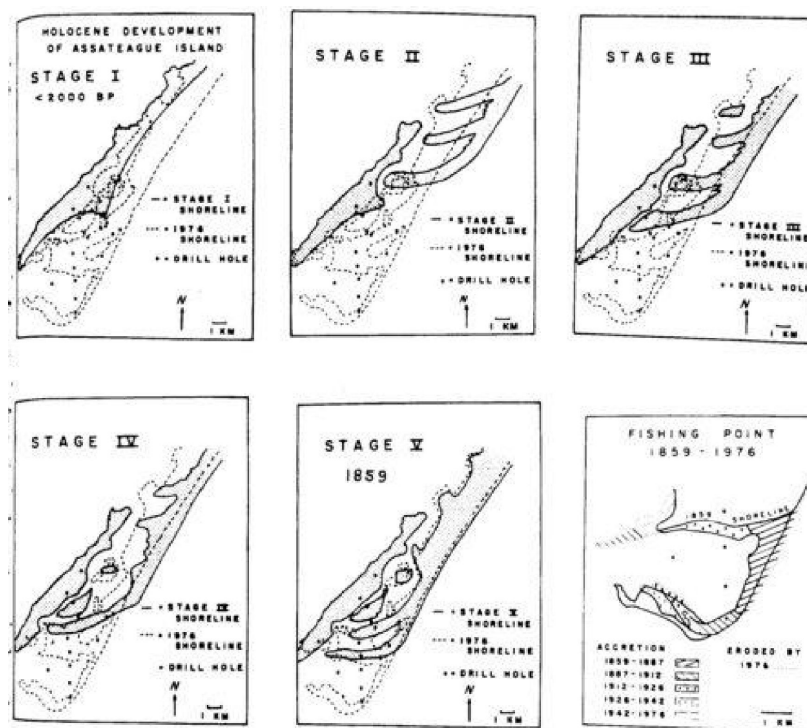


Figure 86: Stages of Holocene development of the large recurved spit complex at the southern end of Assateague Island, Virginia-MD (Goettle, 1981).



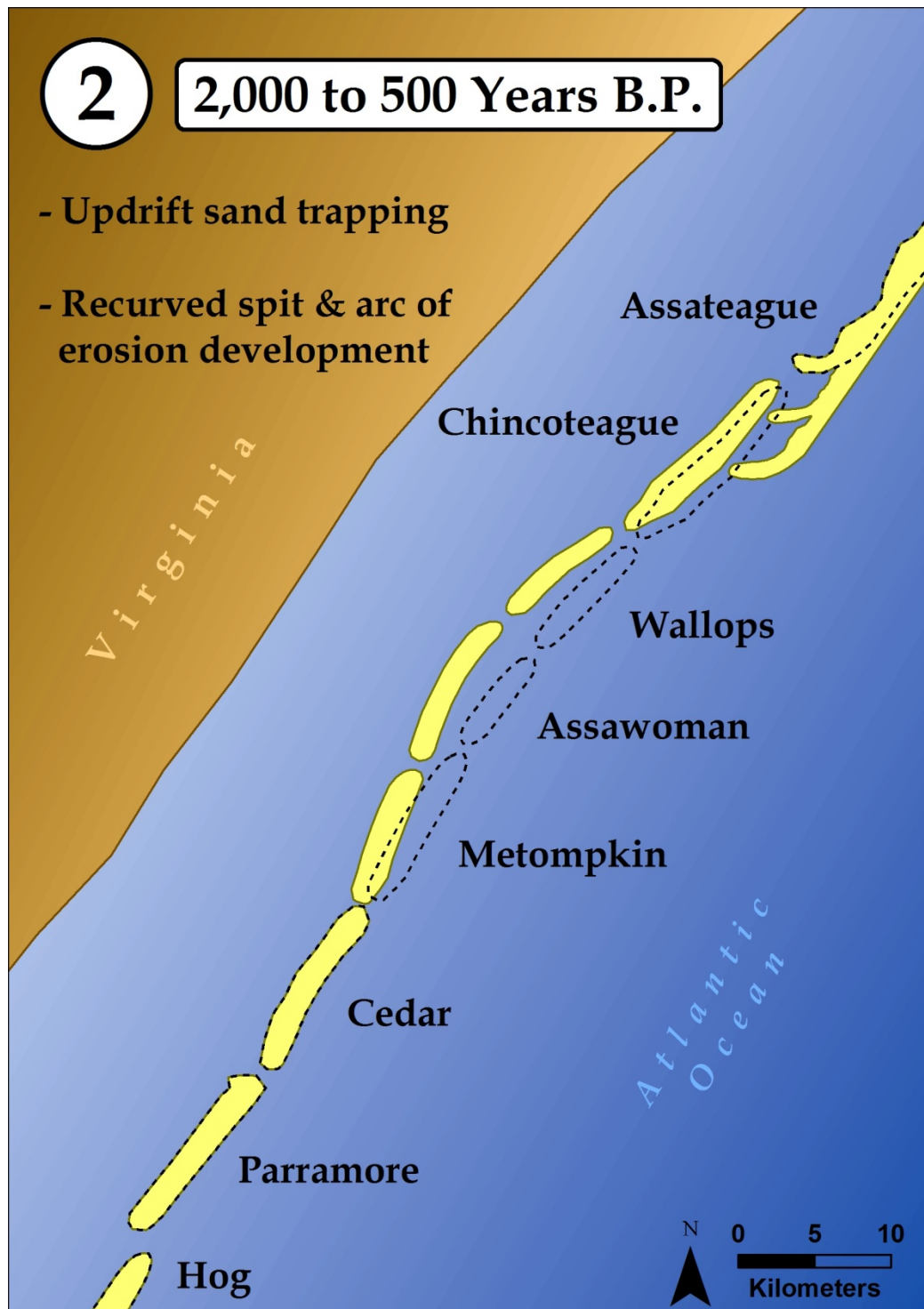


Figure 87: Stage 2 of the six-stage model of coastal change and barrier island system evolution. Stage 2 occurred 2000 to 500 years ago and reflects updrift sand trapping, the development of recurved spits, and an arc of erosion initiation.

### **Stage 3 (500 to 200 years B.P.): Continued Spit Development and Southern Extension of the Large Arc of Erosion**

In Stage 3 the arc of erosion extends further southward, creating an ever-larger zone of anomalous erosion (Figure 88). The cascading and cumulative effects of long-term sediment starvation along the Virginia barrier islands become more pronounced. About 500 to 200 years before the present, Wallops, Assawoman, and Metompkin are now affected by the arc of erosion. In addition, as a result of rapid barrier-island rollover, these Holocene barrier islands are transgressing toward the Pleistocene mainland more quickly, thereby making the arc more pronounced geographically. The effects of these processes are quite apparent when examining aerial photography or satellite imagery of the region (Figure 69). Consequently, Wallops, Assawoman, and Metompkin Islands are much closer to the Pleistocene mainland than the islands to the north and south. In fact, the widest distances between the Pleistocene mainland and outer barrier island shoreline are found at the far southern reaches of the Virginia Eastern Shore.

The acute effects of the large arc of erosion (i.e., a sediment supply deficient) propagate in a southerly direction sequentially from island to island. The continued growth of the recurved spit complex captured sediment that would otherwise nourish the downdrift barrier islands. As such, the continued lack of sediment supply to downdrift barrier islands enables the extension or propagation of the arc of erosion in a southerly direction through time.

In Figure 88 Wallops and Assawoman Islands have fused together and Metompkin Island is fully enveloped by the arc of erosion. In addition, Cedar Island possibly begins to be affected by the arc of erosion and initiates the transformation to

rapid transgression. Notably, Parramore Island is still not affected by the large arc of erosion and continues to display clockwise rotational instability.

#### **Stage 4 (200 to 150 years B.P.): Morphodynamic Changes to Cedar Island, Virginia**

The current recurved spit complex (i.e., Fishing Point) has prograded in a southwesterly direction approximately 8 km since 1859 (Goettle, 1981). The further development of the recurved spit complex means large sediment quantities continue to be sequestered at the southern end of Assateague Island. Furthermore, the ever-enlarging large arc of erosion enveloped Cedar Island and began to affect shoreline behavior, as documented throughout the historical period of record (1852–2010). In addition, storms may now have the ability to influence the behavior of Cedar Island to a greater degree because of the overall deficiency in the sediment budget (i.e., barrier islands become lower in profile thus easier to overwash during tropical or extratropical storms).

Cedar Island suffered from sustained retreat rates because of the lack of sediment and storm impacts. Cedar Island begins to evolve from a mixed-energy, tide-dominated barrier island to a mixed-energy, wave-dominated barrier island that is a low-profile, washover-dominated transgressive barrier island with a thin veneer of sand incrementally rolling over backbarrier marsh (Figures 89–92). In addition, Figure 93 documents the long-term and short-term linear regression retreat change rates of Cedar's non-inlet-influenced, open-ocean shoreline (-5.5 m/yr and -15.4 m/yr, respectively) and the long-term linear regression change rate of tidal prism for Wachapreague Inlet ( $-2.67 \times 10^4$  m<sup>3</sup>/yr).



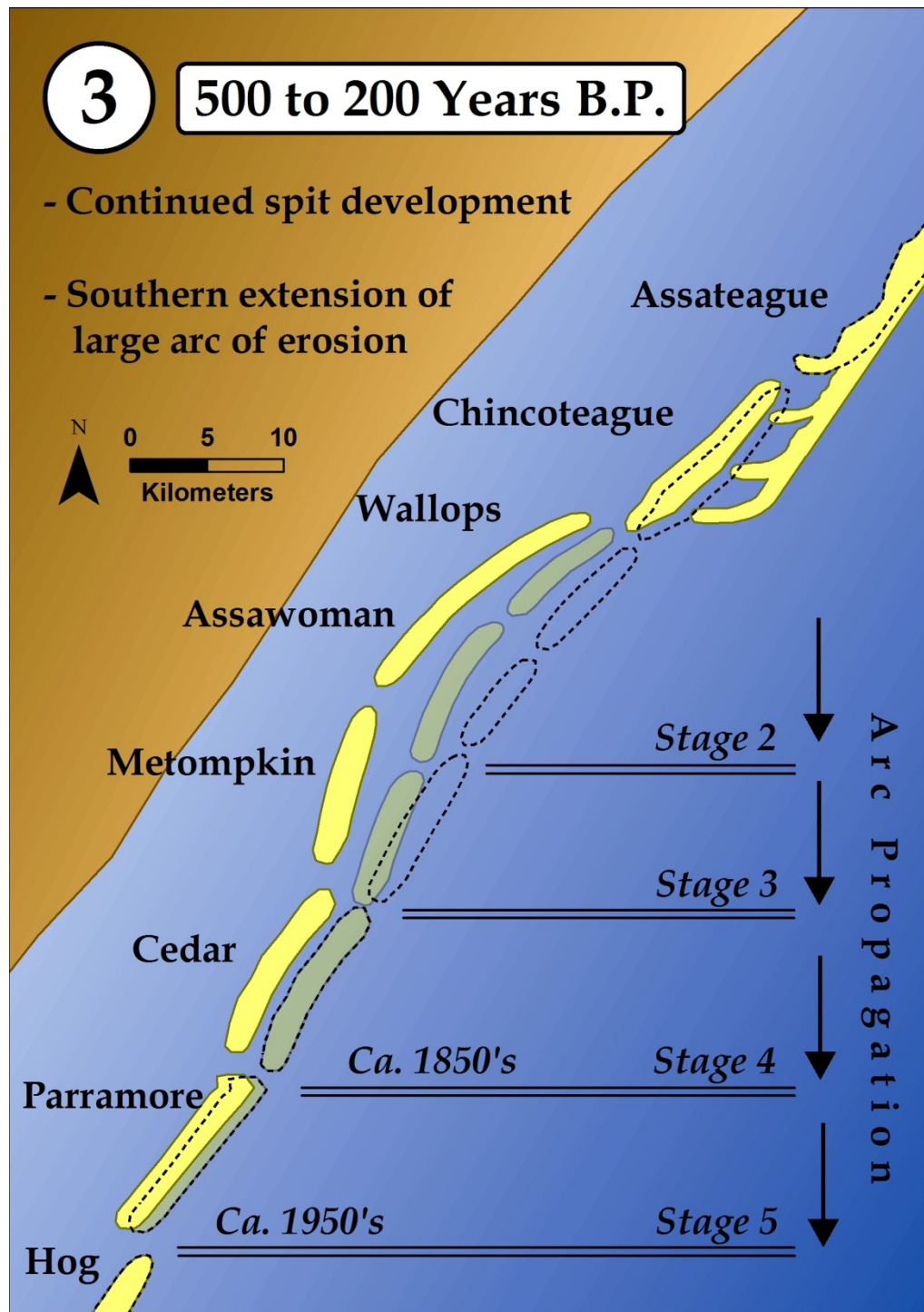


Figure 88: Stage 3 of the six-stage model of coastal change and barrier island system evolution. Stage 3 occurred 500–200 years ago. The arc of erosion propagated southward as a series of stages in response to updrift sediment trapping at the large recurved spit complex at the southern end of Assateague Island, Virginia–Maryland. As it propagated southward, the arc of erosion enveloped Cedar Island by the 1850s (end of Stage 4) and enveloped Parramore by the 1950s (end of Stage 5).



**Figure 89:** Sparse remnants of the cedar maritime forest on the northern end of Cedar Island, Virginia in April 2010. USGS topographic sheets from the 1950s and 1960s illustrate 10 to 20 foot dune ridges and a fairly extensive forest (Gaunt, 1991).



**Figure 90:** A thin sand veneer covers the breach closure area on Cedar Island's bay-backed, open-ocean shoreline. April 21, 2010.



**Figure 91: View is from beach looking west across the backbarrier marsh along the northern, marsh-backed, open-ocean shoreline (Cell 3) of Cedar Island, Virginia in April 2008. Note the position of the immobile red truck (upper left).**



**Figure 92: View is south along the berm crest of Cedar Island, Virginia during a GPS shoreline survey along Cell 3 in April 2010 (~2 years after the previous photo [Fig. 75]). The same red truck is now buried in sand on the active foreshore near the same general area of the previous photo.**



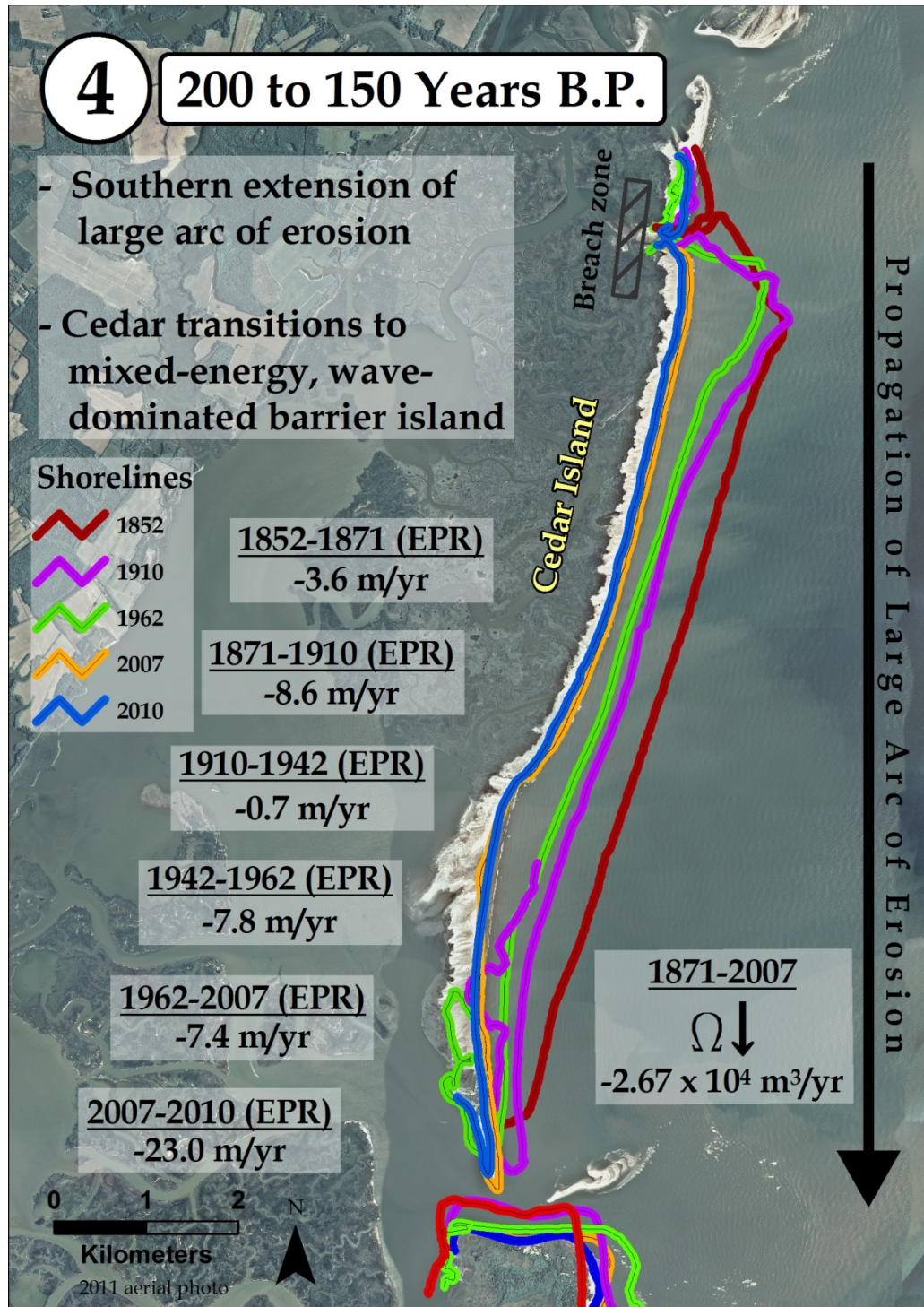


Figure 93: Stage 4 of the six-stage model of coastal change and barrier-island system evolution. Stage 4 was 200 to 150 years before present and demonstrates morphodynamic changes of Cedar Island including the progressive southern extension of the large arc of erosion and transition from mixed-energy, tide-dominated barrier island to a mixed-energy, wave-dominated barrier island. Omega symbol ( $\Omega$ ) represents tidal prism.

### **Stage 5 (50 to 40 years B.P.): Morphodynamic Changes to Parramore Island, Virginia**

In Stage 5 the large arc of erosion continues its southerly propagation and now begins to affect Parramore Island, circa 1940s to 1950s. Parramore Island experienced a distinct change from shoreline advance to retreat because the large arc of erosion has decreased sediment supply, which is a primary sediment source to Parramore's open-ocean shorelines. Parramore Island is now transforming from a high-profile, regressive barrier island with a classic drumstick shape to a lower profile, transgressive, mixed-energy, wave-dominated barrier island that has become more vulnerable to storm impacts.

Storm surge, overwash, and salt spray penetration affect areas of healthy vegetation and produce substantial eco-geomorphic changes now clearly evident along Parramore Island. The maritime forest located along the high-profile beach and dune ridges has been severely degraded to the point of complete collapse. As a result of the rapid shoreline retreat, habitat change is occurring at a brisk pace in the interior of Parramore Island. Freshwater ponds and marsh (i.e., cat eye ponds) behind the most seaward dune ridge converts to brackish to saline lagoons fronting Italian Ridge. Saltwater spray severely impacts the maritime forest on Italian Ridge and produces extensive canopy loss and tree die-offs. Dead trees (i.e., snags) now dominate the barrier island landscape, whereas 14 years ago, Parramore Island had a healthy, full tree canopy.

Various researchers from the Virginia Coast Reserve, Long-Term Ecological Research program collected the following series of oblique aerial photos from light aircraft dating from the years 2003 to 2011 (Figures 94–98). These images qualitatively

document the changes to a segment of the north-central, open-ocean shoreline of Parramore Island (Cell 3). The photos were selected because they demonstrate changes to the general area near the “crossover trail” (the long linear manmade path evident in all the photos). The crossover trail allows unimpeded travel from Club Canal on the estuarine side to the beach on the ocean side of Parramore Island and is maintained by the Virginia Institute of Marine Science. And finally, Figure 99 demonstrates the extension of the large arc of erosion and documents the long-term and short-term linear regression retreat change rates of the non-inlet-influenced, open-ocean shoreline of Parramore Island (-4.1 m/yr and -12.2 m/yr, respectively) and the short-term linear regression change rate of tidal prism for Wachapreague Inlet ( $+2.04 \times 10^6 \text{ m}^3/\text{yr}$ ).



**Figure 94: Parramore Island circa 1976. Note the home of a caretaker along the backshore and the broad, extensive, and full tree canopy. Image provided by Stephen Leatherman.**





**Figure 95:** Low oblique aerial photo of Parramore Island, Virginia taken on October 13, 2003. Note the dune ridge fronting the beach with an extensive stand of trees and vegetation with scattered fallen trees along the foreshore. The trees on Italian Ridge in the background have a full, healthy canopy.



**Figure 96:** Low oblique aerial photo of Parramore Island, Virginia taken September 21, 2005. Note the area of trees and vegetation fronting the beach have experienced thinning and die-off. A number of dead trees are now apparent decreasing in number in a landward direction.



**Figure 97:** Low oblique aerial photo of Parramore Island, Virginia taken on November 28, 2009. Note the areas of overwash and salt marsh inundation with an absence of trees and vegetation fronting the beach. Dead trees are more extensive.



**Figure 98:** Low oblique aerial photo of Parramore Island, Virginia taken on August 31, 2010. Note the extensive washover fans, large areas of salt marsh inundation fronting Italian Ridge, and rapid retreat of the shoreline.



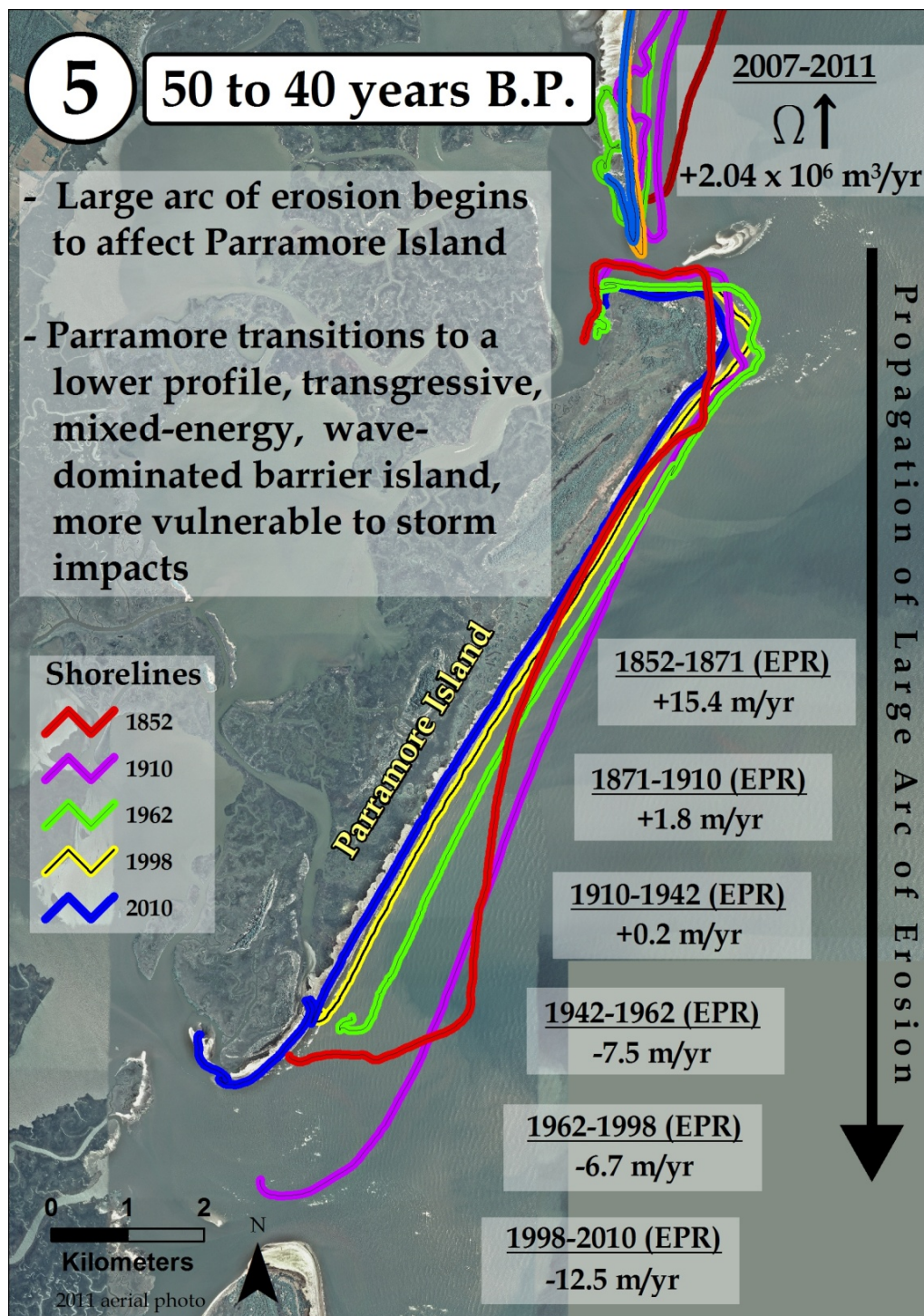


Figure 99: Stage 5 of the six-stage model of coastal change and barrier island system evolution. Stage 5 was 50 to 40 years before the present and demonstrates the morphodynamics changes of Parramore Island. The arc of erosion reaches Parramore Island and thus begins its transformation from a high-profile, regressive barrier island with a classic drumstick shape to a lower profile transgressive, mixed-energy, wave-dominated barrier island that has become more vulnerable to storm impacts. Omega symbol ( $\Omega$ ) represents tidal prism.

### **Stage 6 (10 to 100 years into the future): Evolution of the Parramore–Cedar Barrier Island and Wachapreague Tidal Inlet System**

In Stage 6 Parramore Island evolves into a mixed-energy, wave-dominated barrier island that is a low-profile, washover-dominated, transgressive barrier island (Figure 100). Parramore Island experiences intense eco-geomorphic changes just as Cedar Island did in its past. For example, Cedar Island—hence its name—previously had many trees that are no longer present on the island (Figure 89). Thus, Parramore Island is a modern analog to what happened on Cedar Island in the past and the other updrift islands to its north (i.e., Metompkin, Assawoman, and Wallops). At the current rates of shoreline change, Parramore Island may well resemble Cedar Island in just a few decades. The events leading up to this will include the complete disappearance of the maritime forest along Italian Ridge; the island's shoreline will retreat to relict dune ridges (e.g., Italian Ridge); the island will fully complete its transition to a mixed-energy, wave-dominated morphology; and the central or southern portions of Parramore Island may breach and fragment. In conclusion, Parramore Island will be characterized as a low-profile, washover-dominated barrier island with a thin sand veneer that rapidly rolls over the remaining backbarrier wetlands.

Also in Stage 6, Cedar Island will continue to rapidly roll over, particularly along the northern, marsh-backed shoreline. Breaching will continue at both the Coast Guard breach area and at the southern breaching zone (i.e., Cedar Island breach) along the bay-backed shoreline. Moreover, Cedar Island may fragment into three components: a northern, central, and southern Cedar Island. Finally, the tidal prism at Wachapreague Inlet will continue to increase, thus leading to a larger ebb-tidal delta.



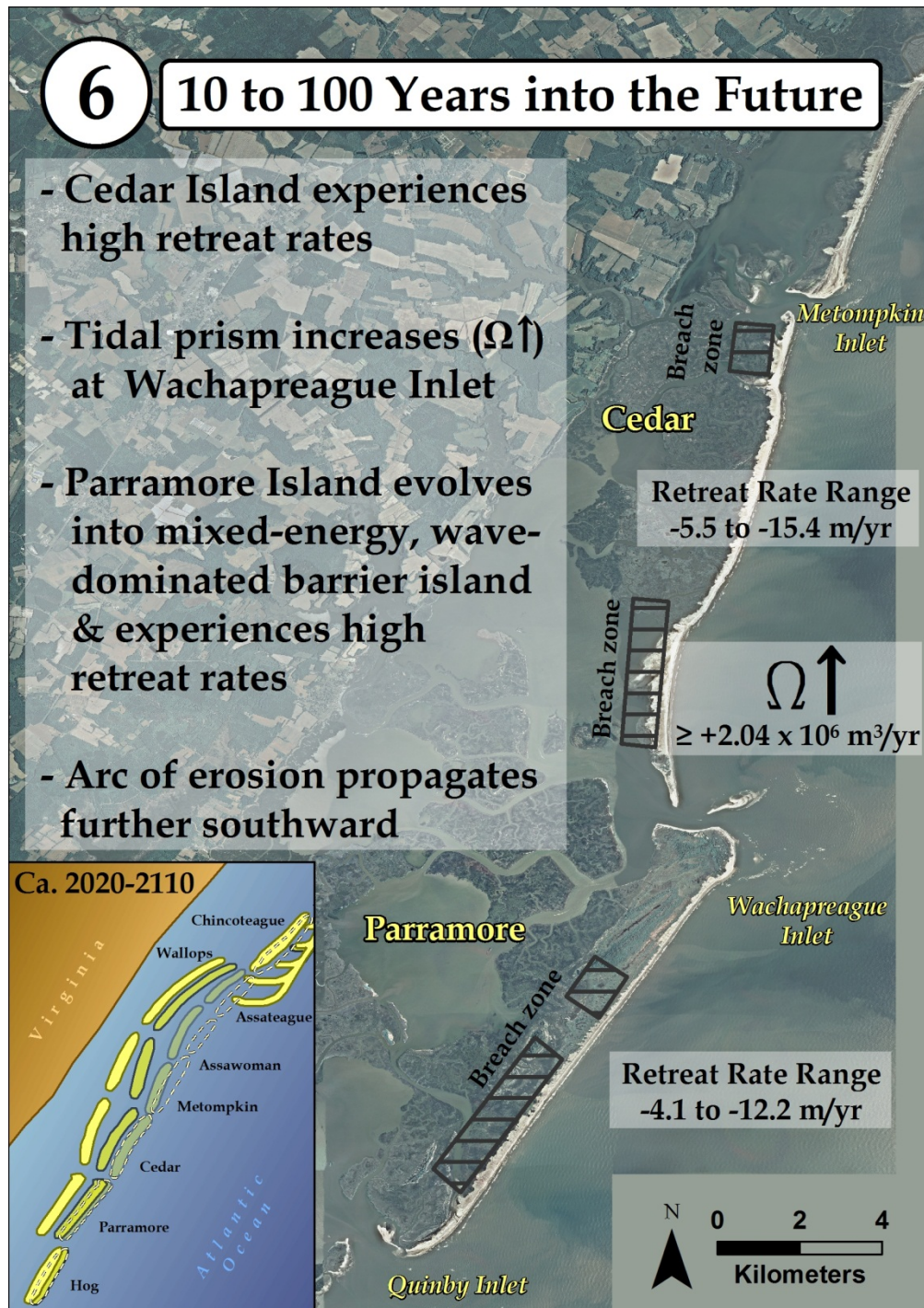


Figure 100: Stage 6 of the six-stage model of coastal change and barrier island system evolution. Stage 6 projects 10–100 years into the future. Parramore Island evolves into a mixed-energy, wave-dominated barrier island and Cedar Island fragments into three segments. Wachapreague Inlet’s tidal prism increases and thereby enlarges the ebb-tidal delta and establishes a flood-tidal delta in the backbarrier bay, which further exacerbates sediment supply shortages by sequestering ever-larger sediment quantities on the inlet shoals. Omega symbol ( $\Omega$ ) represents tidal prism.

Finally, Figure 101 was photographed from the International Space Station on April 16, 2008. Parramore Island is located in the center with the majority of Cedar Island to the north (left side of image). This photograph graphically demonstrates several of the processes currently producing changes along the Parramore–Cedar barrier-island system. Note the offset of the shoreline along the bay-backed portion of Cedar Island (Cell 4), which shows the effects of island breaching. In addition, the shoreline of Parramore Island is straightening, typified by the erosion of the northern meaty end of the drumstick. Most notably, the ebb-tidal delta fronting Wachapreague Inlet and the waves breaking along its surface show a larger and more elongated ebb-tidal delta than in previous imagery. All of these developments are fundamental changes to the Parramore–Cedar barrier-island system and represent harbingers of the future. In summary, the Parramore–Cedar barrier-island system is rapidly changing and these developments potentially foreshadow other future changes of the Holocene barrier islands along the entire southern Delmarva Peninsula. The shortage of sediment supply; the extension of the long arc of erosion; relative sea level rise; and the more recent increase in tidal prism, updrift island breaching, and increased vulnerability to storm impacts have combined to force significant and lasting changes to the Parramore and Cedar barrier island system and Wachapreague Inlet.



ISS016E036243

**Figure 101: Vertical aerial photograph of Cedar, Parramore, and Hog Islands from the International Space Station, taken on April 16, 2008.**

## **CHAPTER SEVEN: CONCLUSIONS**

### **Summary of the Study**

This dissertation is a study of the shoreline and tidal inlet changes of the Parramore–Cedar barrier-island and Wachapreague tidal inlet system through the integration of a variety of geospatial data sets over a range of spatial and temporal scales. The time-series analysis examined outer shoreline and tidal inlet changes using NOS topographic sheets, GPS shoreline position surveys, NOS hydrographic sheets, bathymetric surveys, and aerial photography. The primary goal of the research is to determine the drivers of change to the Parramore–Cedar barrier-island system and to propose a model of coastal change and barrier evolution along the southern Delmarva Peninsula. The study addresses three primary objectives: 1) quantify the rate, magnitude, and direction of shoreline change along Parramore and Cedar Islands across a range of temporal scales and geomorphic zones; 2) quantify the cross-sectional areas of Wachapreague Inlet, Virginia over the historical period of record and determine if tidal prism and ebb-tidal delta volumes are stable, increasing, or decreasing; and 3) test the three-stage model of “runaway transgression” proposed by FitzGerald et al. (2004) where relative sea-level rise is proposed to cause an increase in tidal prism and ebb-tidal delta volume through increased sediment trapping, thus causing the eventual degradation to the adjacent barrier-island system.

## Conclusions of the Findings

The following is a summary of the major findings of this research and their relation to coastal change and the evolution of the Parramore–Cedar barrier-island and Wachapreague tidal inlet system:

1. Parramore Island's non-inlet-influenced, open-ocean shoreline (Cells 3 and 4) experienced a long-term linear regression retreat rate of -4.1 m/yr from 1852 to 1998 and nearly a three-fold increase to -12.2 m/yr over the short term from 1998 to 2010. The retreat rate across the entire period of record (1852–2010) for Parramore is -5.0 m/yr. All shoreline cells for Parramore Island experience either a transition from advance to retreat or an increase from low to high retreat rates when comparing long-term (1852–1998) to short-term (1998–2010) linear regression rates. The end point rates segmented into incremental time periods identify a change in prevailing shoreline behavior from retreat to advance at the 1942 to 1962 time period.
2. Cedar Island's non-inlet-influenced, open-ocean shoreline (Cells 3 and 4) experienced a long-term linear regression retreat rate of -5.5 m/yr from 1852 to 2007 and also nearly a three-fold increase to -15.4 m/yr over the short term from 2007 to 2010. The retreat rate across the entire period of record (1852–2010) for Cedar is -6.1 m/yr. The shoreline cells of Cedar Island overwhelmingly display sustained retreat over the long term (1852–2007) with an increase in retreat rate during the short term (2007–2010). The shoreline data from 2007 to 2010 for the southern, bay-backed shoreline of Cedar Island demonstrate the effects of beach

widening and shoreline advancement following the closure of an ephemeral breach in 2007.

3. The pattern of clockwise rotational instability along Parramore Island's outer shoreline over the long term as documented by Leatherman et al. (1982) has evolved into sustained rapid retreat, whereas Cedar Island has transitioned from in-place narrowing (Gaunt, 1991) to rapid barrier rollover and landward migration through overwash and inlet/breach processes. In other words, the Parramore–Cedar barrier-island system is experiencing a fundamental adjustment in its pattern of historical shoreline movement exemplified by the steady increase in retreat rates over the period of record and further magnified by rapid retreat rates over the short term.
4. Wachapreague Inlet slowly migrated in a southerly direction from 1852 to 2010. The southern tip of Cedar Island migrated in a southerly direction at a linear regression rate of +0.9 m/yr from 1852 to 2007. In contrast, the southern tip of Cedar Island migrated in a northerly direction at -83.8 m/yr from 2007 to 2010. The Wachapreague inlet-throat shoreline of Parramore Island demonstrated low to moderate rates of southerly migration from 1852 to 1998 with a linear regression rate of -2.0 m/yr. However, the rate of southerly migration nearly doubled to -3.9 m/yr from 1998 to 2010. These shoreline-change results document higher rates of southerly migration of Wachapreague Inlet than the 1-m/yr rate calculated by DeAlteris and Byrne (1975).



5. The historical cross-sectional areas for Wachapreague Inlet, Virginia were 1845 m<sup>2</sup> in 1852, 4473 m<sup>2</sup> in 1871, 4737 m<sup>2</sup> in 1911, 4572 m<sup>2</sup> in 1934, 4047 m<sup>2</sup> in 1972, 4398 m<sup>2</sup> in 2007, 4735 m<sup>2</sup> in 2010 (April), 5014 m<sup>2</sup> in 2010 (August), and 5210 m<sup>2</sup> in 2011. Over the long term from 1871 to 2007, cross-sectional area was characterized by relative stability with a distinct increase over the short term from 2007 to 2011.
6. The maximum depth of Wachapreague Inlet, Virginia increased from 18.3 m in 1871 to 20.9 m in 2011, and the inlet width decreased from 640 m in 1871 to 445 m in 2011.
7. For Wachapreague Inlet, Virginia, the calculated tidal prisms and ebb-tidal delta volumes are  $2.33 \times 10^7$  m<sup>3</sup> and  $7.55 \times 10^6$  m<sup>3</sup> in 1852,  $5.29 \times 10^7$  m<sup>3</sup> and  $2.07 \times 10^7$  m<sup>3</sup> in 1871,  $5.57 \times 10^7$  m<sup>3</sup> and  $2.21 \times 10^7$  m<sup>3</sup> in 1911,  $5.39 \times 10^7$  m<sup>3</sup> and  $2.12 \times 10^7$  m<sup>3</sup> in 1934,  $4.82 \times 10^7$  m<sup>3</sup> and  $1.85 \times 10^7$  m<sup>3</sup> in 1972,  $5.20 \times 10^7$  m<sup>3</sup> and  $2.03 \times 10^7$  m<sup>3</sup> in 2007,  $5.57 \times 10^7$  m<sup>3</sup> and  $2.21 \times 10^7$  m<sup>3</sup> in 2010 (April),  $5.88 \times 10^7$  m<sup>3</sup> and  $2.36 \times 10^7$  m<sup>3</sup> in 2010 (August), and  $6.09 \times 10^7$  m<sup>3</sup> and  $2.46 \times 10^7$  m<sup>3</sup> in 2011, respectively.
8. Tidal prism and ebb-tidal delta volumes at Wachapreague Inlet fluctuated from 1871 to 2011 with tidal prism ranging between  $4.82 \times 10^7$  m<sup>3</sup> and  $6.09 \times 10^7$  m<sup>3</sup> and ebb-tidal delta volumes ranging between  $1.85 \times 10^7$  m<sup>3</sup> and  $2.46 \times 10^7$  m<sup>3</sup>. From 1871 to 2007, the long-term linear regression rates of change were -2.4 m<sup>2</sup>/yr for cross-sectional area,  $-2.67 \times 10^4$  m<sup>3</sup>/yr for tidal prism, and  $-1.26 \times 10^4$  m<sup>3</sup>/yr for ebb-tidal delta volume. However, from 2007 to 2011, the short-term

linear regression rates of change switched to high rates of increase with  $+186.1 \text{ m}^2/\text{yr}$  for cross-sectional area,  $+2.04 \times 10^6 \text{ m}^3/\text{yr}$  for tidal prism, and  $+9.89 \times 10^5 \text{ m}^3/\text{yr}$  for ebb-tidal delta volume. Overall, from 1871 to 2007, cross-sectional area, tidal prism and ebb-tidal delta volumes were characterized by relative stability to a slight decrease with a distinct increase more recently from 2007 to 2011.

9. The barrier-island and tidal inlet evolution model of Fitzgerald et al. (2004) is tested by examining changes in tidal prism and ebb-tidal delta volumes at Wachapreague Inlet in response to tidal prism fluctuations and the impact on adjacent barrier-island shorelines of Cedar and Parramore Islands. The relatively stable tidal prism volumes during the past 136 years (1871–2007) with a modest increase over the short term (2007–2011) possibly indicate the barrier-island system has entered the initial stages of the three-stage runaway transgression model (Fitzgerald et al. 2004). The increase in tidal prism from 1972 to 2007 and the distinct increase in tidal prism from 2007 to 2011 may signal the impacts of relative sea-level rise and a subsequent enlargement of open water in the bay in response to wetland degradation. Also, increased sediment volumes were likely deposited on the ebb-tidal delta in comparison to long-term trends.
10. The morphodynamic changes and degradation of the Parramore–Cedar barrier-island system appear to be in response to a complementary interaction of the following set of coastal-change drivers: a) the southern propagation of the expanding large arc of erosion (i.e., deficit in sediment supply creating an anomalous erosion zone) operating downdrift (south) of Assateague Island,

Maryland-Virginia, b) relative sea-level rise and recent increases in tidal prism at Wachapreague Inlet, Virginia, c) episodic updrift island breaching north of Wachapreague Inlet along Cedar Island, Virginia and other barrier islands to the north of Cedar, and d) storm impacts and the increased vulnerability to storm impacts over time. Of these four coastal-change drivers, the southern propagation of the large arc of erosion appears to be the primary driver of coastal evolution along the Parramore–Cedar barrier island system. By the 1950's, the large arc of erosion affected the Parramore–Cedar barrier island system, which is before any significant increases occurred in tidal prism at Wachapreague Inlet, Virginia. Moreover, the short-term (2007-2011) morphodynamics of Wachapreague Inlet and the adjacent shorelines of Parramore and Cedar Islands support the hypothesis the barrier island system has recently (no earlier than 1972) entered the initial stages of the three-stage model of runaway transgression (Fitzgerald et al., 2004). Sediment supply is further exacerbated by updrift island breaching, as documented along the outer shoreline of Cedar Island. The combination of these factors has led to a weakened barrier-island system undergoing fundamental morphodynamic changes and incapable of responding to shoreline impacts from an increase in storm frequency or magnitude.

11. This research presents a model of coastal change and barrier-island evolution along the southern Delmarva Peninsula. The six-stage model accounts for changes in sediment supply, relative sea-level rise, updrift island breaching, and increased vulnerability to storm impacts, but not inlet processes. Shoreline change data

indicate that Cedar Island has experienced sustained retreat rates across the entire period of record, whereas Parramore Island depicts a distinct shift from shoreline advance to rapid retreat. Parramore Island is a classic mixed-energy, tide-dominated barrier island that is now experiencing severe erosion along its entire outer shoreline, whereas the morphology of Cedar Island has already evolved into a mixed-energy, wave-dominated barrier island. Cedar Island has experienced the impact of the arc of erosion during the entire period of record as reflected in the high long-term retreat rates, whereas the arc of erosion did not affect Parramore Island until approximately 100 years later (circa 1950s). The short-term rate changes indicate the processes controlling shoreline trends (e.g., longshore sediment transport, relative sea-level rise, island breaching, storm impacts, etc.) have intensified or changed relative to the long term. Short-term shoreline or bathymetric changes that depart from historical trends are significant because these developments may indicate wider patterns of barrier-island change for the entire Virginia Eastern Shore and perhaps large expanses of mixed-energy coasts along the U.S. Atlantic seaboard.

12. The model of coastal change and barrier-island evolution along the southern Delmarva Peninsula consists of six progressive stages. Stage One ( $\geq 2000$  years B.P.) depicts the original shoreline of the northern and central barrier islands along the Virginia coastline, the lack of the recurved spit complex at southern Assateague Island, and the absence of the arc of erosion south of Assateague Island. Stage Two (2000 to 500 years B.P.) displays updrift sand trapping at

southern Assateague Island through the development of a progressive series of recurved spits and a gradual expansion of the arc of erosion caused by shortages in downdrift sediment supply. Stage Three (500 to 200 years B.P.) outlines the southern propagation of the arc of erosion through various stages along the Virginia coastline because of continued sediment trapping and recurved spit development at the southern end of Assateague Island that leads to the southern extension of the large arc of erosion. In Stage Three, Chincoteague Island is becoming sheltered from open-ocean processes because of continued southerly spit progradation at the southern end of Assateague Island and the arc of erosion becomes more pronounced and extends further southward to encompass Wallops, Assawoman, and Metompkin Islands. In Stage Four (200 to 150 years B.P.), the southern extension of the large arc of erosion reaches Cedar Island and effectively transforms Cedar from a mixed-energy, tide-dominated barrier island to a mixed-energy, wave-dominated barrier island that experiences island narrowing and rapid landward roll over onto backbarrier salt marsh. In Stage Five (50 to 40 years B.P.), the large arc of erosion begins to affect Parramore Island and thus initiates Parramore's transition to a lower profile, transgressive, mixed-energy, wave-dominated barrier island that is more vulnerable to storm impacts. In Stage Six (10 to 100 years into the future), Parramore Island evolves into a mixed-energy, wave-dominated barrier island that is low profile and washover dominated and has perhaps fragmented into a northern island centered around Italian Ridge and a smaller rapidly retreating southern component. Cedar Island is

even more low profile and has possibly fragmented into a small northern inlet- and breach- influenced shoreline, an open-ocean, marsh-backed segment that experiences rapid roll over, and a southern component bounded by a new entrained inlet at the ephemeral breach location and Wachapreague Inlet. Finally, the tidal prism at Wachapreague Inlet continues to increase, allowing larger water volumes to move through the inlet, thus sequestering ever-larger sediment quantities on the ebb- and flood tidal deltas and, as a result, further exacerbating downdrift sediment starvation along northern Parramore Island. If the prevailing pattern of the southern extension of the large arc of erosion continues into the future, then Hog Island will be the next island gradually enveloped by the southward propagating arc of erosion.

## **Future Research**

Future research needs include the continued monitoring of shoreline and tidal inlet behavior of the Parramore–Cedar barrier-island system in order to further quantify the effects of a rise in relative sea level, a sediment budget, updrift island breaching, and increased storminess upon the barrier-island system. In addition, continued bathymetric surveys of the cross-sectional area and the direct measurement of tidal discharge at Wachapreague Inlet—and others along the Virginia Eastern Shore—are critical to the determination of whether tidal prism is significantly increasing over the short term and the implications to the entire Virginia Eastern Shore. An expansion of this research is warranted to further investigate the six-stage model of coastal change and barrier evolution. These efforts may include the following: 1) the quantification of backbarrier changes in wetland area using aerial photography for the available period of record, 2) quantification of a sediment budget for the entire Virginia Eastern Shore including offshore sediment sources and sinks, and 3) quantification of the sand volume of the large recurved spit complex at the southern end of Assateague Island. Finally, the management of uncertainty will require proactive engagement and policy development from the various stakeholders along the Virginia Eastern Shore such as the National Park Service at Assateague National Seashore, the National Aeronautics and Space Administration facility at Wallops Island, The Nature Conservancy, the states of Maryland and Virginia, and private landowners.

## **APPENDIX A: PARRAMORE ISLAND SHORELINE RESULTS**

Appendix A (24 pages): Parramore Island shoreline results by shoreline cell and long term (1852-1998) and short term (1998-2010) time periods using the various statistical measurements. Individual pages by shoreline cell for the following: 1) long-term and short-term rates of shoreline change and net shoreline movement, 2) comparison of long-term and short-term shoreline change rate statistics, 3) linear regression statistics, and 4) weighted linear regression statistics. The long-term and short-term categories are further subdivided by progressively more modern and shorter timeframes within the categories. The individual temporal timeframes within the categories are also segmented and analyzed by the data points contained within the timeframes. A total of four appendix pages exist for each shoreline cell in Appendices A.



Cell 0: Northern, Bay-Side Shoreline															
Long-Term and Short-Term Rates of Shoreline Change and Net Shoreline Movement															
1852 to							07/98 to								
	1871	1910	1942	1962	1998	2010		05/99	05/00	10/00	04/02	05/05	04/06	06/07	04/10
EPR	-1.9	-2.3	-1.6	-0.7	x	-0.9	EPR	x	x	x	x	x	x	x	x
LRR	x	-2.2	-1.6	-0.7	x	-0.8	LRR	x	x	x	x	x	x	x	x
LR2	x	0.97	0.89	0.58	x	0.67	LR2	x	x	x	x	x	x	x	x
NSM	-37.0	-133.4	-141.9	-78.7	x	-146.3	NSM	x	x	x	x	x	x	x	x
SMP	13	1	1	7	x	5	SMP	x	x	x	x	x	x	x	x
1871 to							05/99 to								
	1910	1942	1962	1998	2010		05/00	10/00	04/02	05/05	04/06	06/07	04/10		
EPR	-1.8	-1.1	-0.4	x	-0.6	EPR	-6.5	-3.7	x	-1.9	-1.4	-1.7	-1.5		
LRR	x	-1.1	-0.5	x	-0.6	LRR	x	-4.3	x	-1.5	-1.2	-1.3	-1.3		
LR2	x	0.87	0.47	x	0.52	LR2	x	0.80	x	0.68	0.62	0.73	0.80		
NSM	-69.8	-78.3	-39.2	x	-89.5	NSM	-7.0	-5.3	x	-11.2	-9.5	-13.7	-17.0		
SMP	1	1	7	x	5	SMP	2	2	x	2	2	2	2		
1910 to							05/00 to								
	1942	1962	1998	2010		10/00	04/02	05/05	04/06	06/07	04/10				
EPR	-0.3	-2.0	x	-0.9	EPR	6.1	x	-0.7	-0.4	-0.9	-0.6				
LRR	x	-1.9	x	-1.1	LRR	x	x	-1.0	-0.7	-0.9	-0.8				
LR2	x	0.69	x	0.64	LR2	x	x	0.54	0.50	0.56	0.61				
NSM	-8.4	-106.2	x	-94.5	NSM	2.2	x	-3.7	-2.2	-6.1	-6.4				
SMP	1	1	x	1	SMP	4	x	4	4	4	4				
1942 to							10/00 to								
	1962	1998	2010		04/02	05/05	04/06	06/07	04/10						
EPR	1.0	x	-0.6	EPR	x	-1.3	-0.8	-1.3	-0.9						
LRR	x	x	-0.7	LRR	x	x	-0.9	-1.1	-0.9						
LR2	x	x	0.37	LR2	x	x	0.78	0.83	0.68						
NSM	19.8	x	-39.2	NSM	x	-5.9	-4.4	-8.4	-8.6						
SMP	7	x	5	SMP	x	4	4	4	4						
1962 to							04/02 to								
	1998	2010		05/05	04/06	06/07	04/10								
EPR	x	-1.2	EPR	x	x	x	x								
LRR	x	x	LRR	x	x	x	x								
LR2	x	x	LR2	x	x	x	x								
NSM	x	-58.8	NSM	x	x	x	x								
SMP	x	5	SMP	x	x	x	x								
1998 to							05/05 to								
	2010		04/06	06/07	04/10										
EPR	x	EPR	1.6	-1.2	-0.5										
LRR	x	LRR	x	-1.3	-0.7										
LR2	x	LR2	x	0.39	0.47										
NSM	x	NSM	1.5	-2.5	-2.7										
SMP	x	SMP	4	4	4										
04/06 to							06/07 to								
	06/07	04/10		04/10											
EPR	-3.6	-1.1	EPR	-0.1											
LRR	x	-0.9	LRR	x											
LR2	x	0.45	LR2	x											
NSM	-4.0	-4.2	NSM	-0.3											
SMP	4	4	SMP	4											
06/07 to							04/10 to								
	04/10														
EPR	-0.1														
LRR	x														
LR2	x														
NSM	-0.3														
SMP	4														
EPR: End Point Rate (m/yr), LRR: Linear Regression Rate (m/yr),															
LR2: R-Squared of LRR, NSM : Net Shoreline Movement (m),															
SMP: Sample size (total number of transects).															
(x) symbol indicates shoreline for year unavailable or a minimum															
of three shorelines necessary for a regression rate.															
(-) sign indicates retreat & a positive integer signals advance.															

Cell 0: Northern, Bay-Side Shoreline															
Comparison of Long-Term and Short-Term Shoreline Change Rate Statistics															
1852 to							07/98 to								
	1871	1910	1942	1962	1998	2010		05/99	05/00	10/00	04/02	05/05	04/06	06/07	04/10
EPR	-1.9	-2.3	-1.6	-0.7	x	-0.9	EPR	x	x	x	x	x	x	x	x
LRR	x	-2.2	-1.6	-0.7	x	-0.8	LRR	x	x	x	x	x	x	x	x
WLR	x	x	-1.4	-0.7	x	-0.8	WLR	x	x	x	x	x	x	x	x
LMS	x	-2.3	-1.4	-0.8	x	-0.8	LMS	x	x	x	x	x	x	x	x
SMP	13	1	1	7	x	5	SMP	x	x	x	x	x	x	x	x
1871 to							05/99 to								
	1910	1942	1962	1998	2010			05/00	10/00	04/02	05/05	04/06	06/07	04/10	
EPR		-1.8	-1.1	-0.4	x	-0.6	EPR		-6.5	-3.7	x	-1.9	-1.4	-1.7	-1.5
LRR		x	-1.1	-0.5	x	-0.6	LRR		x	-4.3	x	-1.5	-1.2	-1.3	-1.3
WLR		x	-1.0	-0.4	x	-0.7	WLR		x	x	x	x	x	x	x
LMS		x	-1.1	-0.4	x	-0.6	LMS		x	-3.7	x	-1.5	-1.1	-1.3	-1.5
SMP		1	1	7	x	5	SMP		2	2	x	2	2	2	2
1910 to							05/00 to								
		1942	1962	1998	2010				10/00	04/02	05/05	04/06	06/07	04/10	
EPR			-0.3	-2.0	x	-0.9	EPR			6.1	x	-0.7	-0.4	-0.9	-0.6
LRR			x	-1.9	x	-1.1	LRR			x	x	-1.0	-0.7	-0.9	-0.8
WLR			x	-2.5	x	-0.9	WLR			x	x	x	x	x	x
LMS			x	-2.0	x	-0.9	LMS			x	x	-0.7	-0.8	-1.2	-0.9
SMP			1	1	x	1	SMP			4	x	4	4	4	4
1942 to							10/00 to								
			1962	1998	2010					04/02	05/05	04/06	06/07	04/10	
EPR				1.0	x	-0.6	EPR				x	-1.3	-0.8	-1.3	-0.9
LRR				x	x	-0.7	LRR				x	x	-0.9	-1.1	-0.9
WLR				x	x	-0.8	WLR				x	x	x	x	x
LMS				x	x	-0.6	LMS				x	x	-0.8	-1.1	-1.1
SMP				7	x	5	SMP				x	4	4	4	4
1962 to							04/02 to								
				1998	2010						05/05	04/06	06/07	04/10	
EPR					x	-1.2	EPR					x	x	x	x
LRR					x	x	LRR					x	x	x	x
WLR					x	x	WLR					x	x	x	x
LMS					x	x	LMS					x	x	x	x
SMP					x	5	SMP					x	x	x	x
1998 to							05/05 to								
					2010							04/06	06/07	04/10	
EPR						x	EPR						1.6	-1.2	-0.5
LRR						x	LRR						x	-1.3	-0.7
WLR						x	WLR						x	x	x
LMS						x	LMS						x	-1.2	-0.7
SMP						x	SMP						4	4	4
							04/06 to								
													06/07	04/10	
EPR: End Point Rate (m/yr), LRR: Linear Regression Rate (m/yr),							EPR							-3.6	-1.1
WLR: Weighted Linear Regression (m/yr), LMS: Least Median							LRR							x	-0.9
of Squares (m/yr), SMP: Sample size (total number of transects).							WLR							x	x
(x) symbol indicates shoreline for year unavailable, or a minimum							LMS							x	-1.1
of three shorelines necessary for a regression rate, or							SMP							4	4
shorelines have identical positional accuracies for WLR.							06/07 to								
														04/10	
							EPR							-0.1	
							LRR							x	
							WLR							x	
							LMS							x	
							SMP							4	

Cell 0: Northern, Bay-Side Shoreline															
Linear Regression Statistics															
1852 to							07/98 to								
	1871	1910	1942	1962	1998	2010		05/99	05/00	10/00	04/02	05/05	04/06	06/07	04/10
LRR	x	-2.2	-1.6	-0.7	x	-0.8	LRR	x	x	x	x	x	x	x	x
LR2	x	0.97	0.89	0.58	x	0.67	LR2	x	x	x	x	x	x	x	x
LSE	x	15.3	27.1	31.8	x	33.9	LSE	x	x	x	x	x	x	x	x
LCI	x	4.7	1.7	1.4	x	0.8	LCI	x	x	x	x	x	x	x	x
SMP	x	1	1	7	x	5	SMP	x	x	x	x	x	x	x	x
1871 to							05/99 to								
	1910	1942	1962	1998	2010			05/00	10/00	04/02	05/05	04/06	06/07	04/10	
LRR	x	-1.1	-0.5	x	-0.6	LRR	x	-4.3	x	-1.5	-1.2	-1.3	-1.3		
LR2	x	0.87	0.47	x	0.52	LR2	x	0.80	x	0.68	0.62	0.73	0.80		
LSE	x	22.2	33.3	x	33.4	LSE	x	2.4	x	2.8	2.8	2.4	2.2		
LCI	x	5.6	5.7	x	1.4	LCI	x	28.5	x	2.6	1.4	0.9	0.6		
SMP	x	1	7	x	5	SMP	x	2	x	2	2	2	2		
1910 to							05/00 to								
	1942	1962	1998	2010				10/00	04/02	05/05	04/06	06/07	04/10		
LRR	x	-1.9	x	-1.1	LRR	x	x	-1.0	-0.7	-0.9	-0.9				
LR2	x	0.69	x	0.64	LR2	x	x	0.54	0.50	0.56	0.61				
LSE	x	46.4	x	40.9	LSE	x	x	2.6	2.4	2.2	2.3				
LCI	x	15.8	x	2.4	LCI	x	x	8.4	1.9	1.1	0.7				
SMP	x	1	x	1	SMP	x	x	4	4	4	4				
1942 to							10/00 to								
	1962	1998	2010					04/02	05/05	04/06	06/07	04/10			
LRR	x	x	-0.7	LRR	x	x	-0.9	-1.1	-0.9						
LR2	x	x	0.37	LR2	x	x	0.78	0.83	0.68						
LSE	x	x	47.7	LSE	x	x	1.7	1.6	1.9						
LCI	x	x	12.3	LCI	x	x	5.2	1.3	0.9						
SMP	x	x	5	SMP	x	x	4	4	4						
1962 to							04/02 to								
	1998	2010						05/05	04/06	06/07	04/10				
LRR	x	x	LRR	x	x	x	x								
LR2	x	x	LR2	x	x	x	x								
LSE	x	x	LSE	x	x	x	x								
LCI	x	x	LCI	x	x	x	x								
SMP	x	x	SMP	x	x	x	x								
1998 to							05/05 to								
	2010							04/06	06/07	04/10					
LRR	x	LRR	x	-1.3	-0.7										
LR2	x	LR2	x	0.39	0.47										
LSE	x	LSE	x	2.2	1.8										
LCI	x	LCI	x	18.7	2.1										
SMP	x	SMP	x	4	4										
04/06 to															
											06/07	04/10			
LRR											x	-0.9			
LR2											x	0.45			
LSE											x	2.2			
LCI											x	9.6			
SMP											x	4			
06/07 to															
												04/10			
LRR												x			
LR2												x			
LSE												x			
LCI												x			
SMP												x			
LRR: Linear Regression Rate (m/yr), LR2: R-squared of LRR															
LSE: Standard Error of LRR, LCI: Confidence Interval 95%of LRR															
SMP: Sample size (total number of transects).															
(x) symbol indicates shoreline for year unavailable or a minimum of three shorelines necessary for a regression rate.															
(-) sign indicates retreat & a positive integer signals advance.															

Cell 0: Northern, Bay-Side Shoreline															
Weighted Linear Regression Statistics															
1852 to							07/98 to								
	1871	1910	1942	1962	1998	2010		05/99	05/00	10/00	04/02	05/05	04/06	06/07	04/10
WLR	x	x	-1.4	-0.7	x	-0.8	WLR	x	x	x	x	x	x	x	x
WR2	x	x	0.91	0.45	x	0.72	WR2	x	x	x	x	x	x	x	x
WSE	x	x	1.5	2.7	x	3.1	WSE	x	x	x	x	x	x	x	x
WCI	x	x	1.4	1.9	x	0.8	WCI	x	x	x	x	x	x	x	x
SMP	x	x	1	7	x	5	SMP	x	x	x	x	x	x	x	x
1871 to							05/99 to								
	1910	1942	1962	1998	2010		05/00	10/00	04/02	05/05	04/06	06/07	04/10		
WLR	x	-1.0	-0.4	x	-0.7	WLR	x	x	x	x	x	x	x		
WR2	x	0.88	0.34	x	0.64	WR2	x	x	x	x	x	x	x		
WSE	x	1.2	3.2	x	3.5	WSE	x	x	x	x	x	x	x		
WCI	x	4.7	9.0	x	1.4	WCI	x	x	x	x	x	x	x		
SMP	x	1	7	x	5	SMP	x	x	x	x	x	x	x		
1910 to							05/00 to								
	1942	1962	1998	2010		10/00	04/02	05/05	04/06	06/07	04/10				
WLR	x	-2.5	x	-0.9	WLR	x	x	x	x	x	x				
WR2	x	0.70	x	0.76	WR2	x	x	x	x	x	x				
WSE	x	4.1	x	4.2	WSE	x	x	x	x	x	x				
WCI	x	21.3	x	1.6	WCI	x	x	x	x	x	x				
SMP	x	1	x	1	SMP	x	x	x	x	x	x				
1942 to							10/00 to								
	1962	1998	2010		04/02	05/05	04/06	06/07	04/10						
WLR	x	x	-0.8	WLR	x	x	x	x	x						
WR2	x	x	0.58	WR2	x	x	x	x	x						
WSE	x	x	4.9	WSE	x	x	x	x	x						
WCI	x	x	8.5	WCI	x	x	x	x	x						
SMP	x	x	5	SMP	x	x	x	x	x						
1962 to							04/02 to								
	1998	2010		05/05	04/06	06/07	04/10								
WLR	x	x	x	x	x	x	x								
WR2	x	x	x	x	x	x	x								
WSE	x	x	x	x	x	x	x								
WCI	x	x	x	x	x	x	x								
SMP	x	x	x	x	x	x	x								
1998 to							05/05 to								
	2010		04/06	06/07	04/10										
WLR	x	x	x	x	x										
WR2	x	x	x	x	x										
WSE	x	x	x	x	x										
WCI	x	x	x	x	x										
SMP	x	x	x	x	x										
WLR: Weighted Linear Regression (m/yr), WR2: R-squared of WLR							04/06 to								
WSE: Standard Error of WLR, WCI: Confidence Interval 95%											06/07	04/10			
of WLR, SMP: Sample size (total number of transects).							WLR					x	x		
(x) symbol indicates shoreline for year unavailable, or a minimum							WR2					x	x		
of three shorelines necessary for a regression rate, or							WSE					x	x		
shorelines have identical positional accuracies for WLR.							WCI					x	x		
(-) sign indicates retreat & a positive integer signals advance.							SMP					x	x		
							04/06 to								
													04/10		
WLR													x		
WR2													x		
WSE													x		
WCI													x		
SMP													x		

Cell 1: Wachapreague Inlet-Throat Shoreline															
Long-Term and Short-Term Rates of Shoreline Change and Net Shoreline Movement															
1852 to							07/98 to								
	1871	1910	1942	1962	1998	2010		05/99	05/00	10/00	04/02	05/05	04/06	06/07	04/10
EPR	1.4	0.0	-1.5	-1.8	-1.7	-1.8	EPR	-6.0	2.2	-0.1	x	-3.3	-3.2	-3.7	-3.6
LRR	x	-0.1	-1.4	-1.9	-2.0	-2.0	LRR	x	2.6	1.4	x	-3.4	-3.6	-3.9	-3.9
LR2	x	0.54	0.64	0.79	0.87	0.90	LR2	x	0.33	0.27	x	0.60	0.67	0.75	0.83
NSM	27.0	1.4	-131.5	-198.8	-243.8	-286.0	NSM	-4.5	4.1	-0.3	x	-22.6	-24.8	-33.2	-42.1
SMP	23	23	23	23	23	23	SMP	23	23	23	x	23	23	23	23
1871 to							05/99 to								
	1910	1942	1962	1998	2010			05/00	10/00	04/02	05/05	04/06	06/07	04/10	
EPR	-0.7	-2.2	-2.5	-2.1	-2.3	EPR	8.0	3.0	x	-3.0	-2.9	-3.5	-3.4		
LRR	x	-2.2	-2.6	-2.4	-2.4	LRR	x	4.1	x	-3.9	-3.9	-4.2	-4.1		
LR2	x	0.81	0.89	0.92	0.94	LR2	x	0.47	x	0.69	0.67	0.75	0.83		
NSM	-25.5	-158.5	-225.8	-270.8	-313.0	NSM	8.6	4.3	x	-18.1	-20.3	-28.6	-37.6		
SMP	23	23	23	23	23	SMP	23	23	x	23	23	23	23		
1910 to							05/00 to								
	1942	1962	1998	2010				10/00	04/02	05/05	04/06	06/07	04/10		
EPR	-4.1	-3.8	-2.8	-2.9	EPR	-12.0	x	-5.4	-4.9	-5.3	-4.7				
LRR	x	-3.9	-2.8	-2.7	LRR	x	x	-5.2	-4.8	-5.0	-4.7				
LR2	x	0.99	0.92	0.93	LR2	x	x	0.83	0.81	0.85	0.88				
NSM	-132.9	-200.3	-245.3	-287.4	NSM	-4.4	x	-26.7	-28.9	-37.2	-46.2				
SMP	23	23	23	23	SMP	23	x	23	23	23	23				
1942 to							10/00 to								
	1962	1998	2010					04/02	05/05	04/06	06/07	04/10			
EPR	-3.4	-2.0	-2.3	EPR	x	-4.9	-4.4	-4.9	-4.4						
LRR	x	-1.9	-2.1	LRR	x	x	-4.6	-4.8	-4.5						
LR2	x	0.89	0.92	LR2	x	x	0.78	0.81	0.85						
NSM	-67.3	-112.3	-154.5	NSM	x	-22.3	-24.5	-32.9	-41.9						
SMP	23	23	23	SMP	x	23	23	23	23						
1962 to							04/02 to								
	1998	2010						05/05	04/06	06/07	04/10				
EPR	-1.2	-1.8	EPR	x	x	x	x								
LRR	x	-1.7	LRR	x	x	x	x								
LR2	x	0.89	LR2	x	x	x	x								
NSM	-45.0	-87.1	NSM	x	x	x	x								
SMP	23	23	SMP	x	x	x	x								
1998 to							05/05 to								
	2010							04/06	06/07	04/10					
EPR	-3.6	EPR	-2.3	-5.1	-4.0										
LRR	x	LRR	x	-5.2	-4.1										
LR2	x	LR2	x	0.77	0.87										
NSM	-42.1	NSM	-2.2	-10.6	-19.5										
SMP	23	SMP	23	23	23										
							04/06 to								
								06/07	04/10						
EPR: End Point Rate (m/yr), LRR: Linear Regression Rate (m/yr),							EPR	-7.5	-4.3						
LR2: R-Squared of LRR, NSM: Net Shoreline Movement (m),							LRR	x	-4.1						
SMP: Sample size (total number of transects).							LR2	x	0.85						
(x) symbol indicates shoreline for year unavailable or a minimum							NSM	-8.4	-17.3						
of three shorelines necessary for a regression rate.							SMP	23	23						
(-) sign indicates retreat & a positive integer signals advance.							06/07 to								
										04/10					
EPR							EPR			-3.1					
LRR							LRR			x					
LR2							LR2			x					
NSM							NSM			-9.0					
SMP							SMP			23					

Cell 1: Wachapreague Inlet-Throat Shoreline															
Comparison of Long-Term and Short-Term Shoreline Change Rate Statistics															
1852 to							07/98 to								
	1871	1910	1942	1962	1998	2010		05/99	05/00	10/00	04/02	05/05	04/06	06/07	04/10
EPR	1.4	0.0	-1.5	-1.8	-1.7	-1.8	EPR	-6.0	2.2	-0.1	x	-3.3	-3.2	-3.7	-3.6
LRR	x	-0.1	-1.4	-1.9	-2.0	-2.0	LRR	x	2.6	1.4	x	-3.4	-3.6	-3.9	-3.9
WLR	x	x	-1.8	-2.1	-2.0	-2.3	WLR	x	x	x	x	x	x	x	x
LMS	x	0.0	-1.2	-2.1	-2.0	-2.1	LMS	x	2.2	1.9	x	0.7	-3.4	-3.6	-3.4
SMP	23	23	23	23	23	23	SMP	23	23	23	x	23	23	23	23
1871 to							05/99 to								
	1910	1942	1962	1998	2010			05/00	10/00	04/02	05/05	04/06	06/07	04/10	
EPR		-0.7	-2.2	-2.5	-2.1	-2.3	EPR		-6.5	3.0	x	-3.0	-2.9	-3.5	-3.4
LRR		x	-2.2	-2.6	-2.4	-2.4	LRR		x	4.1	x	-3.9	-3.9	-4.2	-4.1
WLR		x	-2.4	-2.7	-2.1	-2.5	WLR		x	x	x	x	x	x	x
LMS		x	-2.2	-2.8	-2.3	-2.3	LMS		x	3.0	x	-3.5	-4.3	-4.6	-4.2
SMP		23	23	23	23	23	SMP		23	23	x	23	23	23	23
1910 to							05/00 to								
		1942	1962	1998	2010				10/00	04/02	05/05	04/06	06/07	04/10	
EPR			-4.1	-3.8	-2.8	-2.9	EPR			-12.0	x	-5.4	-4.9	-5.3	-4.7
LRR			x	-3.9	-2.8	-2.7	LRR			x	x	-5.2	-4.8	-5.0	-4.7
WLR			x	-3.8	-2.1	-2.6	WLR			x	x	x	x	x	x
LMS			x	-3.8	-2.8	-2.3	LMS			x	x	-5.3	-4.8	-4.8	-5.2
SMP			23	23	23	23	SMP			23	x	23	23	23	23
1942 to							10/00 to								
			1962	1998	2010					04/02	05/05	04/06	06/07	04/10	
EPR				-3.4	-2.0	-2.3	EPR				x	-4.9	-4.4	-4.9	-4.4
LRR				x	-1.9	-2.1	LRR				x	x	-4.6	-4.8	-4.5
WLR				x	-1.8	-2.1	WLR				x	x	x	x	x
LMS				x	-2.0	-1.9	LMS				x	x	-4.6	-4.7	-4.4
SMP				23	23	23	SMP				x	23	23	23	23
1962 to							04/02 to								
				1998	2010						05/05	04/06	06/07	04/10	
EPR					-1.2	-1.8	EPR					x	x	x	x
LRR					x	-1.7	LRR					x	x	x	x
WLR					x	-2.0	WLR					x	x	x	x
LMS					x	-1.8	LMS					x	x	x	x
SMP					23	23	SMP					x	x	x	x
1998 to							05/05 to								
					2010							04/06	06/07	04/10	
EPR						-3.6	EPR						-2.3	-5.1	-4.0
LRR						x	LRR						x	-5.2	-4.1
WLR						x	WLR						x	x	x
LMS						x	LMS						x	-5.1	-4.1
SMP						23	SMP						23	23	23
EPR: End Point Rate (m/yr), LRR: Linear Regression Rate (m/yr), WLR: Weighted Linear Regression (m/yr), LM S: Least Median of Squares (m/yr), SMP: Sample size (total number of transect (x) symbol indicates shoreline for year unavailable, or a minimum of three shorelines necessary for a regression rate, or shorelines have identical positional accuracies for WLR.															
04/06 to															
							EPR							06/07	04/10
							LRR							-7.5	-4.3
							WLR							x	-4.1
							LMS							x	x
							SMP							x	-4.3
														23	23
06/07 to															
							EPR								04/10
							LRR								-3.1
							WLR								x
							LMS								x
							SMP								23

EPR: End Point Rate (m/yr), LRR: Linear Regression Rate (m/yr),  
WLR: Weighted Linear Regression (m/yr), LMS: Least Median  
of Squares (m/yr), SMP: Sample size (total number of transect  
(x) symbol indicates shoreline for year unavailable, or a minimum  
of three shorelines necessary for a regression rate, or  
shorelines have identical positional accuracies for WLR.

Cell 1: Wachapreague Inlet-Throat Shoreline															
Linear Regression Statistics															
1852 to							07/98 to								
	1871	1910	1942	1962	1998	2010		05/99	05/00	10/00	04/02	05/05	04/06	06/07	04/10
LRR	x	-0.1	-1.4	-1.9	-2.0	-2.0	LRR	x	2.6	1.4	x	-3.4	-3.6	-3.9	-3.9
LR2	x	0.54	0.64	0.79	0.87	0.90	LR2	x	0.33	0.27	x	0.60	0.67	0.75	0.83
LSE	x	21.3	54.1	53.3	47.1	44.1	LSE	x	5.2	4.4	x	7.0	6.5	6.6	7.0
LCI	x	6.5	3.3	1.8	1.1	0.8	LCI	x	50.5	11.0	x	4.2	2.5	1.9	1.5
SMP	x	23	23	23	23	23	SMP	x	23	23	x	23	23	23	23
1871 to							05/99 to								
	1910	1942	1962	1998	2010			05/00	10/00	04/02	05/05	04/06	06/07	04/10	
LRR		x	-2.2	-2.6	-2.4	-2.4	LRR		x	4.1	x	-3.9	-3.9	-4.2	-4.1
LR2		x	0.81	0.89	0.92	0.94	LR2		x	0.47	x	0.69	0.67	0.75	0.83
LSE		x	49.5	41.3	38.3	35.0	LSE		x	4.3	x	7.0	6.5	6.4	7.1
LCI		x	12.5	2.6	1.3	0.8	LCI		x	51.4	x	6.5	3.3	2.3	1.8
SMP		x	23	23	23	23	SMP		x	23	x	23	23	23	23
1910 to							05/00 to								
		1942	1962	1998	2010				10/00	04/02	05/05	04/06	06/07	04/10	
LRR			x	-3.9	-2.8	-2.7	LRR			x	x	-5.2	-4.8	-5.0	-4.7
LR2			x	0.99	0.92	0.93	LR2			x	x	0.83	0.81	0.85	0.88
LSE			x	11.9	36.4	31.9	LSE			x	x	2.2	4.0	4.6	6.4
LCI			x	4.1	2.4	1.2	LCI			x	x	7.1	3.3	2.3	2.0
SMP			x	23	23	23	SMP			x	x	23	23	23	23
1942 to							10/00 to								
			1962	1998	2010					04/02	05/05	04/06	06/07	04/10	
LRR				x	-1.9	-2.1	LRR				x	x	-4.6	-4.8	-4.5
LR2				x	0.89	0.92	LR2				x	x	0.78	0.81	0.85
LSE				x	22.2	20.3	LSE				x	x	4.7	5.2	6.7
LCI				x	7.0	1.6	LCI				x	x	14.3	4.4	3.1
SMP				x	23	23	SMP				x	x	23	23	23
1962 to							04/02 to								
				1998	2010						05/05	04/06	06/07	04/10	
LRR					x	-1.7	LRR					x	x	x	x
LR2					x	0.89	LR2					x	x	x	x
LSE					x	16.9	LSE					x	x	x	x
LCI					x	6.1	LCI					x	x	x	x
SMP					x	23	SMP					x	x	x	x
1998 to							05/05 to								
					2010							04/06	06/07	04/10	
LRR						x	LRR						x	-5.2	-4.1
LR2						x	LR2						x	0.77	0.87
LSE						x	LSE						x	3.6	3.3
LCI						x	LCI						x	31.5	3.8
SMP						x	SMP						x	23	23
LRR: Linear Regression Rate (m/yr), LR2: R-squared of LRR															
LSE: Standard Error of LRR, LCI: Confidence Interval 95%of LRR															
SMP: Sample size (total number of transects).															
(x) symbol indicates shoreline for year unavailable or a minimum															
of three shorelines necessary for a regression rate.															
(-) sign indicates retreat & a positive integer signals advance.															
06/07 to															
														04/10	
LRR							LRR								x
LR2							LR2								x
LSE							LSE								x
LCI							LCI								x
SMP							SMP								x

Cell 1: Wachapreague Inlet-Throat Shoreline															
Weighted Linear Regression Statistics															
1852 to							07/98 to								
	1871	1910	1942	1962	1998	2010		05/99	05/00	10/00	04/02	05/05	04/06	06/07	04/10
WLR	x	x	-1.8	-2.1	-2.0	-2.3	WLR	x	x	x	x	x	x	x	x
WR2	x	x	0.80	0.87	0.94	0.93	WR2	x	x	x	x	x	x	x	x
WSE	x	x	3.0	2.9	2.8	4.1	WSE	x	x	x	x	x	x	x	x
WCI	x	x	2.7	1.5	0.7	0.7	WCI	x	x	x	x	x	x	x	x
SMP	x	x	23	23	23	23	SMP	x	x	x	x	x	x	x	x
1871 to							05/99 to								
	1910	1942	1962	1998	2010		05/00	10/00	04/02	05/05	04/06	06/07	04/10		
WLR	x	-2.4	-2.7	-2.1	-2.5	WLR	x	x	x	x	x	x	x		
WR2	x	0.89	0.93	0.94	0.95	WR2	x	x	x	x	x	x	x		
WSE	x	2.7	2.3	2.7	3.8	WSE	x	x	x	x	x	x	x		
WCI	x	10.4	2.2	1.0	0.8	WCI	x	x	x	x	x	x	x		
SMP	x	23	23	23	23	SMP	x	x	x	x	x	x	x		
1910 to							05/00 to								
	1942	1962	1998	2010		10/00	04/02	05/05	04/06	06/07	04/10				
WLR	x	-3.8	-2.1	-2.6	WLR	x	x	x	x	x	x				
WR2	x	0.98	0.91	0.95	WR2	x	x	x	x	x	x				
WSE	x	1.1	3.1	4.0	WSE	x	x	x	x	x	x				
WCI	x	5.5	1.9	1.1	WCI	x	x	x	x	x	x				
SMP	x	23	23	23	SMP	x	x	x	x	x	x				
1942 to							10/00 to								
	1962	1998	2010		04/02	05/05	04/06	06/07	04/10						
WLR	x	-1.8	-2.1	WLR	x	x	x	x	x						
WR2	x	0.93	0.91	WR2	x	x	x	x	x						
WSE	x	2.3	3.2	WSE	x	x	x	x	x						
WCI	x	5.0	1.9	WCI	x	x	x	x	x						
SMP	x	23	23	SMP	x	x	x	x	x						
1962 to							04/02 to								
	1998	2010		05/05	04/06	06/07	04/10								
WLR	x	-2.0	WLR	x	x	x	x								
WR2	x	0.82	WR2	x	x	x	x								
WSE	x	3.9	WSE	x	x	x	x								
WCI	x	10.8	WCI	x	x	x	x								
SMP	x	23	SMP	x	x	x	x								
1998 to							05/05 to								
	2010		04/06	06/07	04/10										
WLR	x	WLR	x	x	x										
WR2	x	WR2	x	x	x										
WSE	x	WSE	x	x	x										
WCI	x	WCI	x	x	x										
SMP	x	SMP	x	x	x										
WLR: Weighted Linear Regression (m/yr), WR2: R-squared of WLR							04/06 to								
WSE: Standard Error of WLR, WCI: Confidence Interval 95%										06/07	04/10				
of WLR, SMP: Sample size (total number of transects).							WLR				x	x			
(x) symbol indicates shoreline for year unavailable, or a minimum							WR2				x	x			
of three shorelines necessary for a regression rate, or							WSE				x	x			
shorelines have identical positional accuracies for WLR.							WCI				x	x			
(-) sign indicates retreat & a positive integer signals advance.							SMP				x	x			
							04/06 to								
											04/10				
WLR							WLR				x				
WR2							WR2				x				
WSE							WSE				x				
WCI							WCI				x				
SMP							SMP				x				



Cell 2: Northern, Inlet-Influenced, Open-Ocean Shoreline															
Long-Term and Short-Term Rates of Shoreline Change and Net Shoreline Movement															
1852 to							07/98 to								
	1871	1910	1942	1962	1998	2010		05/99	05/00	10/00	04/02	05/05	04/06	06/07	04/10
EPR	7.5	3.1	3.5	3.1	1.1	-0.4	EPR	-44.5	-38.2	-32.2	-11.0	-12.7	-9.3	-12.7	-16.2
LRR	x	2.8	3.0	3.0	1.4	0.1	LRR	x	-37.9	-33.2	-10.3	-9.8	-7.1	-8.2	-11.6
LR2	x	0.61	0.69	0.65	0.41	0.20	LR2	x	0.76	0.70	0.47	0.54	0.59	0.63	0.66
NSM	144.0	179.5	314.4	327.6	160.1	-58.5	NSM	-33.5	-69.7	-70.5	-41.3	-86.2	-71.7	-112.2	-190.3
SMP	38	38	38	48	48	54	SMP	39	39	39	21	39	39	39	39
1871 to							05/99 to								
	1910	1942	1962	1998	2010			05/00	10/00	04/02	05/05	04/06	06/07	04/10	
EPR		1.8	2.7	2.7	0.5	-1.2	EPR		-33.8	-25.8	-5.3	-8.7	-5.5	-9.7	-14.3
LRR		x	2.7	2.8	1.0	-0.6	LRR		x	-27.6	-5.0	-6.2	-4.2	-6.0	-10.4
LR2		x	0.69	0.63	0.42	0.24	LR2		x	0.79	0.24	0.57	0.65	0.68	0.64
NSM		71.3	193.9	223.2	60.8	-159.8	NSM		-36.2	-37.0	-15.8	-52.7	-38.2	-78.7	-156.8
SMP		48	48	54	54	54	SMP		39	39	21	39	39	39	39
1910 to							05/00 to								
		1942	1962	1998	2010				10/00	04/02	05/05	04/06	06/07	04/10	
EPR			4.2	2.1	-0.7	-2.5	EPR			-12.2	-2.0	-3.3	-0.3	-6.0	-12.2
LRR			x	2.3	-0.8	-2.5	LRR			-10.1	-1.5	-3.3	-1.7	-4.3	-10.1
LR2			x	0.53	0.30	0.41	LR2			0.67	0.13	0.85	0.84	0.81	0.67
NSM			136.5	112.1	-60.1	-250.4	NSM			-120.6	-3.8	-16.6	-2.0	-42.5	-120.6
SMP			39	39	39	39	SMP			39	21	39	39	39	39
1942 to							10/00 to								
			1962	1998	2010					04/02	05/05	04/06	06/07	04/10	
EPR				-1.2	-3.5	-5.7	EPR				-0.4	-3.4	-0.2	-6.3	-12.6
LRR				x	-3.7	-5.3	LRR				x	-17.7	-2.0	-5.1	-12.1
LR2				x	0.72	0.76	LR2				x	0.83	0.86	0.80	0.65
NSM				-24.4	-196.6	-386.9	NSM				-0.6	-15.7	-1.2	-41.7	-119.8
SMP				39	39	39	SMP				21	39	39	39	39
1962 to							04/02 to								
				1998	2010						05/05	04/06	06/07	04/10	
EPR				-4.7	-7.6		EPR					-24.9	-15.0	-17.4	-16.3
LRR				x	-6.9		LRR					x	-17.4	-16.8	0.9
LR2				x	0.89		LR2					x	0.81	0.81	0.89
NSM				-172.2	-362.5		NSM					-75.7	-59.9	-89.1	-135.3
SMP				39	39		SMP					21	21	21	21
1998 to							05/05 to								
					2010							04/06	06/07	04/10	
EPR					-16.2		EPR						15.1	-12.5	-21.0
LRR					x		LRR						x	-13.1	-23.5
LR2					x		LR2						x	0.35	0.82
NSM					-190.3		NSM						14.5	-26.0	-104.1
SMP					39		SMP						39	39	39
							04/06 to								
													06/07	04/10	
EPR: End Point Rate (m/yr), LRR: Linear Regression Rate (m/yr),							EPR							-36.5	-29.7
LR2: R-Squared of LRR, NSM: Net Shoreline Movement (m),							LRR							x	-29.2
SMP: Sample size (total number of transects).							LR2							x	0.97
(x) symbol indicates shoreline for year unavailable or a minimum							NSM							-40.5	-118.6
of three shorelines necessary for a regression rate.							SMP							39	39
(-) sign indicates retreat & a positive integer signals advance.							06/07 to								
														04/10	
							EPR								-27.1
							LRR								x
							LR2								x
							NSM								-78.1
							SMP								39

Cell 2: Northern, Inlet-Influenced, Open-Ocean Shoreline															
Comparison of Long-Term and Short-Term Shoreline Change Rate Statistics															
1852 to							07/98 to								
	1871	1910	1942	1962	1998	2010		05/99	05/00	10/00	04/02	05/05	04/06	06/07	04/10
EPR	7.5	3.1	3.5	3.1	1.1	-0.4	EPR	-44.5	-38.2	-32.2	-11.0	-12.7	-9.3	-12.7	-16.2
LRR	x	2.8	3.0	3.0	1.4	0.1	LRR	x	-37.9	-33.2	-10.3	-9.8	-7.1	-8.2	-11.6
WLR	x	x	3.1	2.9	-0.3	-1.8	WLR	x	x	x	x	x	x	x	x
LMS	x	3.1	2.8	2.6	1.5	0.6	LMS	x	-30.5	-24.9	-10.3	-23.5	-7.0	-8.2	-10.8
SMP	38	38	38	48	48	54	SMP	39	39	39	21	39	39	39	39
1871 to							05/99 to								
	1910	1942	1962	1998	2010			05/00	10/00	04/02	05/05	04/06	06/07	04/10	
EPR		1.8	2.7	2.7	0.5	-1.2	EPR		-33.8	-25.8	-5.3	-8.7	-5.5	-9.7	-14.3
LRR		x	2.7	2.8	1.0	-0.6	LRR		x	-27.6	-5.0	-6.2	-4.2	-6.0	-10.4
WLR		x	2.8	2.9	-0.8	-2.2	WLR		x	x	x	x	x	x	x
LMS		x	2.7	2.7	1.1	0.0	LMS		x	-16.6	-5.3	-7.7	-1.9	-3.1	-6.4
SMP		48	48	54	54	54	SMP		39	39	21	39	39	39	39
1910 to							05/00 to								
		1942	1962	1998	2010				10/00	04/02	05/05	04/06	06/07	04/10	
EPR			4.2	2.1	-0.7	-2.5	EPR			-2.2	-2.0	-3.3	-0.3	-6.0	-12.2
LRR			x	2.3	-0.8	-2.5	LRR			x	-1.5	-3.3	-1.7	-4.3	-10.1
WLR			x	1.6	-2.8	-3.1	WLR			x	x	x	x	x	x
LMS			x	2.1	-1.0	-3.9	LMS			x	-2.0	-4.5	-1.7	-3.2	-5.1
SMP			39	39	39	39	SMP			39	21	39	39	39	39
1942 to							10/00 to								
			1962	1998	2010					04/02	05/05	04/06	06/07	04/10	
EPR				-1.2	-3.5	-5.7	EPR				-0.4	-3.4	-0.2	-6.3	-12.6
LRR				x	-3.7	-5.3	LRR				x	-17.7	-2.0	-5.1	-12.1
WLR				x	-3.8	-6.1	WLR				x	x	x	x	x
LMS				x	-3.5	-5.6	LMS				x	-4.3	-2.8	-4.2	-13.5
SMP				39	39	39	SMP				21	39	39	39	39
1962 to							04/02 to								
				1998	2010						05/05	04/06	06/07	04/10	
EPR					-4.7	-7.6	EPR					-24.9	-15.0	-17.4	-16.9
LRR					x	-6.9	LRR					x	-17.4	-16.8	-16.3
WLR					x	-8.4	WLR					x	x	x	x
LMS					x	-7.4	LMS					x	-15.5	-16.2	-16.3
SMP					39	39	SMP					21	21	21	21
1998 to							05/05 to								
					2010							04/06	06/07	04/10	
EPR						-16.2	EPR						15.1	-12.5	-21.0
LRR						x	LRR						x	-13.1	-23.5
WLR						x	WLR						x	x	x
LMS						x	LMS						x	-12.6	-21.9
SMP						39	SMP						39	39	39
							04/06 to								
													06/07	04/10	
EPR: End Point Rate (m/yr), LRR: Linear Regression Rate (m/yr),							EPR							-36.5	-29.7
WLR: Weighted Linear Regression (m/yr), LMS: Least Median							LRR							x	-29.2
of Squares (m/yr), SMP: Sample size (total number of transects							WLR							x	x
(x) symbol indicates shoreline for year unavailable, or a minimum							LMS							x	-27.5
of three shorelines necessary for a regression rate, or							SMP							39	39
shorelines have identical positional accuracies for WLR.							06/07 to								
														04/10	
							EPR							-27.1	
							LRR							x	
							WLR							x	
							LMS							x	
							SMP							39	

Cell 2: Northern, Inlet-Influenced, Open-Ocean Shoreline															
Linear Regression Statistics															
1852 to							07/98 to								
	1871	1910	1942	1962	1998	2010		05/99	05/00	10/00	04/02	05/05	04/06	06/07	04/10
LRR	x	2.8	3.0	3.0	1.4	0.1	LRR	x	-37.9	-33.2	-10.3	-9.8	-7.1	-8.2	-11.6
LR2	x	0.61	0.69	0.65	0.41	0.20	LR2	x	0.76	0.70	0.47	0.54	0.59	0.63	0.66
LSE	x	71.6	80.2	85.5	129.5	176.5	LSE	x	22.3	21.2	17.2	43.5	40.3	38.1	41.8
LCI	x	21.8	4.9	3.3	3.2	3.7	LCI	x	218.1	52.5	19.1	25.2	15.1	10.8	8.8
SMP	x	38	38	48	48	54	SMP	x	39	39	21	39	39	39	39
1871 to							05/99 to								
	1910	1942	1962	1998	2010		05/00	10/00	04/02	05/05	04/06	06/07	04/10		
LRR	x	2.7	2.8	1.0	-0.6	LRR	x	-27.6	-5.0	-6.2	-4.2	-6.0	-10.4		
LR2	x	0.69	0.63	0.42	0.24	LR2	x	0.79	0.2	0.57	0.65	0.68	0.64		
LSE	x	78.6	88.4	124.8	170.2	LSE	x	13.5	15.8	40.9	36.3	35.0	42.1		
LCI	x	19.8	8.3	4.5	4.3	LCI	x	163.0	31.7	35.5	17.6	12.2	10.5		
SMP	x	48	54	54	54	SMP	x	39	21	39	39	39	39		
1910 to							05/00 to								
	1942	1962	1998	2010		10/00	04/02	05/05	04/06	06/07	04/10				
LRR	x	2.3	-0.8	-2.5	LRR	x	-1.5	-3.3	-1.7	-4.3	-10.1				
LR2	x	0.53	0.30	0.41	LR2	x	0.1	0.85	0.84	0.81	0.67				
LSE	x	102.7	132.6	153.0	LSE	x	14.6	18.8	20.7	25.6	41.0				
LCI	x	35.0	8.9	5.9	LCI	x	129.1	37.1	14.5	11.8	12.8				
SMP	x	39	39	39	SMP	x	21	39	39	39	39				
1942 to							10/00 to								
	1962	1998	2010		04/02	05/05	04/06	06/07	04/10						
LRR	x	-3.7	-5.3	LRR	x	-17.7	-2.0	-5.1	-12.1						
LR2	x	0.72	0.76	LR2	x	0.8	0.86	0.80	0.65						
LSE	x	73.5	90.5	LSE	x	24.8	22.7	28.5	43.9						
LCI	x	23.2	7.1	LCI	x	95.2	43.9	21.2	19.1						
SMP	x	39	39	SMP	x	21	39	39	39						
1962 to							04/02 to								
	1998	2010		05/05	04/06	06/07	04/10								
LRR	x	-6.9	LRR	x	-17.4	-16.8	-16.3								
LR2	x	0.89	LR2	x	0.81	0.81	0.89								
LSE	x	79.6	LSE	x	23.6	21.4	19.0								
LCI	x	28.6	LCI	x	101.2	24.2	10.3								
SMP	x	39	SMP	x	21	21	21								
1998 to							05/05 to								
	2010		04/06	06/07	04/10										
LRR	x	LRR	x	-13.1	-23.5										
LR2	x	LR2	x	0.35	0.82										
LSE	x	LSE	x	21.7	24.2										
LCI	x	LCI	x	187.9	28.0										
SMP	x	SMP	x	39	39										
04/06 to															
											06/07	04/10			
LRR											x	-29.2			
LR2											x	0.97			
LSE											x	11.7			
LCI											x	51.3			
SMP											x	39.0			
06/07 to															
												04/10			
LRR												x			
LR2												x			
LSE												x			
LCI												x			
SMP												x			
LRR: Linear Regression Rate (m/yr), LR2: R-squared of LRR															
LSE: Standard Error of LRR, LCI: Confidence Interval 95%of LRR															
SMP: Sample size (total number of transects).															
(x) symbol indicates shoreline for year unavailable or a minimum															
of three shorelines necessary for a regression rate.															
(-) sign indicates retreat & a positive integer signals advance.															

Cell 2: Northern, Inlet-Influenced, Open-Ocean Shoreline															
Weighted Linear Regression Statistics															
1852 to							07/98 to								
	1871	1910	1942	1962	1998	2010		05/99	05/00	10/00	04/02	05/05	04/06	06/07	04/10
WLR	x	x	3.1	2.9	-0.3	-1.8	WLR	x	x	x	x	x	x	x	x
WR2	x	x	0.80	0.60	0.36	0.29	WR2	x	x	x	x	x	x	x	x
WSE	x	x	4.3	6.7	12.7	23.3	WSE	x	x	x	x	x	x	x	x
WCI	x	x	3.9	4.0	3.5	4.5	WCI	x	x	x	x	x	x	x	x
SMP	x	x	38	48	48	54	SMP	x	x	x	x	x	x	x	x
1871 to							05/99 to								
	1910	1942	1962	1998	2010		05/00	10/00	04/02	05/05	04/06	06/07	04/10		
WLR	x	2.8	2.9	-0.8	-2.2	WLR	x	x	x	x	x	x	x		
WR2	x	0.79	0.58	0.43	0.35	WR2	x	x	x	x	x	x	x		
WSE	x	4.3	7.3	12.1	23.6	WSE	x	x	x	x	x	x	x		
WCI	x	16.5	10.9	4.6	5.2	WCI	x	x	x	x	x	x	x		
SMP	x	48	54	54	54	SMP	x	x	x	x	x	x	x		
1910 to							05/00 to								
	1942	1962	1998	2010		10/00	04/02	05/05	04/06	06/07	04/10				
WLR	x	1.6	-2.8	-3.1	WLR	x	x	x	x	x	x				
WR2	x	0.44	0.63	0.51	WR2	x	x	x	x	x	x				
WSE	x	9.1	11.1	22.1	WSE	x	x	x	x	x	x				
WCI	x	47.1	6.9	6.0	WCI	x	x	x	x	x	x				
SMP	x	39	39	39	SMP	x	x	x	x	x	x				
1942 to							10/00 to								
	1962	1998	2010		04/02	05/05	04/06	06/07	04/10						
WLR	x	-3.8	-6.1	WLR	x	x	x	x	x						
WR2	x	0.78	0.74	WR2	x	x	x	x	x						
WSE	x	7.6	16.9	WSE	x	x	x	x	x						
WCI	x	16.5	10.0	WCI	x	x	x	x	x						
SMP	x	39	39	SMP	x	x	x	x	x						
1962 to							04/02 to								
	1998	2010		05/05	04/06	06/07	04/10								
WLR	x	-8.4	WLR	x	x	x	x								
WR2	x	0.81	WR2	x	x	x	x								
WSE	x	18.2	WSE	x	x	x	x								
WCI	x	50.9	WCI	x	x	x	x								
SMP	x	39	SMP	x	x	x	x								
1998 to							05/05 to								
	2010		04/06	06/07	04/10										
WLR	x	WLR	x	x	x										
WR2	x	WR2	x	x	x										
WSE	x	WSE	x	x	x										
WCI	x	WCI	x	x	x										
SMP	x	SMP	x	x	x										
WLR: Weighted Linear Regression (m/yr), WR2: R-squared of WLR							04/06 to								
WSE: Standard Error of WLR, WCI: Confidence Interval 95%												06/07	04/10		
of WLR, SMP: Sample size (total number of transects).							WLR						x	x	
(x) symbol indicates shoreline for year unavailable, or a minimum							WR2						x	x	
of three shorelines necessary for a regression rate, or							WSE						x	x	
shorelines have identical positional accuracies for WLR.							WCI						x	x	
(-) sign indicates retreat & a positive integer signals advance.							SMP						x	x	
							04/06 to								
							<td></td> <td></td> <td></td> <td></td> <td></td> <td></td> <td>04/10</td>							04/10	
							WLR							x	
							WR2							x	
							WSE							x	
							WCI							x	
							SMP							x	

Cell 3: North-Central, Open-Ocean Shoreline																
Long-Term and Short-Term Rates of Shoreline Change and Net Shoreline Movement																
1852 to							07/98 to									
	1871	1910	1942	1962	1998	2010		05/99	05/00	10/00	04/02	05/05	04/06	06/07	04/10	
EPR	15.4	6.4	4.2	2.1	-0.1	-1.0	EPR	-7.3	-4.9	-9.1	-1.8	-8.0	-7.2	-10.1	-12.5	
LRR	x	5.7	3.6	1.8	-0.3	-1.5	LRR	x	-4.8	-7.7	-2.4	-7.3	-7.4	-9.0	-11.4	
LR2	x	0.69	0.61	0.36	0.07	0.17	LR2	x	0.68	0.68	0.35	0.74	0.83	0.86	0.89	
NSM	298.0	369.1	376.4	226.9	-16.3	-162.6	NSM	-5.5	-9.0	-20.0	-6.9	-54.5	-55.9	-89.2	-146.3	
SMP	96	96	96	96	96	96	SMP	96	96	96	96	96	96	96	96	
1871 to							05/99 to									
	1910	1942	1962	1998	2010			05/00	10/00	04/02	05/05	04/06	06/07	04/10		
EPR		1.8	1.1	-0.8	-2.5	-3.3	EPR		-3.2	-10.1	-0.5	-8.1	-7.2	-10.3	-12.8	
LRR		x	1.1	-0.4	-2.4	-3.4	LRR		x	-8.6	-0.5	-7.6	-7.7	-9.5	-12.1	
LR2		x	0.53	0.31	0.41	0.59	LR2		x	0.63	0.33	0.72	0.82	0.86	0.89	
NSM		71.1	78.4	-71.2	-314.3	-460.6	NSM		-3.5	-14.5	-1.4	-49.0	-50.4	-83.7	-140.8	
SMP		96	96	96	96	96	SMP		96	96	96	96	96	96	96	
1910 to							05/00 to									
		1942	1962	1998	2010				10/00	04/02	05/05	04/06	06/07	04/10		
EPR			0.2	-2.7	-4.4	-5.3	EPR			-30.4	1.1	-9.2	-7.9	-11.4	-13.9	
LRR			x	-2.4	-4.6	-5.5	LRR			x	3.3	-8.3	-8.2	-10.2	-13.0	
LR2			x	0.55	0.73	0.83	LR2			x	0.39	0.72	0.81	0.85	0.89	
NSM			7.3	-142.2	-385.4	-531.7	NSM			-11.1	2.1	-45.6	-47.0	-80.3	-137.4	
SMP			96	96	96	96	SMP			96	96	96	96	96	96	
1942 to							10/00 to									
			1962	1998	2010					04/02	05/05	04/06	06/07	04/10		
EPR				-7.5	-7.0	-7.9	EPR				8.5	-7.5	-6.5	-10.4	-13.2	
LRR				x	-7.0	-7.6	LRR				x	-8.6	-8.4	-10.7	-13.8	
LR2				x	1.00	0.99	LR2				x	0.69	0.78	0.83	0.89	
NSM				-149.5	-392.6	-539.0	NSM				13.1	-34.5	-35.9	-69.2	-126.3	
SMP				96	96	96	SMP				96	96	96	96	96	
1962 to							04/02 to									
				1998	2010						05/05	04/06	06/07	04/10		
EPR					-6.7	-8.1	EPR					-15.7	-12.2	-16.1	-17.4	
LRR					x	-7.8	LRR					x	-13.1	-15.1	-17.4	
LR2					x	0.98	LR2					x	0.95	0.94	0.96	
NSM					-243.1	-389.5	NSM					-47.6	-49.1	-82.3	-139.4	
SMP					96	96	SMP					96	96	96	96	
1998 to							05/05 to									
					2010							04/06	06/07	04/10		
EPR						-12.5	EPR						-1.5	-16.7	-18.6	
LRR						x	LRR						x	-17.1	-19.8	
LR2						x	LR2						x	0.78	0.96	
NSM						-146.3	NSM						-1.4	-34.7	-91.8	
SMP						96	SMP						96	96	96	
EPR: End Point Rate (m/yr), LRR: Linear Regression Rate (m/yr),							04/06 to									
LR2: R-Squared of LRR, NSM: Net Shoreline Movement (m),							06/07								04/10	
SMP: Sample size (total number of transects).							EPR <td>-30.0</td> <td>-22.7</td>								-30.0	-22.7
(x) symbol indicates shoreline for year unavailable or a minimum							LRR <td>x</td> <td>-22.1</td>								x	-22.1
of three shorelines necessary for a regression rate.							LR2 <td>x</td> <td>0.99</td>								x	0.99
(-) sign indicates retreat & a positive integer signals advance.							NSM <td>-28.8</td> <td>-90.4</td>								-28.8	-90.4
							SMP <td>96</td> <td>96</td>								96	96
							06/07 to								04/10	
							EPR <td>-19.9</td>								-19.9	
							LRR <td>x</td>								x	
							LR2 <td>x</td>								x	
							NSM <td>-57.1</td>								-57.1	
							SMP <td>96</td>								96	

Cell 3: North-Central, Open-Ocean Shoreline																
Comparison of Long-Term and Short-Term Shoreline Change Rate Statistics																
1852 to							07/98 to									
	1871	1910	1942	1962	1998	2010		05/99	05/00	10/00	04/02	05/05	04/06	06/07	04/10	
EPR	15.4	6.4	4.2	2.1	-0.1	-1.0	EPR	-7.3	-4.9	-9.1	-1.8	-8.0	-7.2	-10.1	-12.5	
LRR	x	5.7	3.6	1.8	-0.3	-1.5	LRR	x	-4.8	-7.7	-2.4	-7.3	-7.4	-9.0	-11.4	
WLR	x	x	3.0	1.2	-2.8	-4.1	WLR	x	x	x	0.3	x	x	x	x	
LMS	x	6.3	3.6	-0.4	-0.6	-3.0	LMS	x	-4.9	-7.4	-3.6	-7.6	-7.5	-8.1	-8.2	
SMP	96	96	96	96	96	96	SMP	96	96	96	96	96	96	96	96	
1871 to							05/99 to									
	1910	1942	1962	1998	2010			05/00	10/00	04/02	05/05	04/06	06/07	04/10		
EPR		1.8	1.1	-0.8	-2.5	-3.3	EPR		-3.2	-10.1	-0.5	-8.1	-7.2	-10.3	-12.8	
LRR		x	1.1	-0.4	-2.4	-3.4	LRR		x	-8.6	-0.5	-7.6	-7.7	-9.5	-12.1	
WLR		x	1.0	-1.0	-4.5	-5.2	WLR		x	x	x	x	x	x	x	
LMS		x	1.1	-0.5	-3.1	-4.9	LMS		x	-9.7	0.2	-7.0	-7.6	-8.3	-8.7	
SMP		96	96	96	96	96	SMP		96	96	96	96	96	96	96	
1910 to							05/00 to									
		1942	1962	1998	2010				10/00	04/02	05/05	04/06	06/07	04/10		
EPR			0.2	-2.7	-4.4	-5.3	EPR			-30.4	1.1	-9.2	-7.9	-11.4	-13.9	
LRR			x	-2.4	-4.6	-5.5	LRR			x	3.3	-8.3	-8.2	-10.2	-13.0	
WLR			x	-3.6	-6.0	-5.9	WLR			x	x	x	x	x	x	
LMS			x	-2.7	-4.8	-7.7	LMS			x	1.2	-8.6	-8.1	-9.0	-10.8	
SMP			96	96	96	96	SMP			96	96	96	96	96	96	
1942 to							10/00 to									
			1962	1998	2010					04/02	05/05	04/06	06/07	04/10		
EPR				-7.5	-7.0	-7.9	EPR				8.5	-7.5	-6.5	-10.4	-13.2	
LRR				x	-7.0	-7.6	LRR				x	-8.6	-8.4	-10.7	-13.8	
WLR				x	-6.9	-7.9	WLR				x	x	x	x	x	
LMS				x	-7.0	-7.6	LMS				x	-7.7	-9.2	-12.2	-14.9	
SMP				96	96	96	SMP				96	96	96	96	96	
1962 to							04/02 to									
				1998	2010						05/05	04/06	06/07	04/10		
EPR					-6.7	-8.1	EPR					-15.7	-12.2	-16.1	-17.4	
LRR					x	-7.8	LRR					x	-13.1	-15.1	-17.4	
WLR					x	-8.5	WLR					x	x	x	x	
LMS					x	-8.0	LMS					x	-12.7	-14.8	-17.3	
SMP					96	96	SMP					96	96	96	96	
1998 to							05/05 to									
					2010							04/06	06/07	04/10		
EPR						-12.5	EPR						-1.5	-16.7	-18.6	
LRR						x	LRR						x	-17.1	-19.8	
WLR						x	WLR						x	x	x	
LMS						x	LMS						x	-16.7	-19.1	
SMP						96	SMP						96	96	96	
EPR: End Point Rate (m/yr), LRR: Linear Regression Rate (m/yr), WLR: Weighted Linear Regression (m/yr), LMS: Least Median of Squares (m/yr), SMP: Sample size (total number of transects (x) symbol indicates shoreline for year unavailable, or a minimum of three shorelines necessary for a regression rate, or shorelines have identical positional accuracies for WLR.							04/06 to									
														06/07	04/10	
															-30.0	-22.7
															x	-22.1
															x	x
															x	-21.2
															96	96
							06/07 to									
														04/10		
							EPR							-19.9		
							LRR							x		
							WLR							x		
							LMS							x		
							SMP							96		

Cell 3: North-Central, Open-Ocean Shoreline															
Linear Regression Statistics															
1852 to							07/98 to								
	1871	1910	1942	1962	1998	2010		05/99	05/00	10/00	04/02	05/05	04/06	06/07	04/10
LRR	x	5.7	3.6	1.8	-0.3	-1.5	LRR	x	-4.8	-7.7	-2.4	-7.3	-7.4	-9.0	-11.4
LR2	x	0.69	0.61	0.36	0.07	0.17	LR2	x	0.68	0.68	0.35	0.74	0.83	0.86	0.89
LSE	x	140.3	141.9	159.1	204.2	218.9	LSE	x	3.8	5.8	8.6	11.4	10.5	12.9	17.7
LCI	x	42.7	8.7	5.5	4.6	3.8	LCI	x	37.4	14.3	9.6	5.8	3.7	3.5	3.6
SMP	x	96	96	96	96	96	SMP	x	96	96	96	96	96	96	96
1871 to							05/99 to								
	1910	1942	1962	1998	2010		05/00	10/00	04/02	05/05	04/06	06/07	04/10		
LRR	x	1.1	-0.4	-2.4	-3.4	LRR	x	-8.6	-0.5	-7.6	-7.7	-9.5	-12.1		
LR2	x	0.53	0.31	0.41	0.59	LR2	x	0.63	0.3	0.72	0.82	0.86	0.89		
LSE	x	77.9	100.9	138.5	150.0	LSE	x	5.9	8.6	12.6	11.3	13.5	18.0		
LCI	x	19.7	6.3	4.5	3.5	LCI	x	71.4	17.3	8.6	4.9	4.4	4.3		
SMP	x	96	96	96	96	SMP	x	96	96	96	96	96	96		
1910 to							05/00 to								
	1942	1962	1998	2010		10/00	04/02	05/05	04/06	06/07	04/10				
LRR	x	-2.4	-4.6	-5.5	LRR	x	3.3	-8.3	-8.2	-10.2	-13.0				
LR2	x	0.55	0.73	0.83	LR2	x	0.39	0.72	0.81	0.85	0.89				
LSE	x	77.2	89.8	93.8	LSE	x	8.8	14.6	12.3	14.1	18.1				
LCI	x	26.3	6.0	3.6	LCI	x	78.0	16.1	7.3	5.9	5.1				
SMP	x	96	96	96	SMP	x	96	96	96	96	96				
1942 to							10/00 to								
	1962	1998	2010		04/02	05/05	04/06	06/07	04/10						
LRR	x	-7.0	-7.6	LRR	x	-8.6	-8.4	-10.7	-13.8						
LR2	x	1.00	0.99	LR2	x	0.69	0.78	0.83	0.89						
LSE	x	12.6	31.1	LSE	x	19.9	14.5	15.8	19.0						
LCI	x	4.0	2.5	LCI	x	76.5	13.9	9.0	6.8						
SMP	x	96	96	SMP	x	96	96	96	96						
1962 to							04/02 to								
	1998	2010		05/05	04/06	06/07	04/10								
LRR	x	-7.8	LRR	x	-13.1	-15.1	-17.4								
LR2	x	0.98	LR2	x	0.95	0.94	0.96								
LSE	x	40.0	LSE	x	8.2	10.0	11.1								
LCI	x	14.4	LCI	x	35.4	11.3	6.1								
SMP	x	96	SMP	x	96	96	96								
1998 to							05/05 to								
	2010		04/06	06/07	04/10										
LRR	x	LRR	x	-17.1	-19.8										
LR2	x	LR2	x	0.78	0.96										
LSE	x	LSE	x	12.0	9.4										
LCI	x	LCI	x	104.1	10.9										
SMP	x	SMP	x	96	96										
04/06 to							06/07	04/10							
LRR: Linear Regression Rate (m/yr), LR2: R-squared of LRR							x	-22.1							
LSE: Standard Error of LRR, LCI: Confidence Interval 95%of LRR							x	0.99							
SMP: Sample size (total number of transects).							x	6.5							
(x) symbol indicates shoreline for year unavailable or a minimum of three shorelines necessary for a regression rate.							x	28.4							
(-) sign indicates retreat & a positive integer signals advance.							x	96							
06/07 to							04/10								
LRR							x								
LR2							x								
LSE							x								
LCI							x								
SMP							x								

Cell 3: North-Central, Open-Ocean Shoreline																	
Weighted Linear Regression Statistics																	
		1852 to							07/98 to								
		1871	1910	1942	1962	1998	2010			05/99	05/00	10/00	04/02	05/05	04/06	06/07	04/10
WLR		x	x	3.0	1.2	-2.8	-4.1	WLR		x	x	x	x	x	x	x	x
WR2		x	x	0.62	0.26	0.42	0.64	WR2		x	x	x	x	x	x	x	x
WSE		x	x	0.6	10.3	16.9	19.4	WSE		x	x	x	x	x	x	x	x
WCI		x	x	7.5	5.4	4.3	3.4	WCI		x	x	x	x	x	x	x	x
SMP		x	x	96	96	96	96	SMP		x	x	x	x	x	x	x	x
		1871 to							05/99 to								
		1910	1942	1962	1998	2010			05/00	10/00	04/02	05/05	04/06	06/07	04/10		
WLR		x	1.0	-1.0	-4.5	-5.2	WLR		x	x	x	x	x	x	x	x	
WR2		x	0.61	0.25	0.76	0.82	WR2		x	x	x	x	x	x	x	x	
WSE		x	4.2	7.8	11.9	14.4	WSE		x	x	x	x	x	x	x	x	
WCI		x	16.3	7.7	4.2	3.0	WCI		x	x	x	x	x	x	x	x	
SMP		x	96	96	96	96	SMP		x	x	x	x	x	x	x	x	
		1910 to							05/00 to								
		1942	1962	1998	2010			10/00	04/02	05/05	04/06	06/07	04/10				
WLR		x	-3.6	-6.0	-5.9	WLR		x	x	x	x	x	x				
WR2		x	0.54	0.93	0.87	WR2		x	x	x	x	x	x				
WSE		x	6.8	6.9	12.6	WSE		x	x	x	x	x	x				
WCI		x	35.4	4.2	3.4	WCI		x	x	x	x	x	x				
SMP		x	96	96	96	SMP		x	x	x	x	x	x				
		1942 to							10/00 to								
		1962	1998	2010			04/02	05/05	04/06	06/07	04/10						
WLR		x	-6.9	-7.9	WLR		x	x	x	x	x						
WR2		x	1.00	0.97	WR2		x	x	x	x	x						
WSE		x	1.3	7.1	WSE		x	x	x	x	x						
WCI		x	2.8	4.2	WCI		x	x	x	x	x						
SMP		x	96	96	SMP		x	x	x	x	x						
		1962 to							04/02 to								
		1998	2010			05/05	04/06	06/07	04/10								
WLR		x	-8.5	WLR		x	x	x	x								
WR2		x	0.95	WR2		x	x	x	x								
WSE		x	9.2	WSE		x	x	x	x								
WCI		x	25.6	WCI		x	x	x	x								
SMP		x	96	SMP		x	x	x	x								
		1998 to							05/05 to								
		2010			04/06	06/07	04/10										
WLR		x	WLR		x	x	x										
WR2		x	WR2		x	x	x										
WSE		x	WSE		x	x	x										
WCI		x	WCI		x	x	x										
SMP		x	SMP		x	x	x										
WLR: Weighted Linear Regression (m/yr), WR2: R-squared of WLR								04/06 to									
WSE: Standard Error of WLR, WCI: Confidence Interval 95%								06/07 04/10									
of WLR, SMP: Sample size (total number of transects).								WLR							x	x	
(x) symbol indicates shoreline for year unavailable, or a minimum								WR2							x	x	
of three shorelines necessary for a regression rate, or								WSE							x	x	
shorelines have identical positional accuracies for WLR.								WCI							x	x	
(-) sign indicates retreat & a positive integer signals advance.								SMP							x	x	
		04/06 to							04/10								
		04/06	06/07	04/10			WLR									x	
							WR2									x	
							WSE									x	
							WCI									x	
							SMP									x	



Cell 4: Southern, Washover-Dominated, Open-Ocean Shoreline															
Long-Term and Short-Term Rates of Shoreline Change and Net Shoreline Movement															
1852 to							07/98 to								
	1871	1910	1942	1962	1998	2010		05/99	05/00	10/00	04/02	05/05	04/06	06/07	04/10
EPR	16.8	0.7	-2.2	-5.9	-7.0	-7.5	EPR	-16.5	-12.7	-17.4	-7.8	-11.8	-10.4	-12.3	-14.6
LRR	x	-0.4	-3.6	-6.9	-8.3	-8.9	LRR	x	-12.5	-15.7	-8.4	-10.8	-10.3	-11.1	-13.2
LR2	x	0.32	0.28	0.62	0.78	0.84	LR2	x	0.89	0.87	0.59	0.87	0.91	0.94	0.94
NSM	324.4	43.2	-195.8	-646.7	-1028.7	-1194.6	NSM	-12.4	-23.2	-38.0	-29.2	-80.1	-80.5	-108.9	-171.8
SMP	88	88	56	86	86	88	SMP	87	87	87	87	87	87	87	87
1871 to							05/99 to								
	1910	1942	1962	1998	2010		05/00	10/00	04/02	05/05	04/06	06/07	04/10		
EPR	-7.3	-9.0	-10.7	-10.7	-10.9	EPR	-10.3	-17.7	-5.6	-11.1	-9.6	-11.8	-14.4		
LRR	x	-9.0	-10.6	-11.0	-11.2	LRR	x	-16.0	-5.6	-10.2	-9.8	-10.9	-13.2		
LR2	x	0.97	0.95	0.97	0.98	LR2	x	0.77	0.36	0.83	0.88	0.91	0.92		
NSM	-281.2	-640.4	-974.3	-1356.3	-1519.0	NSM	-11.1	-25.4	-16.7	-66.8	-67.2	-96.0	-157.8		
SMP	88	56	86	86	88	SMP	88	88	88	88	88	88	88		
1910 to							05/00 to								
	1942	1962	1998	2010		10/00	04/02	05/05	04/06	06/07	04/10				
EPR	-9.8	-12.9	-12.0	-12.3	EPR	-39.3	-2.1	-11.2	-9.5	-12.1	-14.8				
LRR	x	-11.5	-12.1	-12.2	LRR	x	-0.5	-10.2	-9.6	-11.0	-13.6				
LR2	x	0.98	0.99	1.00	LR2	x	0.24	0.80	0.86	0.89	0.91				
NSM	-317.0	-677.4	-1059.4	-1237.8	NSM	-14.3	-5.6	-55.7	-56.2	-84.9	-146.8				
SMP	56	86	86	88	SMP	88	88	88	88	88	88				
1942 to							10/00 to								
	1962	1998	2010		04/02	05/05	04/06	06/07	04/10						
EPR	-14.9	-11.4	-11.8	EPR	5.7	-9.0	-7.5	-10.6	-13.9						
LRR	x	-11.2	-11.3	LRR	x	-10.2	-9.5	-11.1	-14.2						
LR2	x	0.98	0.99	LR2	x	0.76	0.83	0.87	0.90						
NSM	-295.9	-640.4	-799.4	NSM	8.8	-41.4	-41.9	-70.6	-132.5						
SMP	56	56	56	SMP	87	88	88	88	88						
1962 to							04/02 to								
	1998	2010		05/05	04/06	06/07	04/10								
EPR	-10.5	-11.5	EPR	-16.7	-12.8	-15.6	-17.8								
LRR	x	-11.3	LRR	x	-13.8	-14.8	-17.6								
LR2	x	0.99	LR2	x	0.95	0.96	0.96								
NSM	-382.0	-549.3	NSM	-50.9	-51.3	-79.7	-142.5								
SMP	86	87	SMP	87	87	87	87								
1998 to							05/05 to								
	2010		04/06	06/07	04/10										
EPR	-14.6	EPR	-0.5	-14.1	-18.4										
LRR	x	LRR	x	-14.4	-19.7										
LR2	x	LR2	x	0.79	0.95										
NSM	-171.8	NSM	-0.5	-29.2	-91.1										
SMP	87	SMP	88	88	88										
04/06 to							06/07 to								
	06/07	04/10													
EPR	-25.9	-22.7													
LRR	x	-22.5													
LR2	x	0.98													
NSM	-28.7	-90.6													
SMP	88	88													
06/07 to							04/10								
	04/10														
EPR	-21.5														
LRR	x														
LR2	x														
NSM	-61.9														
SMP	88														
EPR: End Point Rate (m/yr), LRR: Linear Regression Rate (m/yr), LR2: R-Squared of LRR, NSM: Net Shoreline Movement (m), SMP: Sample size (total number of transects). (x) symbol indicates shoreline for year unavailable or a minimum of three shorelines necessary for a regression rate. (-) sign indicates retreat & a positive integer signals advance.															

Cell 4: Southern, Washover-Dominated, Open-Ocean Shoreline															
Comparison of Long-Term and Short-Term Shoreline Change Rate Statistics															
1852 to							07/98 to								
	1871	1910	1942	1962	1998	2010		05/99	05/00	10/00	04/02	05/05	04/06	06/07	04/10
EPR	16.8	0.7	-2.2	-5.9	-7.0	-7.5	EPR	-16.5	-12.7	-17.4	-7.8	-11.8	-10.4	-12.3	-14.6
LRR	x	-0.4	-3.6	-6.9	-8.3	-8.9	LRR	x	-12.5	-15.7	-8.4	-10.8	-10.3	-11.1	-13.2
WLR	x	x	-4.7	-7.8	-9.5	-10.8	WLR	x	x	x	x	x	x	x	x
LMS	x	0.7	-4.0	-9.6	-10.6	-11.1	LMS	x	-12.4	-15.2	-11.9	-11.2	-10.5	-11.2	-11.4
SMP	88	88	56	86	86	88	SMP	87	87	87	87	87	87	87	87
1871 to							05/99 to								
	1910	1942	1962	1998	2010		05/00	10/00	04/02	05/05	04/06	06/07	04/10		
EPR	-7.3	-9.0	-10.7	-10.7	-10.9	EPR	-10.3	-17.7	-5.6	-11.1	-9.6	-11.8	-14.4		
LRR	x	-9.0	-10.6	-11.0	-11.2	LRR	x	-16.0	-5.6	-10.2	-9.8	-10.9	-13.2		
WLR	x	-9.1	-11.1	-11.2	-11.9	WLR	x	x	x	x	x	x	x		
LMS	x	-9.0	-10.6	-11.6	-12.0	LMS	x	-16.9	-4.8	-10.9	-9.8	-10.8	-10.8		
SMP	88	56	86	86	88	SMP	88	88	88	88	88	88	88		
1910 to							05/00 to								
	1942	1962	1998	2010		10/00	04/02	05/05	04/06	06/07	04/10				
EPR	-9.8	-12.9	-12.0	-12.3	EPR	-39.3	-2.1	-11.2	-9.5	-12.1	-14.8				
LRR	x	-11.5	-12.1	-12.2	LRR	x	-0.5	-10.2	-9.6	-11.0	-13.6				
WLR	x	-12.3	-11.8	-12.2	WLR	x	x	x	x	x	x				
LMS	x	-12.6	-12.1	-12.3	LMS	x	-2.3	-10.6	-9.8	-10.6	-11.1				
SMP	56	86	86	88	SMP	88	88	88	88	88	88				
1942 to							10/00 to								
	1962	1998	2010		04/02	05/05	04/06	06/07	04/10						
EPR	-14.9	-11.4	-11.8	EPR	5.7	-9.0	-7.5	-10.6	-13.9						
LRR	x	-11.2	-11.3	LRR	x	-10.2	-9.5	-11.1	-14.2						
WLR	x	-10.9	-11.3	WLR	x	x		x	x						
LMS	x	-11.1	-11.2	LMS	x	-9.1	-10.1	-12.6	-14.4						
SMP	56	56	56	SMP	87	88	88	88	88						
1962 to							04/02 to								
	1998	2010		05/05	04/06	06/07	04/10								
EPR	-10.5	-11.5	EPR	-16.7	-12.8	-15.6	-17.8								
LRR	x	-11.3	LRR	x	-13.8	-14.8	-17.6								
WLR	x	-11.9	WLR	x	x	x	1.0								
LMS	x	-11.4	LMS	x	-13.4	-14.4	-14.6								
SMP	86	87	SMP	87	87	87	87								
1998 to							05/05 to								
	2010		04/06	06/07	04/10										
EPR	-14.6	EPR	-0.5	-14.1	-18.4										
LRR	x	LRR	x	-14.4	-19.7										
WLR	x	WLR	x	x	x										
LMS	x	LMS	x	-13.9	-19.3										
SMP	87	SMP	88	88	88										
EPR: End Point Rate (m/yr), LRR: Linear Regression Rate (m/yr), WLR: Weighted Linear Regression (m/yr), LMS: Least Median of Squares (m/yr), SMP: Sample size (total number of transects). (x) symbol indicates shoreline for year unavailable, or a minimum of three shorelines necessary for a regression rate, or shorelines have identical positional accuracies for WLR.															
04/06 to							06/07 to								
	06/07	04/10		06/07	04/10										
EPR	-25.9	-22.7	EPR	-25.9	-22.7										
LRR	x	-22.5	LRR	x	-22.5										
WLR	x	x	WLR	x	x										
LMS	x	-21.8	LMS	x	-21.8										
SMP	88	88	SMP	88	88										
06/07 to							04/10 to								
	04/10		04/10		04/10										
EPR	-21.5	EPR	-21.5												
LRR	x	LRR	x												
WLR	x	WLR	x												
LMS	x	LMS	x												
SMP	88	SMP	88												

Cell 4: Southern, Washover-Dominated, Open-Ocean Shoreline															
Linear Regression Statistics															
1852 to							07/98 to								
	1871	1910	1942	1962	1998	2010		05/99	05/00	10/00	04/02	05/05	04/06	06/07	04/10
LRR	x	-0.4	-3.6	-6.9	-8.3	-8.9	LRR	x	-12.5	-15.7	-8.4	-10.8	-10.3	-11.1	-13.2
LR2	x	0.32	0.28	0.62	0.78	0.84	LR2	x	0.89	0.87	0.59	0.87	0.91	0.94	0.94
LSE	x	249.6	278.4	252.9	236.2	227.0	LSE	x	4.1	6.0	10.6	10.7	9.9	10.2	14.7
LCI	x	75.9	17.2	10.0	5.5	4.2	LCI	x	39.7	15.0	11.8	5.4	3.5	2.8	3.0
SMP	x	88	56	86	86	88	SMP	x	87	87	87	87	87	87	87
1871 to							05/99 to								
	1910	1942	1962	1998	2010		05/00	10/00	04/02	05/05	04/06	06/07	04/10		
LRR	x	-9.0	-10.6	-11.0	-11.2	LRR	x	-16.0	-5.6	-10.2	-9.8	-10.9	-13.2		
LR2	x	0.97	0.95	0.97	0.98	LR2	x	0.77	0.4	0.83	0.88	0.91	0.92		
LSE	x	39.8	98.2	82.4	84.3	LSE	x	7.8	11.1	11.8	10.4	10.9	15.6		
LCI	x	10.0	13.6	3.2	2.8	LCI	x	93.7	25.4	8.1	4.6	3.6	3.7		
SMP	x	56	86	86	88	SMP	x	88	88	88	88	88	88		
1910 to							05/00 to								
	1942	1962	1998	2010		10/00	04/02	05/05	04/06	06/07	04/10				
LRR	x	-11.5	-12.1	-12.2	LRR	x	-0.5	-10.2	-9.6	-11.0	-13.6				
LR2	x	0.98	0.99	1.00	LR2	x	0.24	0.80	0.86	0.89	0.91				
LSE	x	50.7	43.1	35.6	LSE	x	10.6	13.5	11.3	11.7	16.3				
LCI	x	17.2	5.2	1.7	LCI	x	93.9	15.4	6.7	4.9	4.7				
SMP	x	86	86	88	SMP	x	88	88	88	88	88				
1942 to							10/00 to								
	1962	1998	2010		04/02	05/05	04/06	06/07	04/10						
LRR	x	-11.2	-11.3	LRR	x	-10.2	-9.5	-11.1	-14.2						
LR2	x	0.98	0.99	LR2	x	0.76	0.83	0.87	0.90						
LSE	x	55.4	40.5	LSE	x	18.5	13.2	13.2	17.6						
LCI	x	17.5	3.2	LCI	x	70.9	12.8	7.6	6.3						
SMP	x	56	56	SMP	x	88	88	88	88						
1962 to							04/02 to								
	1998	2010		05/05	04/06	06/07	04/10								
LRR	x	-11.3	LRR	x	-13.8	-14.8	-17.6								
LR2	x	0.99	LR2	x	0.95	0.96	0.96								
LSE	x	28.9	LSE	x	9.3	8.2	11.1								
LCI	x	10.4	LCI	x	39.9	9.2	6.1								
SMP	x	87	SMP	x	87	87	87								
1998 to							05/05 to								
	2010		04/06	06/07	04/10										
LRR	x	LRR	x	-14.4	-19.7										
LR2	x	LR2	x	0.79	0.95										
LSE	x	LSE	x	10.7	10.9										
LCI	x	LCI	x	92.6	12.7										
SMP	x	SMP	x	88	88										
04/06 to							06/07 to								
					06/07	04/10									
LRR					x	-22.5									
LR2					x	0.98									
LSE					x	4.2									
LCI					x	18.5									
SMP					x	88									
06/07 to							04/10 to								
						04/10									
LRR						x									
LR2						x									
LSE						x									
LCI						x									
SMP						x									
LRR: Linear Regression Rate (m/yr), LR2: R-squared of LRR															
LSE: Standard Error of LRR, LCI: Confidence Interval 95%of LRR															
SMP: Sample size (total number of transects).															
(x) symbol indicates shoreline for year unavailable or a minimum															
of three shorelines necessary for a regression rate.															
(-) sign indicates retreat & a positive integer signals advance.															

Cell 4: Southern, Washover-Dominated, Open-Ocean Shoreline															
Weighted Linear Regression Statistics															
1852 to							07/98 to								
	1871	1910	1942	1962	1998	2010		05/99	05/00	10/00	04/02	05/05	04/06	06/07	04/10
WLR	x	x	-4.7	-7.8	-9.5	-10.8	WLR	x	x	x	x	x	x	x	x
WR2	x	x	0.46	0.74	0.92	0.94	WR2	x	x	x	x	x	x	x	x
WSE	x	x	14.5	13.9	13.6	0.9	WSE	x	x	x	x	x	x	x	x
WCI	x	x	13.2	8.2	3.7	3.0	WCI	x	x	x	x	x	x	x	x
SMP	x	x	56	86	86	88	SMP	x	x	x	x	x	x	x	x
1871 to							05/99 to								
	1910	1942	1962	1998	2010			05/00	10/00	04/02	05/05	04/06	06/07	04/10	
WLR		x	-9.1	-11.1	-11.2	-11.9	WLR		x	x	x	x	x	x	x
WR2		x	0.98	0.96	0.99	0.99	WR2		x	x	x	x	x	x	x
WSE		x	2.2	6.3	5.5	7.4	WSE		x	x	x	x	x	x	x
WCI		x	8.3	11.8	2.4	2.2	WCI		x	x	x	x	x	x	x
SMP		x	56	86	86	88	SMP		x	x	x	x	x	x	x
1910 to							05/00 to								
		1942	1962	1998	2010				10/00	04/02	05/05	04/06	06/07	04/10	
WLR			x	-12.3	-11.8	-12.2	WLR			x	x	x	x	x	x
WR2			x	0.97	0.99	1.00	WR2			x	x	x	x	x	x
WSE			x	4.5	4.3	5.1	WSE			x	x	x	x	x	x
WCI			x	23.3	5.4	1.8	WCI			x	x	x	x	x	x
SMP			x	86	86	88	SMP			x	x	x	x	x	x
1942 to							10/00 to								
			1962	1998	2010					04/02	05/05	04/06	06/07	04/10	
WLR				x	-10.9	-11.3	WLR				x	x	x	x	x
WR2				x	0.99	0.99	WR2				x	x	x	x	x
WSE				x	5.7	5.3	WSE				x	x	x	x	x
WCI				x	12.5	3.1	WCI				x	x	x	x	x
SMP				x	56	56	SMP				x	x	x	x	x
1962 to							04/02 to								
				1998	2010						05/05	04/06	06/07	04/10	
WLR					x	-11.9	WLR					x	x	x	x
WR2					x	0.98	WR2					x	x	x	x
WSE					x	6.6	WSE					x	x	x	x
WCI					x	18.5	WCI					x	x	x	x
SMP					x	87	SMP					x	x	x	x
1998 to							05/05 to								
					2010							04/06	06/07	04/10	
WLR						x	WLR						x	x	x
WR2						x	WR2						x	x	x
WSE						x	WSE						x	x	x
WCI						x	WCI						x	x	x
SMP						x	SMP						x	x	x
WLR: Weighted Linear Regression (m/yr), WR2: R-squared of WLR							04/06 to								
WSE: Standard Error of WLR, WCI: Confidence Interval 95%													06/07	04/10	
of WLR, SMP: Sample size (total number of transects).							WLR							x	x
(x) symbol indicates shoreline for year unavailable, or a minimum							WR2							x	x
of three shorelines necessary for a regression rate, or							WSE							x	x
shorelines have identical positional accuracies for WLR.							WCI							x	x
(-) sign indicates retreat & a positive integer signals advance.							SMP							x	x
							04/06 to								
															04/10
WLR							WLR								x
WR2							WR2								x
WSE							WSE								x
WCI							WCI								x
SMP							SMP								x

Cell 5: Southern Spit Shoreline															
Long-Term and Short-Term Rates of Shoreline Change and Net Shoreline Movement															
1852 to							07/98 to								
	1871	1910	1942	1962	1998	2010		05/99	05/00	10/00	04/02	05/05	04/06	06/07	04/10
EPR	11.4	19.6	x	x	x	-2.9	EPR	x	x	x	x	x	x	x	x
LRR	x	20.2	x	x	x	-3.7	LRR	x	x	x	x	x	x	x	x
LR2	x	0.97	x	x	x	0.17	LR2	x	x	x	x	x	x	x	x
NSM	220.6	1137.8	x	x	x	-463.1	NSM	x	x	x	x	x	x	x	x
SMP	11	11	x	x	x	11	SMP	x	x	x	x	x	x	x	x
1871 to							05/99 to								
	1910	1942	1962	1998	2010			05/00	10/00	04/02	05/05	04/06	06/07	04/10	
EPR		30.7	x	x	x	-3.2	EPR		x	x	x	x	x	x	x
LRR		x	x	x	x	-5.8	LRR		x	x	x	x	x	x	x
LR2		x	x	x	x	0.27	LR2		x	x	x	x	x	x	x
NSM		1187.4	x	x	x	-444.5	NSM		x	x	x	x	x	x	x
SMP		25	x	x	x	25	SMP		x	x	x	x	x	x	x
1910 to							05/00 to								
	1942	1962	1998	2010					10/00	04/02	05/05	04/06	06/07	04/10	
EPR			x	x	x	-16.3	EPR			x	x	x	x	x	x
LRR			x	x	x	x	LRR			x	x	x	x	x	x
LR2			x	x	x	x	LR2			x	x	x	x	x	x
NSM			x	x	x	-1631.9	NSM			x	x	x	x	x	x
SMP			x	x	x	25	SMP			x	x	x	x	x	x
1942 to							10/00 to								
	1962	1998	2010							04/02	05/05	04/06	06/07	04/10	
EPR				x	x	x	EPR				x	x	x	x	x
LRR				x	x	x	LRR				x	x	x	x	x
LR2				x	x	x	LR2				x	x	x	x	x
NSM				x	x	x	NSM				x	x	x	x	x
SMP				x	x	x	SMP				x	x	x	x	x
1962 to							04/02 to								
	1998	2010									05/05	04/06	06/07	04/10	
EPR				x	x		EPR				x	x	x	x	x
LRR				x	x		LRR				x	x	x	x	x
LR2				x	x		LR2				x	x	x	x	x
NSM				x	x		NSM				x	x	x	x	x
SMP				x	x		SMP				x	x	x	x	x
1998 to							05/05 to								
	2010											04/06	06/07	04/10	
EPR						x	EPR					-10.3	-35.9	-17.5	
LRR						x	LRR					x	-36.5	-18.2	
LR2						x	LR2					x	0.88	0.74	
NSM						x	NSM					-9.9	-74.4	-86.4	
SMP						x	SMP					7	7	7	
							04/06 to								
													06/07	04/10	
EPR: End Point Rate (m/yr), LRR: Linear Regression Rate (m/yr),							EPR						-79.3	-32.9	
LR2: R-Squared of LRR, NSM : Net Shoreline Movement (m),							LRR						x	-29.3	
SMP: Sample size (total number of transects).							LR2						x	0.78	
(x) symbol indicates shoreline for year unavailable or a minimum							NSM						-88.0	-131.1	
of three shorelines necessary for a regression rate.							SMP						26	26	
(-) sign indicates retreat & a positive integer signals advance.															
							06/07 to								
														04/10	
EPR							EPR							-14.2	
LRR							LRR							x	
LR2							LR2							x	
NSM							NSM							-41.0	
SMP							SMP							27	

Cell 5: Southern Spit Shoreline																					
Comparison of Long-Term and Short-Term Shoreline Change Rate Statistics																					
		1852 to								07/98 to											
		1871	1910	1942	1962	1998	2010			05/99	05/00	10/00	04/02	05/05	04/06	06/07	04/10				
EPR		11.4	19.6	x	x	x	-2.9	EPR		x	x	x	x	x	x	x	x				
LRR		x	20.2	x	x	x	-3.7	LRR		x	x	x	x	x	x	x	x				
WLR		x	x	x	x	x	-9.9	WLR		x	x	x	x	x	x	x	x				
LMS		x	19.9	x	x	x	-4.9	LMS		x	x	x	x	x	x	x	x				
SMP		11	11	x	x	x	11	SMP		x	x	x	x	x	x	x	x				
		1871 to								05/99 to											
		1910	1942	1962	1998	2010			05/00	10/00	04/02	05/05	04/06	06/07	04/10						
EPR			30.7	x	x	x	-3.2	EPR		x	x	x	x	x	x	x	x				
LRR			x	x	x	x	-5.8	LRR		x	x	x	x	x	x	x	x				
WLR			x	x	x	x	-12.4	WLR		x	x	x	x	x	x	x	x				
LMS			x	x	x	x	-3.3	LMS		x	x	x	x	x	x	x	x				
SMP			25	x	x	x	25	SMP		x	x	x	x	x	x	x	x				
		1910 to								05/00 to											
				1942	1962	1998	2010				10/00	04/02	05/05	04/06	06/07	04/10					
EPR				x	x	x	-16.3	EPR			x	x	x	x	x	x	x	x			
LRR				x	x	x	x	LRR			x	x	x	x	x	x	x				
WLR				x	x	x	x	WLR			x	x	x	x	x	x	x				
LMS				x	x	x	x	LMS			x	x	x	x	x	x	x				
SMP				x	x	x	25	SMP			x	x	x	x	x	x	x				
		1942 to								10/00 to											
					1962	1998	2010					04/02	05/05	04/06	06/07	04/10					
EPR					x	x	x	EPR				x	x	x	x	x	x	x			
LRR					x	x	x	LRR				x	x	x	x	x	x	x			
WLR					x	x	x	WLR				x	x	x	x	x	x	x			
LMS					x	x	x	LMS				x	x	x	x	x	x	x			
SMP					x	x	x	SMP				x	x	x	x	x	x	x			
		1962 to								04/02 to											
						1998	2010						05/05	04/06	06/07	04/10					
EPR						x	x	EPR					x	x	x	x	x	x			
LRR						x	x	LRR					x	x	x	x	x	x			
WLR						x	x	WLR					x	x	x	x	x	x			
LMS						x	x	LMS					x	x	x	x	x	x			
SMP						x	x	SMP					x	x	x	x	x	x			
		1998 to								05/05 to											
							2010							04/06	06/07	04/10					
EPR							x	EPR						-10.3	-35.9	-17.5					
LRR							x	LRR						x	-36.5	-18.2					
WLR							x	WLR						x	x	x					
LMS							x	LMS						x	-30.3	-17.8					
SMP							x	SMP						7	7	7					
										04/06 to											
															06/07	04/10					
EPR: End Point Rate (m/yr), LRR: Linear Regression Rate (m/yr),								EPR								-79.3	-32.9				
WLR: Weighted Linear Regression (m/yr), LMS: Least Median								LRR								x	-29.3				
of Squares (m/yr), SMP: Sample size (total number of transects).								WLR								x	x				
(x) symbol indicates shoreline for year unavailable, or a minimum								LMS								x	-29.0				
of three shorelines necessary for a regression rate, or								SMP								26	26				
shorelines have identical positional accuracies for WLR.																					
										06/07 to											
																04/10					
								EPR									-14.2				
								LRR									x				
								WLR									x				
								LMS									x				
								SMP									27				

Cell 5: Southern Spit Shoreline															
Linear Regression Statistics															
1852 to							07/98 to								
	1871	1910	1942	1962	1998	2010		05/99	05/00	10/00	04/02	05/05	04/06	06/07	04/10
LRR	x	20.2	x	x	x	-3.7	LRR	x	x	x	x	x	x	x	x
LR2	x	0.97	x	x	x	0.17	LR2	x	x	x	x	x	x	x	x
LSE	x	128.9	x	x	x	759.5	LSE	x	x	x	x	x	x	x	x
LCI	x	39.2	x	x	x	26.8	LCI	x	x	x	x	x	x	x	x
SMP	x	11	x	x	x	11	SMP	x	x	x	x	x	x	x	x
1871 to							05/99 to								
	1910	1942	1962	1998	2010		05/00	10/00	04/02	05/05	04/06	06/07	04/10		
LRR	x	x	x	x	-5.8	LRR	x	x	x	x	x	x	x		
LR2	x	x	x	x	0.27	LR2	x	x	x	x	x	x	x		
LSE	x	x	x	x	1037.0	LSE	x	x	x	x	x	x	x		
LCI	x	x	x	x	129.9	LCI	x	x	x	x	x	x	x		
SMP	x	x	x	x	1	SMP	x	x	x	x	x	x	x		
1910 to							05/00 to								
	1942	1962	1998	2010		10/00	04/02	05/05	04/06	06/07	04/10				
LRR	x	x	x	x	LRR	x	x	x	x	x	x				
LR2	x	x	x	x	LR2	x	x	x	x	x	x				
LSE	x	x	x	x	LSE	x	x	x	x	x	x				
LCI	x	x	x	x	LCI	x	x	x	x	x	x				
SMP	x	x	x	x	SMP	x	x	x	x	x	x				
1942 to							10/00 to								
	1962	1998	2010		04/02	05/05	04/06	06/07	04/10						
LRR	x	x	x	LRR	x	x	x	x	x						
LR2	x	x	x	LR2	x	x	x	x	x						
LSE	x	x	x	LSE	x	x	x	x	x						
LCI	x	x	x	LCI	x	x	x	x	x						
SMP	x	x	x	SMP	x	x	x	x	x						
1962 to							04/02 to								
	1998	2010		05/05	04/06	06/07	04/10								
LRR	x	x	LRR	x	x	x	x								
LR2	x	x	LR2	x	x	x	x								
LSE	x	x	LSE	x	x	x	x								
LCI	x	x	LCI	x	x	x	x								
SMP	x	x	SMP	x	x	x	x								
1998 to							05/05 to								
	2010		04/06	06/07	04/10										
LRR	x	LRR	x	-36.5	-18.2										
LR2	x	LR2	x	0.88	0.74										
LSE	x	LSE	x	20.1	25.2										
LCI	x	LCI	x	174.3	29.2										
SMP	x	SMP	x	7	7										
04/06 to							06/07 to								
	06/07	04/10													
LRR	x	-29.3	LRR	x	0.78										
LR2	x	40.8	LR2	x	178.0										
LSE	x	26	LSE												
LCI			LCI												
SMP			SMP												
06/07 to							04/10								
LRR	x	LRR													
LR2	x	LR2													
LSE	x	LSE													
LCI	x	LCI													
SMP	x	SMP													
LRR: Linear Regression Rate (m/yr), LR2: R-squared of LRR															
LSE: Standard Error of LRR, LCI: Confidence Interval 95%of LRR															
SMP: Sample size (total number of transects).															
(x) symbol indicates shoreline for year unavailable or a minimum of three shorelines necessary for a regression rate.															
(-) sign indicates retreat & a positive integer signals advance.															

Cell 5: Southern Spit Shoreline															
Weighted Linear Regression Statistics															
1852 to							07/98 to								
	1871	1910	1942	1962	1998	2010		05/99	05/00	10/00	04/02	05/05	04/06	06/07	04/10
WLR	x	x	x	x	x	-9.9	WLR	x	x	x	x	x	x	x	x
WR2	x	x	x	x	x	0.68	WR2	x	x	x	x	x	x	x	x
WSE	x	x	x	x	x	66.0	WSE	x	x	x	x	x	x	x	x
WCI	x	x	x	x	x	20.8	WCI	x	x	x	x	x	x	x	x
SMP	x	x	x	x	x	11	SMP	x	x	x	x	x	x	x	x
1871 to							05/99 to								
	1910	1942	1962	1998	2010			05/00	10/00	04/02	05/05	04/06	06/07	04/10	
WLR		x	x	x	x	-12.4	WLR		x	x	x	x	x	x	x
WR2		x	x	x	x	0.78	WR2		x	x	x	x	x	x	x
WSE		x	x	x	x	76.9	WSE		x	x	x	x	x	x	x
WCI		x	x	x	x	82.6	WCI		x	x	x	x	x	x	x
SMP		x	x	x	x	25	SMP		x	x	x	x	x	x	x
1910 to							05/00 to								
		1942	1962	1998	2010				10/00	04/02	05/05	04/06	06/07	04/10	
WLR			x	x	x	x	WLR			x	x	x	x	x	x
WR2			x	x	x	x	WR2			x	x	x	x	x	x
WSE			x	x	x	x	WSE			x	x	x	x	x	x
WCI			x	x	x	x	WCI			x	x	x	x	x	x
SMP			x	x	x	x	SMP			x	x	x	x	x	x
1942 to							10/00 to								
			1962	1998	2010					04/02	05/05	04/06	06/07	04/10	
WLR				x	x	x	WLR				x	x	x	x	x
WR2				x	x	x	WR2				x	x	x	x	x
WSE				x	x	x	WSE				x	x	x	x	x
WCI				x	x	x	WCI				x	x	x	x	x
SMP				x	x	x	SMP				x	x	x	x	x
1962 to							04/02 to								
				1998	2010						05/05	04/06	06/07	04/10	
WLR					x	x	WLR					x	x	x	x
WR2					x	x	WR2					x	x	x	x
WSE					x	x	WSE					x	x	x	x
WCI					x	x	WCI					x	x	x	x
SMP					x	x	SMP					x	x	x	x
1998 to							05/05 to								
					2010							04/06	06/07	04/10	
WLR						x	WLR						x	x	x
WR2						x	WR2						x	x	x
WSE						x	WSE						x	x	x
WCI						x	WCI						x	x	x
SMP						x	SMP						x	x	x
WLR: Weighted Linear Regression (m/yr), WR2: R-squared of WLR							04/06 to								
WSE: Standard Error of WLR, WCI: Confidence Interval 95%													06/07	04/10	
of WLR, SMP: Sample size (total number of transects).							WLR							x	x
(x) symbol indicates shoreline for year unavailable, or a minimum							WR2							x	x
of three shorelines necessary for a regression rate, or							WSE							x	x
shorelines have identical positional accuracies for WLR.							WCI							x	x
(-) sign indicates retreat & a positive integer signals advance.							SMP							x	x
04/06 to							04/06 to								
															04/10
WLR							WLR								x
WR2							WR2								x
WSE							WSE								x
WCI							WCI								x
SMP							SMP								x



## **APPENDIX B: CEDAR ISLAND SHORELINE RESULTS**

Appendix B (24 pages): Cedar Island shoreline results by shoreline cell and long term (1852-2007) and short term (2007-2010) time periods using various statistical measurements. Individual pages by shoreline cell for the following: 1) long-term and short-term rates of shoreline change and net shoreline movement, 2) comparison of long-term and short-term shoreline change rate statistics, 3) linear regression statistics, and 4) weighted linear regression statistics. The long-term and short-term categories are further subdivided by progressively more modern and shorter timeframes within the categories. The individual temporal timeframes within the categories are also segmented and analyzed by the data points contained within the timeframes. A total of four appendix pages exist for each shoreline cell in Appendices B.

Cell 0: Metompkin Inlet-Influenced Shoreline												
Long-Term and Short-Term Rates of Shoreline Change and Net Shoreline Movement												
1852 to								06/2007 to				
	1871	1910	1933	1942	1962	2007	2010		05/08	04/09	04/10	
EPR	x	-3.0	x	x	-2.8	x	-1.2	EPR	x	x	x	
LRR	x	x	x	x	-2.8	x	-1.4	LRR	x	x	x	
LR2	x	x	x	x	0.99	x	0.57	LR2	x	x	x	
NSM	x	-173.2	x	x	-312.8	x	-189.5	NSM	x	x	x	
SMP	x	14	x	x	14	x	14	SMP	x	x	x	
1871 to								05/2008 to				
		1910	1933	1942	1962	2007	2010			04/09	04/10	
EPR		x	x	x	x	x	x	EPR		x	x	
LRR		x	x	x	x	x	x	LRR		x	x	
LR2		x	x	x	x	x	x	LR2		x	x	
NSM		x	x	x	x	x	x	NSM		x	x	
SMP		x	x	x	x	x	x	SMP		x	x	
1910 to								04/2009 to				
			1933	1942	1962	2007	2010				04/10	
EPR			x	x	-2.7	x	-0.2	EPR			x	
LRR			x	x	x	x	-0.2	LRR			x	
LR2			x	x	x	x	0.17	LR2			x	
NSM			x	x	-139.6	x	-16.4	NSM			x	
SMP			x	x	14	x	14	SMP			x	
1933 to												
				1942	1962	2007	2010					
EPR				x	x	x	x					
LRR				x	x	x	x					
LR2				x	x	x	x					
NSM				x	x	x	x					
SMP				x	x	x	x					
1942 to												
					1962	2007	2010					
EPR					x	x	x					
LRR					x	x	x					
LR2					x	x	x					
NSM					x	x	x					
SMP					x	x	x					
1962 to												
						2007	2010					
EPR						x	2.6					
LRR						x	x					
LR2						x	x					
NSM						x	123.3					
SMP						x	14					
EPR: End Point Rate (m/yr), LRR: Linear Regression Rate (m/yr), LR2: R-Squared of LRR,												
NSM: Net Shoreline Movement (m), and SMP: Sample size (total number of transects).												
(x) symbol indicates shoreline for year unavailable or a minimum of three shorelines necessary for a regression rate.												
(-) sign indicates retreat & a positive integer signals advance.												

Cell 0: Metompkin Inlet-Influenced Shoreline												
Comparison of Long-Term and Short-Term Shoreline Change Rate Statistics												
1852 to								06/2007 to				
	1871	1910	1933	1942	1962	2007	2010		05/08	04/09	04/10	
EPR	x	-3.0	x	x	-2.8	x	-1.2	EPR	x	x	x	
LRR	x	x	x	x	-2.8	x	-1.4	LRR	x	x	x	
WLR	x	x	x	x	-2.8	x	-0.2	WLR	x	x	x	
LMS	x	x	x	x	-2.8	x	-1.6	LMS	x	x	x	
SMP	x	14	x	x	14	x	14	SMP	x	x	x	
1871 to								05/2008 to				
		1910	1933	1942	1962	2007	2010			04/09	04/10	
EPR		x	x	x	x	x	x	EPR		x	x	
LRR		x	x	x	x	x	x	LRR		x	x	
WLR		x	x	x	x	x	x	WLR		x	x	
LMS		x	x	x	x	x	x	LMS		x	x	
SMP		x	x	x	x	x	x	SMP		x	x	
1910 to								04/2009 to				
			1933	1942	1962	2007	2010				04/10	
EPR			x	x	-2.7	x	-0.2	EPR			x	
LRR			x	x	x	x	-0.2	LRR			x	
WLR			x	x	x	x	1.2	WLR			x	
LMS			x	x	x	x	-0.2	LMS			x	
SMP			x	x	14	x	14	SMP			x	
1933 to												
				1942	1962	2007	2010					
EPR				x	x	x	x					
LRR				x	x	x	x					
WLR				x	x	x	x					
LMS				x	x	x	x					
SMP				x	x	x	x					
1942 to												
					1962	2007	2010					
EPR					x	x	x					
LRR					x	x	x					
WLR					x	x	x					
LMS					x	x	x					
SMP					x	x	x					
1962 to												
						2007	2010					
EPR						x	2.6					
LRR						x	x					
WLR						x	x					
LMS						x	x					
SMP						x	14					
EPR: End Point Rate (m/yr), LRR: Linear Regression Rate (m/yr), WLR: Weighted Linear Regression (m/yr),												
LMS: Least Median of Squares (m/yr), SMP: Sample size (total number of transects).												
(x) symbol indicates shoreline for year unavailable, or a minimum of three shorelines necessary for a regression rate, or shorelines have identical positional accuracies for WLR. (-) sign indicates retreat & a positive integer signals advance.												

Cell 0: Metompkin Inlet-Influenced Shoreline												
Linear Regression Statistics												
1852 to								06/2007 to				
	1871	1910	1933	1942	1962	2007	2010		05/08	04/09	04/10	
LRR	x	x	x	x	-2.8	x	-1.4	LRR	x	x	x	
LR2	x	x	x	x	0.99	x	0.57	LR2	x	x	x	
LSE	x	x	x	x	18.0	x	107.3	LSE	x	x	x	
LCI	x	x	x	x	2.9	x	3.9	LCI	x	x	x	
SMP	x	x	x	x	14	x	14	SMP	x	x	x	
1871 to								05/2008 to				
		1910	1933	1942	1962	2007	2010			04/09	04/10	
LRR		x	x	x	x	x	x	LRR		x	x	
LR2		x	x	x	x	x	x	LR2		x	x	
LSE		x	x	x	x	x	x	LSE		x	x	
LCI		x	x	x	x	x	x	LCI		x	x	
SMP		x	x	x	x	x	x	SMP		x	x	
1910 to								05/2008 to				
			1933	1942	1962	2007	2010				04/10	
LRR			x	x	x	x	-0.2	LRR			x	
LR2			x	x	x	x	0.17	LR2			x	
LSE			x	x	x	x	107.0	LSE			x	
LCI			x	x	x	x	19.2	LCI			x	
SMP			x	x	x	x	14	SMP			x	
1933 to												
				1942	1962	2007	2010					
LRR				x	x	x	x					
LR2				x	x	x	x					
LSE				x	x	x	x					
LCI				x	x	x	x					
SMP				x	x	x	x					
1942 to												
					1962	2007	2010					
LRR					x	x	x					
LR2					x	x	x					
LSE					x	x	x					
LCI					x	x	x					
SMP					x	x	x					
1962 to												
						2007	2010					
LRR						x	x					
LR2						x	x					
LSE						x	x					
LCI						x	x					
SMP						x	x					
LRR: Linear Regression Rate (m/yr), LR2: R-squared of LRR, LSE: Standard Error of LRR,												
LCI: Confidence Interval 95% of LRR , SMP : Sample size (total number of transects).												
(x) symbol indicates shoreline for year unavailable or a minimum of three shorelines necessary for a regression rate.												
(-) sign indicates retreat & a positive integer signals advance.												

Cell 0: Metompkin Inlet-Influenced Shoreline												
Weighted Linear Regression Statistics												
1852 to								06/2007 to				
	1871	1910	1933	1942	1962	2007	2010		05/08	04/09	04/10	
WLR	x	x	x	x	-2.8	x	-0.2	WLR	x	x	x	
WR2	x	x	x	x	0.99	x	0.15	WR2	x	x	x	
WSE	x	x	x	x	1.0	x	11.4	WSE	x	x	x	
WCI	x	x	x	x	2.4	x	5.0	WCI	x	x	x	
SMP	x	x	x	x	14	x	14	SMP	x	x	x	
1871 to								05/2008 to				
		1910	1933	1942	1962	2007	2010			04/09	04/10	
WLR		x	x	x	x	x	x	WLR		x	x	
WR2		x	x	x	x	x	x	WR2		x	x	
WSE		x	x	x	x	x	x	WSE		x	x	
WCI		x	x	x	x	x	x	WCI		x	x	
SMP		x	x	x	x	x	x	SMP		x	x	
1910 to								04/2009 to				
			1933	1942	1962	2007	2010				04/10	
WLR			x	x	x	x	1.2	WLR			x	
WR2			x	x	x	x	0.36	WR2			x	
WSE			x	x	x	x	9.9	WSE			x	
WCI			x	x	x	x	18.8	WCI			x	
SMP			x	x	x	x	14	SMP			x	
1933 to												
				1942	1962	2007	2010					
WLR				x	x	x	x					
WR2				x	x	x	x					
WSE				x	x	x	x					
WCI				x	x	x	x					
SMP				x	x	x	x					
1942 to												
					1962	2007	2010					
WLR					x	x	x					
WR2					x	x	x					
WSE					x	x	x					
WCI					x	x	x					
SMP					x	x	x					
1962 to												
						2007	2010					
WLR						x	x					
WR2						x	x					
WSE						x	x					
WCI						x	x					
SMP						x	x					
WLR: Weighted Linear Regression (m/yr), WR2: R-squared of WLR, WSE: Standard Error of WLR,												
WCI: Confidence Interval 95% of WLR, SMP: Sample size (total number of transects).												
(x) symbol indicates shoreline for year unavailable, or a minimum of three shorelines necessary for a regression rate, or shorelines have identical positional accuracies for WLR. (-) sign indicates retreat & a positive integer signals advance.												

Cell 1: Coast Guard Breach Shoreline												
Long-Term and Short-Term Rates of Shoreline Change and Net Shoreline Movement												
1852 to								06/2007 to				
	1871	1910	1933	1942	1962	2007	2010		05/08	04/09	04/10	
EPR	x	-2.4	-1.3	-0.9	-0.6	-1.0	-1.0	EPR	-21.3	6.4	4.7	
LRR	x	x	-1.5	-1.1	-0.7	-0.9	-0.9	LRR	x	6.6	7.6	
LR2	x	x	0.72	0.79	0.51	0.71	0.75	LR2	x	0.16	0.39	
NSM	x	-140.3	-102.3	-81.0	-63.0	-158.6	-154.7	NSM	-19.5	12.0	13.5	
SMP	x	1	1	4	4	4	4	SMP	6	6	6	
1871 to								05/2008 to				
		1910	1933	1942	1962	2007	2010			04/09	04/10	
EPR		x	x	x	x	x	x	EPR		27.8	16.8	
LRR		x	x	x	x	x	x	LRR		x	16.7	
LR2		x	x	x	x	x	x	LR2		x	0.75	
NSM		x	x	x	x	x	x	NSM		27.0	33.0	
SMP		x	x	x	x	x	x	SMP		7	6	
1910 to								04/2009 to				
			1933	1942	1962	2007	2010				04/10	
EPR			1.6	2.4	1.3	-0.4	-0.7	EPR			2.0	
LRR			x	2.2	1.4	-0.5	-0.9	LRR			x	
LR2			x	0.92	0.77	0.13	0.38	LR2			x	
NSM			38.0	78.0	68.2	-34.5	-65.5	NSM			2.0	
SMP			1	1	1	1	1	SMP			7	
1933 to												
				1942	1962	2007	2010					
EPR				1.9	1.0	-0.4	-0.3					
LRR				x	0.9	-0.6	-0.6					
LR2				x	0.81	0.60	0.42					
NSM				16.4	28.3	-36.6	-26.1					
SMP				7	7	7	7					
1942 to												
					1962	2007	2010					
EPR					0.6	-0.8	-0.6					
LRR					x	-1.1	-0.9					
LR2					x	0.77	0.54					
NSM					12.2	-53.0	-42.6					
SMP					8	7	7					
1962 to												
						2007	2010					
EPR						-1.7	-1.3					
LRR						x	-1.5					
LR2						x	0.68					
NSM						-64.9	-62.2					
SMP						7	6					
EPR: End Point Rate (m/yr), LRR: Linear Regression Rate (m/yr), LR2: R-Squared of LRR,												
NSM : Net Shoreline Movement (m), and SMP : Sample size (total number of transects).												
(x) symbol indicates shoreline for year unavailable or a minimum of three shorelines necessary for a regression rate.												
(-) sign indicates retreat & a positive integer signals advance.												

Cell 1: Coast Guard Breach Shoreline												
Comparison of Long-Term and Short-Term Shoreline Change Rate Statistics												
1852 to								06/2007 to				
	1871	1910	1933	1942	1962	2007	2010		05/08	04/09	04/10	
EPR	x	-2.4	-1.3	-0.9	-0.6	-1.0	-1.0	EPR	-21.3	6.4	4.7	
LRR	x	x	-1.5	-1.1	-0.7	-0.9	-0.9	LRR	x	6.6	7.6	
WLR	x	x	x	0.8	-0.5	-1.1	-1.1	WLR	x	x	x	
LMS	x	-2.5	-1.3	-81.0	-0.2	-1.0	-1.0	LMS	x	6.3	10.1	
SMP	x	1	1	4	4	4	4	SMP	6	6	6	
1871 to								05/2008 to				
		1910	1933	1942	1962	2007	2010			04/09	04/10	
EPR		x	x	x	x	x	x	EPR		27.8	16.8	
LRR		x	x	x	x	x	x	LRR		x	16.7	
WLR		x	x	x	x	x	x	WLR		x	x	
LMS		x	x	x	x	x	x	LMS		x	x	
SMP		x	x	x	x	x	x	SMP		7	6	
1910 to								04/2009 to				
			1933	1942	1962	2007	2010				04/10	
EPR			1.6	2.4	1.3	-0.4	-0.7	EPR			2.0	
LRR			x	2.2	1.4	-0.5	-0.9	LRR			x	
WLR			x	2.5	1.0	-1.4	-1.7	WLR			x	
LMS			x	2.4	1.6	1.3	-1.7	LMS			x	
SMP			1	1	1	1	1	SMP			7	
1933 to												
				1942	1962	2007	2010					
EPR				1.9	1.0	-0.4	-0.3					
LRR				x	0.9	-0.6	-0.6					
WLR				x	0.8	-0.9	-0.8					
LMS				x	1.0	-0.6	-0.6					
SMP				7	7	7	7					
1942 to												
					1962	2007	2010					
EPR					0.6	-0.8	-0.6					
LRR					x	-1.1	-0.9					
WLR					x	-1.2	-0.9					
LMS					x	-0.8	-0.9					
SMP					8	7	7					
1962 to												
						2007	2010					
EPR						-1.7	-1.3					
LRR						x	-1.5					
WLR						x	-1.4					
LMS						x	-1.3					
SMP						7	6					
EPR: End Point Rate (m/yr), LRR: Linear Regression Rate (m/yr), WLR: Weighted Linear Regression (m/yr),												
LMS: Least Median of Squares (m/yr), SMP: Sample size (total number of transects).												
(x) symbol indicates shoreline for year unavailable, or a minimum of three shorelines necessary for a regression rate, or shorelines have identical positional accuracies for WLR. (-) sign indicates retreat & a positive integer signals advance.												

Cell 1: Coast Guard Breach Shoreline												
Linear Regression Statistics												
1852 to								06/2007 to				
	1871	1910	1933	1942	1962	2007	2010		05/08	04/09	04/10	
LRR	x	x	-1.5	-1.1	-0.7	-0.9	-0.9	LRR	x	6.6	7.6	
LR2	x	x	0.72	0.79	0.51	0.71	0.75	LR2	x	0.16	0.39	
LSE	x	x	53.9	30.6	40.7	35.8	33.4	LSE	x	20.6	17.1	
LCI	x	x	11.5	3.8	1.9	1.0	0.7	LCI	x	197.0	34.3	
SMP	x	x	1	4	4	4	4	SMP	x	6	6	
1871 to								05/2008 to				
		1910	1933	1942	1962	2007	2010			04/09	04/10	
LRR		x	x	x	x	x	x	LRR		x	16.7	
LR2		x	x	x	x	x	x	LR2		x	0.75	
LSE		x	x	x	x	x	x	LSE		x	12.4	
LCI		x	x	x	x	x	x	LCI		x	113.2	
SMP		x	x	x	x	x	x	SMP		x	6	
1910 to								04/2009 to				
			1933	1942	1962	2007	2010				04/10	
LRR			x	2.2	1.4	-0.5	-0.9	LRR			x	
LR2			x	0.92	0.77	0.13	0.38	LR2			x	
LSE			x	15.3	20.6	50.7	50.4	LSE			x	
LCI			x	8.2	2.4	2.2	1.5	LCI			x	
SMP			x	1	1	1	1	SMP			x	
1933 to												
				1942	1962	2007	2010					
LRR				x	0.9	-0.6	-0.6					
LR2				x	0.81	0.60	0.42					
LSE				x	8.8	25.4	24.5					
LCI				x	5.4	2.4	1.1					
SMP				x	7	7	7					
1942 to												
					1962	2007	2010					
LRR					x	-1.1	-0.9					
LR2					x	0.77	0.54					
LSE					x	26.2	21.0					
LCI					x	7.1	1.7					
SMP					x	7	7					
1962 to												
						2007	2010					
LRR						x	-1.5					
LR2						x	0.68					
LSE						x	18.1					
LCI						x	6.0					
SMP						x	6					
LRR: Linear Regression Rate (m/yr), LR2: R-squared of LRR, LSE: Standard Error of LRR,												
LCI: Confidence Interval 95% of LRR , SMP: Sample size (total number of transects).												
(x) symbol indicates shoreline for year unavailable or a minimum of three shorelines necessary for a regression rate.												
(-) sign indicates retreat & a positive integer signals advance.												



Cell 1: Coast Guard Breach Shoreline												
Weighted Linear Regression Statistics												
1852 to								06/2007 to				
	1871	1910	1933	1942	1962	2007	2010		05/08	04/09	04/10	
WLR	x	x	x	-0.9	-0.5	-1.1	-1.1	WLR	x	x	x	
WR2	x	x	x	0.71	0.27	0.81	0.72	WR2	x	x	x	
WSE	x	x	x	1.8	2.7	3.2	3.5	WSE	x	x	x	
WCI	x	x	x	4.0	2.2	0.9	0.8	WCI	x	x	x	
SMP	x	x	x	4	4	4	4	SMP	x	x	x	
1871 to								05/2008 to				
		1910	1933	1942	1962	2007	2010			04/09	04/10	
WLR		x	x	x	x	x	x	WLR		x	x	
WR2		x	x	x	x	x	x	WR2		x	x	
WSE		x	x	x	x	x	x	WSE		x	x	
WCI		x	x	x	x	x	x	WCI		x	x	
SMP		x	x	x	x	x	x	SMP		x	x	
1910 to								04/2009 to				
			1933	1942	1962	2007	2010				04/10	
WLR			x	2.5	1.0	-1.4	-1.7	WLR			x	
WR2			x	0.94	0.49	0.74	0.76	WR2			x	
WSE			x	0.9	1.9	4.1	4.5	WSE			x	
WCI			x	7.7	3.1	1.5	1.3	WCI			x	
SMP			x	1	1	1	1	SMP			x	
1933 to												
				1942	1962	2007	2010					
WLR				x	0.8	-0.9	-0.8					
WR2				x	0.80	0.83	0.44					
WSE				x	0.6	2.3	3.2					
WCI				x	4.6	1.7	1.2					
SMP				x	7	7	7					
1942 to												
					1962	2007	2010					
WLR					x	-1.2	-0.9					
WR2					x	0.88	0.52					
WSE					x	2.9	3.5					
WCI					x	5.2	2.0					
SMP					x	7	7					
1962 to												
						2007	2010					
WLR						x	-1.4					
WR2						x	0.55					
WSE						x	4.5					
WCI						x	11.6					
SMP						x	6					
WLR: Weighted Linear Regression (m/yr), WR2: R-squared of WLR, WSE: Standard Error of WLR,												
WCI: Confidence Interval 95% of WLR, SMP: Sample size (total number of transects).												
(x) symbol indicates shoreline for year unavailable, or a minimum of three shorelines necessary for a regression rate, or shorelines have identical positional accuracies for WLR. (-) sign indicates retreat & a positive integer signals advance.												

Cell 2: Northern, Breach-Influenced, Open-Ocean Shoreline												
Long-Term and Short-Term Rates of Shoreline Change and Net Shoreline Movement												
1852 to								06/2007 to				
	1871	1910	1933	1942	1962	2007	2010		05/08	04/09	04/10	
EPR	x	-1.6	-0.6	-1.2	-2.0	-4.7	-5.1	EPR	-13.9	-11.7	-23.3	
LRR	x	x	-0.8	-1.0	-1.6	-4.3	-5.3	LRR	x	-11.6	-22.1	
LR2	x	x	0.74	0.71	0.57	0.67	0.75	LR2	x	0.86	0.81	
NSM	x	-90.5	-50.3	-108.5	-218.9	-736.4	-803.8	NSM	-12.7	-22.0	-67.2	
SMP	x	19	19	20	20	20	20	SMP	20	20	20	
1871 to								05/2008 to				
		1910	1933	1942	1962	2007	2010			04/09	04/10	
EPR		x	x	x	x	x	x	EPR		-9.6	-27.7	
LRR		x	x	x	x	x	x	LRR		x	-27.8	
LR2		x	x	x	x	x	x	LR2		x	0.85	
NSM		x	x	x	x	x	x	NSM		-9.3	-54.5	
SMP		x	x	x	x	x	x	SMP		20	20	
1910 to								04/2009 to				
			1933	1942	1962	2007	2010				04/10	
EPR			1.7	-0.6	-2.6	-6.9	-7.4	EPR			-45.4	
LRR			x	-0.1	-2.6	-7.5	-8.3	LRR			x	
LR2			x	0.48	0.54	0.84	0.89	LR2			x	
NSM			40.2	-20.1	-135.3	-675.1	-744.8	NSM			-45.2	
SMP			19	19	19	19	19	SMP			20	
1933 to												
				1942	1962	2007	2010					
EPR				-6.4	-5.8	-9.3	-9.8					
LRR				x	-5.8	-9.4	-9.9					
LR2				x	0.89	0.94	0.96					
NSM				-54.5	-164.9	-682.5	-749.1					
SMP				20	20	20	20					
1942 to												
					1962	2007	2010					
EPR					-5.6	-9.7	-10.2					
LRR					x	-10.0	-10.4					
LR2					x	0.96	0.97					
NSM					-110.4	-628.0	-695.3					
SMP					20	20	20					
1962 to												
						2007	2010					
EPR						-11.5	-12.2					
LRR						x	-11.9					
LR2						x	0.98					
NSM						-517.5	-584.5					
SMP						20	20					
EPR: End Point Rate (m/yr), LRR: Linear Regression Rate (m/yr), LR2: R-Squared of LRR,												
NSM : Net Shoreline Movement (m), and SMP : Sample size (total number of transects).												
(x) symbol indicates shoreline for year unavailable or a minimum of three shorelines necessary for a regression rate.												
(-) sign indicates retreat & a positive integer signals advance.												

Cell 2: Northern, Breach-Influenced, Open-Ocean Shoreline												
Comparison of Long-Term and Short-Term Shoreline Change Rate Statistics												
1852 to								06/2007 to				
	1871	1910	1933	1942	1962	2007	2010		05/08	04/09	04/10	
EPR	x	-1.6	-0.6	-1.2	-2.0	-4.7	-5.1	EPR	-13.9	-11.7	-23.3	
LRR	x	x	-0.8	-1.0	-1.6	-4.3	-5.3	LRR	x	-11.6	-22.1	
WLR	x	x	x	-1.1	-2.0	-7.3	-7.8	WLR	x	x	x	
LMS	x	-1.6	-0.6	0.0	-2.1	-1.5	-7.7	LMS	x	-11.8	-21.9	
SMP	x	19	19	20	20	20	20	SMP	20	20	20	
1871 to								05/2008 to				
		1910	1933	1942	1962	2007	2010			04/09	04/10	
EPR		x	x	x	x	x	x	EPR		-9.6	-27.7	
LRR		x	x	x	x	x	x	LRR		x	-27.8	
WLR		x	x	x	x	x	x	WLR		x	x	
LMS		x	x	x	x	x	x	LMS		x	-26.9	
SMP		x	x	x	x	x	x	SMP		20	20	
1910 to								04/2009 to				
			1933	1942	1962	2007	2010				04/10	
EPR			1.7	-0.6	-2.6	-6.9	-7.4	EPR			-45.4	
LRR			x	-0.1	-2.6	-7.5	-8.3	LRR			x	
WLR			x	-0.7	-3.6	-9.6	-10.0	WLR			x	
LMS			x	-0.6	-3.0	-5.2	-10.2	LMS			x	
SMP			19	19	19	19	19	SMP			20	
1933 to												
				1942	1962	2007	2010					
EPR				-6.4	-5.8	-9.3	-9.8					
LRR				x	-5.8	-9.4	-9.9					
WLR				x	-5.7	-10.1	-10.5					
LMS				x	-5.8	-9.3	-9.9					
SMP				20	20	20	20					
1942 to												
					1962	2007	2010					
EPR					-5.6	-9.7	-10.2					
LRR					x	-10.0	-10.4					
WLR					x	-10.3	-10.7					
LMS					x	-9.7	-10.0					
SMP					20	20	20					
1962 to												
						2007	2010					
EPR						-11.5	-12.2					
LRR						x	-11.9					
WLR						x	-11.9					
LMS						x	-12.4					
SMP						20	20					
EPR: End Point Rate (m/yr), LRR: Linear Regression Rate (m/yr), WLR: Weighted Linear Regression (m/yr),												
LMS: Least Median of Squares (m/yr), SMP: Sample size (total number of transects).												
(x) symbol indicates shoreline for year unavailable, or a minimum of three shorelines necessary for a regression rate, or shorelines have identical positional accuracies for WLR. (-) sign indicates retreat & a positive integer signals advance.												

Cell 2: Northern, Breach-Influenced, Open-Ocean Shoreline												
Linear Regression Statistics												
1852 to								06/2007 to				
	1871	1910	1933	1942	1962	2007	2010		05/08	04/09	04/10	
LRR	x	x	-0.8	-1.0	-1.6	-4.3	-5.3	LRR	x	-11.6	-22.1	
LR2	x	x	0.74	0.71	0.57	0.67	0.75	LR2	x	0.86	0.81	
LSE	x	x	70.5	63.4	79.1	194.4	201.4	LSE	x	4.0	13.3	
LCI	x	x	15.1	4.1	3.0	4.6	3.8	LCI	x	37.9	26.7	
SMP	x	x	19	20	20	20	20	SMP	x	20	20	
1871 to								05/2008 to				
	1910	1933	1942	1962	2007	2010			04/09	04/10		
LRR		x	x	x	x	x	x	LRR		x	-27.8	
LR2		x	x	x	x	x	x	LR2		x	0.85	
LSE		x	x	x	x	x	x	LSE		x	14.4	
LCI		x	x	x	x	x	x	LCI		x	131.6	
SMP		x	x	x	x	x	x	SMP		x	20	
1910 to								04/2009 to				
		1933	1942	1962	2007	2010				04/10		
LRR			x	-0.1	-2.6	-7.5	-8.3	LRR			x	
LR2			x	0.48	0.54	0.84	0.89	LR2			x	
LSE			x	45.2	64.5	140.0	133.0	LSE			x	
LCI			x	24.2	7.4	6.1	4.1	LCI			x	
SMP			x	19	19	19	19	SMP			x	
1933 to												
			1942	1962	2007	2010						
LRR				x	-5.8	-9.4	-9.9					
LR2				x	0.89	0.94	0.96					
LSE				x	17.9	72.3	65.7					
LCI				x	11.1	5.5	2.9					
SMP				x	20	20	20					
1942 to												
					1962	2007	2010					
LRR						x	-10.0	-10.4				
LR2						x	0.96	0.97				
LSE						x	82.4	65.7				
LCI						x	22.2	4.9				
SMP						x	20	20				
1962 to												
						2007	2010					
LRR							x	-11.9				
LR2							x	0.98				
LSE							x	23.4				
LCI							x	7.8				
SMP							x	20				
LRR: Linear Regression Rate (m/yr), LR2: R-squared of LRR, LSE: Standard Error of LRR,												
LCI: Confidence Interval 95% of LRR , SMP: Sample size (total number of transects).												
(x) symbol indicates shoreline for year unavailable or a minimum of three shorelines necessary for a regression rate.												
(-) sign indicates retreat & a positive integer signals advance.												

Cell 2: Northern, Breach-Influenced, Open-Ocean Shoreline												
Weighted Linear Regression Statistics												
1852 to								06/2007 to				
	1871	1910	1933	1942	1962	2007	2010		05/08	04/09	04/10	
WLR	x	x	x	-1.1	-2.0	-7.3	-7.8	WLR	x	x	x	
WR2	x	x	x	0.71	0.56	0.86	0.87	WR2	x	x	x	
WSE	x	x	x	0.7	5.3	17.4	17.1	WSE	x	x	x	
WCI	x	x	x	4.0	3.2	4.4	3.7	WCI	x	x	x	
SMP	x	x	x	20	20	20	20	SMP	x	x	x	
1871 to								05/2008 to				
		1910	1933	1942	1962	2007	2010			04/09	04/10	
WLR		x	x	x	x	x	x	WLR		x	x	
WR2		x	x	x	x	x	x	WR2		x	x	
WSE		x	x	x	x	x	x	WSE		x	x	
WCI		x	x	x	x	x	x	WCI		x	x	
SMP		x	x	x	x	x	x	SMP		x	x	
1910 to								04/2009 to				
			1933	1942	1962	2007	2010				04/10	
WLR			x	-0.7	-3.6	-9.6	-10.0	WLR			x	
WR2			x	0.47	0.67	0.95	0.94	WR2			x	
WSE			x	2.6	4.2	11.0	10.9	WSE			x	
WCI			x	22.9	6.9	4.0	3.2	WCI			x	
SMP			x	19	19	19	19	SMP			x	
1933 to												
				1942	1962	2007	2010					
WLR				x	-5.7	-10.1	-10.5					
WR2				x	0.76	0.98	0.96					
WSE				x	0.6	7.1	7.5					
WCI				x	4.6	4.0	2.8					
SMP				x	20	20	20					
1942 to												
					1962	2007	2010					
WLR					x	-10.3	-10.7					
WR2					x	0.98	0.96					
WSE					x	9.0	8.5					
WCI					x	16.2	4.7					
SMP					x	20	20					
1962 to												
						2007	2010					
WLR						x	-11.9					
WR2						x	0.95					
WSE						x	5.8					
WCI						x	14.9					
SMP						x	20					
WLR: Weighted Linear Regression (m/yr), WR2: R-squared of WLR, WSE: Standard Error of WLR,												
WCI: Confidence Interval 95% of WLR, SMP: Sample size (total number of transects).												
(x) symbol indicates shoreline for year unavailable, or a minimum of three shorelines necessary for a regression rate, or shorelines have identical positional accuracies for WLR. (-) sign indicates retreat & a positive integer signals advance.												

Cell 3: North-Central, Marsh-Backed, Open-Ocean Shoreline												
Long-Term and Short-Term Rates of Shoreline Change and Net Shoreline Movement												
1852 to								06/2007 to				
	1871	1910	1933	1942	1962	2007	2010		05/08	04/09	04/10	
EPR	-3.6	-6.0	-4.5	-4.1	-4.8	-5.5	-5.8	EPR	-9.1	-10.0	-23.0	
LRR	x	-6.9	-4.9	-4.4	-4.5	-5.3	-5.7	LRR	x	-10.0	-22.0	
LR2	x	0.98	0.94	0.89	0.91	0.93	0.94	LR2	x	0.87	0.83	
NSM	-69.4	-350.6	-369.7	-371.5	-526.3	-859.1	-925.4	NSM	-8.3	-18.9	-66.3	
SMP	32	102	102	102	102	102	102	SMP	102	102	102	
1871 to								05/2008 to				
		1910	1933	1942	1962	2007	2010			04/09	04/10	
EPR		-8.6	-5.9	-5.0	-5.5	-5.9	-6.3	EPR		-10.9	-29.5	
LRR		x	-6.1	-5.2	-5.1	-5.5	-5.9	LRR		x	-29.6	
LR2		x	0.91	0.87	0.91	0.96	0.96	LR2		x	0.88	
NSM		-331.1	-367.3	-357.1	-495.8	-807.3	-878.4	NSM		-10.6	-58.0	
SMP		32	32	32	32	32	32	SMP		102	102	
1910 to								04/2009 to				
			1933	1942	1962	2007	2010				04/10	
EPR			-0.8	-0.7	-3.4	-5.2	-5.7	EPR			-47.7	
LRR			x	-0.7	-3.2	-5.6	-6.2	LRR			x	
LR2			x	0.65	0.63	0.89	0.92	LR2			x	
NSM			-19.1	-20.9	-175.8	-508.6	-574.8	NSM			-47.4	
SMP			102	102	102	102	102	SMP			102	
1933 to												
				1942	1962	2007	2010					
EPR				-0.2	-5.5	-6.7	-7.3					
LRR				x	-5.9	-7.0	-7.4					
LR2				x	0.85	0.98	0.98					
NSM				-1.8	-156.7	-489.5	-555.7					
SMP				102	102	102	102					
1942 to												
					1962	2007	2010					
EPR					-7.8	-7.5	-8.2					
LRR					x	-7.5	-7.9					
LR2					x	0.99	0.99					
NSM					-154.9	-487.7	-553.9					
SMP					102	102	102					
1962 to												
						2007	2010					
EPR						-7.4	-8.3					
LRR						x	-7.9					
LR2						x	0.99					
NSM						-332.8	-399.1					
SMP						102	102					
EPR: End Point Rate (m/yr), LRR: Linear Regression Rate (m/yr), LR2: R-Squared of LRR,												
NSM : Net Shoreline Movement (m), and SMP : Sample size (total number of transects).												
(x) symbol indicates shoreline for year unavailable or a minimum of three shorelines necessary for a regression rate.												
(-) sign indicates retreat & a positive integer signals advance.												

Cell 3: North-Central, Marsh-Backed, Open-Ocean Shoreline												
Comparison of Long-Term and Short-Term Shoreline Change Rate Statistics												
1852 to								06/2007 to				
	1871	1910	1933	1942	1962	2007	2010		05/08	04/09	04/10	
EPR	-3.6	-6.0	-4.5	-4.1	-4.8	-5.5	-5.8	EPR	-9.1	-10.0	-23.0	
LRR	x	-6.9	-4.9	-4.4	-4.5	-5.3	-5.7	LRR	x	-10.0	-22.0	
WLR	x	x	x	-4.0	-4.6	-6.2	-6.6	WLR	x	x	x	
LMS	x	-6.0	-4.8	-4.5	-4.6	-5.0	-6.3	LMS	x	-10.0	-21.8	
SMP	32	102	102	102	102	102	102	SMP	x	102	102	
1871 to								05/2008 to				
		1910	1933	1942	1962	2007	2010			04/09	04/10	
EPR		-8.6	-5.9	-5.0	-5.5	-5.9	-6.3	EPR		-10.9	-29.5	
LRR		x	-6.1	-5.2	-5.1	-5.5	-5.9	LRR		x	-29.6	
WLR		x	x	-4.6	-5.0	-6.1	-6.5	WLR		x	x	
LMS		x	-5.9	-5.7	-5.3	-5.9	-6.2	LMS		x	-27.6	
SMP		32	32	32	32	32	32	SMP		102	102	
1910 to								04/2009 to				
			1933	1942	1962	2007	2010				04/10	
EPR			-0.8	-0.7	-3.4	-5.2	-5.7	EPR			-47.7	
LRR			x	-0.7	-3.2	-5.6	-6.2	LRR			x	
WLR			x	-0.6	-4.3	-6.8	-7.2	WLR			x	
LMS			x	-0.6	-2.9	-5.8	-7.3	LMS			x	
SMP			102	102	102	102	102	SMP			102	
1933 to												
				1942	1962	2007	2010					
EPR				-0.2	-5.5	-6.7	-7.3					
LRR				x	-5.9	-7.0	-7.4					
WLR				x	-6.9	-7.3	-7.7					
LMS				x	-5.6	-7.0	-7.5					
SMP				102	102	102	102					
1942 to												
					1962	2007	2010					
EPR					-7.8	-7.5	-8.2					
LRR					x	-7.5	-7.9					
WLR					x	-7.5	-7.9					
LMS					x	-7.5	-7.9					
SMP					102	102	102					
1962 to												
						2007	2010					
EPR						-7.4	-8.3					
LRR						x	-7.9					
WLR						x	-8.0					
LMS						x	-8.0					
SMP						102	102					
EPR: End Point Rate (m/yr), LRR: Linear Regression Rate (m/yr), WLR: Weighted Linear Regression (m/yr),												
LMS: Least Median of Squares (m/yr), SMP: Sample size (total number of transects).												
(x) symbol indicates shoreline for year unavailable, or a minimum of three shorelines necessary for a regression rate, or shorelines have identical positional accuracies for WLR. (-) sign indicates retreat & a positive integer signals advance.												

**Cell 3: North-Central, Marsh-Backed, Open-Ocean Shoreline**  
Linear Regression Statistics

1852 to								06/2007 to			
	1871	1910	1933	1942	1962	2007	2010	05/08	04/09	04/10	
LRR	x	-6.9	-4.9	-4.4	-4.5	-5.3	-5.7	LRR	x	-10.0	-22.0
LR2	x	0.98	0.94	0.89	0.91	0.93	0.94	LR2	x	0.87	0.83
LSE	x	45.9	70.3	73.5	68.5	84.1	86.1	LSE	x	3.8	14.7
LCI	x	14.0	12.2	4.1	2.4	1.9	1.6	LCI	x	36.6	29.4
SMP	x	102	102	102	102	102	102	SMP	x	102	102
1871 to								05/2008 to			
	1910	1933	1942	1962	2007	2010		04/09	04/10		
LRR	x	-6.1	-5.2	-5.1	-5.5	-5.9	LRR	x	-29.6		
LR2	x	0.91	0.87	0.91	0.96	0.96	LR2	x	0.88		
LSE	x	84.0	79.0	65.5	61.8	62.7	LSE	x	14.7		
LCI	x	23.9	6.2	3.0	1.7	1.3	LCI	x	134.9		
SMP	x	32	32	32	32	32	SMP	x	102		
1910 to								04/2009 to			
		1933	1942	1962	2007	2010			04/10		
LRR		x	-0.7	-3.2	-5.6	-6.2	LRR		x		
LR2		x	0.65	0.63	0.89	0.92	LR2		x		
LSE		x	22.4	57.8	79.1	77.8	LSE		x		
LCI		x	12.0	6.6	3.4	2.4	LCI		x		
SMP		x	102	102	102	102	SMP		x		
1933 to											
			1942	1962	2007	2010					
LRR			x	-5.9	-7.0	-7.4					
LR2			x	0.85	0.98	0.98					
LSE			x	41.6	39.2	39.7					
LCI			x	25.7	3.0	1.8					
SMP			x	102	102	102					
1942 to											
				1962	2007	2010					
LRR				x	-7.5	-7.9					
LR2				x	0.99	0.99					
LSE				x	25.2	30.4					
LCI				x	6.8	2.2					
SMP				x	102	102					
1962 to											
					2007	2010					
LRR					x	-7.9					
LR2					x	0.99					
LSE					x	30.8					
LCI					x	10.3					
SMP					x	102					
LRR: Linear Regression Rate (m/yr), LR2: R-squared of LRR, LSE: Standard Error of LRR,											
LCI: Confidence Interval 95% of LRR , SMP: Sample size (total number of transects).											
(x) symbol indicates shoreline for year unavailable or a minimum of three shorelines necessary for a regression rate.											
(-) sign indicates retreat & a positive integer signals advance.											



### Cell 3: North-Central, Marsh-Backed, Open-Ocean Shoreline

#### Weighted Linear Regression Statistics

1852 to								06/2007 to			
	1871	1910	1933	1942	1962	2007	2010		05/08	04/09	04/10
WLR	x	x	x	-4.0	-4.6	-6.2	-6.6	WLR	x	x	x
WR2	x	x	x	0.87	0.91	0.96	0.96	WR2	x	x	x
WSE	x	x	x	4.2	4.4	6.7	7.7	WSE	x	x	x
WCI	x	x	x	4.0	2.5	1.6	1.6	WCI	x	x	x
SMP	x	x	x	102	102	102	102	SMP	x	x	x
1871 to								05/2008 to			
		1910	1933	1942	1962	2007	2010			04/09	04/10
WLR		x	x	-4.6	-5.0	-6.1	-6.5	WLR		x	x
WR2		x	x	0.85	0.92	0.98	0.97	WR2		x	x
WSE		x	x	4.4	3.8	4.5	6.2	WSE		x	x
WCI		x	x	5.8	2.7	1.2	1.4	WCI		x	x
SMP		x	x	32	32	32	32	SMP		x	x
1910 to								04/2009 to			
			1933	1942	1962	2007	2010				04/10
WLR			x	-0.6	-4.3	-6.8	-7.2	WLR			x
WR2			x	0.67	0.71	0.97	0.96	WR2			x
WSE			x	1.3	4.7	5.8	6.8	WSE			x
WCI			x	11.4	7.8	2.1	2.0	WCI			x
SMP			x	102	102	102	102	SMP			x
1933 to											
				1942	1962	2007	2010				
WLR				x	-6.9	-7.3	-7.7				
WR2				x	0.92	0.99	0.98				
WSE				x	3.0	3.0	5.4				
WCI				x	21.9	1.7	2.0				
SMP				x	102	102	102				
1942 to											
					1962	2007	2010				
WLR					x	-7.5	-7.9				
WR2					x	1.00	0.98				
WSE					x	2.8	6.1				
WCI					x	5.0	3.3				
SMP					x	102	102				
1962 to											
						2007	2010				
WLR						x	-8.0				
WR2						x	0.96				
WSE						x	7.7				
WCI						x	19.6				
SMP						x	102				
WLR: Weighted Linear Regression (m/yr), WR2: R-squared of WLR, WSE: Standard Error of WLR,											
WCI: Confidence Interval 95% of WLR, SMP: Sample size (total number of transects).											
(x) symbol indicates shoreline for year unavailable, or a minimum of three shorelines necessary for a regression rate, or shorelines have identical positional accuracies for WLR. (-) sign indicates retreat & a positive integer signals advance.											

Cell 4: South-Central, Bay-Backed, Open-Ocean Shoreline												
Long-Term and Short-Term Rates of Shoreline Change and Net Shoreline Movement												
1852 to								06/2007 to				
	1871	1910	1933	1942	1962	2007	2010		05/08	04/09	04/10	
EPR	-5.7	-7.7	-5.7	-5.6	-6.0	-7.1	-7.0	EPR	-7.8	10.3	-2.3	
LRR	x	-7.9	-6.3	-5.8	-5.8	-6.7	-6.9	LRR	x	10.5	0.7	
LR2	x	0.98	0.93	0.93	0.95	0.96	0.97	LR2	x	0.53	0.47	
NSM	-109.9	-446.9	-469.7	-510.2	-657.6	-1099.5	-1106.0	NSM	-7.1	19.5	-6.5	
SMP	60	60	60	60	60	60	60	SMP	60	60	60	
1871 to								05/2008 to				
		1910	1933	1942	1962	2007	2010			04/09	04/10	
EPR		-8.7	-5.8	-5.6	-6.0	-7.3	-7.2	EPR		27.4	0.3	
LRR		x	-6.0	-5.5	-5.6	-6.9	-7.1	LRR		x	0.2	
LR2		x	0.86	0.85	0.90	0.94	0.96	LR2		x	0.33	
NSM		-336.9	-359.8	-400.3	-547.6	-989.6	-996.1	NSM		26.6	0.6	
SMP		60	60	60	60	60	60	SMP		60	60	
1910 to								04/2009 to				
			1933	1942	1962	2007	2010				04/10	
EPR			-1.0	-2.0	-4.0	-6.7	-6.6	EPR			-26.1	
LRR			x	-1.7	-4.0	-7.1	-7.4	LRR			x	
LR2			x	0.56	0.74	0.90	0.93	LR2			x	
NSM			-22.9	-63.4	-210.7	-652.7	-659.2	NSM			-26.0	
SMP			60	60	60	60	60	SMP			60	
1933 to												
				1942	1962	2007	2010					
EPR				-4.7	-6.6	-8.6	-8.3					
LRR				x	-6.8	-8.7	-8.7					
LR2				x	0.86	0.96	0.97					
NSM				-40.5	-187.8	-629.8	-636.3					
SMP				60	60	60	60					
1942 to												
					1962	2007	2010					
EPR					-7.4	-9.1	-8.8					
LRR					x	-9.2	-9.1					
LR2					x	0.99	0.99					
NSM					-147.4	-589.3	-595.8					
SMP					60	60	60					
1962 to												
						2007	2010					
EPR						-9.8	-9.3					
LRR						x	-9.5					
LR2						x	0.99					
NSM						-441.9	-448.4					
SMP						60	60					
EPR: End Point Rate (m/yr), LRR: Linear Regression Rate (m/yr), LR2: R-Squared of LRR,												
NSM: Net Shoreline Movement (m), and SMP: Sample size (total number of transects).												
(x) symbol indicates shoreline for year unavailable or a minimum of three shorelines necessary for a regression rate.												
(-) sign indicates retreat & a positive integer signals advance.												

Cell 4: South-Central, Bay-Backed, Open-Ocean Shoreline												
Comparison of Long-Term and Short-Term Shoreline Change Rate Statistics												
1852 to								06/2007 to				
	1871	1910	1933	1942	1962	2007	2010		05/08	04/09	04/10	
EPR	-5.7	-7.7	-5.7	-5.6	-6.0	-7.1	-7.0	EPR	-7.8	10.3	-2.3	
LRR	x	-7.9	-6.3	-5.8	-5.8	-6.7	-6.9	LRR	x	10.5	0.7	
WLR	x	x	x	-5.6	-5.8	-7.7	-7.7	WLR	x	x	x	
LMS	x	-7.8	-6.4	-5.9	-6.0	-6.0	-6.9	LMS	x	9.8	1.0	
SMP	60	60	60	60	60	60	60	SMP	60	60	60	
1871 to								05/2008 to				
		1910	1933	1942	1962	2007	2010			04/09	04/10	
EPR		-8.7	-5.8	-5.6	-6.0	-7.3	-7.2	EPR		27.4	0.3	
LRR		x	-6.0	-5.5	-5.6	-6.9	-7.1	LRR		x	0.2	
WLR		x	x	-5.2	-5.6	-8.1	-8.0	WLR		x	x	
LMS		x	-5.9	-5.6	-5.1	-5.8	-7.5	LMS		x	0.3	
SMP		60	60	60	60	60	60	SMP		60	60	
1910 to								04/2009 to				
			1933	1942	1962	2007	2010				04/10	
EPR			-1.0	-2.0	-4.0	-6.7	-6.6	EPR			-26.1	
LRR			x	-1.7	-4.0	-7.1	-7.4	LRR			x	
WLR			x	-2.0	-4.9	-8.5	-8.4	WLR			x	
LMS			x	-1.9	-3.9	-5.2	-8.2	LMS			x	
SMP			60	60	60	60	60	SMP			60	
1933 to												
				1942	1962	2007	2010					
EPR				-4.7	-6.6	-8.6	-8.3					
LRR				x	-6.8	-8.7	-8.7					
WLR				x	-7.1	-9.2	-9.0					
LMS				x	-6.6	-8.7	-9.0					
SMP				60	60	60	60					
1942 to												
					1962	2007	2010					
EPR					-7.4	-9.1	-8.8					
LRR					x	-9.2	-9.1					
WLR					x	-9.3	-9.1					
LMS					x	-9.1	-9.2					
SMP					60	60	60					
1962 to												
						2007	2010					
EPR						-9.8	-9.3					
LRR						x	-9.5					
WLR						x	-9.5					
LMS						x	-9.2					
SMP						60	60					
EPR: End Point Rate (m/yr), LRR: Linear Regression Rate (m/yr), WLR: Weighted Linear Regression (m/yr),												
LMS: Least Median of Squares (m/yr), SMP: Sample size (total number of transects).												
(x) symbol indicates shoreline for year unavailable, or a minimum of three shorelines necessary for a regression rate, or shorelines have identical positional accuracies for WLR. (-) sign indicates retreat & a positive integer signals advance.												

**Cell 4: South-Central, Bay-Backed, Open-Ocean Shoreline**  
Linear Regression Statistics

1852 to								06/2007 to			
	1871	1910	1933	1942	1962	2007	2010		05/08	04/09	04/10
LRR	x	-7.9	-6.3	-5.8	-5.8	-6.7	-6.9	LRR	x	10.5	0.7
LR2	x	0.98	0.93	0.93	0.95	0.96	0.97	LR2	x	0.53	0.47
LSE	x	39.5	71.7	72.6	65.1	83.1	79.8	LSE	x	13.5	15.9
LCI	x	12.0	4.8	3.0	1.9	1.6	1.3	LCI	x	129.0	31.9
SMP	x	60	60	60	60	60	60	SMP	x	60	60
1871 to								05/2008 to			
	1910	1933	1942	1962	2007	2010			04/09	04/10	
LRR	x	-6.0	-5.5	-5.6	-6.9	-7.1	LRR	x	x	0.2	
LR2	x	0.86	0.85	0.90	0.94	0.96	LR2	x	x	0.33	
LSE	x	92.6	85.2	73.3	89.9	83.8	LSE	x	x	21.5	
LCI	x	26.4	6.7	3.3	2.4	1.8	LCI	x	x	196.4	
SMP	x	60	60	60	60	60	SMP	x	x	60	
1910 to								04/2009 to			
		1933	1942	1962	2007	2010				04/10	
LRR		x	-1.7	-4.0	-7.1	-7.4	LRR			x	
LR2		x	0.56	0.74	0.90	0.93	LR2			x	
LSE		x	46.1	63.1	102.4	91.3	LSE			x	
LCI		x	24.7	7.2	4.5	2.8	LCI			x	
SMP		x	60	60	60	60	SMP			x	
1933 to											
			1942	1962	2007	2010					
LRR			x	-6.8	-8.7	-8.7					
LR2			x	0.86	0.96	0.97					
LSE			x	50.0	66.8	56.6					
LCI			x	30.8	5.1	2.5					
SMP			x	60	60	60					
1942 to											
				1962	2007	2010					
LRR				x	-9.2	-9.1					
LR2				x	0.99	0.99					
LSE				x	41.3	38.4					
LCI				x	11.1	2.8					
SMP				x	60	60					
1962 to											
					2007	2010					
LRR					x	-9.5					
LR2					x	0.99					
LSE					x	30.3					
LCI					x	10.1					
SMP					x	60					

EPR: End Point Rate (m/yr), LRR: Linear Regression Rate (m/yr), WLR: Weighted Linear Regression (m/yr),

LMS: Least Median of Squares (m/yr), SMP: Sample size (total number of transects).

(x) symbol indicates shoreline for year unavailable or a minimum of three shorelines necessary for a regression rate.

(-) sign indicates retreat & a positive integer signals advance.

Cell 4: South-Central, Bay-Backed, Open-Ocean Shoreline												
Weighted Linear Regression Statistics												
1852 to								06/2007 to				
	1871	1910	1933	1942	1962	2007	2010		05/08	04/09	04/10	
WLR	x	x	x	-5.6	-5.8	-7.7	-7.7	WLR	x	x	x	
WR2	x	x	x	0.94	0.96	0.97	0.97	WR2	x	x	x	
WSE	x	x	x	4.0	3.8	7.5	7.5	WSE	x	x	x	
WCI	x	x	x	2.7	1.7	1.6	1.4	WCI	x	x	x	
SMP	x	x	x	60	60	60	60	SMP	x	x	x	
1871 to								05/2008 to				
		1910	1933	1942	1962	2007	2010			04/09	04/10	
WLR		x	x	-5.2	-5.6	-8.1	-8.0	WLR		x	x	
WR2		x	x	0.87	0.92	0.97	0.97	WR2		x	x	
WSE		x	x	4.7	4.3	7.5	7.5	WSE		x	x	
WCI		x	x	6.1	3.0	2.0	1.7	WCI		x	x	
SMP		x	x	60	60	60	60	SMP		x	x	
1910 to								04/2009 to				
			1933	1942	1962	2007	2010				04/10	
WLR			x	-2.0	-4.9	-8.5	-8.4	WLR			x	
WR2			x	0.61	0.80	0.97	0.97	WR2			x	
WSE			x	2.7	4.6	7.5	7.6	WSE			x	
WCI			x	23.3	7.6	2.8	2.2	WCI			x	
SMP			x	60	60	60	60	SMP			x	
1933 to												
				1942	1962	2007	2010					
WLR				x	-7.1	-9.2	-9.0					
WR2				x	0.90	0.99	0.98					
WSE				x	3.6	5.2	6.2					
WCI				x	26.3	2.9	2.3					
SMP				x	60	60	60					
1942 to												
					1962	2007	2010					
WLR					x	-9.3	-9.1					
WR2					x	0.99	0.98					
WSE					x	4.5	6.6					
WCI					x	8.1	3.6					
SMP					x	60	60					
1962 to												
						2007	2010					
WLR						x	-9.5					
WR2						x	0.97					
WSE						x	7.5					
WCI						x	19.3					
SMP						x	60					
WLR: Weighted Linear Regression (m/yr), WR2: R-squared of WLR, WSE: Standard Error of WLR,												
WCI: Confidence Interval 95% of WLR, SMP: Sample size (total number of transects).												
(x) symbol indicates shoreline for year unavailable, or a minimum of three shorelines necessary for a regression rate, or shorelines have identical positional accuracies for WLR. (-) sign indicates retreat & a positive integer signals advance.												

Cell 5: Southern Spit, Open-Ocean Shoreline												
Long-Term and Short-Term Rates of Shoreline Change and Net Shoreline Movement												
1852 to								06/2007 to				
	1871	1910	1933	1942	1962	2007	2010		05/08	04/09	04/10	
EPR	-8.3	-4.1	-3.5	-5.7	-3.7	-3.7	-4.1	EPR	-9.5	-9.3	-26.0	
LRR	x	-3.8	-3.3	-4.5	-3.6	-3.5	-3.6	LRR	x	-9.3	-24.6	
LR2	x	0.81	0.79	0.84	0.83	0.89	0.91	LR2	x	0.90	0.83	
NSM	-160.5	-238.9	-282.1	-513.5	-402.1	-571.9	-646.1	NSM	-8.6	-17.5	-74.7	
SMP	22	22	13	17	22	22	22	SMP	35	35	32	
1871 to								05/2008 to				
	1910	1933	1942	1962	2007	2010			04/09	04/10		
EPR		-1.2	-1.6	-4.7	-2.6	-2.7	-3.2	EPR		-9.1	-32.9	
LRR		x	-1.8	-3.9	-2.9	-2.9	-3.1	LRR		x	-33.0	
LR2		x	0.78	0.68	0.71	0.82	0.86	LR2		x	0.87	
NSM		-47.7	-101.9	-335.9	-235.5	-368.9	-441.9	NSM		-8.9	-64.6	
SMP		29	13	17	29	29	29	SMP		35	32	
1910 to								04/2009 to				
		1933	1942	1962	2007	2010				04/10		
EPR			0.6	-7.4	-3.6	-3.2	-3.9	EPR			-54.9	
LRR			x	-4.9	-3.7	-3.3	-3.5	LRR			x	
LR2			x	0.43	0.45	0.78	0.85	LR2			x	
NSM			13.7	-238.7	-187.8	-315.0	-389.8	NSM			-54.6	
SMP			13	17	29	32	32	SMP			32	
1933 to												
			1942	1962	2007	2010						
EPR				-25.7	-6.2	-5.1	-5.9					
LRR				x	-4.8	-4.0	-4.5					
LR2				x	0.37	0.71	0.81					
NSM				-220.0	-177.1	-372.4	-450.4					
SMP				13	13	13	13					
1942 to												
					1962	2007	2010					
EPR						4.0	-1.7	-2.7				
LRR						x	-2.1	-2.9				
LR2						x	0.52	0.61				
NSM						79.8	-107.9	-181.4				
SMP						17	17	17				
1962 to												
						2007	2010					
EPR							-3.0	-4.3				
LRR							x	-3.7				
LR2							x	0.83				
NSM							-133.4	-206.4				
SMP							29	29				
EPR: End Point Rate (m/yr), LRR: Linear Regression Rate (m/yr), LR2: R-Squared of LRR,												
NSM : Net Shoreline Movement (m), and SMP : Sample size (total number of transects).												
(x) symbol indicates shoreline for year unavailable or a minimum of three shorelines necessary for a regression rate.												
(-) sign indicates retreat & a positive integer signals advance.												

Cell 5: Southern Spit, Open-Ocean Shoreline												
Comparison of Long-Term and Short-Term Shoreline Change Rate Statistics												
1852 to								06/2007 to				
	1871	1910	1933	1942	1962	2007	2010		05/08	04/09	04/10	
EPR	-8.3	-4.1	-3.5	-5.7	-3.7	-3.7	-4.1	EPR	-9.5	-9.3	-26.0	
LRR	x	-3.8	-3.3	-4.5	-3.6	-3.5	-3.6	LRR	x	-9.3	-24.6	
WLR	x	x	x	-5.1	-3.5	-3.2	-3.5	WLR	x	x	x	
LMS	x	-4.1	-3.3	-4.9	-3.3	-3.2	-3.8	LMS	x	-9.1	-23.6	
SMP	22	22	13	17	22	22	22	SMP	35	35	32	
1871 to								05/2008 to				
		1910	1933	1942	1962	2007	2010			04/09	04/10	
EPR		-1.2	-1.6	-4.7	-2.6	-2.7	-3.2	EPR		-9.1	-32.9	
LRR		x	-1.8	-3.9	-2.9	-2.9	-3.1	LRR		x	-33.0	
WLR		x	x	-4.8	-2.9	-2.7	-3.1	WLR		x	x	
LMS		x	-1.6	-3.8	-2.9	-2.9	-3.1	LMS		x	-31.0	
SMP		29	13	17	29	29	29	SMP		35	32	
1910 to								04/2009 to				
			1933	1942	1962	2007	2010				04/10	
EPR			0.6	-7.4	-3.6	-3.2	-3.9	EPR			-54.9	
LRR			x	-4.9	-3.7	-3.3	-3.5	LRR			x	
WLR			x	-6.7	-2.2	-2.6	-3.2	WLR			x	
LMS			x	-7.2	-3.6	-2.9	-3.7	LMS			x	
SMP			13	17	29	32	32	SMP			32	
1933 to												
				1942	1962	2007	2010					
EPR				-25.7	-6.2	-5.1	-5.9					
LRR				x	-4.8	-4.0	-4.5					
WLR				x	-1.3	-3.4	-4.1					
LMS				x	-6.1	-3.6	-5.3					
SMP				13	13	13	13					
1942 to												
					1962	2007	2010					
EPR					4.0	-1.7	-2.7					
LRR					x	-2.1	-2.9					
WLR					x	-2.5	-3.2					
LMS					x	-1.7	-3.2					
SMP					17	17	17					
1962 to												
						2007	2010					
EPR						-3.0	-4.3					
LRR						x	-3.7					
WLR						x	-3.9					
LMS						x	-4.2					
SMP						29	29					
EPR: End Point Rate (m/yr), LRR: Linear Regression Rate (m/yr), WLR: Weighted Linear Regression (m/yr),												
LMS: Least Median of Squares (m/yr), SMP: Sample size (total number of transects).												
(x) symbol indicates shoreline for year unavailable, or a minimum of three shorelines necessary for a regression rate, or shorelines have identical positional accuracies for WLR. (-) sign indicates retreat & a positive integer signals advance.												

### Cell 5: Southern Spit, Open-Ocean Shoreline

#### Linear Regression Statistics

1852 to								06/2007 to				
	1871	1910	1933	1942	1962	2007	2010		05/08	04/09	04/10	
LRR	x	-3.8	-3.3	-4.5	-3.6	-3.5	-3.6	LRR	x	-9.3	-24.6	
LR2	x	0.81	0.79	0.84	0.83	0.89	0.91	LR2	x	0.90	0.83	
LSE	x	64.9	75.8	90.6	81.3	72.9	70.0	LSE	x	2.3	16.8	
LCI	x	19.7	5.1	4.2	2.7	1.5	1.2	LCI	x	21.6	33.7	
SMP	x	22	13	17	22	22	22	SMP	x	35	32	
1871 to								05/2008 to				
	1910	1933	1942	1962	2007	2010			04/09	04/10		
LRR		x	-1.8	-3.9	-2.9	-2.9	-3.1	LRR		x	-33.0	
LR2		x	0.78	0.68	0.71	0.82	0.86	LR2		x	0.87	
LSE		x	42.5	107.6	94.1	76.9	72.4	LSE		x	17.9	
LCI		x	12.1	14.1	10.2	2.5	1.7	LCI		x	163.6	
SMP		x	13	17	29	29	29	SMP		x	32	
1910 to								04/2009 to				
		1933	1942	1962	2007	2010				04/10		
LRR			x	-4.9	-3.7	-3.3	-3.5	LRR			x	
LR2			x	0.43	0.45	0.78	0.85	LR2			x	
LSE			x	130.4	124.6	82.9	71.7	LSE			x	
LCI			x	69.8	25.2	7.6	3.4	LCI			x	
SMP			x	17	29	32	32	SMP			x	
1933 to												
			1942	1962	2007	2010						
LRR				x	-4.8	-4.0	-4.5					
LR2				x	0.37	0.71	0.81					
LSE				x	132.6	95.6	82.1					
LCI				x	81.8	7.2	3.6					
SMP				x	13	13	13					
1942 to												
				1962	2007	2010						
LRR					x	-2.1	-2.9					
LR2					x	0.52	0.61					
LSE					x	89.8	78.9					
LCI					x	24.2	5.8					
SMP					x	17	17					
1962 to												
					2007	2010						
LRR						x	-3.7					
LR2						x	0.83					
LSE						x	44.1					
LCI						x	14.7					
SMP						x	29					
EPR: End Point Rate (m/yr), LRR: Linear Regression Rate (m/yr), WLR: Weighted Linear Regression (m/yr),												
LMS: Least Median of Squares (m/yr), SMP: Sample size (total number of transects).												
(x) symbol indicates shoreline for year unavailable or a minimum of three shorelines necessary for a regression rate.												
(-) sign indicates retreat & a positive integer signals advance.												



Cell 5: Southern Spit, Open-Ocean Shoreline												
Weighted Linear Regression Statistics												
1852 to								06/2007 to				
	1871	1910	1933	1942	1962	2007	2010		05/08	04/09	04/10	
WLR	x	x	x	-5.1	-3.5	-3.2	-3.5	WLR	x	x	x	
WR2	x	x	x	0.89	0.78	0.88	0.86	WR2	x	x	x	
WSE	x	x	x	5.1	6.2	5.6	7.4	WSE	x	x	x	
WCI	x	x	x	3.7	3.1	1.2	1.4	WCI	x	x	x	
SMP	x	x	x	17	22	22	22	SMP	x	x	x	
1871 to								05/2008 to				
		1910	1933	1942	1962	2007	2010			04/09	04/10	
WLR		x	x	-4.8	-2.9	-2.7	-3.1	WLR		x	x	
WR2		x	x	0.78	0.68	0.81	0.77	WR2		x	x	
WSE		x	x	6.4	6.6	5.9	8.0	WSE		x	x	
WCI		x	x	12.8	9.3	2.0	2.2	WCI		x	x	
SMP		x	x	17	29	29	29	SMP		x	x	
1910 to								04/2009 to				
			1933	1942	1962	2007	2010				04/10	
WLR			x	-6.7	-2.2	-2.6	-3.2	WLR			x	
WR2			x	0.62	0.28	0.74	0.69	WR2			x	
WSE			x	7.5	10.0	7.0	9.6	WSE			x	
WCI			x	66.0	31.2	6.8	7.2	WCI			x	
SMP			x	17	29	32	32	SMP			x	
1933 to												
				1942	1962	2007	2010					
WLR				x	-1.3	-3.4	-4.1					
WR2				x	0.21	0.81	0.79					
WSE				x	9.6	7.4	9.3					
WCI				x	70.0	4.2	3.5					
SMP				x	13	13	13					
1942 to												
					1962	2007	2010					
WLR					x	-2.5	-3.2					
WR2					x	0.66	0.64					
WSE					x	9.9	11.4					
WCI					x	17.7	6.3					
SMP					x	17	17					
1962 to												
						2007	2010					
WLR						x	-3.9					
WR2						x	0.68					
WSE						x	11.0					
WCI						x	28.1					
SMP						x	29					
WLR: Weighted Linear Regression (m/yr), WR2: R-squared of WLR, WSE: Standard Error of WLR,												
WCI: Confidence Interval 95% of WLR, SMP: Sample size (total number of transects).												
(x) symbol indicates shoreline for year unavailable, or a minimum of three shorelines necessary for a regression rate, or shorelines have identical positional accuracies for WLR. (-) sign indicates retreat & a positive integer signals advance.												

## REFERENCES

## REFERENCES

- Anders, F.J. & Byrnes, M.R., 1991. Accuracy of shoreline change rates as determined from maps and aerial photographs. *Shore and Beach*, 59(1), pp. 17–26.
- Belknap, D.F. & Kraft, J.C., 1985. Influence of antecedent geology on stratigraphic preservation potential and evolution of Delaware's barrier system. *Marine Geology*, 63, pp. 235–262.
- Boak, E.H. & Turner, I.L., 2005. Shoreline definition and detection: a review. *Journal of Coastal Research*, 21(4), pp. 688–703.
- Boon, J.D., 1975. Tidal discharge asymmetry in a salt marsh drainage system. *Limnology and Oceanography*, 20(1), pp. 71–80.
- Boothroyd, J.C., 1985. Tidal inlets and tidal deltas. In R.A. Davis, ed. *Coastal Sedimentary Environments*. New York: Springer-Verlag. pp.445-532.
- Bruun, P., 1962. Sea-level rise as a cause of shore erosion. *Journal Waterways and Harbours Division*, 88(1-3), pp.117-30.
- Boon, J.D. & Byrne, R.J., 1981. On basin hypsometry and the morphodynamic response of coastal inlet systems. *Marine Geology*, 40, pp. 27–48.
- Bruun, P. & Gerritsen, F., 1959. Natural by-passing of sand at coastal inlets. *Journal of the Waterways and Harbor Division*, ASCE, 85, pp. 75–107.
- Byrne, R.J., Dealteris, J.T. & Bullock, P.A., 1974. Channel stability in tidal inlets. *Proceedings of the 14th Coastal Engineering Conference*, ASCE, pp. 1585–1604.
- Byrne, R.J., Bullock, P. & Tyler, D.G., 1975. Response characteristics of a tidal inlet: A case study. In L.E. Cronin, ed. *Estuarine Research v.2*. New York: Academic Press. pp. 201–216.
- Byrnes, M.R., 1988. *Holocene geology and migration of a low-profile barrier island system, Metompkin Island, Virginia*. Ph.D. dissertation. Oceanography Department, Old Dominion University, p. 419.

- Byrnes, M.R. & Hiland, M.W., 1995. Large-scale sediment transport patterns on the continental shelf and influence on shoreline response: St. Andrew Sound, Georgia to Nassau Sound, Florida, USA. *Marine Geology*, 126, pp. 19–43.
- Byrnes, M.R., McBride, R.A. & Hiland, M.W., 1991. Accuracy standards and development of a national shoreline change data base. *Proceedings of Coastal Sediments '91*, ASCE, pp. 1027–1042.
- Byrnes, M.R., Crowell, M. & Fowler, C., 2003. Shoreline mapping and change analysis: Technical considerations and management implications. *Journal of Coastal Research*, (Special Issue 38), pp. 1–4.
- Byrnes, M.R., McBride, R.A., Tao, Q. & Duvic, L., 1995. Historical shoreline dynamics along the Chenier Plain of southwestern Louisiana. *Gulf Coast Association of Geological Societies Transactions*, XLV, pp. 113–122.
- Crowell, M., Leatherman, S.P. & Buckley, M.K., 1993. Shoreline change rate analysis: long term versus short term data. *Shore and Beach*, 61(2), pp. 13–20.
- Crowell, M., Douglas, B.C. & Leatherman, S.P., 1997. On forecasting future U.S. shoreline positions: A test of algorithms. *Journal of Coastal Research*, 13(4), pp. 1245–1255.
- Crowell, M., Leatherman, S.P. & Buckley, M.K., 1991. Historical shoreline change: Error analysis and mapping accuracy. *Journal of Coastal Research*, 7(3), pp. 839–852.
- Curry, J.R., 1964. Transgressions and regressions. *Papers in Marine Geology*, pp. 175–203.
- Davis, R.A. & Fox, W.T., 1974. Coastal dynamics on Cedar Island, Virginia. *Technical report—Williams College*, 11, p. 66 p.
- Davis, R.A. & Hayes, M.O., 1984. What is a wave-dominated coast? *Marine Geology*, 60, pp. 313–329.
- Davis, R.A. & Fitzgerald, D.M., 2004. *Beaches and Coasts*. Malden, MA: Blackwell Publishing.
- Davis, R.E., Dolan, R. & Demme, G., 1993. Synoptic climatology of Atlantic Coast north-easters. *International Journal of Climatology*, 13, pp. 171–189.
- DeAlteris, J.T. & Byrne, R.J., 1975. The recent history of Wachapreague Inlet, Virginia. In L.E. Cronin, ed. *Estuarine Research*. New York: Academic Press. pp. 167–181.

De Beaumont, E., 1845. In P. Bertrand, ed. *Lecons de Geologie Pratique*. Paris. pp. 223-252.

Demarest, J.M. & Leatherman, S.P., 1985. Mainland influence on coastal transgression: Delmarva Peninsula. *Marine Geology*, 63, pp. 19–33.

Dolan, R., & Davis, R.E., 1992. An intensity scale for Atlantic coast northeast storms. *Journal of Coastal Research*, 8(4), pp. 840-853.

Dolan, R., Hayden, B. & Jones, C., 1979. Barrier island configuration. *Science*, 204(4391), pp. 401–403.

Dolan, R., Fenster, M.S. & Holme, S.J., 1991. Temporal analysis of shoreline recession and accretion. *Journal of Coastal Research*, 7(3), pp. 723–744.

Douglas, B.C., 1991. Global sea level rise. *Journal of Geophysical Research*, 96(C4), pp. 6981-6992.

Douglas, B.C., Crowell, M. & Honeycutt, M.G., 2002. Discussion of Fenster, M.S.; Dolan, R.; and Morton, R.A., 2001. Coastal storms and shoreline change: signal or noise? *Journal of Coastal Research*, 18(2), pp. 388-390.

Ellis, M.Y., 1978. *Coastal Mapping Handbook*, U.S. Department of Commerce, U.S. Department of Interior, Washington DC, p. 199.

Engelhart, S.E., Horton, B.P. & Kemp, A.C., 2011. Holocene sea level changes along the United States' Atlantic Coast. *Oceanography*, 24(2), pp. 70–79.

Fenster, M. & Dolan, R., 1994. Large-scale reversals in shoreline trends along the U.S. mid-Atlantic coast. *Geology*, 22, pp. 543–546.

Fenster, M. & Dolan, R., 1996. Assessing the impact of tidal inlets on adjacent barrier island shorelines. *Journal of Coastal Research*, 12(1), pp. 294–310.

Fenster, M.S., Dolan, R. & Elder, J.F., 1993. A new method for predicting shoreline positions from historical data. *Journal of Coastal Research*, 9(1), pp. 147–171.

Fenster, M.S., Dolan, R. & Morton, R.A., 2001. Coastal storms and shoreline change: Signal or noise? *Journal of Coastal Research*, 17(3), pp. 714–720.

Fenster, M.S., Honeycutt, M.G. & Gowan, C., 2003. The impact of storms on shoreline change along the mid-Atlantic coast. *Proceedings of Coastal Sediments '03*, ASCE, p. 13.

- Fenster, M.S., McBride, R.A., Trembanis, A., Richardson, T., & Nebel, S., 2011. A field test of the theoretical evolution of a mixed-energy barrier coast to a regime of accelerated sea-level rise. In *Proceedings of Coastal Sediments '11*. Miami, FL, 2011. ASCE.
- Field, M.E. & Duane, D.B., 1976. Post-Pleistocene history of the United States inner continental shelf: Significance to origin of barrier islands. *Geological Society of America Bulletin*, 87, pp. 691–702.
- Fisher, J.J., 1968. Barrier island formation: Discussion. *Geological Society of America Bulletin*, 79(10), pp. 1421–1426.
- Fitzgerald, D.M., 1982. Sediment bypassing at mixed energy tidal inlets. *Proceedings of the 18th Coastal Engineering Conference*, ASCE, pp. 1094–1118.
- Fitzgerald, D.M., 1984. Interactions between the ebb-tidal delta and landward shoreline: Price Inlet, South Carolina. *Journal of Sedimentary Petrology*, 54(4), pp. 1303–1318.
- Fitzgerald, D.M., 1988. Shoreline erosional-depositional processes associated with tidal inlets. In D.G. Aubrey & L. Weishar, eds. *Hydrodynamics and Sediment Dynamics of Tidal Inlets*. New York: Springer-Verlag. pp. 186–225.
- Fitzgerald, D.M. & Fitzgerald, S.A., 1977. Factors influencing tidal inlet throat geometry. *Proceedings of Coastal Sediments '77*, ASCE, pp. 563–581.
- Fitzgerald, D.M., Penland, S. & Nummedal, D., 1984. Control of barrier island shape by inlet sediment bypassing: East Frisian Islands, West Germany. *Marine Geology*, 60, pp. 355–376.
- Fitzgerald, D.M., Argow, B.A. & Buynevich, I.V., 2003. Rising sea level and its effects on backbarrier marshes and tidal flats, tidal inlets, and adjacent barrier shorelines. *Proceedings of Coastal Sediments '03*, ASCE, p. 14.
- Fitzgerald, D.M., Buynevich, I. & Argow, B., 2004. Model of tidal inlet and barrier island dynamics in a regime of accelerated sea level rise. *Journal of Coastal Research*, (SI 39), pp. 789–795.
- Fitzgerald, D.M., Fenster, M.S., Argow, B.A. & Buynevich, I.V., 2008. Coastal impacts due to sea-level rise. *Annual Review of Earth and Planetary Sciences*, 36, pp. 601–647.
- Fitzgerald, D.M., Kulp, M., Hughes, Z., Georgiou, I., Miner, M., Penland, S., & Howes, N., 2007. Impacts of rising sea level to backbarrier wetlands, tidal inlets, and barrier islands: Barataria coast, Louisiana. *Proceedings of Coastal Sediments '07*, ASCE, p. 14.

Fontolan, G., Pillon, S., Delli Quadri, F., & Bezzi, A., 2007. Sediment storage at tidal inlets in northern Adriatic lagoons: Ebb-tidal delta morphodynamics, conservation and sand use strategies. *Estuarine, Coastal and Shelf Science*, 75, pp. 261–277.

Fontolan, G., 2010. Walton and Adams (1976) formula conversion. *Personal correspondence*.

Galgano, F.A., 1998. *Geomorphic analysis of U.S. east coast shoreline behavior and the influence of tidal inlets on coastal configuration*. Ph.D. Dissertation. College Park: University of Maryland.

Galgano, F.A., 2007. Types and causes of beach erosion anomaly areas in the U.S. east coast barrier island system: Stabilized tidal inlets. *Middle States Geographer*, 40, pp. 158–170.

Galgano, F.A., 2009. Beach erosion adjacent to stabilized microtidal inlets. *Middle States Geographer*, 42, pp. 18–32.

Galvin, C. 2000. 'Comment on Sea Level Rise Shown to Drive Coastal Erosion', *EOS Transactions* 81 (38), pp. 437-440.

Gaunt, C.H., 1991. Recent evolution and potential causal mechanisms of Cedar Island, Virginia, 1852–1986. *Proceedings of Coastal Sediments '91*, ASCE, pp. 2335–2349.

Gilbert, G.K., 1885. Lake Bonneville. In *Monograph 1*. U.S. Geologic Survey. p.438.

Glaeser, J.D., 1978. Global distribution of barrier islands in terms of tectonic setting. *The Journal of Geology*, 86, pp. 283–297.

Goettle, M.S., 1981. Geological development of the southern portion of Assateague Island, Virginia. *Northeastern Geology*, 3(3-4), pp. 278–282.

Halsey, S.D., 1979. Nexus: new model of barrier island development, in Leatherman, S. P., ed., *Barrier Islands*: New York, Academic Press, pp. 185-210.

Hanley, J.T. & McBride, R.A., 2011. Repetitive breaching on Cedar Island, Virginia, USA: History, geomorphology, and deposits. In *ASCE Coastal Sediments 2011*. Miami, FL, 2011.

Hapke, C.J., Himmelstoss, E.A., Kratzmann, M., List, J.H., and Thieler, E.R., 2010. National assessment of shoreline change: Historical shoreline change along the New England and Mid-Atlantic coasts: U.S. Geological Survey Open-File Report 2010-1118, p. 57.

Harper, S. (2002, September 14). Eastern Shore's Welcome Fire. *The Virginian-Pilot*, p. B1.

Harris, M.S., 1992. *The geomorphology of Hog Island, Virginia: a mid-Atlantic coast barrier*. Master's thesis. Department of Environmental Sciences, University of Virginia, p.70.

Hayes, M.O., 1979. Barrier island morphology as a function of tidal and wave regime. In S.P. Leatherman, ed. *Barrier Islands from the Gulf of St. Lawrence to the Gulf of Mexico*. New York: Academic Press. pp. 1–27.

Hayes, M.O., 1980. General morphology and sediment patterns in tidal inlets. *Sedimentary Geology*, 26, pp. 135–156.

Hayes, M.O., 1994. The Georgia Bight barrier system. In R.A. Davis, ed. *Geology of Holocene Barrier Islands*. Berlin: Springer-Verlag. pp. 233–304.

Hobbs, C.H., Krantz, D.E. & Wikel, G.L., 2008. Coastal Processes and Offshore Geology. In C. Bailey, ed. *The Geology of Virginia*. College of William and Mary. p.44.

Honeycutt, M.G. & Krantz, D.E., 2003. Influence of the geologic framework on spatial variability in long-term shoreline change, Cape Henlopen to Rehoboth Beach, Delaware. *Journal of Coastal Research*, (Special Issue 38), pp. 147-167.

Honeycutt, M.G., Crowell, M. & Douglas, B.C., 2001. Shoreline-position forecastings: Impact of storms, rate-calculation methodologies, and temporal scales. *Journal of Coastal Research*, 17(3), pp. 721–730.

Hoyt, J.H., 1967. Barrier island formation. *Geological Society of America Bulletin*, 78, pp. 1125–1136.

Inman, D.L. & Nordstrom, C.E., 1971. On the tectonic and morphologic classification of coasts. *The Journal of Geology*, 79(1), pp. 1–21.

IPCC, 2007. *Climate change 2007: The physical science basis, summary for policy-makers*. Cambridge, UK: Contrib. Work. Group I Fourth Assess. Rep. Intergov. Panel Climate Change.

Jarrett, J.T., 1976. *Tidal prism-inlet area relationships*. Vicksburg, MS: U.S. Army Corps of Engineers, Waterways Experiment Station, p. 55.

Komar, P.D., 1976. *Beach Processes and Sedimentation*. Englewood Cliffs, NJ: Prentice-Hall.



Kraft, J.C. & Chrzastowski, M.J., 1985. Costal stratigraphy sequences. In: R.A. Davis (Ed.), *Coastal Sedimentary Environments*, p. 625–664.

Kraft, J.C., Biggs, R.B. & Halsey, S.D., 1973. Morphology and vertical sedimentary sequence models in holocene transgressive barrier systems. *Coastal Geomorphology*, pp. 321–354.

Leatherman, S.P. & Douglas, B.C., 2003. Sea level and coastal erosion require large-scale monitoring. *Eos*, 84(2), pp. 13,16.

Leatherman, S.P., Rice, T.E. & Goldsmith, V., 1982. Virginia barrier island configuration: A reappraisal. *Science*, 215(4530), pp. 285–287.

Leatherman, S.P., Zhang, K. & Douglas, B.C., 2000. Sea level rise shown to drive coastal erosion. *Eos*, 81(6), pp. 55–57.

Leatherman, S.P., Zhang, K. & Douglas, B.C., 2000. Reply to: Pilkey et al., 2000., Galvin, C., 2000., and Sallenger, et al., 2000. Comment: Leatherman, S.P., et al., 2000. Sea rise level shown to drive coastal erosion. *Eos*, 81(6). *Eos*, 81(38), pp. 437, 439, 441.

McBride, R.A., 1999. Spatial and temporal distribution of historical and active tidal inlets: Delmarva Peninsula and New Jersey, USA. *Proceedings of Coastal Sediments '99*, ASCE, pp. 1505–1521.

McBride, R.A. & Byrnes, M.R., 1997. Regional variations in shore response along barrier island systems of the Mississippi River delta plain: Historical change and future prediction. *Journal of Coastal Research*, 13, pp. 628–655.

McBride, R.A., Byrnes, M.R. & Hiland, M.W., 1995. Geomorphic response-type model for barrier coastlines: A regional perspective. *Marine Geology*, 126, pp. 143–159.

McGee, W.D., 1890. Encroachments from the sea. *Forum*, 9, pp. 437–449.

Merchant, D.C., 1987. Spatial accuracy specification for large scale topographic maps. *Photogrammetric Engineering and Remote Sensing*, 53, pp. 958–961.

Miner, M.D., Fitzgerald, D.M. & Kulp, M.A., 2007. 1880 to 2005 morphologic evolution of a transgressive tidal inlet, Little Pass Timbalier, Louisiana. In *Proceedings of Coastal Sediments '07*. New Orleans, 2007. ASCE.

Moffat and Nichol Engineers, 1986. *Wallops Island Shore Protection Study*. Wallops Island, Virginia: NASA, Goddard Space Flight Facility.

- Moore, L.J., 2000. Shoreline mapping techniques. *Journal of Coastal Research*, 16(1), pp. 111–124.
- Moore, L.J., Ruggiero, P. & List, J.H., 2006. Comparing mean high water and high water line shorelines: should proxy-datum offsets be incorporated into shoreline change analysis. *Journal of Coastal Research*, 22(4), pp. 894–905.
- Morton, R.A., 1977. Historical shoreline changes and their causes, Texas Gulf Coast. *Gulf Coast Association of Geological Societies, Transactions*, 27, pp. 352–364.
- Morton, R.A., 1979. Temporal and spatial variations in shoreline changes and their implications, examples from the Texas Gulf Coast. *Journal of Sedimentary Petrology*, 49, pp. 1101–1112.
- Morton, R.A. & Donaldson, A.C., 1973. Sediment distribution and evolution of tidal deltas along a tide-dominated shoreline, Wachapreague, Virginia. *Sedimentary Geology*, 10, pp. 285–299.
- Morton, R.A. & Miller, T.L., 2005. *National assessment of shoreline change: Part 2, historical shoreline changes and associated coastal land loss along the U.S. southeast Atlantic coast*. Open-File Report 2005-1401. St. Petersburg, FL: U.S. Geological Survey, p. 35.
- Moyer, K.S., 2007. *An assessment of an ephemeral breach along Cedar Island, Virginia*. Master's Thesis. Environmental Science and Policy, George Mason University, p. 101.
- Nebel, S. & Trembanis, N., 2010. Shoreline analysis: Decadal scale patterns (1852–2007) from Cedar Island, Virginia. In *Northeastern Section (45th Annual) and Southeastern Section (59th Annual) Joint Meeting*. Baltimore, 2010. Geological Society of America.
- Nebel, S.H., Trembanis, A.C. & Barber, D.C., 2012. Shoreline analysis and barrier island dynamics: Decadal scale patterns from Cedar Island, Virginia. *Journal of Coastal Research*, 28(2), pp. 332–341.
- NOAA Tides and Currents, 2006. [Online] Available at: <http://tidesandcurrents.noaa.gov/tides06/tab2ec2b.html#44> [Accessed 28 February 2011].
- NOAA, 2009. *Sea level variations of the United States 1854–2006*. Technical Report NOS CO-OPS 053. Silver Spring, MD: National Oceanic and Atmospheric Administration, National Ocean Service.
- Nummedal, D. & Fischer, I.A., 1978. Process-response models for depositional shorelines: The German and the Georgia Bights. *Proceedings of the 16th Coastal Engineering Conference*, ASCE, pp. 1215–1231.

- O'Brien, M.P., 1931. Estuary tidal prisms related to entrance areas. *Civil Engineering*, 1(8), pp. 738–739.
- O'Brien, M.P., 1969. Equilibrium flow areas of inlets on sandy coasts. *Journal of the Waterways and Harbors Division*, 95(WW1), pp. 43–52.
- Oertel, G.F., 1985. The barrier island system. *Marine Geology*, 63, pp. 1–18.
- Oertel, G.F., Kearney, M.S., Leatherman, S.P. & Woo, H., 1989. Anatomy of a barrier platform: Outer barrier lagoon, southern Delmarva Peninsula, Virginia. *Marine Geology*, 88, pp. 303–318.
- Oertel, G.F. & Kraft, J.C., 1994. New Jersey and Delmarva barrier islands. In R.A. Davis Jr., ed. *Geology of Barrier Islands*. Heidelberg, Germany: Springer-Verlag. pp. 207–232.
- Otvos, E.G., 1970. Development and migration of barrier islands, northern Gulf of Mexico. *Geological Society of America Bulletin*, 81, pp. 241–246.
- Pajak, M.J. & Leatherman, S., 2002. The high water line as shoreline indicator. *Journal of Coastal Research*, 18(2), pp. 329–337.
- Pilkey, O. H., Young, R. S., and Bush, D. M., 2000. 'Comment on Sea Level Rise Shown to Drive Coastal Erosion', *EOS Transactions* 81 (38), pp. 437–441.
- Rice, T.E. & Leatherman, S.P., 1983. Barrier island dynamics: The Eastern Shore of Virginia. *Southeastern Geology*, 24(3), pp. 125–137.
- Rice, T.E., Niedoroda, A.W. & Pratt, A.P., 1976. *The coastal processes and geology: Virginia barrier islands*. The Virginia Coast Reserve Study. The Nature Conservancy, Arlington, VA, pp. 109–382.
- Richardson, T.M. & McBride, R.A., 2007. Historical shoreline changes and morphodynamics of Parramore Island, Virginia (1852–2006). In *Coastal Sediments '07*. New Orleans, 2007. ASCE.
- Richardson, T.M. & McBride, R.A., 2010. Investigating a model of barrier-island and tidal-inlet evolution along the southern Delmarva Peninsula with historical shoreline and bathymetric data (1852 to 2009). In *Northeastern Section (45th Annual) and Southeastern Section (59th Annual) Joint Meeting*. Baltimore, 2010. Geological Society of America.
- Richardson, T.M. & McBride, R.A., 2011. Historical shoreline changes and morphodynamics of Cedar Island, Virginia, USA: 1852–2010. In *Proceedings of Coastal Sediments '11*. Miami, FL, 2011. ASCE.

Rosati, J.D., 2005. Concepts in sediment budgets. *Journal of Coastal Research*, 21, 307-322.

Sallenger, A.H., Fletcher, C., Thieler, E.R. & Howd, P., 2000. Comment: Leatherman, S.P., et al., 2000. Sea rise level shown to drive coastal erosion. *Eos*, 81(6). *Eos*, 81(38), p. 436.

Schwartz, M.L., 1973. *Barrier islands (Benchmark papers in geology, v. 9)*. Stroudsburg, PA: Dowden, Hutchinson & Ross.

Seabergh, W.C., 2007. Inlets and entrances, tidal inlet short course: Coastal inlet hydraulics. In *Coastal Sediments '07*. New Orleans, 2007. ASCE.

Seminack, C., October 2011. Personal communication on Jarrett (1976) feet to meters conversion.

Sha, L.P., 1989. Sand transport patterns in the ebb-tidal delta off Texel Inlet, Wadden Sea, The Netherlands. *Marine Geology*, 86, pp. 137–154.

Sha, L.P. & Van Den Berg, J.H., 1993. Variation in ebb-tidal delta geometry along the coast of the Netherlands and the German Bight. *Journal of Coastal Research*, 9(3), pp. 730–746.

Shalowitz, A.L., 1964. *Shore and sea boundaries*. Publication 10-1, Vol 2. Washington, DC: Coast and Geodetic Survey, U.S. Department of Commerce, p. 581.

St. Petersburg Coastal and Marine Science Center, 2011. *Coastal Change Hazards: Hurricanes and Extreme Storms*. [Online] Available at: <http://coastal.er.usgs.gov/hurricanes/norida/photo-comparisons/virginia.html> [Accessed December 2011].

Swift, D.J.P., 1975. Barrier-island genesis: Evidence from the central Atlantic shelf, eastern U.S.A. *Sedimentary Geology*, 14, pp. 1–43.

The Nature Conservancy, 2011. *Virginia Eastern Shore*. [Online] Available at: <http://www.nature.org/ourinitiatives/regions/northamerica/unitedstates/virginia/placesweprotect/virginia-coast-reserve.xml> [Accessed June 2010].

Thieler, E.R., Himmelstoss, E.A., Zichichi, J.L. & Ergul, A., 2008. *Digital Shoreline Analysis System (DSAS) version 4.0—an ArcGIS extension for calculating shoreline change*. Open-File Report 2008-1278. Woods Hole, MA: U.S. Geological Survey, p. 79.

Townend, I., 2005. An examination of empirical stability relationships for UK estuaries. *Journal of Coastal Research*, 21(5), pp.1042–1053.

USGS, 2011. *Coastal Change Hazards: Hurricanes and Extreme Storms*. [Online] Available at: <http://coastal.er.usgs.gov/hurricanes/norida/photo-comparisons/virginia.html> [Accessed April 2011].

VIMS, Fate, S., April 2011. Personal communication on shoaling patterns at Wachapreague Inlet while on-site for tidal inlet bathymetric survey.

Walton, T.L. & Adams, W.D., 1976. Capacity of inlet outer bars to store sand. *Proceedings of the 15th Coastal Engineering Conference*, ASCE, pp. 1919–1937.

Wikel, G.L. 2008. *Variability in Geologic Framework and Shoreline Change: Assateague and Wallops Islands, Eastern Shore of Virginia*. M.S. Thesis. The College of William and Mary in Virginia. p. 210.

Zervas, C., 2001. *Sea level variations of the United States 1854–1999*. NOAA Technical Report NOS CO-OPS 36. Silver Spring, MD: National Oceanographic and Atmospheric Administration, National Ocean Service.

Zhang, K., 1998. *Twentieth Century Storm Activity and Sea Level Rise Along the U.S. East Coast and Their Impact on Shoreline Position*. Ph.D. Dissertation. College Park, MD: University of Maryland.

Zhang, K., Douglas, B.C. & Leatherman, S.P., 1997. East coast storm surges provide unique climate record. *Eos*, 78(37), pp. 389, 396-397.

Zhang, K., Douglas, B.C. & Leatherman, S.P., 2001. Beach erosion potential for severe nor'easters. *Journal of Coastal Research*, 17(2), pp. 309-321.

Zhang, K., Douglas, B. & Leatherman, S., 2002. Do storms cause long-term beach erosion along the U.S. east barrier coast? *The Journal of Geology*, 110, pp. 493–502.

Zhang, K., Douglas, B.C. & Leatherman, S.P., 2004. Global warming and coastal erosion. *Climate Change*, 64, pp. 41–58.

## **CURRICULUM VITAE**

Trent Michael Richardson graduated from Marion Senior High School (Marion, Virginia) in 1993. He received a Bachelor of Arts in Geography and a Bachelor of Arts in Political Science from Mary Washington College (Fredericksburg, Virginia) in 1997. He also graduated from George Mason University (Fairfax, Virginia) in 1999 as a Master of Science in Geographic and Cartographic Sciences. Trent is currently employed as a Program Analyst at the Bureau of Ocean Energy Management within the United States Department of the Interior (Washington, DC). Email: [trent.richardson@boem.gov](mailto:trent.richardson@boem.gov)